UNITED STATES
DEPARTMENT OF INTERIOR
GEOLOGICAL SURVEY

SEAFLOOR GEOLOGIC HAZARDS, SEDIMENTOLOGY, AND BATHYMETRY: NAVARIN BASIN PROVINCE, NORTHWESTERN BERING SEA

Paul R. Carlson and Herman A. Karl

OPEN-FILE REPORT 81-1217

Menlo Park, California
1981

CONTENTS

INTRODUCTION

The study area, referred to in this report as the Navarin basin province, is located on the outer continental shelf and upper slope in the northwestern Bering Sea (Fig. 1). The area is bounded on the northwest by the US-USSR Convention line of 1867, on the southwest by the base of the continental slope and extends to within 100 km of St. Matthew Island to the northeast and St. Paul Island to the southeast. This region potentially contains significant vast accumulations of oil and gas and is likely to be the subject of extensive exploration activity.

The principal purpose of this report is to provide preliminary interpretations of seafloor hazards and related sediment and microfaunal studies of the Navarin Basin province preparatory to OCS lease sale 83. Several geologic processes that are active in Navarin Basin province are potentially hazardous to commercial development and will be discussed in this report.

Previous Studies

Prior to the summer of 1980, systematic geohazard surveys data had not been conducted in the Navarin Basin province. However, several earlier marine geology and geophysics cruises had collected dredge samples and seismic data adjacent to and within part of the province. A thick sedimentary sequence that underlies much of the present study area was first discovered on a 1970 cruise of the R/V Bartlett (Scholl and others, 1975, 1976). Marlow and others (1976) named this 10-15 km thick sedimentary sequence of Mesozoic and Cenozoic age deposits Navarin Basin. However, detailed mapping of the "acoustic basement" was not completed until seismic-reflection surveys of 1976, 1977, and 1980 provided multi-channel seismic coverage necessary to allow delineation of the northwest-trending basins (Marlow and others, 1981).

Bathymetric maps of the Bering Sea constructed by Pratt and Walton (1972) and Schumacher (1976), include very limited bathymetric data from the Navarin area. We have made a more detailed bathymetric map of the study area by combining the bathymetric data obtained on the DISCOVERER cruise of 1980 with data from several U. S. Geological Survey cruises during the past decade (Scholl and Marlow, 1970; Scholl, Buffington, and Marlow, 1976; Marlow and Cooper, 1979 and 1980).

Lisitsyn (1966) Russians published the first generalized maps of sediment distribution in the study area; without access to the original data, we only have been able to extract a few data points along the northern border of the Navarin province that we are using to supplement our sediment distribution maps. Data from the University of Washington cores and grab samples, some of which were collected in the eastern part of Navarin Basin (Knebel, 1972), are of much greater use. Other studies that provide comparative sedimentologic data have been conducted on nearby parts of the Bering Sea (Anadyr Basin, Kummer and Creager, 1971; Bristol Bay, Sharma and others, 1972; Norton Basin, Nelson and others, 1974, McManus and others, 1977, Kvenvolden and others, 1979, Drake and others, 1980; St. George Basin, Gardner and others, 1980; Vallier and others, 1980).

Although oceanographic data have been gathered from the Bering Sea for at least 100 years (Dall, N.H., 1881 to Cacchione and others, in press) and by scientists from numerous countries (e.g. USSR-Natarov, 1963; Japan-Takenouti and Ohtani, 1974; U.S.A.-Hughes and others, 1974), very little is known about the details of circulation and other oceanographic parameters within the Navarin Basin province. These other studies have involved water mass characteristics (Sayles and others, 1979) or large scale circulation (Hughes and others, 1974) of the entire Bering Sea or the deep Aleutian Basin or have concentrated on movement and characteristics of the water in and through the major outlets, the Bering Strait (Coachman and others, 1975) or the passes in the Aleutian Chain (Favorite, 1974).

Sea-ice is often present throughout of the Navarin basin province for about five months of the year (January through May). Whereas the average monthly limit of sea-ice in the Bering Sea has been determined (Webster, 1979), little is known about the movement and deformation of the sea-ice field (Tabata, 1974). The increasing availability of satellite imagery (Muench, 1974; Ahlnas and Wendler, 1980) together with winter field work (Drake and others, 1979; Parquette and Bourke, 1980) will provide needed detailed information helping to delineate the sea-ice fields in the Navarin Basin province.

Data Collection

The principal sources of data for this study have been the seismic-reflection profiles and sediment samples collected on the 1980 R/V DISCOVERER cruise (Figs. 2 and 3).

The geophysical systems used on the 1980 Navarin Basin cruise were as follows:

System	Resolution
1. Air gun (40 in ^{3})	5 - 10 m
2. Minisparker (800 J)	1 - 3 m
3. 3.5 kHz	1 m

The bottom samplers used were: gravity corer, dredge, and grab samplers. Suspended particulate samples were collected at the sea surface and near the seafloor.

Spacing between geophysical tracklines was approximately 30 km and seafloor geological samples were taken at intersections of track lines and at selected sites deemed geologically significant. Navigational control was LORAN C updated with satellite positioning.

Some additional data were collected in 1980 from the USGC POLAR STAR and the R/V S. P. LEE. We are also incorporating into our data base seismic-reflection records that were collected over the past fifteen years by the U.S.G.S. for resource evaluation (Marlow and others, 1981). Other sources of data include studies by the University of Washington and Alaska, Russian, and Japanese scientists (e.g. Knebel, 1972; Sharma, 1979; Lisitsyn, 1966; Takenouti and Ohtani, 1974).

Acknowledgments

We acknowledge the assistance provided by the officers and crew of the NOAA Ship DISCOVERER (July 2 - August 22, 1980) in collecting seismic reflection profiles along 6700 km of track lines (Fig. 2), 300 suspended samples, and 115 bottom samples (Fig. 3; 104 gravity cores, 10 grab samples, and 1 dredge haul). NOAA officers and survey technicians provided navigational control.

On the cruise of the U.S.C.G. cutter POLAR STAR (May 2 - 29, 1980), Rick Herrera (USGS representative), with assistance from Coast Guard personnel, collect 55 samples (Fig. 3; 22 gravity cores and 33 grab samples).

This study was funded jointly by the U.S. Geological Survey and by the Bureau of Land Management through interagency agreement with the National Oceanic and Atmospheric Administration, as part of the Outer Continental Shelf Environmental Assessment Program.

REFERENCES CITED

Ahlnas, K. and Wendler, G., 1980, Meteorological parameters affecting the location of the ice edge in the Bering Sea: Transactions Am. Geophys. Union, EOS, v. 61, p. 1006.

Cacchione, D. A., Drake, D. E., and Wiberg, P., in press, Velocity and bottom-stress measurements in the bottom boundary layer, outer Norton Sound, Alaska: in Nio, S. D., ed., Holocene marine sedimentation.

Coachman, L. K., Aagaard, K., and Tripp, R. B., 1975, Bering Strait, The regional physical oceanography: Seattle, Univ. of Washington Press, 186 p.

Dall, N. H., 1881, Hydrologie des Bering-Meeres und der benachbarten Gewasser: Pet. Geog. Mitt., v. 27, p. 361-380.

Drake, D. E., Totman, C. E., and Wiberg, P. L., 1979, Sediment transport during the winter on the Yukon prodelta Norton Sound, Alaska: Journal of Sedimentary Petrology, v. 49, p. 1171-1180.

Drake, D. E., Cacchione, D. A., Muench, R. D., and Nelson, C. H., 1980, Sediment transport in Norton Sound, Alaska: Marine Geology, v. 36, p. 97-126.

Favorite, F., 1974, Flow into the Bering Sea through Aleutian island passes: in Hood, D. W. and Kelley, E. J., ed., Oceanography of the Bering Sea. Inst. Mar. Sci., Univ. Alaska Occas. Publ. 2, p. 3-37.

Gardner, J. V., Dean, W. E., and Vallier, T. L., 1980, Sedimentology and geochemistry of the surface sediments, outer continental shelf, southern Bering Sea: Marine Geology, v. 35, p. 299-329.

Hughes, F. W., Coachman, L. K., and Aagaard, K., 1974, Circulation, transport and water exchange in the western Bering Sea: in Hood, D. W. and Kelley, E. J., ed., Oceanography of the Bering Sea. Univ. Alaska Inst. Marine Science, Occas. Publ. 2, p. 59-98.

Knebel, H. J., 1972, Holocene sedimentary framework of the east-central Bering Sea continental shelf: Ph.D. thesis, Univ. Washington, Seattle, 186 p.

Kummer, J. T., and Creager, J. S., 1971, Marine geology and Cenozoic history of the Gulf of Anadyr: Marine Geology, v. 10, p. 257-280.

Kvenvolden, K. A., Nelson, C. H., Thor, D. R., Larsen, M. C., Redden, G. D., Rapp, J. V., and Des Marias, D. J., 1979, Biogenic and thermogenic gas in gas-charged sediment of Norton Sound, Alaska: Offshore Technology Conference, Houston, Texas, Proceedings, v. 1, p. 479-486.

Lisitsyn, A. P., 1966, Protessy Sovremennogo Osodko' obrazovaniya v Beringovom More: Akad. Nauk SSR Inst. Okeal., Moskva, 574 p. (Recent sedimentation in the Bering Sea: Israel Program for Sci. Translations, 1969, Jerusalem; U.S. Dept. of Commerce, Clearinghouse for Federal Sci. Tech. Info., Springfield, VA, 614 p.).

Marlow, M. S., Scholl, D. W., Cooper, A. K., and Buffington, E. C., 1976, Structure and Evolution of Bering Sea shelf south of St. Lawrence Island, Bulletin of the American Association of Petroleum Geologists, v. 60, no. 1, p. 161-183.

Marlow, M. S., and Cooper, A. K., 1979, Multichannel seismic reflection profiles collected in 1977 in the northern Bering Sea: U.S. Geological Survey open-file report 79-1147.

Marlow, M. S. and Cooper, A. K., 1980, Multichannel seismic reflection profiles collected in 1976 in the southern Bering Sea shelf: U.S. Geological Survey open-file report 80-389.

Marlow, M. S., Cooper, A. K., Parker, A. W., and Childs, J. R., 1981, Isopach map of strata above acoustic basement in the Bering Sea: U.S. Geological Survey miscellaneous field studies map MF-1164

Marlow, M. S., Carlson, P. R., Cooper, A. K., Karl, H. A., McLean, H., McMullin, R., and Lynch, M. B., 1981, Resource report for proposed OCS sale number 83 Navarin Basin, Alaska: U.S. Geological Survey open-file report 81-252, 82 p.

McManus, D. A., Kolla, Venkatarathnam, Hopkins, D. M., and Nelson, C. H., 1977, Distribution of bottom sediments on the continental shelf, northern Bering Sea: U.S. Geological Survey Prof. Paper 759-C, 31 p.

Muench, R. D., 1974, Satellite observations of Bering Sea ice: in Hood, D. W. and Takenouti, Y., eds., Bering Sea oceanography: an update: Univ. Alaska, Inst. Marine Science, Report No. 75-2, p. 191-192.

Nelson, C. H., Hopkins, D. M., and Scholl, D. W., 1974, Tectonic setting and Cenozoic sedimentary history of the Bering Sea, in Herman, Yvonne, ed., Marine geology and oceanography of the Arctic seas: New York, Springer-Verlag, p. 119-140.

Paquette, R. G. and Bourke, R. H., 1980, Winter conditions in the Bering Sea: Transactions Am. Geophys. Union, EOS, v. 61, p. 1006.

Pratt, R. and Walton, F., 1974, Bathymetric map of the Bering Shelf: Geological Society of America, Boulder, Colorado.

Sayles, M. A., Aagaard, K., and Coachman, L. K., 1979, Oceanographic atlas of the Bering Sea Basin: Seattle, Univ. of Washington Press, 155 p.

Scholl, D. W., Buffington, E. C., and Marlow, M. S., 1975, Plate tectonics and the structural evolution of the Aleutian Bering Sea region, in Forbes, R. B., ed., Contributions to the geology of the Bering Sea Basin and adjacent regions: Geol. Soc. of America Spec. Paper 151, p. 1-32.

Scholl, D. W., Buffington, E. C., Marlow, M. S., 1976, Aleutian-Bering Sea region seismic reflection profiles: U.S. Geol. Survey Open-File Rept. 76-748.

Schumacher, G. M., 1976, Bathymetric map of the Aleutian Trench and Bering Sea U.S. Geological Survey open-file map 76-821, scale 1:2,500,000.

Sharma, G. D., Naidu, A. S., and Hood, D. W., 1972, Bristol Bay: model contemporary graded shelf: Am. Assoc. Petroleum Geologists, v. 56, p. 2000-2012.

Sharma, G. D., 1979, The Alaska shelf, hydrographic, sedimentary, and geochemical environment: Springer-Verlag, New York, 498 p.

Tabata, T., 1974, Movement and deformation of drift ice as observed with sea ice radar: in Hood, D. W. and Kelley, E. J., eds., Oceanography of the Bering Sea, Univ. Alaska, Inst. Marine Science, Occas. Publ. 2, p. 373-382.

Takenouti, A. Y. and Ohtani, K., 1974, Currents and water masses in the Bering Sea: a review of Japanese work: in Hood, D. W. and Kelley, E. J., eds., Oceanography of the Bering Sea, Univ. Alaska, Inst. Marine Science, Occas. Publ. 2, p. 39-57.

Vallier, T. L., Underwood, M. B., Gardner, J. V., and Barron, J. A., 1980, Neogene sedimentation on the outer continental margin, southern Bering Sea: Marine Geology, v. 36, p. 269-287.

Webster, B. D., 1979, Ice edge probabilities for the eastern Bering Sea: NOAA Technical Memorandum NWS AR-26, 20 p.

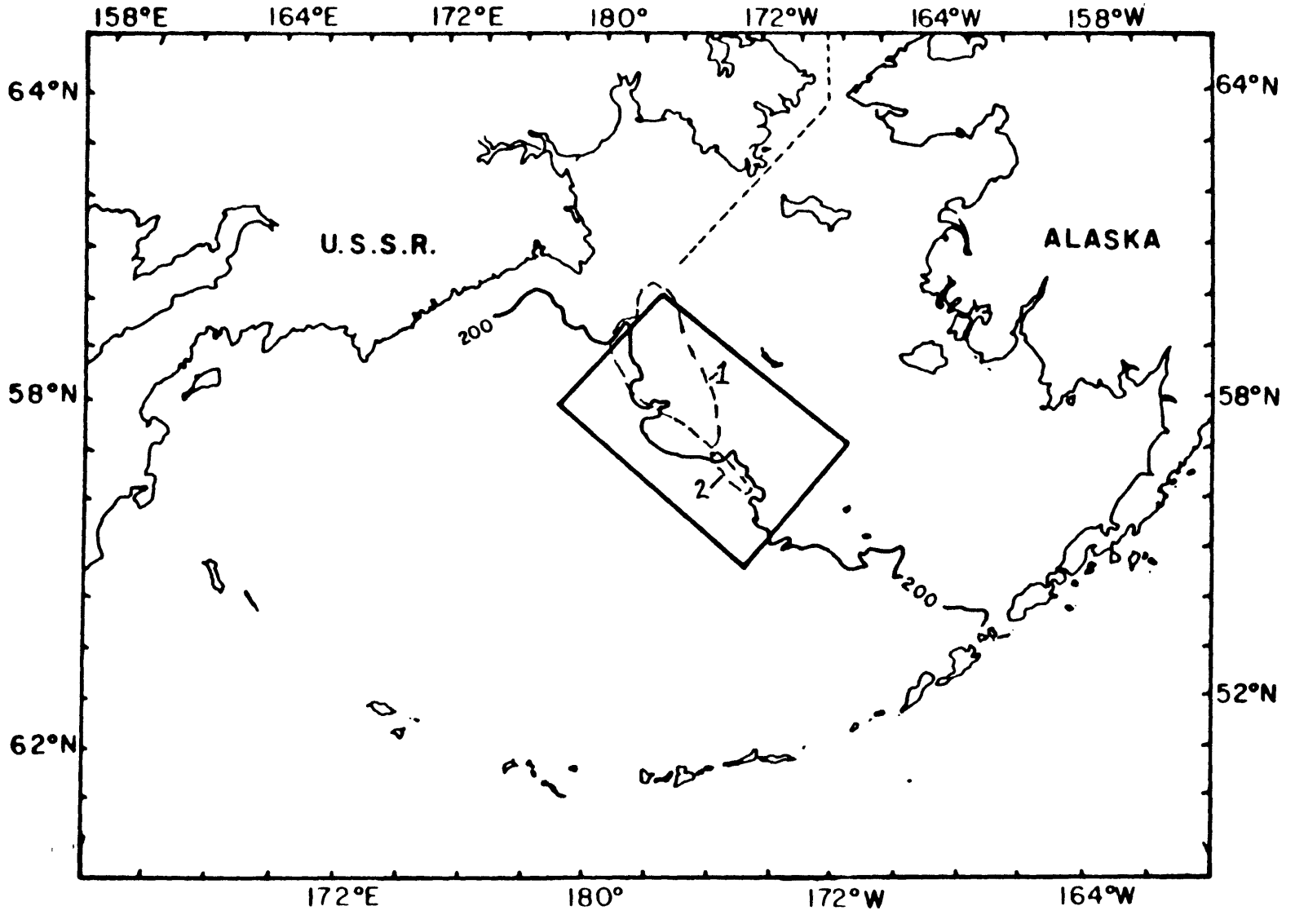

Figure 1. Location map of the study area that includes Navarin(1) and Zhemchug(2) basins as delineated by the 2 km thickness of strata contour (after Marlow and others, 1979).

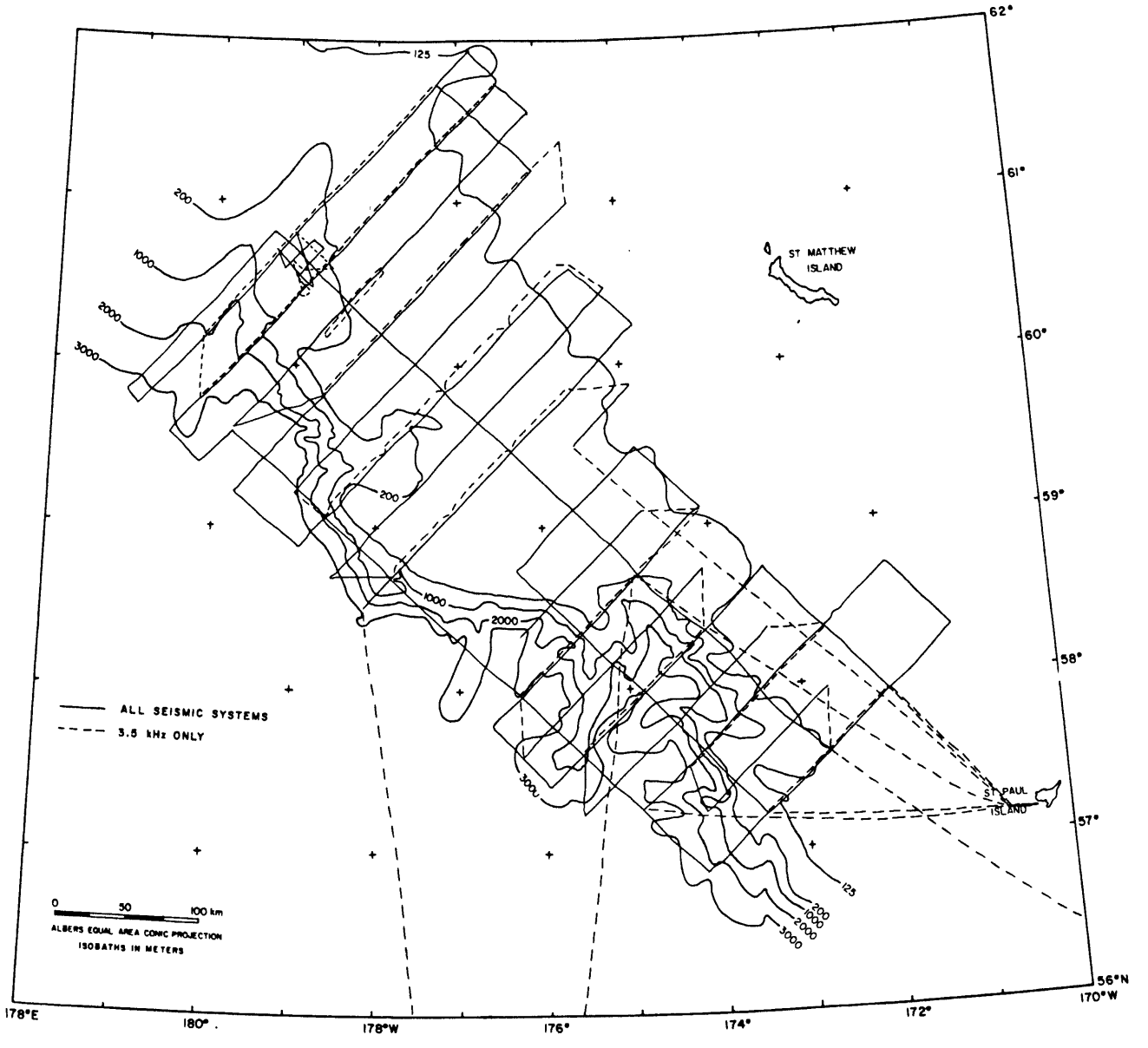

Figure 2. Trackline chart of seismic reflection profiles across the Navarin Basin province, collected on DISCOVERER cruise DC4/5-80-BS/NB.

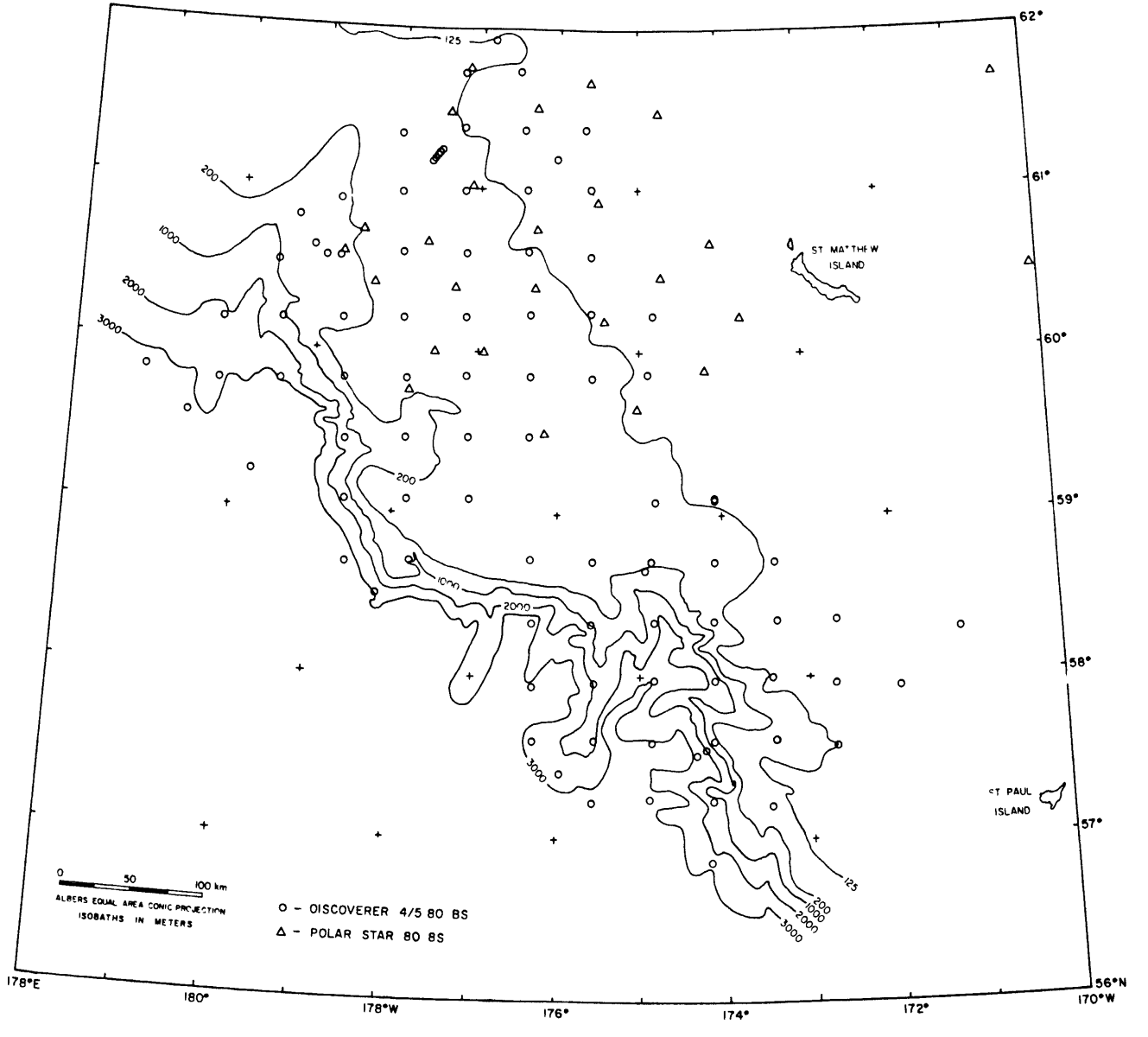

Figure 3. Location map of bottom samples collected in 1980 in Navarin Basin province.

MORPHOLOGY OF NAVARIN BASIN PROVINCE

Paul R. Carlson, Jeffrey M. Fischer, and Herman A. Karl

INTRODUCTION

There are three physiographic provinces in the Navarin study area. These are (1) the flat, wide, 100,000 km^2 continental shelf that extends from the 100 to the 150 m isobath and has an average gradient of 0.02°; (2) the steep, rugged 47,000 km^2 continental slope that extends from the 150 to the 2800 m isobath and has a range of gradients from 3° to 8°; and (3) the 40,000 km^2 rise which extends from the base of the slope to the 3600 m isobath. Three large submarine canyons deeply dissect the outer shelf and slope. Coalescing fans at the mouths of these canyons have contributed in part to the wedge of sediment that forms the continental rise.

The purpose of this chapter is to show a preliminary detailed bathymetric map (Fig. 4) of the Navarin basin province and to discuss characteristics of the principal geomorphic features.

The remoteness of the Navarin basin province has undoubtedly contributed to the lack of detailed published bathymetric maps of the area. Although Soviet scientists have discussed morphologic features of the Bering Sea (Lisitsyn, 1966; Gershanovich, 1968), they have not published detailed maps of the Navarin basin margin. Scholl and others (1970) published a detailed geomorphic diagram of Zhemchug Submarine Canyon and a bathymetric map of the adjacent continental slope that included the southern part of the study area. Four years later Scholl and others (1974) published a map that included the entire continental slope of the Bering Sea. At the same time, Pratt and Walton (1974) released a bathymetric map that included coverage of the Navarin continental shelf. However, both of these maps were contoured using very sparse depth control especially in the northern part of the Navarin basin province.

DATA COLLECTION AND PROCESSING

Shipboard

Depth soundings collected on several cruises by the U.S. Geological Survey scientists were used in compilation of a preliminary bathymetric map of the Navarin Basin province (Fig. 4). The bulk of the soundings were made on the 1980 cruise of the NOAA ship DISCOVERER (DC 4/5-80-BS/NB); supplemental soundings were added to the data set from previous cruises by U.S. Geological Survey ships R/V S. P. LEE and R/V SEA SOUNDER (S3-77-BS,L5-76-BS, L8-77-BS, L5-78-BS, L6-80-BS). Navigation for all cruises included LORAN C and Satellite.

Laboratory

The bathymetric profiles (3.5 and 12 kHz records) were digitized on a Tektronix plotter. Depths were "picked" at 5 minute intervals and at major changes in slope. The digitized data were merged with corrected navigation, computer plotted, and hand contoured at a scale of 1:1,000,000.

THE NAVARIN MARGIN

Shelf

The Bering Sea continental shelf is one of the widest and flattest in the world, is about 700 km wide and has a gradient of 0.02° seaward of the Yukon River delta. By comparison, Shepard (1963) reported a world-wide average for continental shelves of 0.12°. The portion of the Bering shelf that includes the Navarin basin province lies between the 100 m and 150 m isobaths and ranges in width from about 120 km at the northern and southern parts of the study area to a maximum width of about 235 km in the central part (Fig. 4). These boundaries define an area of about 100,000 km^2. The gradient of the Navarin basin shelf averages approximately 0.02° (range 0.01 to 0.03°). Although, the outer continental shelf is cut by three massive submarine canyons, there are no apparent morphologic expressions of these canyons landward of the 125 m isobath.

Slope

The continental slope forming the southeastern boundary of the Navarin Basin province begins at the 150 m isobath and extends to a depth of 2800 m northwest of Zhemchug Canyon (Fig. 4). Southeast of this magnificent canyon the slope abruptly changes gradient at 2400 m. The slope includes an area of about 47,000 km^2. The gradients of the Navarin slope range from 3° to 8° with even steeper gradients over shorter segments of slope. This compares with world-wide average gradient for continental slopes of about 4.3° (Shepard, 1963). The width of the continental slope ranges from 47 km in the middle of the province to 19 km south of Zhemchug Canyon. Exceptions to these width and gradient values are within the three submarine canyons that are deeply incised in the shelf and on either side of Zhemchug Canyon where pronounced ridges extend as much as 105 km seaward of the base of the slope. The longest of these ridges also functions as the northwestern wall of Zhemchug Canyon. These prominent ridges have several hundred to more than a thousand meters of relief.

Submarine Canyons

The three major submarine canyons that cut deeply into the Bering continental margin (Fig. 4) are Navarinsky (named after Cape Navarin), Pervenets, and Zhemchug (both named after Russian research vessels) (Kotenev, 1965). All three canyons head in water depths less than 150 m. Extensive deep-sea fans have been built at the mouths of the canyons in water depths of about 3000 m. Navarinsky is the longest canyon (340 km), Pervenets the shortest (125 km) and Zhemchug intermediate in length (240 km). Both Navarinsky and Zhemchug Canyons are about 100 km wide at the shelf break, but the smaller Pervenets Canyon is only 30 km wide. Wall relief of the three canyons at the shelf break ranges from 700 m for Navarin and 800 m for Pervenets, to a spectacular 2600 m for Zhemchug. Each of the three canyons consist of two main branches or tributaries on the landward side of the shelf break. The two tributaries in Zhemchug Canyon trend 180° away from each other, forming a large trough-shaped basin. Each of these tributaries is about 150 km long. The average gradient along the thalweg of each branch is about 1.2°, but a maximum gradient of 2.2° occurs along the steepest parts of these tributary canyons. In contrast, the two main branches or tributaries in Navarinsky and Pervenets Canyon intersect at a 90° angle. The length of the northern tributary of Navarinsky Canyon is 270 km and the southern 180 km. The thalweg gradients of these broad, shallow branches average 0.33° and 0.50°, respectively. The smaller Pervenets Canyon has a 90 km long northern tributary and a 80 km long southern one. These shorter tributaries average 0.30° and 0.33° in gradient, respectively.

These canyons are incised into Neogene and older more-lithified Paleogene rocks, principally mudstones, that are thought to make up much of Navarin Basin (Marlow and others, 1976). The canyons, especially Zhemchug, are apparently structurally controlled, the structures dating back at least into the Paleogene (Scholl and others, 1975). The major cutting of the canyons probably occurred when glacio-eustatically lowered sea-levels exposed most of the Bering shelf.

Rise

The continental rise in this remote part of the world has been sparsely sounded, but is a prominent enough feature to be easily recognized on profiles that traverse the bounding features - the Bering continental slope and the Aleutian abyssal plain. The rise includes 40,000 km^2 of the Navarin Basin province and begins at the base of the slope, a depth of 2800 m northwest of Zhemchug Canyon and 2400 m south of the canyon, and extends to the 3600 m isobath that marks the beginning of the abyssal plain. The width of the rise averages about 75 km, ranging from a minimum of 25 km northwest of Zhemchug Canyon to a width of more than 100 km adjacent to the mouths of the three large canyons. The gradients across the rise range from a low of 0.5° adjacent to the canyon mouths to 1.8° off the two prominent ridges located northwest of Zhemchug Canyon. Deep-sea channels cross the rise in the area of the canyon mouths and are apparently connected to the submarine canyons. Gravity cores collected near the mouths of the canyons and on the adjacent rise contain sand lenses that indicate deposition by turbidity currents (see Karl and others, this report). Seismic reflection profiles of the rise also

indicate the presence of turbidites which together with the cores suggest that the rise, at least adjacent to the canyons, consists of deep-sea fan deposits. The gradients measured across the rise near the canyons are also similar to gradients reported from other deep-sea fans (Nelson and others, 1970, p. 282-283).

REFERENCES CITED

Gershanovich, D. E., 1968, New data on geomorphology and recent sediments of the Bering Sea and the Gulf of Alaska: Marine Geology v.6, p. 281-296.

Kotenev, B. N., 1965, Submarine valleys in the zone of the continental slope in the Bering Sea: All-Union Research Inst. of Marine Fisheries and Oceanography. Transactions, v. 58, p. 35-44. (U.S. Navy Electronics Lab., San Diego, Ca., NEL Translation 112).

Lisitsyn, A. P., 1966, Recent sedimentation in the Bering Sea (in Russian): Inst. Okeanol. Akad. Nauk USSR, (translated by Israel Program for Scientific Translations, available from U. S. Dept. Commerce, Clearinghouse for Fed. Sci. and Tech. Info. 1969, 614 p.).

Nelson, C. H., Carlson, P. R., Byrne, J. V., and Alpha, T. R., 1970, Development of the Astoria Canyon-Fan physiography and comparison with similar systems: Marine Geology, v. 8, p. 259-291.

Marlow, M. S., Scholl, D. W., Cooper, A. K., and Buffington, E. C., 1976, Structure and evolution of Bering Sea shelf south of St. Lawrence Island: American Assoc. Petroleum Geol. Bull., v. 60, p. 161-183.

Pratt, R. and Walton, F., 1974, Bathymetric map of the Bering shelf: Geological Soc. of America, Boulder, Colo.

Shepard, F. P., 1963, Submarine geology: 2nd. ed. New York, Harper, 557 p.

Scholl, D. W., Alpha, T. R., Marlow, M. S. and Buffington, E. C., 1974, Base map of the Aleutian Bering Sea region: U. S. Geological Survey Map I-879, scale 1:2,500,000.

Scholl, D. W., Buffington, E. C., Hopkins, D. M., and Alpha, T. R., 1970, The structure and origin of large submarine canyons of the Bering Sea: Marine Geology v. 8, p. 187-210.

Scholl, D. W., Buffington, E. C., and Marlow, M. S., 1975, Plate tectonics and the structural evolution of the Aleutian-Bering Sea region: Forbes, R. B., ed., Contributions to the geology of the Bering Sea basin and adjacent regions: Geol. Soc. America Special Paper 151, p. 1-32.

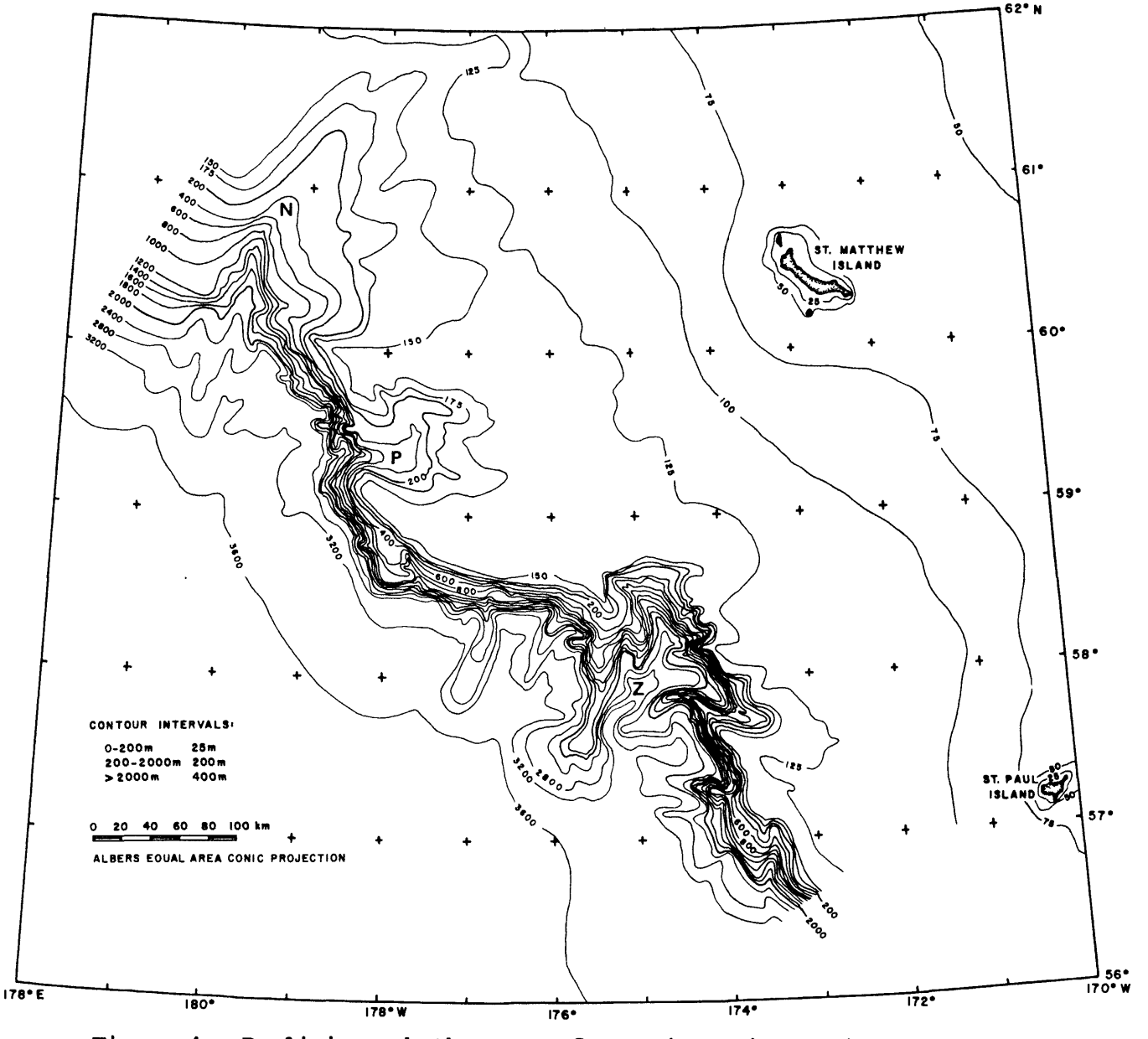

Figure 4. Preliminary bathymetry of Navarin Basin province. Letters N, P, and Z locate the three major submarine canyons, Navarinsky, Pervenets, and Zhemchug.

SUSPENDED PARTICULATE MATTER IN NAVARIN BASIN PROVINCE, SUMMER, 1980

H. A. Karl, B. Lamb, and P. R. Carlson

INTRODUCTION

Distribution, concentration, and composition of particulate matter suspended in the water column reflect oceanographic conditions prevailing in Navarin Basin province. Terrigenous sediment and plankton in large part constitute the total suspended matter (TSM) in the water column. In addition, waves and currents resuspend fine-grained material previously deposited on the bottom. Particulate matter occurs in suspension throughout the water column, but is concentrated at density discontinuities where particles accumulate as they settle. Major concentrations of suspensates occur at the water surface, along density gradients within the thermocline, and near the bottom. Spatial and temporal variations in the distribution, concentration, and composition of suspended sediment define pathways of sediment dispersal and zones of erosion and deposition.

Methods

Samples of TSM were collected at the surface and within 1-2 m of the sea floor. Samples of surface water were collected by casting a PVC bucket from the ship at 4-hour intervals while seismic profiling and 1-2 minutes before coming to a stop at each core station. Water near the bottom was sampled using a 5 liter Niskin bottle modified to close when a weighted line contacted the seabed. Vacuum pumps sucked a 1-4 liter aliquot of water taken from these samples through preweighed 47 mm diameter polycarbonate Nuclepore filters with a nominal pore size of 0.4 um. The filters were rinsed with distilled water and placed in covered plastic petri dishes. Onshore the filters were dried for 24 hours at 50°C and reweighed to an accuracy of 10 ug. In addition, one-half of each filter was combusted for 5-6 hours at 550°C in tared platinum foil crucibles in order to obtain an estimate of organic matter concentration. Concentrations of TSM, organic matter, and ash residue were calculated as milligrams of suspensate per liter of seawater.

RESULTS

During the 1980 DISCOVERER cruise, from July 6 to August 18, we collected 187 surface samples and 38 bottom samples (Fig 5). Table 1 shows the concentrations of TSM, organic matter, and ash residue of those samples processed to date. Concentrations of surface suspended sediment averaged 0.55 mg/l ranging from a low of 0.04 mg/l to a high of 2.32 mg/l. The average bottom TSM concentration, exclusive of 3 contaminated samples (BS-6, BS-12, BS-17) and a non-contaminated sample (BS-18), but one with an unusually high TSM concentration is 1.91 mg/l that is 3.5 times the average surface concentration. By including the highest concentration recorded, 18.32 mg/l, the mean is raised to 2.33 mg/l. The lowest concentration measured was 0.39 mg/l. We have calculated the percent of organic matter in 144 surface samples and 13 near bottom samples. The mean percentage of organic matter for surface

samples is 65.7%; the range is from 12.2% to 95.2%. The organic content of the near bottom samples which have been analyzed is less than half the surface mean averaging 29.1% and ranging from 10.9% to 85.5%.

Maps of the spatial distribution of TSM and ash residue percent (the non-combustible portion of the sample which is taken to be the inverse of the organic matter percentage) reveal several trends. Regionally, concentrations of surface TSM tend to be greater in the southeastern part of the province than elsewhere (Fig. 6). There is no clear cut cross-shelf gradient in concentration. Instead isopleths form lobes, plumes and closures. Although sample coverage is meager, bottom TSM concentrations tend to decrease seaward (Fig. 7). Higher than average concentrations occur at the heads of Pervenets and Zhemchug canyons. Percentage of ash residue in surface samples also tends to be greater in the southeastern part of the area (Fig. 8). A narrow, elongate band of anamolously-low values extending across the upper slope and outer shelf perpendicular to isobaths is an exception to this trend (Fig. 8). Higher percentage occur in the northwest to the east of Pervenets Canyon, and to the southeast of Navarinsky canyon. Except for the transect northeast of Pervenets Canyon, percentages of ash residue in near bottom samples decrease seaward (Fig. 9).

DISCUSSION

Surface TSM

The relatively low concentrations of TSM in the surface water is not surprising in that Navarin Basin lies several hundred kilometers from major sources of terrigenous sediment. The higher concentrations of surface TSM in the southeast in the vicinity of Zhemchug Canyon, over the upper slope and outer shelf, and near Pervenets and Navarinsky Canyons may reflect populations of plankton. Similarly isolated areas of higher TSM values may be the result of concentrated pockets of plankton. This interpretation is conjecture, because no suspended matter compositions have as yet been determined. A major point which must be considered when interpreting our areal distribution of suspended particulates is the time required to sample such an enormous area. Distributions and concentrations may have changed from the first sample collected to the last. Temporal changes in concentrations may in part account for the patchy and convoluted distributions. Alternately, these patterns may reflect eddies in the shelf and slope current systems. The percentage of ash residue tends to be correlated positively with higher TSM concentrations. Ash residue is composed not only of terrigenous debris, but includes the non-combustible, often siliceous, parts of organisms. Diatoms (see Baldauf, this report) dominate and radiolarians (Blueford, this report) are important contributors to the micro-organism assemblages. The siliceous tests of these organisms could contribute to the ash residue.

Near-bottom TSM

Distribution patterns of TSM and ash residue near the bottom of the water column are more readily interpreted than surface distributions. Decreasing gradients seaward suggest less energy is available to resuspend sediment. This might be explained by shoaling surface waves that affect bottom sediments more in shallow water than in deep water. Other oceanic processes affect sedimentation, but not enough is known about Bering Sea shelf currents to discuss the role of various currents on the transport of near bottom sediment.

Three near-bottom samples (BS-6, BS-12, and BS-17) of anamolously high concentrations were discounted as being contaminated. Even discounting these samples, there is a plume of higher than average TSM extending from the shelf towards the head of Pervenets Canyon (Fig. 7). Another plume is located near the head of Zhemchug Canyon. These canyons possibly may modify currents around their heads in such a way as to intensify resuspension of bottom sediment on the adjacent shelf and to draw water from the shelf down canyon. Such canyon effects on shelf sediment dynamics have been postulated elsewhere (Karl, 1980). Alternately, these higher concentrations may reflect greater numbers of benthic and planktonic microorganisms near the canyon heads.

CONCLUSIONS

A substantial number of suspended sediment samples have been collected from a virtually unstudied area of the Bering Sea. The preliminary stage of data reduction does not warrant making detailed statements about the processes that influence sediment dynamics in Navarin basin. Generally, the concentration of total suspended matter near the bottom is more than 3 times that on the surface. This very likely reflects fine-grained material resuspended by currents generated by surface waves but may involve other processes. The patchy distribution of surface suspended sediment suggests not only that plankton may influence the TSM concentrations, but also may reflect complex shelf and slope currents. The submarine canyons may affect both surface and near-bottom distributions by supplying nutrient-rich upwelled water and by modifying current patterns on the adjacent shelf.

REFERENCES CITED

Karl, H. A., 1980, Influence of San Gabriel submarine canyon on narrow shelf sediment dynamics, southern California: Marine Geology, v. 34, p. 61-78.

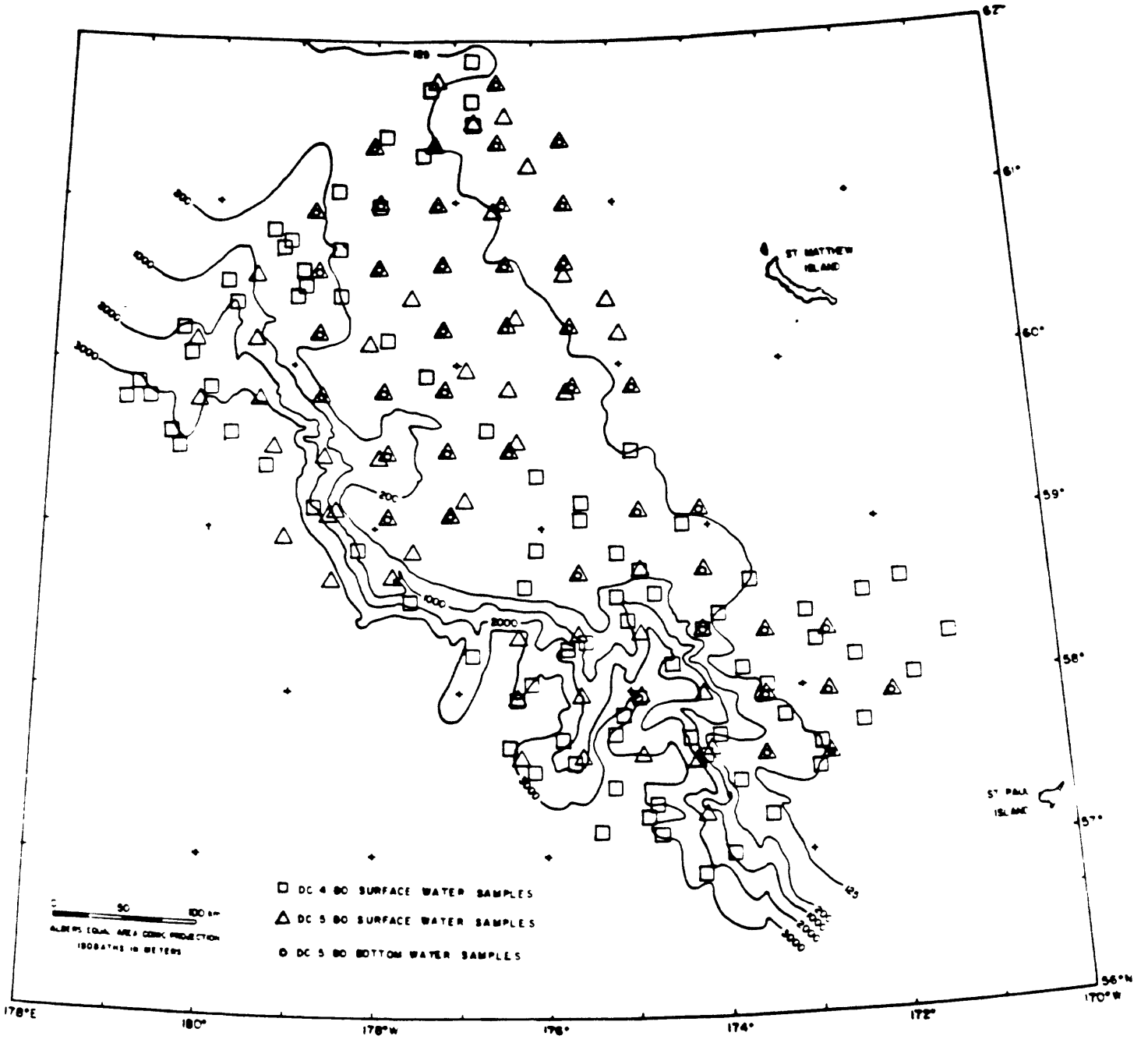

Figure 5. Suspended particulate matter station locations.

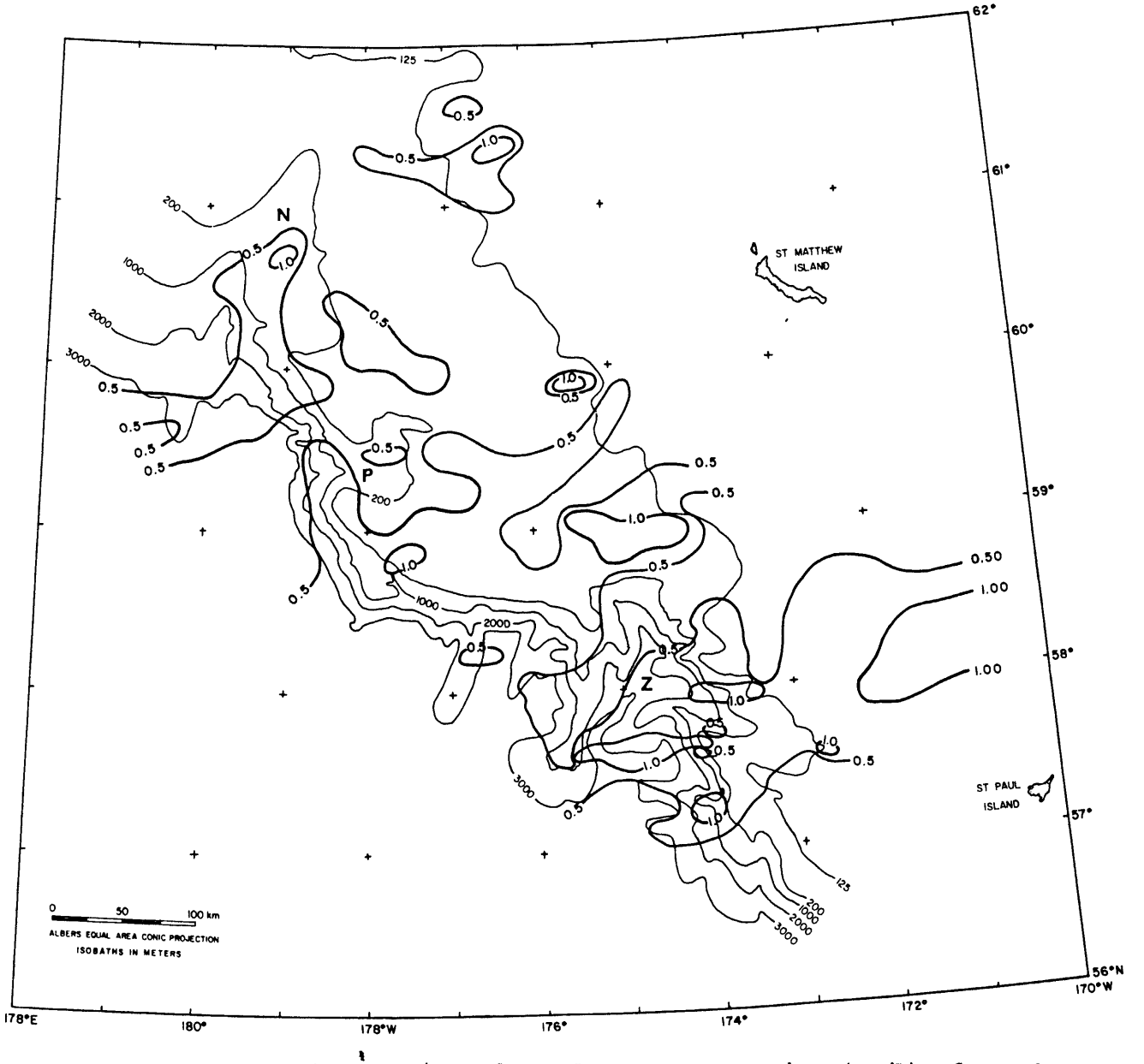

Figure 6. Areal distribution of absolute concentration (mg/l) of total suspended matter collected at the surface. Letters N, P, Z locate Navarinsky, Pervenets, and Zhemchug Canyons.

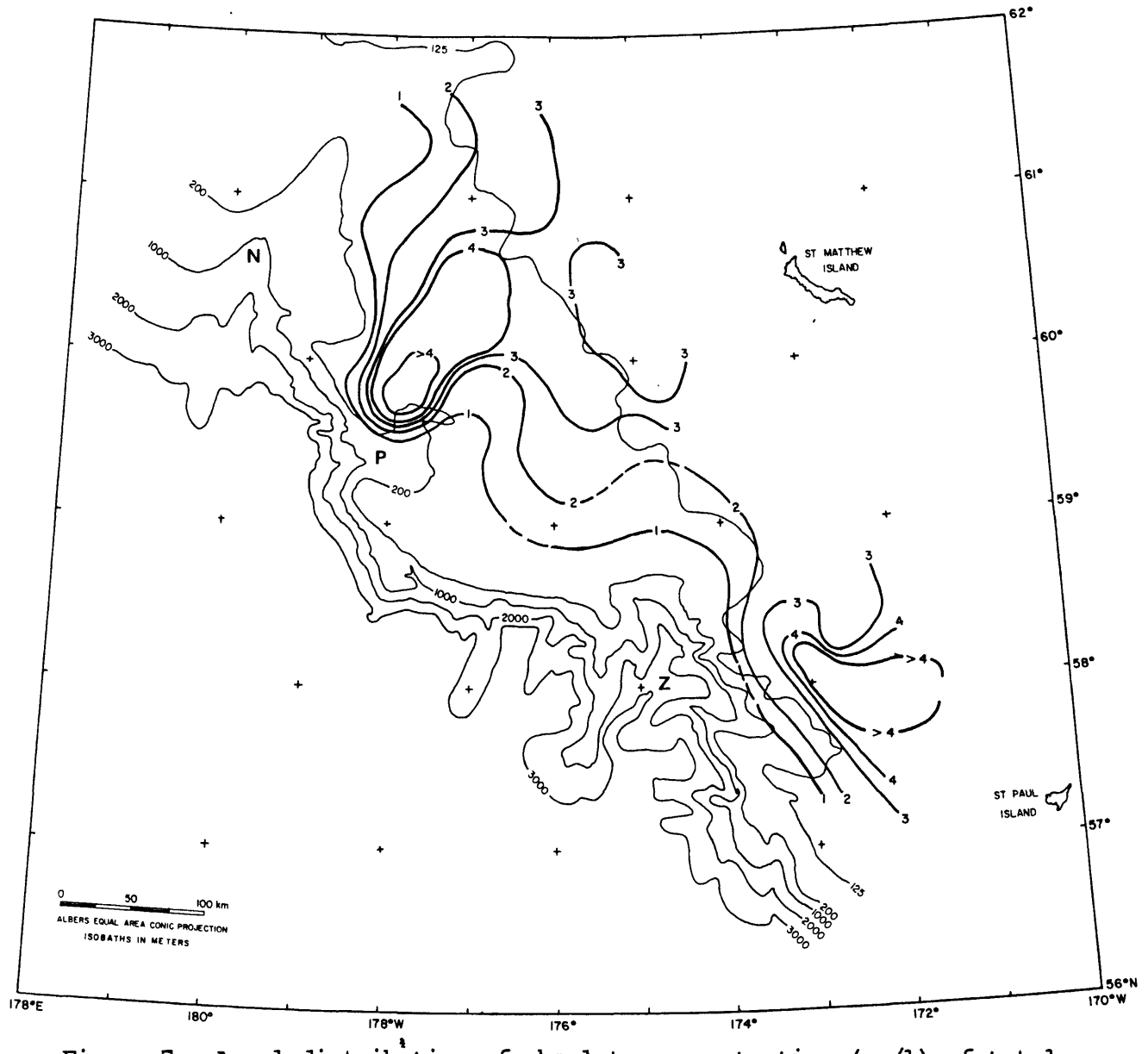

Figure 7. Areal distribution of absolute concentration (mg/l) of total suspended matter collected 1 m above the sea bed. Letters N, P, Z locate Navarinsky, Pervenets, and Zhemchug Canyons.

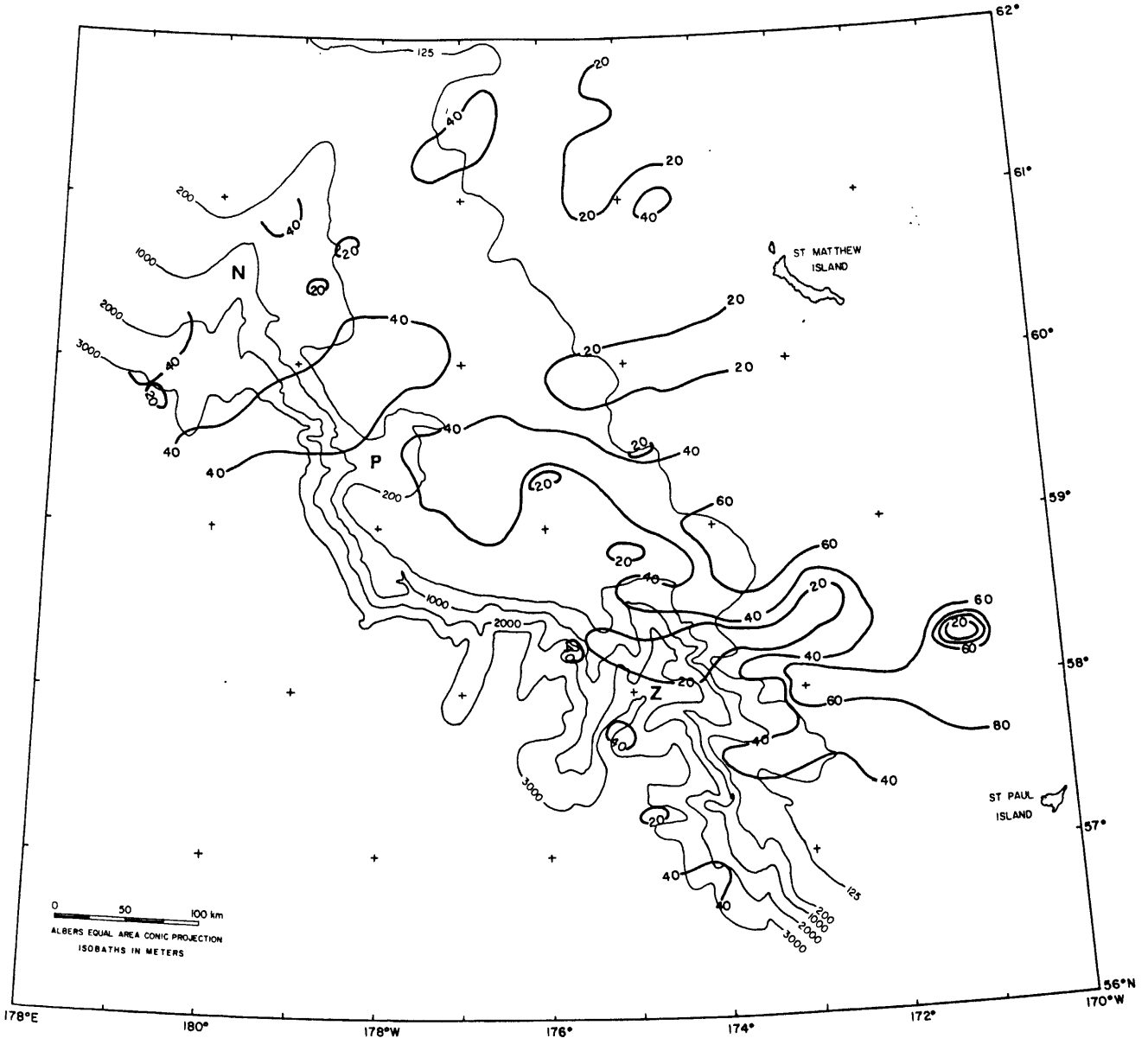

Figure 8. Areal distribution of the percentage of non-combustible material in surface suspended sediment samples. Letters N, P, Z locate Navarinsky, Pervenets, and Zhemchug Canyons.

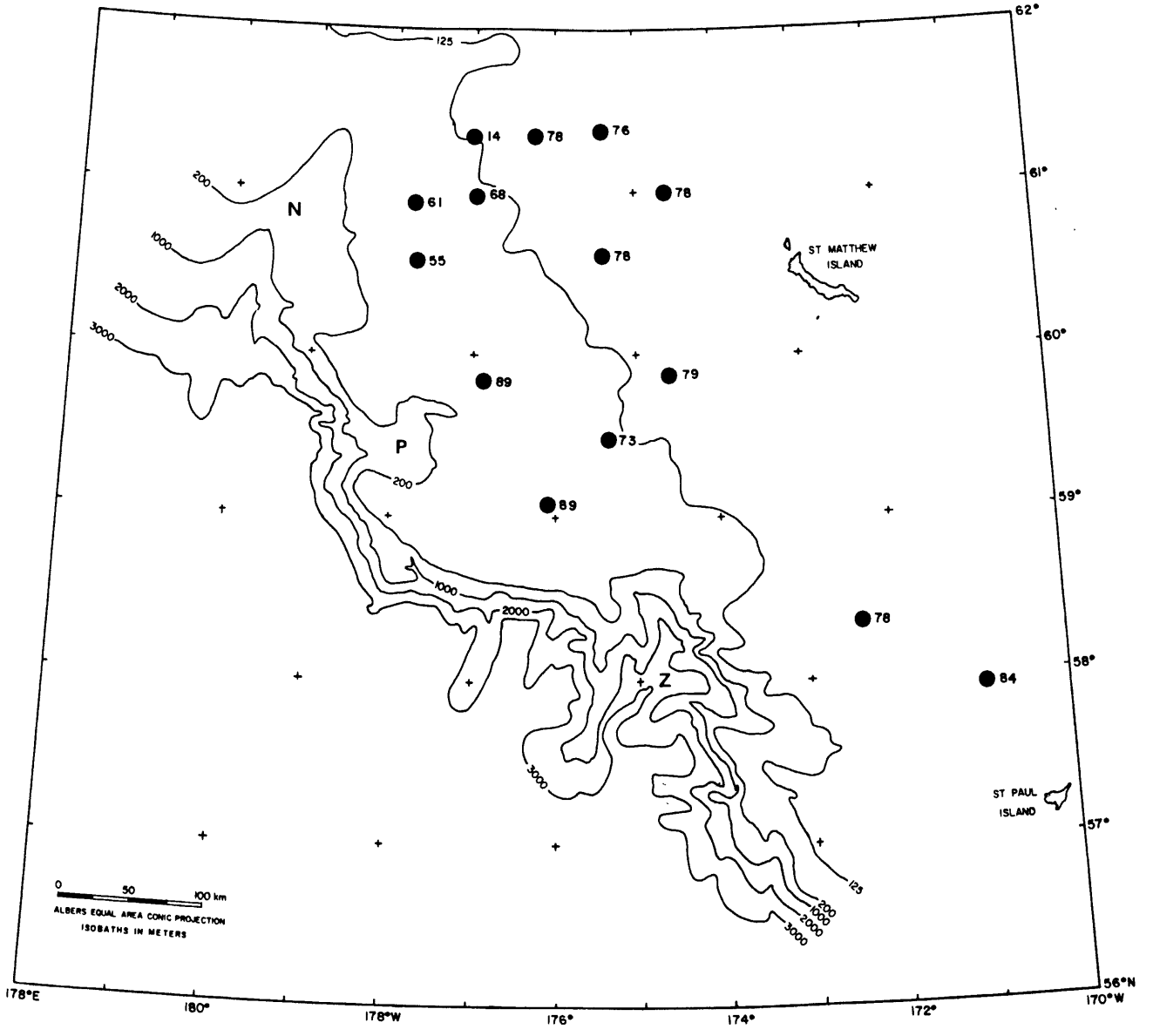

Figure 9. Areal distribution of the percentage of non-combustible material in suspended sediment samples collected 1 m above the sea bed. Letters N, P, Z locate Navarinsky, Pervenets, and Zhemchug Canyons.

Table 1.: Analyses of suspended particulate matter

SAMPLE NO.	DEPTH (m)	TSM[1] (mg/l)	NCM[2] (mg/l)	NCM %	CM[3] (mg/l)	CM %
SS-1	Surface	0.64	0.33	51.3	0.31	48.7
SS-2	"	0.73	0.21	28.0	0.52	72.0
SS-3	"	0.64	0.27	42.9	0.36	57.1
SS-4	"	0.53	0.27	51.7	0.25	48.3
SS-5	"	0.67	0.28	42.5	0.38	57.5
SS-6	"	1.20	0.23	19.0	0.97	81.0
SS-7	"	1.04	0.26	25.0	0.76	75.0
SS-8	"	0.66	0.12	19.3	0.53	80.7
SS-9	"	0.29	0.12	42.6	0.16	57.4
SS-10	"	0.72	0.30	42.0	0.41	58.0
SS-11	"	0.93	0.41	44.4	0.51	55.6
SS-12	"	0.65	0.22	34.7	0.42	65.3
SS-13	"	1.25	0.46	37.4	0.78	62.6
SS-14	"	0.23	0.10	42.7	0.13	47.3
SS-15	"	0.54	0.11	20.8	0.43	79.2
SS-16	"	0.34	0.14	40.3	0.20	59.7
SS-17	"	0.27	0.13	48.8	0.14	51.2
SS-18	"	0.75	0.17	23.7	0.57	76.3
SS-19	"	0.70	0.06	09.5	0.63	90.5
SS-20	"	0.26	0.07	28.7	0.18	71.2
SS-21	"	0.28	0.10	35.5	0.18	64.5
SS-22	"	0.82	0.28	34.1	0.54	65.9
SS-23	"	0.26	0.08	33.7	0.17	66.3
SS-24	"	0.28	0.10	35.8	0.18	64.2
SS-25	"	0.24	0.07	32.8	0.16	67.2
SS-26	"	0.34	0.13	38.9	0.21	61.1
SS-27	"	0.62	0.32	51.5	0.30	48.5
SS-28	"	0.63	0.30	48.5	0.32	51.5
SS-29	"	0.33	0.09	26.8	0.24	73.2
SS-30	"	0.45	0.08	19.4	0.37	80.6
SS-31	"	0.29	0.05	19.8	0.23	80.2
SS-32	"	0.27	0.10	39.5	0.16	60.5
SS-33	"	0.30	0.08	26.1	0.22	73.9
SS-34	"	0.42	0.13	32.5	0.28	67.5
SS-35	"	0.24	0.09	37.1	0.15	62.9
SS-36	"	0.38	0.11	28.8	0.27	71.2
SS-37	"	0.36	0.14	39.6	0.22	60.4
SS-38	"	0.31	0.07	25.4	0.23	74.6
SS-39	"	0.18	0.04	25.7	0.13	74.3
SS-40	"	0.23				
SS-41	"	0.66	0.31	48.1	0.34	51.9
SS-42	"	0.59	0.30	52.1	0.28	48.9
SS-43	"	0.40	0.13	31.8	0.27	58.2
SS-44	"	0.48	0.16	34.6	0.31	65.4
SS-45	"	0.81	0.17	21.4	0.63	78.6
SS-46	"	0.65	0.24	36.8	0.47	63.2
SS-47	"	0.44	0.12	28.5	0.31	71.5

[1] concentration of total suspended matter in the sample

[2] concentration of non-combustible matter in the sample; this matter is assumed to be terrigenous particles and/or the non-combustible parts of organisms.

[3] concentration of combustible matter in the sample; this matter is assumed to be the organic constituents of the total suspended sediment.

* C = contaminated sample.

Table 1.: Analyses of suspended particulate matter (cont'd)

SAMPLE NO.	DEPTH (m)	TSM[1] (mg/l)	NCM[2] (mg/l)	NCM %	CM[3] (mg/l)	CM %
SS-48	Surface	0.46	0.15	32.9	0.31	67.1
SS-49	"	0.38	0.13	34.8	0.25	65.2
SS-50	"	0.50	0.14	29.5	0.35	70.5
SS-51	"	0.34	0.11	34.7	0.22	65.3
SS-52	"	0.40	0.19	44.9	0.20	55.1
SS-53	"	0.40	0.10	26.2	0.29	73.8
SS-54	"	0.35	0.12	34.0	0.23	66.0
SS-55	"	0.41	0.14	35.6	0.26	64.4
SS-56	"	0.58	0.30	52.7	0.27	47.3
SS-57	"	1.76	1.14	65.0	0.62	35.0
SS-58	"	1.66	0.08	04.8	1.58	95.2
SS-59	"	0.49	0.22	45.1	0.27	54.9
SS-60	"	0.62	0.25	41.0	0.36	59.0
SS-61	"	0.66	0.23	34.8	0.43	65.2
SS-62	"	0.35	0.10	29.3	0.24	70.7
SS-63	"	0.35	0.08	25.1	0.26	74.9
SS-64	"	0.38	0.10	27.9	0.27	72.1
SS-65	"	0.44	0.11	25.6	0.32	74.4
SS-66	"	0.38	0.07	19.1	0.31	80.9
SS-67	"	0.80	0.34	42.6	0.46	57.4
SS-68	"	0.74	0.10	14.8	0.63	85.2
SS-69	"	0.44	0.27	62.1	0.16	37.9
SS-70	"	0.72	0.13	19.0	0.58	81.0
SS-71	"	0.60	0.09	14.7	0.51	85.3
SS-72	"	0.51	0.14	27.5	0.37	72.5
SS-73	"	0.50	0.16	32.1	0.34	67.9
SS-74	"	0.57	0.15	26.5	0.42	73.5
SS-75	"	0.60	0.14	24.3	0.46	75.7
SS-76	"	0.46	0.13	30.0	0.32	70.0
SS-77	"	0.57	0.18	52.2	0.39	47.8
SS-78	"	0.37	0.16	48.6	0.21	51.4
SS-79	"	0.94	0.35	37.2	0.59	62.8
SS-80	"	0.31	0.09	29.4	0.22	70.6
SS-81	"	0.59	0.18	31.2	0.40	68.8
SS-82	"	0.66	0.21	17.1	0.45	82.9
SS-83	"	0.61	0.23	38.0	0.38	62.0
SS-84	"	0.28	0.11	39.3	0.17	60.7
SS-85	"	0.32	0.07	22.0	0.25	78.0
SS-86	"	0.33	0.06	19.6	0.26	80.4
SS-87	"	0.78	0.33	42.3	0.45	57.7
SS-88	"	1.47	0.90	61.3	0.56	38.7
SS-89	"	0.53	0.14	26.8	0.39	73.2
SS-90	"	0.40	0.11	28.2	0.28	71.8
SS-91	"	0.92	0.44	47.8	0.48	52.2
SS-92	"	0.44	0.10	23.7	0.33	76.3
SS-93	"	0.41	0.11	26.9	0.30	73.1
SS-94	"	0.26	0.09	34.8	0.17	65.2

Table 1.: Analyses of suspended particulate matter (cont'd)

SAMPLE NO.	DEPTH (m)	TSM[1] (mg/l)	NCM[2] (mg/l)	NCM %	CM[3] (mg/l)	CM %
SS-95	Surface	0.37	0.13	35.8	0.23	64.2
SS-96	"	0.40	0.14	35.4	0.26	64.6
SS-97	"	0.32	0.09	30.6	0.22	69.4
SS-98	"	0.48	0.19	41.3	0.28	58.8
SS-99	"	0.17	0.65	38.0	1.06	62.0
SS-100	"	0.40	0.14	35.5	0.26	64.5
SS-101	"	0.25	0.06	24.6	0.19	75.4
SS-102	"	0.24	0.05	21.6	0.19	78.4
SS-103	"	0.34	0.04	14.1	0.29	85.9
SS-104	"	0.44	0.11	26.7	0.32	73.3
SS-105	"	0.24	0.07	31.6	0.16	83.4
SS-106	"	0.28	0.09	34.6	0.18	65.4
SS-107	"	0.31	0.05	19.1	0.25	80.9
SS-108	"	0.21	0.07	33.5	0.14	66.5
SS-109	"	0.24	0.12	50.0	0.12	50.0
SS-110	"	0.56	0.21	38.8	0.34	65.5
SS-111	"	0.41	0.11	39.5	0.29	60.5
SS-112	"	0.41	0.16	39.8	0.25	60.2
SS-113	"	0.23	0.06	28.8	0.16	71.2
SS-114	"	0.64	0.10	16.9	0.53	83.1
SS-115	"	0.17	0.02	16.8	0.14	83.2
SS-116	"	0.21	0.04	21.2	0.16	78.8
SS-117	"	0.18	0.03	17.6	0.14	82.4
SS-118	"	0.13	0.02	21.5	0.10	78.5
SS-119	"	0.38	0.10	25.9	0.28	74.1
SS-120	"	0.45	0.13	29.6	0.32	70.4
SS-121	"	0.60	0.32	54.3	0.27	45.7
SS-122	"	0.24	0.08	34.9	0.15	65.1
SS-123	"	0.89	0.69	51.7	0.20	48.3
SS-124	"	0.32				
SS-125	"	0.74	0.35	48.2	0.38	51.8
SS-126	"	0.76	0.37	48.7	0.39	51.3
SS-127	"	0.38	0.12	32.3	0.26	67.7
SS-128	"	0.34	0.10	28.0	0.24	72.0
SS-129	"	0.23	0.65	27.9	0.16	72.1
SS-130	"	0.27	0.56	20.2	0.22	79.8
SS-131	"	0.29	0.07	23.2	0.22	76.8
SS-132	"	1.34	0.25	18.2	1.09	81.8
SS-133	"	0.34	0.09	27.0	0.25	73.0
SS-134	"	0.41	0.12	28.0	0.29	72.0
SS-135	"	0.24	0.10	42.0	0.14	58.0
SS-136	"	0.78	0.27	34.0	0.51	66.0
SS-137	"	1.02	0.38	37.0	0.64	63.0
SS-138	"	0.46	0.11	23.0	0.35	77.0
SS-139	"	0.63	0.24	38.0	0.39	62.0
SS-140	"	0.37	0.13	36.0	0.24	64.0

Table 1.: Analyses of suspended particulate matter (cont'd)

SAMPLE NO.	DEPTH (m)	TSM[1] (mg/l)	NCM[2] (mg/l)	NCM %	CM[3] (mg/l)	CM %
SS-141	Surface	0.37	0.15	42.7	0.21	57.3
SS-142	"	0.37	0.13	36.4	0.23	76.2
SS-143	"	0.35	0.19	54.2	0.16	45.8
SS-144	"	0.40	0.35	87.8	0.04	12.2
SS-145	"	0.52	0.27	51.4	0.25	48.6
SS-146A	"	0.56	0.25	44.0	0.31	56.0
SS-146B	"	0.64	0.25	39.0	0.39	61.0
SS-147	"	0.35	0.09	27.0	0.26	73.0
SS-148	"	0.31	0.06	19.0	0.15	81.0
SS-149	"	0.28	0.09	31.0	0.19	69.0
SS-150	"	0.24	-	-	-	-
SS-151	"	0.40	0.02	05.0	0.38	95.0
SS-152	"	0.79	0.23	28.0	0.56	72.0
SS-153	"	0.43	0.16	37.0	0.27	63.0
SS-154	"	0.68	0.27	39.0	0.31	61.0
SS-155	"	0.92	0.34	37.3	0.58	62.7
SS-156	"	0.59	0.14	24.7	0.44	75.3
SS-157	"	0.77	0.34	44.6	0.43	55.4
SS-158	"	1.13	0.19	17.1	0.94	82.9
SS-159	"	0.51	0.14	26.0	0.37	74.0
SS-160A	"	1.22	0.93	76.6	0.28	23.4
SS-160B	"	1.09	0.43	39.0	0.56	61.0
SS-161	"	0.64	0.18	27.9	0.46	72.1
SS-162	"	0.58	0.24	41.6	0.34	58.4
SS-163	"	1.30	0.78	60.1	0.52	39.9
SS-164	"	1.21	0.65	53.5	0.56	46.5
SS-165	"	1.45	0.67	45.8	0.78	54.2
SS-166	"	1.13	0.46	40.4	0.67	59.6
SS-167	"	0.51	0.20	38.5	0.31	61.5
SS-168	"	0.40	0.16	39.0	0.24	84.0
SS-169	"	1.13	0.69	61.1	0.44	38.9
SS-170	"	2.32	0.12	55.8	1.03	44.6
SS-171	"	1.00	0.53	53.3	0.47	46.7
SS-172	"	1.36	0.83	60.9	0.53	39.1
SS-173	"	0.73	0.32	51.0	0.41	49.0
SS-174	"	0.46	0.20	43.7	0.26	56.3
SS-175	"	0.40	0.19	46.8	0.21	53.2
SS-176	"	0.45	0.21	47.1	0.24	52.9
SS-177	"	0.46	0.16	33.2	0.30	66.8
SS-178	"	0.74	0.38	51.2	0.36	48.8
SS-179	"	0.77	0.47	31.3	0.30	68.7
SS-180	"	0.70	0.35	50.5	0.35	49.5
SS-181	"	0.40	0.14	36.3	0.26	63.7
SS-182	"	0.45	0.18	40.2	0.27	59.8
SS-183	"	0.60	0.31	50.4	0.29	49.6
SS-184	"	0.75	0.31	40.9	0.34	59.1
SS-185	"	1.15	0.49	42.6	0.56	57.4

Table 1.: Analyses of suspended particulate matter (cont'd)

SAMPLE NO.	DEPTH (m)	TSM[1] (mg/l)	NCM[2] (mg/l)	NCM %	CM[3] (mg/l)	CM %
BS-1	150	0.41	0.06	14.5	0.35	85.5
BS-2	210	0.54	0.33	60.8	0.21	39.2
BS-3	230	0.39	0.21	55.0	0.17	45.0
BS-4	148	1.51	1.08	67.5	0.42	32.5
BS-5	124	1.97	1.54	78.0	0.43	21.9
BS-6 *	108	214.34C	187.45	87.0	27.85	13.0
BS-7	110	2.19	1.67	76.0	0.42	24.0
BS-8	123	2.35	1.67	70.9	0.68	29.1
BS-9	159	2.31	1.65	71.3	0.66	20.7
BS-10	300	0.50	0.33	65.0	0.17	35.0
BS-11	159	0.71	0.53	73.0	0.18	27.0
BS-12 *	145	376.79C	341.60	90.0	35.10	10.0
BS-13	118	2.35	1.66	70.6	0.69	29.4
BS-14	98	3.79	3.06	81.0	0.73	19.0
BS-15	106	3.73	2.94	78.9	0.78	21.1
BS-16	125	3.82	2.93	76.5	0.89	23.5
BS-17 *	140	59.64C	51.96	87.1	7.68	12.8
BS-18	147	18.32	16.33	89.1	1.99	10.9
BS-19	378	0.74	0.48	64.0	0.26	36.0
BS-20	140	1.75	1.37	78.0	0.38	22.0
BS-21	133	3.47	2.77	80.0	0.70	20.0
BS-22	111	2.70	1.65	61.0	1.05	39.0
BS-23	117	2.20	-	-	-	-
BS-24	151	0.77	0.49	63.0	0.28	37.0
BS-25	140	0.70	0.32	45.0	0.38	55.0
BS-26	147	0.62	0.43	69.6	0.19	30.4
BS-27	137	2.02	1.64	73.4	0.37	26.6
BS-28	128	3.38	2.66	78.7	0.72	21.3
BS-29	117	2.49	1.86	74.0	0.63	26.0
BS-30	105	0.76	6.48	84.0	1.19	15.9
BS-31	120	1.09	2.08	83.0	1.01	17.0
BS-32	112	9.01	7.76	86.0	1.25	14.0
BS-33	145	0.64	0.37	56.6	0.27	43.4
BS-34	119	2.38	1.86	78.0	0.52	22.0
BS-35	109	2.16	1.56	72.4	0.60	27.6
BS-36	117	3.31	2.89	78.0	0.41	22.0
BS-37	134	0.56	0.40	71.2	0.16	29.8
BS-38	142	0.97	0.68	69.8	0.29	30.2
BS-39	165	0.56	0.24	43.2	0.32	56.7
BS-40	122	1.97	1.21	61.2	0.76	38.8
BS-41	129	1.14	0.76	66.5	0.38	33.5
BS-42	136	0.74	0.44	59.4	0.30	40.6

[1] Concentration of total suspended matter in the sample.

[2] Concentration of non-combustible matter in the sample; this matter is assumed to be terrigenous particles and/or the non-combustible parts of organisms.

[3] Concentration of combustible matter in the sample; this matter is assumed to be the organic constituents of the total suspended sediment.

* C = contaminated sample.

TEXTURAL VARIATIONS AND COMPOSITION OF BOTTOM SEDIMENT

H. A. Karl, P. R. Carlson, J. Fischer, K. Johnson, and B. Lamb

In this section we present the available data from our analyses of sediment subsamples taken from gravity cores and grab samples. Subsamples were soaked in H_2O_2 solution to remove organic matter. The samples were then wet sieved at >63 µm to separate mud and sand fractions. If gravel (> 2 mm) was present, it was separated from sand by dry sieving. The percentage of biogenic material in the sand fraction was determined by counting 500 grains under low power magnification.

Sediment sampling stations are plotted in Figure 10. Sediment types are derived from qualitative visual descriptions of surface samples. We consider bulk subsamples from grab samples and discrete subsamples from the upper 35 cm of gravity cores as surface samples. Figure 11 is a contour map of the sand/mud ratios of surface samples. Figures 10 and 11 show two trends. Whereas silts generally characterize the shelf and slope, there is a zone of coarser sediment at the shelf break, on the upper slope, and in the heads of submarine canyons. Also, surficial sediment on the shelf is slightly coarser in the southeastern part of the area than elsehwere. The percentages of various components identified in the sand fraction are shown in Table 2. The small amounts of volcanic glass may be important stratigraphic markers are discussed by Carlson and others elsewhere in this volume.

Characteristics of gravity cores collected along a shelf-to-slope profile are shown in Figure 12. The cores collected on the shelf are representative of many shelf cores in that there is very little variation in texture and structure down core. Cores collected within submarine canyons (see e.g., Core 37, Fig. 12) and deep-sea fan channels often contain lenses and laminae of sand and coarse silt.

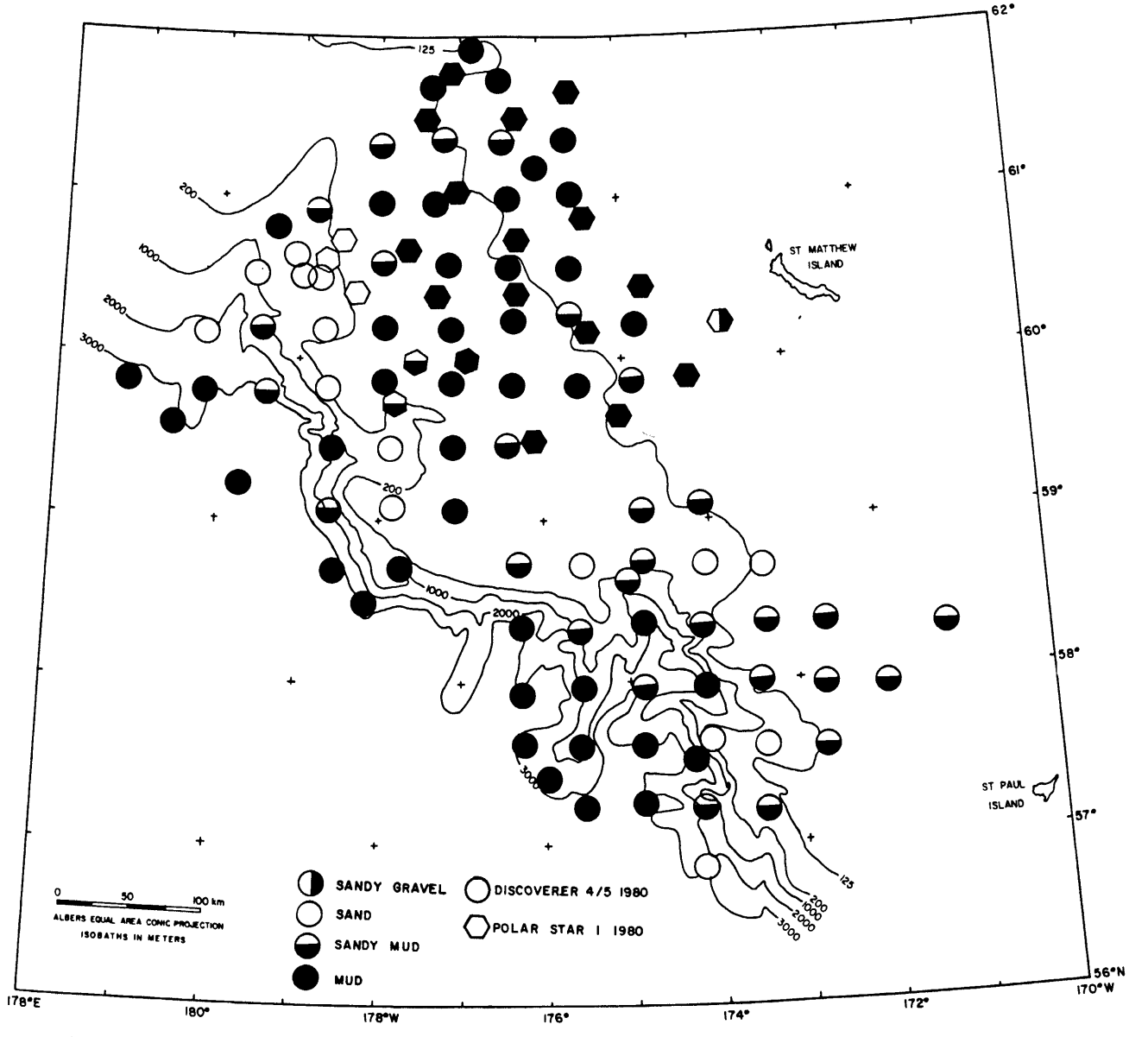

Figure 10. Preliminary map of sediment types in Navarin Basin province derived from visual inspection of core samples onboard ship.

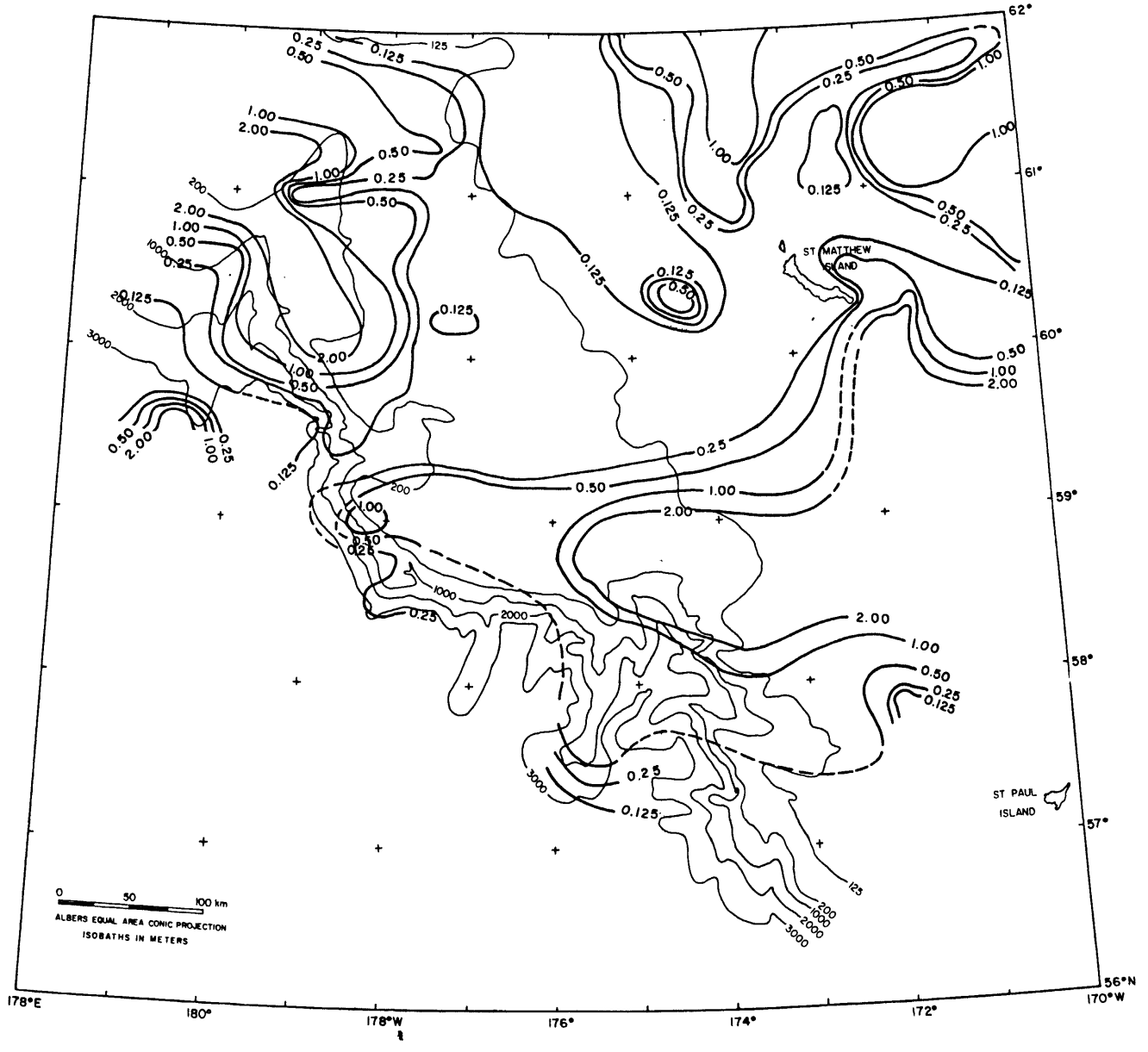

Figure 11. Areal distribution of sand-to-mud ratio for sediment.

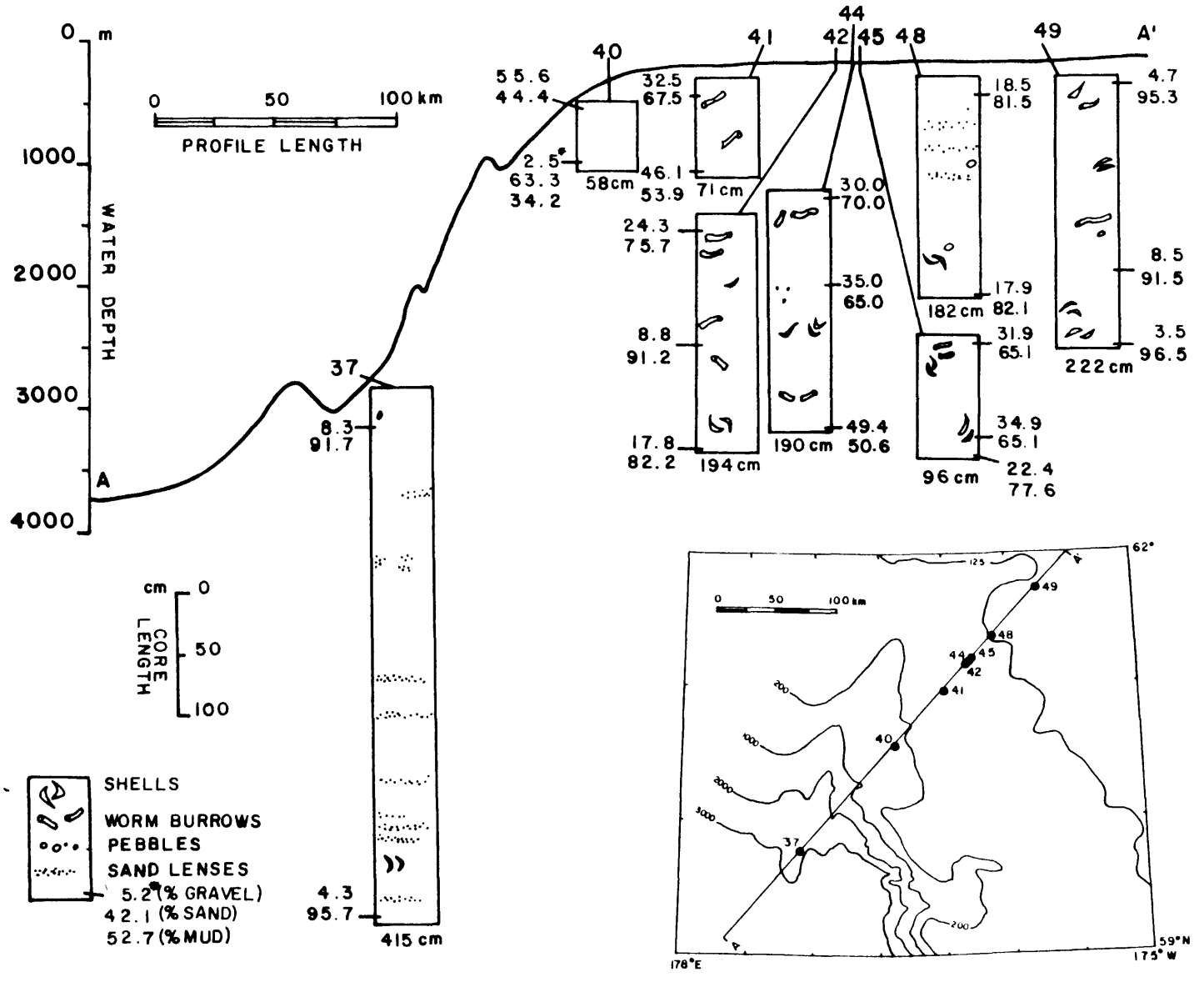

Figure 12. Sedimentary structures observed in gravity cores along bathymetric profile A-A'.

Table 2 Composition of sand fractions (values in percent).

Sample #	Core Interval (cm.)	Minerals and Rock Fragments	Vol. Glass	Diatoms	Rads	Misc.	Water Depth (M)
1		44.8	10.0	44.4	0.8	--	580
2*		96.6	2.8	0.2	0.4		533
4	5-7	96.6	3.0	TR	--	0.4	3,232
12	13-14	4.8	--	92.2	1.0	2.0	3,188
21		93.6	2.8	2.4	0.2	1.0	235
22	25-26	13.6	--	85.2	1.2		2,842
23	8-10	97.6	0.8	1.6	--	TR	110
35		95.2	1.4	3.2	0.2	--	868
38		94.0	1.8	2.2	1.0	TR	990
39		91.8	2.8	4.8	0.6	TR	229
40	5-7	96.4	1.2	1.0	1.2	0.2	230
41	12-13	90.0	--	10.0	TR	--	148
42	12-14	83.4	TR	16.8	--	TR	141
43	5-7	95.2	1.4	3.4	TR	TR	148
44	8-10	93.2	TR	6.8		TR	138
45	8-10	94.8	1.4	3.0	0.4	0.4	137
46	12-14	99.3	--	0.8	TR	--	134
47	5-7	94.8	1.6	3.6	--	--	134
48	11-12	90.2	5.2	4.2	0.4	--	124
60	27-29	62.2	5.0	32.0	--	0.2	106
62	5-7	91.0	2.6	6.4	--	--	125
63	8-10	86.2	0.2	12.6	1.0	--	150
64	9-10	74.8	2.2	22.4	0.6	--	147
65	5-7	19.8	2.0	76.2	1.2	0.8	1,609

Table 2. Composition of sand fractions (values in percent). cont'd

Sample #	Interval (cm.)	Minerals and Rock Fragments	Vol. Glass	Diatoms	Rads	Misc.	Water Depth (M)
75	5-7	23.6	2.0	74.0	0.4	TR	951
77	5-7	89.8	2.8	6.6	0.6	0.2	147
79	11-12	81.2	1.8	16.4	0.2	0.4	136
80	10-11	90.8	0.8	7.8	--	--	128
83	7-10	88.8	1.6	9.6	--	--	105
84	3-4	59.2	0.8	39.6	0.4	--	119
96	9-11	88.0	1.6	10.2	0.2	TR	116
98	5-7	95.2	0.8	2.8	--	1.2	1,610
101	40-42	6.8	0.2	91.8	1.2	--	2,155
102	62-64	83.0	2.4	13.4	TR	0.8	2,960
110		96.0	1.6	2.2	0.2	--	164

*Samples with no values for core interval are grab samples.

CLAY MINERAL DISTRIBUTION IN NAVARIN BASIN, BERING SEA

Kenneth A. Johnson

INTRODUCTION

Previous analyses of clay minerals of Bering Sea sediment are predominantly restricted to the southern reaches of the sea, Hein and others (1976), and Hein and Scholl (1978) reported on clay mineralogical analyses of D.S.D.P. cores in the southern Bering Sea and northern Pacific Ocean. Gardner and others (1980) mapped the distribution of clay minerals in surface sediments in the St. George Basin region just southeast of the Pribilof Islands. This study discusses the distribution of clay minerals in sediments of the Navarin Basin province.

Acknowledgements

Progress of this study was greatly enhanced by discussion with James R. Hein. I would also like to thank Carol Madison and J. Mark Yeats for their assistance during the course of the X-ray work.

METHODS

Subsamples from 58 cores were analyzed and relative percentages of illite, chlorite, smectite and kaolinite were determined (Table 3). Twenty-three of these samples were from near surface (defined as within 35 cm of top of core) sediments. The remainder of samples ranged from 37 to 513 cm in depth. Generally only two samples per core were analyzed, one from the top and bottom of each core. The exception is in core 26 where eight samples were collected from different colored units separated by distinct horizons.

Samples were first treated with equal parts of hydrogen peroxide and Morgan's solution (sodium acetate plus glacial acetic acid diluted with distilled water). Clays were dispersed with a 2% sodium carbonate solution before isolating the less than two micron fraction by centrifugation. This size fraction was saturated with a 1 M $MgCl_2$ solution and subsequently washed twice with distilled water to remove excess salts. Analyses were run on a Picker Integrated high angle diffractometer using nickel filtered copper K radiation at 34 kV and 16 mA. Slides were prepared using the smear technique (Gibbs, 1968) and X-rayed from 3-14° 2θ at 1° per minute. Slides were then glycolated at 65°C for 1 hour and run again at 1° per minute from 3-14° 2θ, and also from 24-26° 2θ at slow scan (1/4° per minute) to distinguish kaolinite and chlorite (Biscaye, 1964).

Peak areas were measured using an electronic planimeter. These values were then multiplied by Biscaye's (1965) weighting factors (4 x 10Å illite peak, 2 x 7Å chlorite peak and 1 x 17Å smectite peak). Relative percentages were calculated by dividing the weighted area of each peak by the total of all three weighted peaks and multiplying by 100. Only clay mineral groups were considered in this study. All minerals whose d-spacing expands to 17Å upon glycolation are called smectite. Kaolinite and chlorite were distinguished by

their respective second -order (3.58Å) and fourth-order (3.54Å) basal diffraction peaks. Values of kaolinite + chlorite are also presented because this analytical method does not always provide clear peak distinction (Martin Vivaldi and Gallego, 1961). Random mixed layering of smectite and illite was seen in all samples. Percentages of expandable layers in these mixed-layer minerals were determined from the charts of Perry and Hower (1970) and Reynolds and Hower (1970).

RESULTS

The distribution of clay minerals in near-surface samples is shown in Figure 13. Areal distribution of smectite was plotted and contoured with a 5% contour interval (Fig. 14). Distribution of other clay minerals did not show any significant trends. The surface distribution of smectite exhibits a band of relatively high concentration (>30%) across the middle of the study area, roughly parallel to the shelf break (Fig. 14). Within this band smectite seems to be slightly more concentrated at the northwest and southeast ends of the study area, roughly coincident with the heads of Navarinsky and Zhemchug canyons. No distinct trend is exhibited by kaolinite + chlorite distribution; however, their concentration also shows a subtle increase in the vicinity of the canyon heads. Conversely, illite distribution, shows a slight decrease in concentration around the canyon heads. No downcore trends could be reliably discerned, due to the irregular sampling intervals throughout this study. However, a downcore increase in chlorite was noticed in approximately 70% of the cores.

DISCUSSION

The average percentages of clay minerals in the Navarin region are similar to those determined by Gardner and others (1980) and Hein and others (1976) in other parts of the Bering Sea (Table 4).

Illite and chlorite are generally believed to have a detrital origin at high latitudes (Biscaye, 1965). Smectite however, while commonly associated with alteration of volcanic rocks, can have both detrital and authigenic origins (Hein and Scholl, 1978; Biscaye, 1965). Detrital smectite is usually not pure smectite, but most often some combination of random and/or ordered illite-smectite interlayers (Reynolds and Hower, 1970). Smectite with 50-70% expandable layers is associated with a detrital origin (Hein and Griggs, 1972) whereas authigenic smectite usually has expandable layers in the 90-100% range (Hein and others, 1979). The smectites from this study were found to contain 50-75% expandable layers, thus implying a detrital origin.

Source Area

The location of the study area, near the center of the Bering Sea, suggests the Navarin area could conceivably be supplied with clay material from many sources. The Yukon and Kuskokwim Rivers, with respective runoff totals of 185 and 45 km^3 per year (Lisitsyn, 1966) are likely sources of much Bering shelf sediment. Problems arise with this source in that modern Yukon and Kuskokwim suspended clay minerals include virtually no smectite (Hein, person. commun., 1981). The Anadyr River, emptying into the Bering Sea just north of the study area has a runoff of 41 km^3 per year (Lisitsyn, 1966). Lisitsyn describes a Cenozoic effusive terrain at the mouth of the Anadyr, that could also supply sediment to the area. The Aleutian island chain also provides a source of volcanic detritus. The smectite distribution throughout the Bering Sea is described by Lisitsyn (1966, p. 57) as being " ... very nonuniform. Its content being very low in the north of the sea, whereas it is the most widespread mineral of the clay fraction in the south." Gardner and others (1980) also note that the highest percentages of smectite occur closest to the Aleutians, but a uniform decrease in smectite concentration away from the Aleutians is not proposed. Comparison of mean smectite percentage between Navarin and southern Bering shelf sediments also agrees with a general decrease in smectite with distance from the Aleutians; however, the distribution determined in this study also precludes a simple trend throughout the Bering Sea.

The Navarin region is one of the least studied and hence hydrographically unknown areas in the Bering Sea. Hughes and others (1974) give a summary of surface current studies that generally show northward flow across this part of the shelf, ultimately passing through the Bering Strait into the Chukchi Sea. However, one must be wary of only using surface currents in discussing clay distribution because bottom currents potentially play the most important role in determining ultimate sites of deposition. Kinder others (1975) and Kinder and Schumacher (1980) propose a hydrographic regime that suggests a source area to the south. Their Bering Slope Current supports the additional possibility of the clay mineral distribution being the product of a reworked sediment source.

REFERENCES CITED

Biscaye, P. E., 1965, Mineralogy and sedimentation of Recent deep sea clay in the Atlantic Ocean and adjacent seas and oceans: Geol. Soc. Amer. Bull., v. 76, p. 803-831.

Biscaye, P. E.,1964, Distinction between kaolinite and chlorite in recent sediments by X-ray diffraction: Amer. Mineralogist, v. 49, p. 1281-1289.

Caroll, D., 1970, Clay minerals: A guide to their X-ray identification: Geol. Soc. Amer. Spec. Paper 126; 80p.

Favorite, F., 1974, Flow into the Bering Sea through Aleutian island passes: in Oceanography of the Bering Sea, D. W. Hood and E. J. Kelley, eds., Institute of Marine Science, Univ. of Alaska, p. 3-37.

Gardner, J. V., Dean, W. E., and Vallier, T. L., 1980, Sedimentology and geochemistry of surface sediments, outer continental shelf, southern Bering Sea: Marine Geology, v. 35, p. 299-329.

Gibbs, R. J., 1968, Clay mineral mounting techniques for X-ray diffraction analysis: A Discussion, Journ. Sed. Pet. v. 38, p. 242-244.

Gibbs, R. J.,1965, Error due to segregation in quantitative clay mineral X-ray diffraction mounting techniques: Amer. Mineralogist, v. 50, p. 741-751.

Griffin, J. and Goldberg, E. D., 1963, Clay mineral distributions in the Pacific Ocean: in The Sea, M. N. Hill, ed., V. III, p. 728-741.

Hein, J. R., Ross, C. R., and Alexander, E. A., 1979a, Mineralogy and diagenesis of surface sediments from D.O.M.E.S. areas A, B, and C: in Marine Geology and Oceanography of the Pacific manganese nodule province, J. L. Bischoff and D. Z. Piper eds., Plenum Publishing Corp. p. 365-396.

Hein, J. R., Bouma, A. H., Hampton, M. A., and Ross, C. R., 1979b, Clay mineralogy, fine grained sediment dispersal, and inferred current patterns, Lower Cook Inlet and Kodiak shelf Alaska; Sedimentary Geol. v. 24, p. 291-306.

Hein, J. R., Yeh H-W, and Alexander, E. A., 1979c, Origin of iron-rich montmorillonite from the manganese nodule belt of the north equatorial Pacific: Clay and Clay Minerals, v. 27, p. 185-194.

Hein, J. R. and Scholl, D. W., 1978, Diagenesis and distribution of late Cenozoic volcanic sediment in the Southern Bering Sea: Geol. Soc. Amer. Bull., v. 89, p. 197-210.

Hein, J. R., Scholl, D. W. and Miller, J., 1978, Episodes of Aleutian Ridge explosive volcanism: Science, v. 199, p. 137-141.

Hein, J. R., Scholl, D. W., and Gutmacher, C. E., 1976, Neogene clay minerals of the far northwest Pacific and southern Bering Sea: Sedimentatin and diagenesis: in A.I.D.E.A. Proceedings, International Clay conference, Mexico City, S. W.Bailey, ed. p. 71-80.

Hughes, F. W., Coachman, L. K., and Aagaard, K., 1974, Circulation, transport, and water exchange in the western Bering Sea: in Oceanography of the Bering Sea, D. W. Hood and E. J. Kelley eds., Inst. of Marine Sciences, Univ. of Alaska, p. 59-98.

Johns, W. D., Grim, R. E., and Bradley, W. F., 1954, Quantitative estimations of clay minerals by diffraction methods: Journ. Sed. Pet. v. 24, p. 242-251.

Kinder, T. H. and Schumacher, J. D., 1980, Circulation over the continental shelf of the southeastern Bering Sea, in The Bering Sea shelf, oceanography and Resources, D. W. Hood, ed., Dept. of Commerce, N.O.A.A.

Kinder, T. H., Coachman, L. K. and Galt, J. A., 1975, The Bering slope current system: Journ. of Physical Oceanog., v. 5, p. 231-244.

Knebel, H. J., 1972, Holocene Sedimentary framework of the east-central Bering Sea continental shelf, Ph.D. Thesis, Univ. of Washington, Seattle, 186 p.

Lisitsyn, A. P., 1966, Recent Sedimentation in the Bering Sea (in Russian): Inst. Okeanol. Akad. Nauk U.S.S.R., (Translated by Israel Program for Scientific Translations, available from U. S. Dept. Commerce, Clearinghouse for Fed. Sci. and Tech. Info., 1969), 614 p.

Martin Vivaldi, J. L. and Gallego, M., 1961, Some problems in the identifications of clay minerals by X-ray diffraction. 1. Chlorite-aolinite mixtures: Clay Minerals Bull. v. 4, p. 288-292.

Naidu, A. S., Burrell, D. C. and Hood, D. W., 1971, Clay mineral composition and geologic significance of some Beaufort Sea sediments: Journ. Sed. Pet. v. 41, p. 691-694.

Perry, E. and Hower, J., 1970, Burial and diagenesis in Gulf Coast pelitic sediments: Clays and clay minerals, v. 18, p. 165-177.

Pierce, J. W. and Siegel, F. R., 1969, Quantification in clay mineral studies of sediments and sedimentary rocks: Journ. Sed. Pet., v. 39, p. 187-193.

Reynolds, R. C. and Hower, J., 1970, The nature of interlayering in mixed layer illite montmorillonite, Clays and clay minerals, v. 18, p. 25-36.

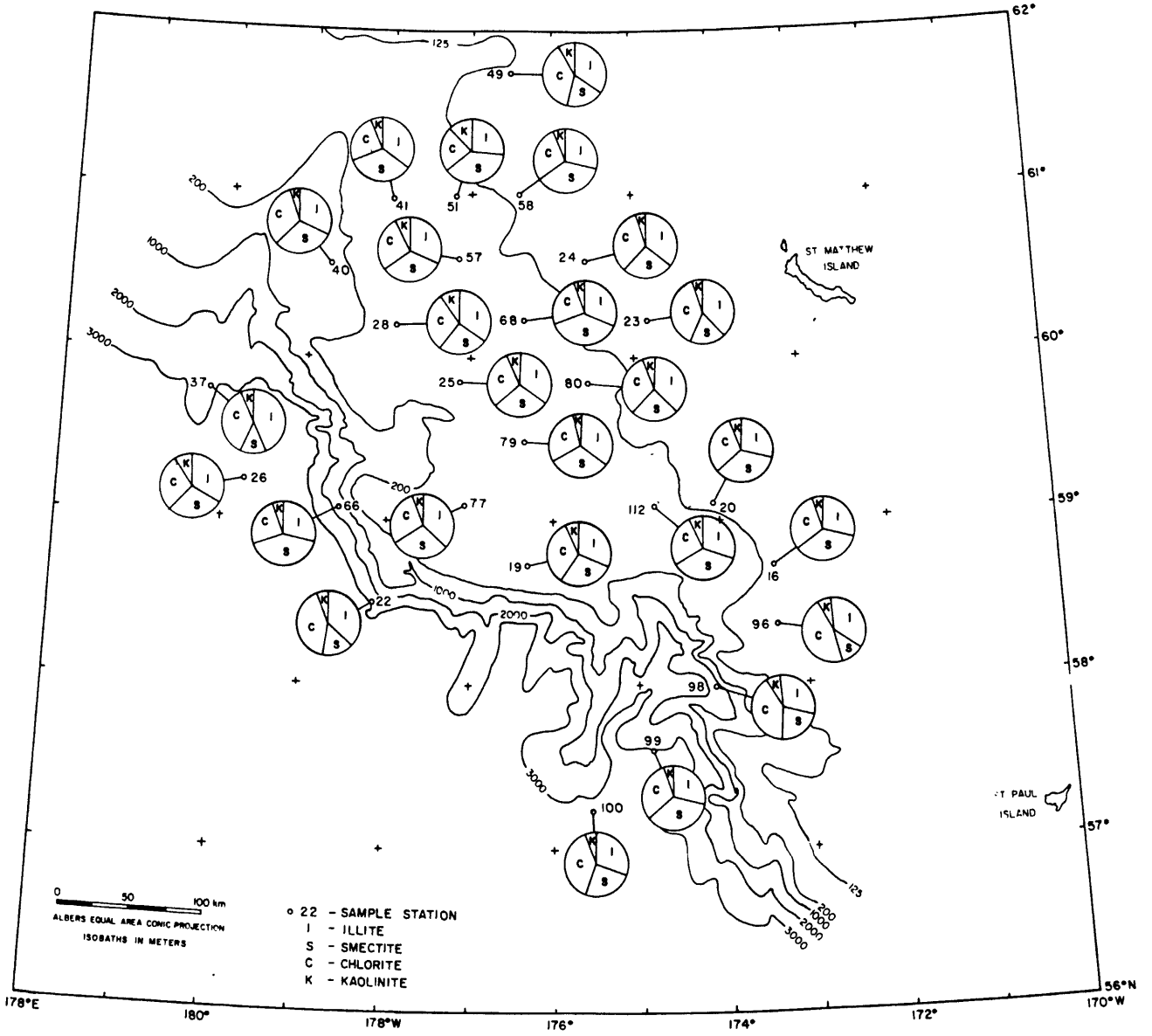

Figure 13. Distribution of relative percentages of clay minerals in surface sediments from Navarin Basin province.

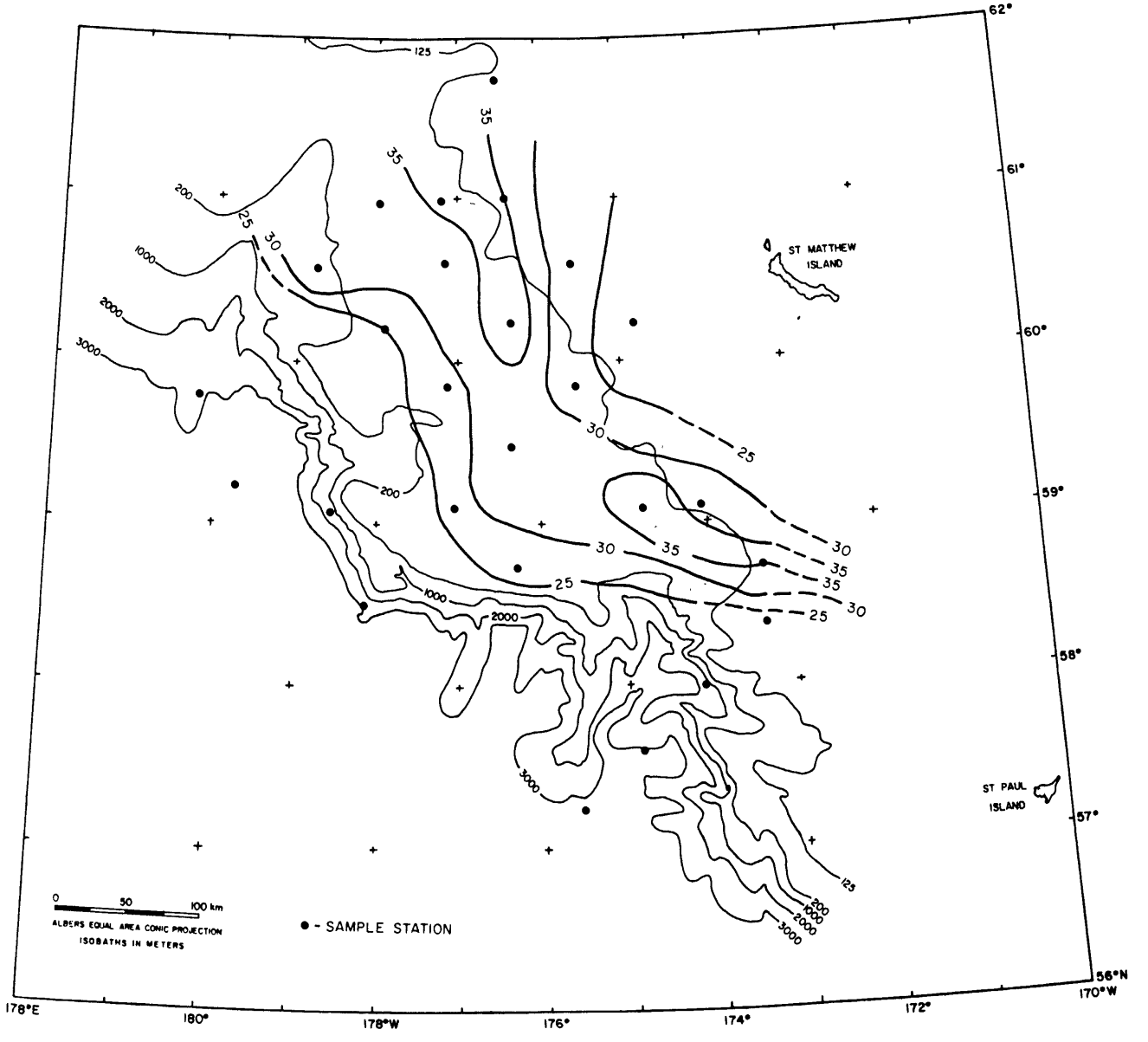

Figure 14. Contour map of relative percentages of smectite in surface sediment. Contour internal 5%.

Table 3. Relative percentages of clay minerals

Core No.	Depth Interval (cm)	Illite	Smectite	Chlorite	Kaolinite	Kaolinite & Chlorite
16G	10-12	29	35	31	5	36
	67-69	29	33	31	7	38
19G	9-11	31	28	34	7	41
	31-32	31	26	35	8	43
20G	10-12	28	34	32	6	38
	94-96	28	29	33	10	43
22G	30-32	36	16	42	6	48
	503-513	41	22	31	6	37
23G	8-10	38	19	38	6	43
	140-142	36	17	41	6	47
24G	10-12	35	27	33	5	38
	94-96	30	34	32	4	36
25G	12-13	34	28	31	7	38
	178-180	36	28	30	6	36
26G	22-24	33	29	29	9	38
	214-216	31	37	25	7	32
	225-230	32	38	24	6	30
	231-232	34	28	31	7	38
	255-260	36	26	31	7	38
	275-280	30	33	29	8	37
	295-300	31	28	34	7	41
	348-350	30	33	29	8	37
28G	12-14	35	25	30	10	40
	70-77	35	25	31	9	40
37G	35-37	42	14	38	6	44
	441	34	16	41	9	50
40G	10-12	32	31	32	5	37
	58	34	31	29	6	35
41G	11-12	34	34	26	6	32
	81	43	12	35	10	45
49G	12-14	33	20	39	8	47
	232	32	23	39	6	45
51G	15-17	27	37	29	7	36
	217	33	29	32	6	38

Table 3. Relative percentages of clay minerals (cont'd)

Core No.	Depth Interval (cm)	Illite	Smectite	Chlorite	Kaolinite	Kaolinite & Chlorite
57G	10-12	31	33	29	7	36
	83	35	30	26	9	35
58G	15-17	29	35	30	6	36
	231	31	32	30	9	39
66G	10-12	30	40	25	6	31
	531	34	28	32	6	38
68G	43-45	32	37	25	6	31
	159	29	35	30	6	36
77G	10-12	37	28	30	5	35
	54	42	28	25	5	30
79G	12-13	34	32	30	4	34
	111	30	34	30	6	36
80G	8-10	36	26	32	6	38
	211	34	26	34	6	40
96G	5-7	34	12	48	6	54
	58-61	33	15	45	7	52
98G	5-7	29	23	41	7	48
	171	36	22	37	5	42
99G	57-58	28	36	32	24	36
	408-431	24	31	40	5	45
100G	24-26	31	25	39	5	44
	382	31	24	41	4	45
112G	6-8	30	36	27	7	34
	74	30	34	28	8	36

Table 4. Comparison of relative percentages of clay minerals from several parts of the Bering Sea.

Mineral	Minimum	Maximum	Mean	Standard deviation
This study				
Smectite	12	40	28.0	6.9
Illite	24	43	32.8	3.8
Kaolinite	4	10	6.6	1.5
Chlorite	24	48	32.6	5.3
Kaolinite + Chlorite	30	54	39.2	5.4
Gardner and others, 1980				
Smectite	13.0	57.5	31.2	9.4
Illite	17.0	47.0	29.8	6.9
Kaolinite	0	11.8	6.0	3.5
Chlorite	24.3	44.3	33.2	5.6
Hein and others, 1976				
Site 184				
Smectite	-	-	31	4
Illite	-	-	30	4
Kaolinite	-	-	10	3
Chlorite	-	-	29	4
Kaolinite & Chlorite	-	-	38	5
Site 185				
Smectite	-	-	32	10
Illite	-	-	30	7
Kaolinite	-	-	7	2
Chlorite	-	-	34	2
Kaolinite + Chlorite	-	-	40	2
Site 188				
Smectite	-	-	32	5
Illite	-	-	26	2
Kaolinite	-	-	8	1
Chlorite	-	-	37	5
Kaolinite + Chlorite	-	-	42	4

CARBON CONTENTS OF NAVARIN BASIN SEDIMENTS

Jeffrey M. Fischer

INTRODUCTION

Carbon plays an important role in sedimentation, even though it is a relatively small component of the sediments. The relation between organic carbon content and depositional environment has long been established (Dow, 1975). Factors such as basin morphology, grain fabric, sedimentation rates, and source areas all affect carbon distribution. Organic matter also has a role in diagenetic processes that affect mineralogy and chemistry of sediments (Lisitsyn, 1972), as well as its bearing as a possible petroleum source. The purpose of this chapter is to discuss the distribution of organic and carbonate carbon in the Navarin Basin province.

Previous work

Various studies of carbon contents for the entire Bering Sea area have been conducted. Gershanovich (1962) and Lisitsyn (1966) discussed variations in carbonate and organic carbon based mainly on data from the western Bering Sea. Carbonate values were universally low, whereas organic carbon showed relatively high concentrations in coastal areas and at the base of the continental slope. Studies of the distribution of carbon in the sediments northeast and southeast of Navarin Basin were conducted by Knebel (1972) and Gardner and others (1980). Both studies showed sediments almost devoid of carbonates; the largest concentrations of organic carbon occurred in the fine-grained sediments.

Methods

Two centimeter subsamples were taken within the top 35 centimeters of 14 of the cores (considered a near surface sample for this study). Each succeeding 100 centimeters length of core was subsampled; subsamples also were taken from the core catchers. Samples were freeze dried, ground to a fine powder, and stored in a dessicator. Analyses for carbonate and organic carbon were done at a commercial laboratory by the direct organic carbon-wet oxidation method (Bush, 1970). Knebel (1972) data were determined on a LECO induction furnace and carbon determinator using the Walkley-Black analysis. Lisitsyn (1966) does not discuss analytical methods.

RESULTS

Values of carbonate and organic carbon from the 52 sample sites are shown as weight percent in table 5. Surface distribution of carbonate is uniformly low and shows little variation (0.04% to 0.22%) throughout the Navarin Basin area (Fig. 15). The total range in carbonate values is small from 0.03% to 0.57%. Some changes were observed down a few cores (Fig. 16); however, in the majority of cores the carbonate percentages were uniformly low.

Organic carbon values in contrast with carbonate values showed greater variance, averaging 0.83% for the entire area and ranging from 0.26% to 1.56%. Figure 17 shows the distribution of organic carbon in surface sediments for the Navarin Basin. Salient features include high organic carbon values on the northwest continental shelf and low values on the southeast continental shelf. In addition, an arcuate band of low percentages of organic carbon content exists parallel to the continental slope at depths of less than 1600 m. Some of the lowest organic carbon values are found at the heads of the largest submarine canyons (Navarinsky and Zhemchug). Comparisons of shelf and slope areas (Table 6) shows that organic carbon in Navarin Basin is concentrated at the base of the continental slope and on the continental shelf west of St. Matthew Island (Fig. 17).

Variation of organic carbon with depth in the cores can be seen in figures 16 and 18. There is a general trend towards lower organic content with depth in those cores collected in water depths greater than 1600 m; however, there are no consistent trends with depth in cores collected on the shelf and upper slope.

DISCUSSION

The consistently low carbonate values show the relative lack of calcareous organisms in the Navarin Basin area. Similar results were obtained to the southeast of the study area by Gardner and others (1980), and to the north of the study area by Knebel (1972). Sporadic increases in carbonate, both at the surface and down core, probably represents the concentrated remains of calcareous organisms.

The primary source of carbon in the Bering Sea is organic carbon (Lisitsyn, 1966). Two sources for this organic carbon are terrestrial and marine. Terrestrial organics are carried to sea via rivers and marine phytoplankton produce organics at sea.

Once organics are in the sea they are influenced by several factors, the most important of which are distance of transport, rate of sedimentation, and grain size. Organic particles are destroyed in transport over large distances; the more prolonged their stay in the water, the higher their degree of decomposition (Lisitsyn, 1959). One exception worth noting is the relatively stable bitumens; however Bordovskiy (1964) has estimated their concentration to be 0.05% or less for organic carbons in the Bering Sea. The rate of sedimentation also affects the concentration of organic carbon; dissolution of organic matter is related to its duration of exposure, so the sooner the organic matter is buried the slower the rate of decay (Lisitsyn, 1972). Finally, in fine grained sediments organic matter is absorbed, and thus preserved, by clays. This negative correlation between organic carbon and grain size has been observed by many scientists (eg., Trask, 1932; Gardner and others, 1980).

The contribution of organic matter from the three largest rivers that enter the Bering Sea, the Anadyr, Kuskokwim, and Yukon, is estimated to be less than 1% of the total organic matter in the Bering Sea (Lisitsyn, 1966).

In addition, these rivers are over 400 km away; these two factors seem to preclude terrestrial sources as significant contributors of organics to the study area.

Most organic carbon in the Bering Sea probably is related to intense diatom blooms that occur in the spring (Lisitsyn, 1966). These blooms are closely related to ice retreat, supply of nutrients from upwelling, spring river runoff, and general turbidity of the seas due to spring storms (Lisitsyn, 1966). Diatoms are significant contributors to sediments at the base of the slope and some northwest shelf regions of the Navarin Basin study area (Karl and others, this report). Comparison of sediment composition to organic carbon distribution shows a postive correlation between areas of diatom concentration and areas of high organic carbon content.

Winnowing and redistribution of sediments by currents can play an important role in the distribution of organic carbon. Relatively low organic carbon values are associated with coarse sediments where currents have winnowed out the fine fractions that contain organic carbon (Gershanovich, 1962). Comparison of sand/mud ratios (Fig. 11, Karl and others, this report) and organic carbon (Fig. 17) shows that the negative correlation of organic carbon and grain size holds for the Navarin Basin province. Where currents predominate, as along the shelf break and at the heads of the submarine canyons, sand content increases with a concommitant reduction in organic carbon. Conversely at the base of the slope where slumped sediment accumulates, where currents are relatively weak, and where muds predominate, the organic carbon content is high. Depletion of organics at the top of the continental margin and accumulation of organics at its' base is normal for continental margins according to Bordovskiy (1965).

Variations of organic carbon percentages on the continental shelf, although not easily understood, are probably due to a variety of factors. The general patchiness may be due in part to differential consumption of the organic matter by the benthic fauna. Low values of organic carbon on the southeast shelf between St. Paul Island and St. Matthew Island (Fig. 17) are consistent with a coarser particle size that perhaps results from a more hydrodynamically active shelf. Alternately, the shelf west of St. Matthews Island has some of the highest organic carbon values found in this study. Correlation of organic carbon (Figs. 17) with particle size of sediments (Fig. 11; Karl and others, this report) shows that the high organic content is accompanied, as would be expected, by fine grained sediments. Both these pieces of evidence seem to indicate an area of little water movement. Indeed Muench and others (1976), have suggested just such an area. Sources for the organics could be diatom blooms transported across the shelf from upwelling along the continental margin. A seasonal cover of ice probably protects this area from the winnowing action of intense winter storms.

CONCLUSIONS

The data for the Navarin Basin province seem to indicate normal trends for an arctic continental margin with a somewhat anomalous area on the shelf west of St. Matthew Island. Carbonate contents are low and in most cases insignificant. Most organic carbon is probably supplied by diatoms and

deposited close to their source. Some of the highest organic carbon percentages were found in sediments from the base of the continental slope. Organic carbon is depleted at shallower depths along the slope. Grain size shows a negative correlation with organic carbon especially on the shelf. The fine grained sediments of the northwest shelf have a higher organic carbon content than the southeast shelf which has low organic carbon possibly due to fines having been removed by winnowing of currents.

REFERENCES CITED

Bordovskiy, O. K., 1965, Accumulation of organic matter in bottom sediments: Marine Geology, vol. 3, p. 33-82.

Bordovskiy, O. K., 1969, Organic matter of Recent sediments of the Caspian Sea: Oceanology, vol. 9, p. 799-807.

Bush, P. R., 1970, A rapid method for the determination of carbonate carbon and organic carbon: Chemical Geology, vol. 6, p. 59-62.

Dow, Wallace G. and Pearson, Daniel B., 1975, Organic matter in Gulf Coast Sediments: 7th Offshore Technology Conference, Houston, Tex., Paper Number OTC 2343.

Gardner, James V., Dean, Walter E., and Vallier, Tracy L., 1980, Sedimentology and geochemistry of surface sediments, outer continental shelf, southern Bering Sea: Marine Geology, v. 35, p. 299-329.

Gershenovich, D. E., 1962, New data on the recent deposits of the Bering Sea: All-Union Scientific Research Institute of Marine Fisheries and Oceanography - Proceedings Vol. XLVI, (Translated by Hulbert Verwey, 1963), p. 128-164.

Kinder, T. H., and Coachman, L. K., 1975, The Bering Slope Current System: Journal of Physical Oceanography, vol. 5, No. 2, p. 231-244.

Kinder, T. H., and Schumacher, J. D., in press, Circulation over the continental shelf of the southeastern Bering Sea: The Bering Sea shelf, oceanography and resources, D. W. Hood (Ed.), Dept. of Commerce, N.O.A.A.

Knebel, Harley J., 1972, Holocene sedimentary framework of the east-central Bering Sea Continental Shelf: Ph.D. Thesis, University of Washington, Seattle, 186 p.

Lisitsyn, A. P., 1959, Bottom sediments of the Bering Sea: in Bezrukov, P. L., (Ed.), Geographical description of the Bering Sea, (Translated by Israel Program for Scientific Translations, available from Office of Technical Services, U. S. Dept. of Commerce, 1964), 188 p.

Lisitsyn, A. P., 1966, Recent sedimentation in the Bering Sea (in Russian): Inst. Okeanol. Akad. Nauk U.S.S.R., (Translated by Israel Program for Scientific Translations, available from U. S. Dept. Commerce, Clearinghouse for Fed. Sci. and Tech. Info., 1969), 614 p.

Lisitsyn, A. P., 1972, Sedimentation in the world ocean: Society of Economic Paleontologists and Mineralogists-Special Publication No. 17, 171 p.

Muench, R. D., and Ahlnas, K., 1976, Ice movement and distribution in the Bering Sea from March to June 1974: Journal of Geophysical Research, vol. 81, No. 24, p. 4467-4476.

Trask, P. D., 1932, Origin and environments of source sediment of petroleum, Gulf Pub. Co., Houston, Tx., 323 p.

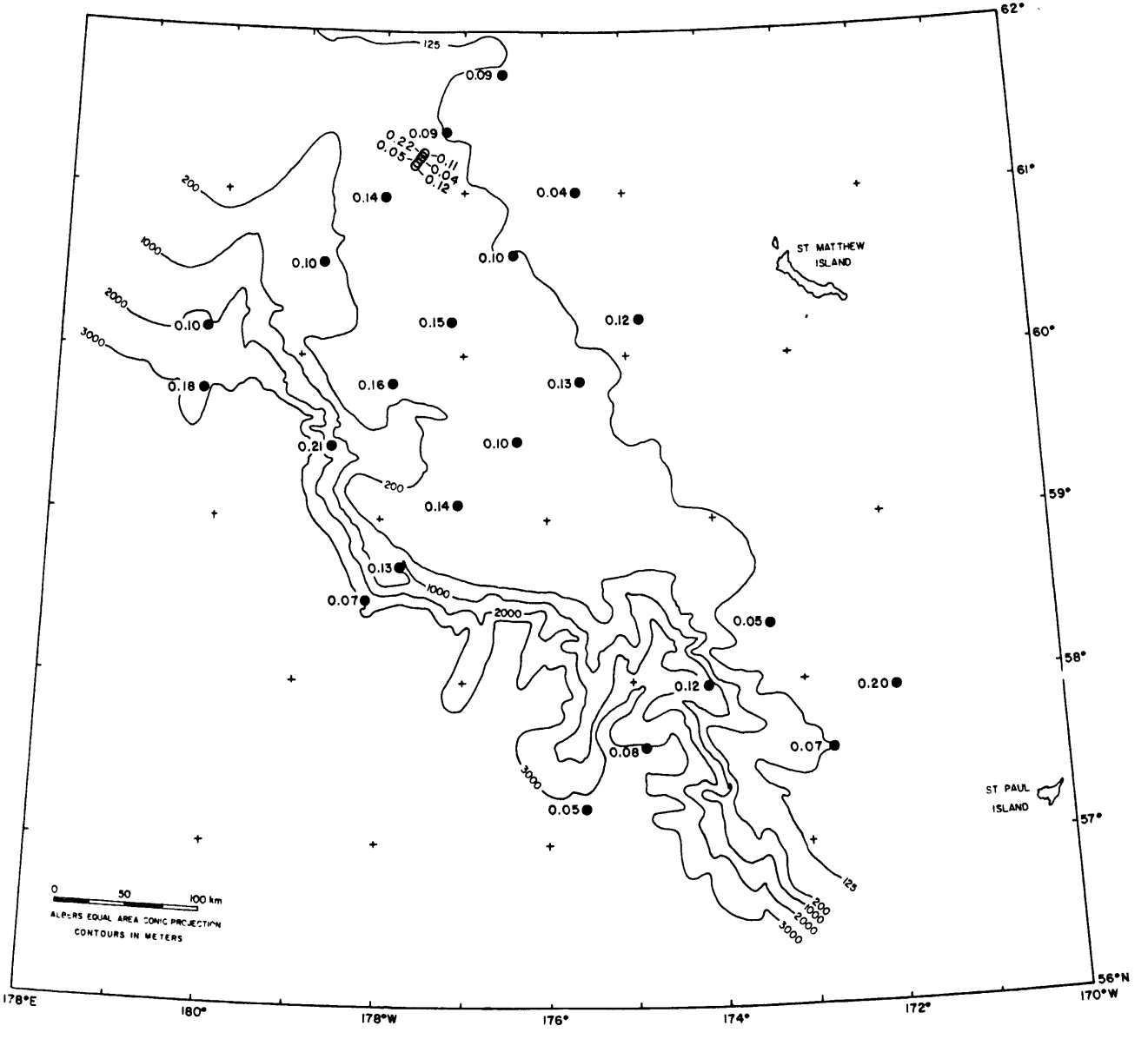

Figure 15. Surface distribution of carbonate carbon (weight percent).

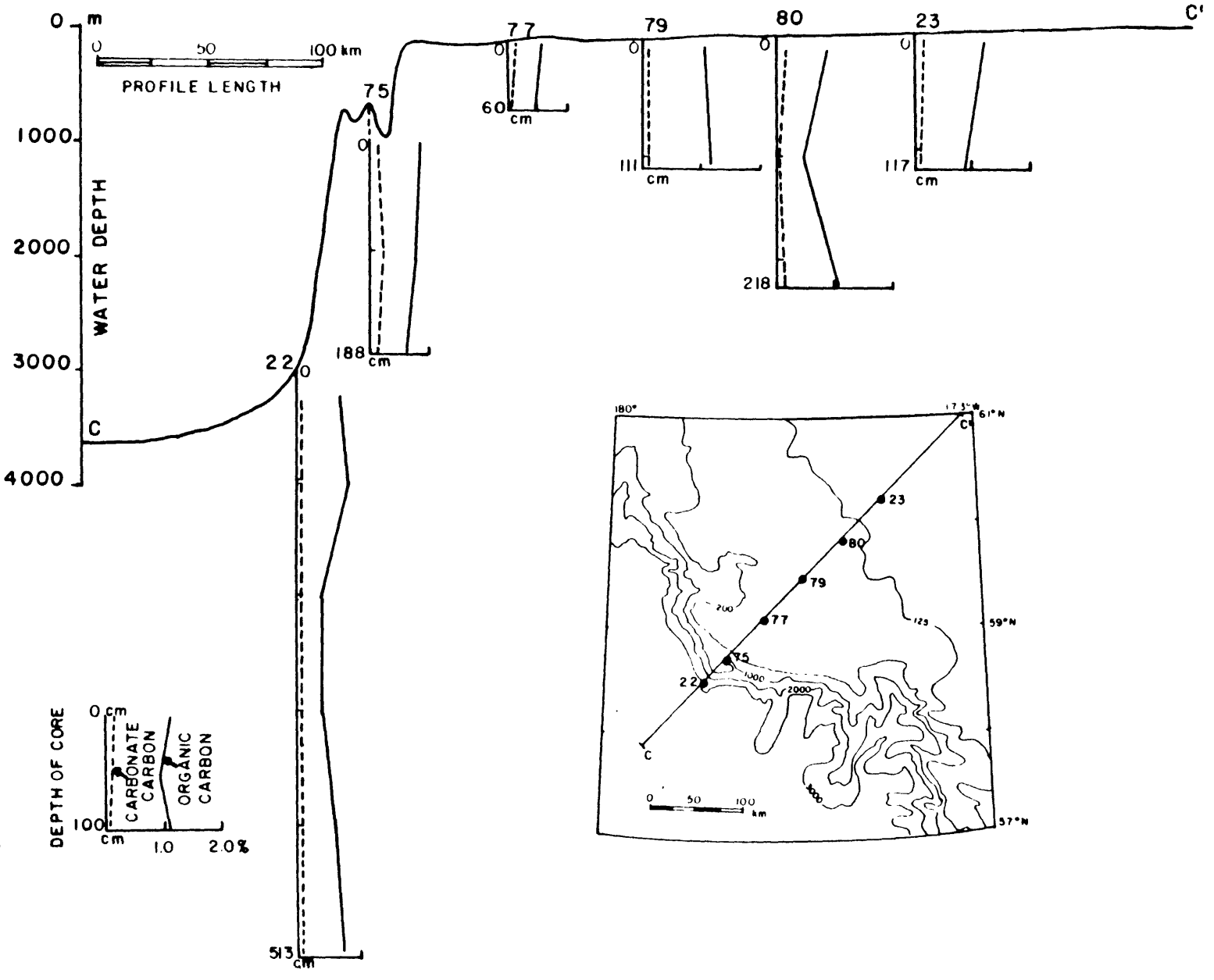

Figure 16. Down core variations of carbonate (dashed line) and organic carbon (solid line) across the Navarin Basin province.

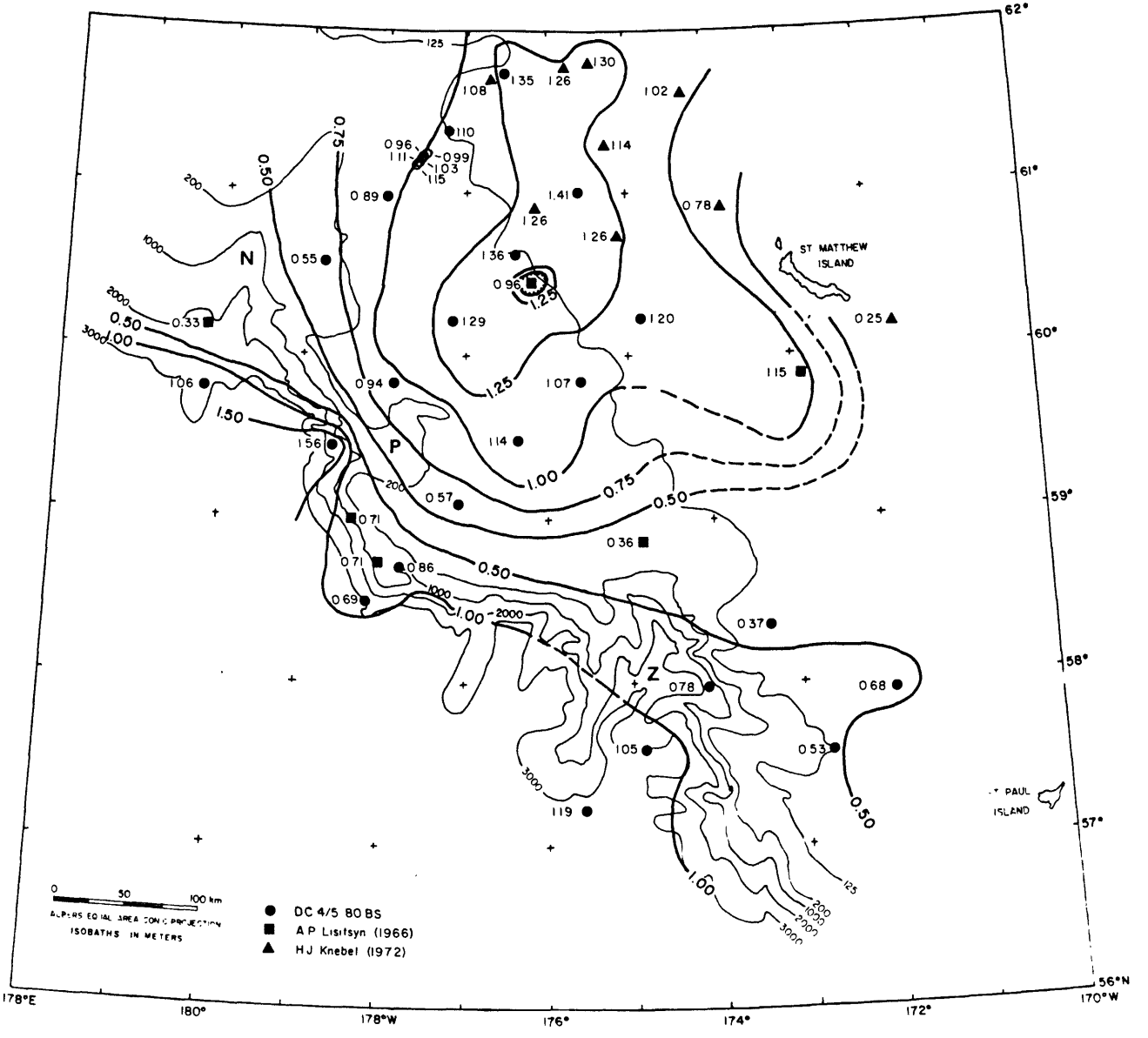

Figure 17. Contour map of weight percents of organic carbon in surface sediments from Navarin Basin province. Contour interval 0.25% on shelf and 0.50% on slope. Letters N, P, Z locate Navarinsky, Pervenets, and Zhemchug Canyons.

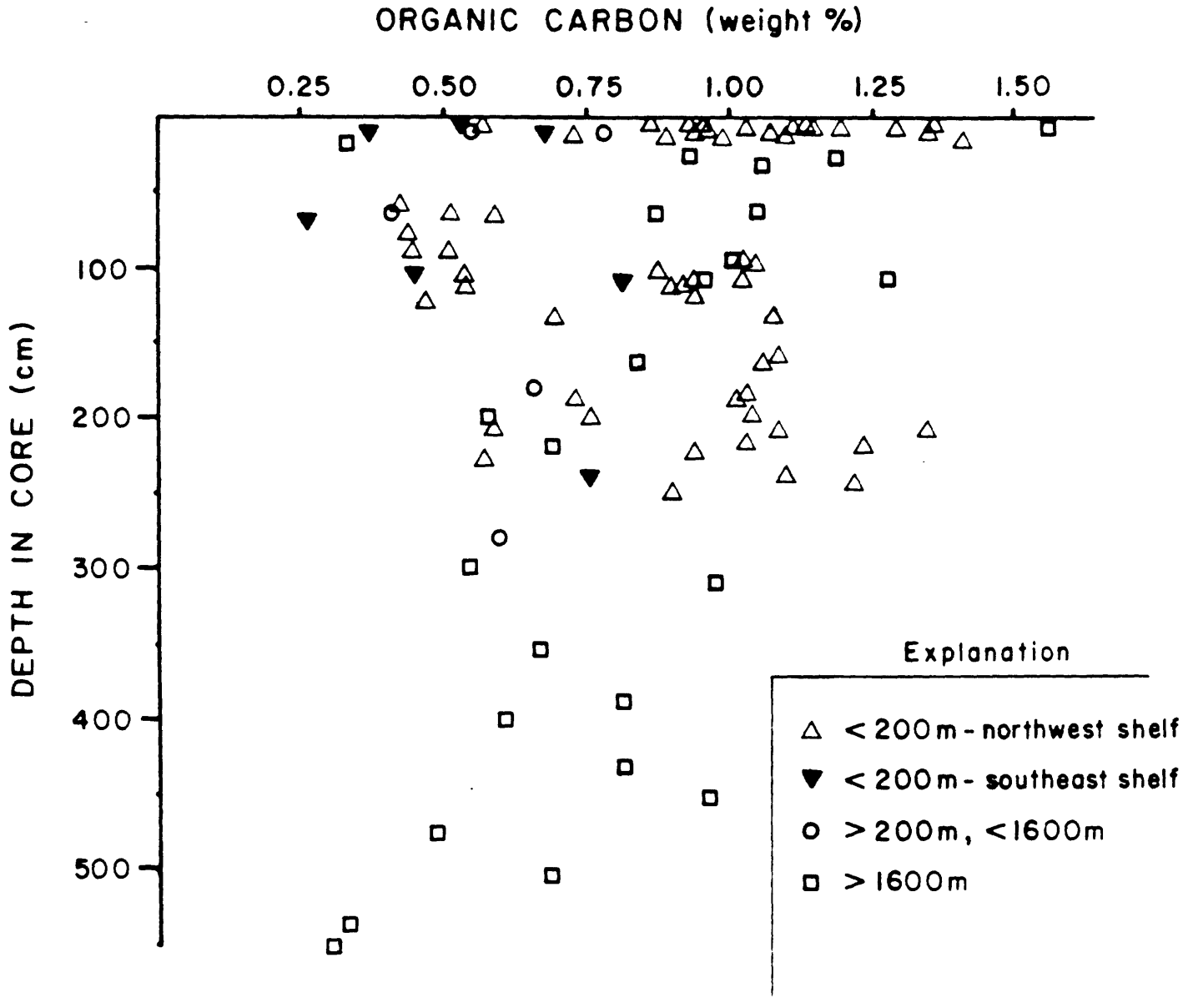

Figure 18. Variation in percent organic carbon with depth in core.

Table 5. Weight percents of organic carbon and carbonate carbon in Navarin Basin Province sediment.

DC 4/5 - 80BS cruise data

Core Number	Depth in core (cm)	Depth of Water (m)	Organic Carbon (%)	Carbonate Carbon (%)
22	28-30	2842	0.93	0.70
	98-100		1.01	0.06
	200-202		0.58	0.06
	300-302		0.55	0.07
	400-402		0.61	0.06
	503-513*		0.69	0.07
23	8-10	110	1.20	0.12
	115-117		0.90	0.06
28	225-227	150	0.94	0.28
32	13-15	150	0.73	0.11
	227-237		0.57	0.11
34	270-280*	210	0.60	0.08
36	18-20	1924	0.33	0.10
	66-68		0.87	0.18
	220-222		0.69	0.17
	354-356		0.67	0.22
	475-477		0.49	0.34
	535-537		0.34	0.38
	539-549*		0.31	0.25
37	35-37	2856	1.06	0.18
	110-112		0.96	0.12
	310-312		0.98	0.23
	441-450*		0.97	0.21
39	0-10**	229	0.44	0.13
40	10-12	230	0.55	0.10
	58-65*		0.41	0.14
41	14-15	148	0.89	0.14
	81-90*		0.51	0.17

* Core catcher
** Grab sample

Table 5. Weight percents of organic carbon and carbonate carbon in Navarin Basin Province sediment. (cont'd)

DC 4/5 - 80BS cruise Data

Core Number	Depth in core (cm)	Depth of Water (m)	Organic Carbon (%)	Carbonate Carbon (%
42	7-8	141	1.15	0.12
	97-98		1.03	0.03
	204-210*		1.09	0.13
43	5-7	148	1.11	0.05
	120-122		0.94	0.07
	246-256*		0.90	0.19
44	8-10	138	1.03	0.04
	112-114		0.94	0.15
	200-210*		0.59	0.02
45	8-10	137	0.96	0.22
	106-116*		0.54	0.14
46	14-15	134	0.99	0.11
	79-80		0.44	0.12
	127-137*	134	0.70	0.20
47	5-7		0.93	0.11
	84-94*		0.45	0.21
48	14-15	124	1.10	0.09
	192-202*		0.76	0.08
49	12-14	108	1.35	0.09
	160-162		1.09	0.13
	232-242*		1.10	0.13
60	17-19	106	1.41	0.04
	134-135		1.08	0.04
	165-167		1.06	0.57
	205-215*		1.35	0.08
61	240-250*	125	1.22	0.13
62	5-7	125	1.36	0.10
	100-102		1.05	0.13
	200-202		1.04	0.17
	214-224*		1.24	0.03

Table 5. Weight percents of organic carbon and carbonate carbon in Navarin Basin Province sediment (cont'd)

DC 4/5 - 80BS cruise Data

Core Number	Depth in core (cm)	Depth of Water (m)	Organic Carbon (%)	Carbonate Carbon (%)
63	8-10	150	1.29	0.15
	115-117		0.92	0.10
	184-194*		1.02	0.16
64	10-11	147	0.94	0.16
	99-109*		0.54	0.09
65	0-2		1.56	0.21
	110-112		1.28	0.14
74	178-188*	920	1.03	0.22
75	5-7		0.86	0.22
	105-107		0.88	0.22
	174-188*		0.73	0.15
76	60-70*	147	0.59	0.05
77	5-7	147	0.57	0.14
	54-64*		0.43	0.05
78	58-68*	147	0.51	0.11
79	5-6	136	1.14	0.10
	101-111*		1.03	0.10
80	11-13	128	1.07	0.13
	125-126		0.47	0.02
	211-221*		1.03	0.16
82	0-10**	105	0.95	0.11
83	12-15	105	0.68	0.20
	112-114		0.81	0.05
	235-241*		0.76	0.05
84	3-5	119	0.53	0.07
	97-107*		0.45	0.02
95	0-10	117	0.39	0.09
96	11-13	116	0.37	0.05
	67-73*		0.26	0.05
98	10-12	1610	0.78	0.12

Table 5. Weight percents of organic carbon and carbonate carbon in Navarin Basin Province sediment. (cont'd)

DC 4/5 - 80BS cruise data

Core Number	Depth in core (cm)	Depth of Water (m)	Organic Carbon (%)	Carbonate Carbon (%)
	171-182*		0.66	0.07
	165-167		0.84	0.06
	408-431*		0.82	0.08
100	28-30	3232	1.19	0.05
	382-392		0.82	0.11

* Core catcher
** Grab sample

Data from H. Knebel (1972)

Core Number	Depth in Core (cm)	Depth of Water (m)	Organic Carbon (%)	Carbonate Carbon (%)
42-140-GR297	0-20	--	1.0	0
42-144-GR301	0-20	--	1.14	0
42-147-GR308	0-20	--	1.08	0
42-149-PC313	0-17	--	1.26	0
42-150-GR314	0-20	--	1.30	0
51-011-GR030	0-20	--	1.26	0
51-109-GR208	0-20	--	0.25	0

Data from A. P. Lizitsyn (1966)

Li-1	Top	--	1.15	--
Li-2	Top	--	0.96	--
Li-3	Top	--	0.33	--
Li-4	Top	--	0.71	--
Li-5	Top	--	0.92	--

Table 6. Organic carbon averages from selected areas in Navarin Basin province (Ave. for DC 4/5-80BS samples)

Location	Number of samples	Organic Carbon (%)		
		Maximum	Minimum	Average
Northwest shelf	56	1.41	0.57	0.89
Southeast shelf	7	0.68	0.37	0.55
200 - 1600 m	5	0.78	0.41	0.60
1600 m	24	1.56	0.69	0.81

SEAFLOOR GEOLOGIC HAZARDS

Paul R. Carlson and Herman A. Karl

INTRODUCTION

Potential geologic hazards in the Navarin Basin province include faulting and earthquakes; seafloor instability due to submarine landslides, sediment transport and erosion, and subsidence or blowouts resulting from disturbance of gas-charged sediment; volcanic activity; and ice. Seafloor instability probably poses the greatest seafloor hazard. The purpose of this chapter is to present preliminary maps and brief discussions of the potential geologic hazards in the study area.

FAULTING AND SEISMICITY

The limited seismic coverage in the Navarin Basin province restricts the interpretation of length, orientation, and age of the faults. The distribution of the faults is shown in figure 19; however, the wide spacing of the tracklines ($\sim$ 30 km) makes correlation from line to line extremely uncertain. Thus, until more seismic lines are available, the only correlation that we have attempted is to connect those points that represent the bounding faults on a graben that is oriented in a northwest-southeast direction (Fig. 19). This graben is about 5 km wide and has been mapped over a distance of nearly 240 km. The maximum apparent relief of this structure (Fig. 20) is about 50 m, resulting from a series of offsets on each side of the down-thrown block. Throw of the individual faults varies from about 10 to 20 m. The graben is buried beneath 130 m of sediment over the depressed block and about 80 m of sediment over the adjacent flat-lying strata. The faults located on lines oriented perpendicular to the long axis of Navarin basin greatly outnumber those on lines that parallel the basin, suggesting a northwest-southeast trend of the faults. This trend is parallel to the basin and to the shelf-break. The majority of these faults occur on the continental slope and outer most shelf.

Many of the faults shown on Figure 19 are mapped from high-resolution seismic-reflection records that have resolution of 1-3 meters; however, none of the faults mapped to date show offset of the Holocene seafloor. Although the ages of the faults are unknown, C^{14} dates of sediment in the southern part of the area indicate accumulation rates of the upper six meters of sediment to be about 25 cm/10^3 yrs. (Askren, 1972). Therefore faults that reach to within three meters of the seafloor may cut sediment as young as 12,000 yrs. B.P. and are considered active.

According to Cooper and others (1976), Marlow and others (1976), and Scholl and others (1975), subduction of the Kula plate beneath the Bering Sea margin apparently ceased in late Mesozoic or early Tertiary and subduction of the Pacific plate shifted to the Aleutian Trench. This transfer tectonically deactivated the Bering Sea margin. The lack of modern seismicity is readily seen on the maps of Alaska earthquake epicenters published by Meyers (1976).

Only six earthquakes have been reported from the Navarin Basin province for the time period prior to 1974, and all were less than magnitude six. These data may be somewhat misleading because of the wide spacing and limited number of seismograph stations in western Alaska.

SEAFLOOR INSTABILITY

Within the broad category of seafloor instability, we have included discussions of three major types; submarine landslides, sediment transport and erosion, and gas-charged sediment.

Submarine Landslides

Submarine landslide is used as an all inclusive term for a variety of slope movements. The preliminary nature of our study makes it impractical at this time to attempt to classify each of the areas of slope movement according to type of movement and type of material.

The continental margin of the Navarin Basin province is incised by three large submarine canyons and it is in association with these canyons that many of the submarine slides have been found (Fig. 21). We have not correlated slide masses from line to line because of the wide spacing between tracklines. None of the slides begin in water shallower than 200 m, several begin below 400 m, and one appears to begin at a depth of greater than 1200 m. The length of the zone affected by down-slope movement is at least 50 km and some of these zones appear to be 25 km wide. Some landslides may affect the upper 200-300 m of the sediment column (Fig. 22). Gravity cores (2-5 m) were collected from a few of the slide masses. These cores recovered a variety of sediment types that range from pebbly mud to sandy mud to very soft, probably oversaturated mud. Preliminary evaluation of the seismic profiles crossing the outer continental shelf and slope suggest that the slope movements vary according to Varnes' (1979) classification from slumps to debris slides to earth flows. The most likely triggering mechanisms of the submarine landslides are agitation of presumed underconsolidated sediment by storm waves, internal waves or tsunamis. Other less likely causes of sliding in this region are prolonged ground shaking during earthquakes, overloading and excessive steepening by erosion and/or rapid sediment accumulation, and buildup of excessive pore-water pressures in underconsolidated clayey sediments due to rapid sedimentation or increase in concentration of bubble-phase gas in the sediment.

Sediment Transport and Erosion

Large Bedforms

Large sediment waves have been found at the heads of Zhemchug, Pervenets, and Navarinsky Submarine Canyons (Fig. 23). The sediment waves in each area are similar. Those at the head of Navarinsky Canyon have been studied in greatest detail. These large bedforms occur on a substrate of silty very fine sand within a 600 to 700 km^2 area between the 215 and 450 m isobaths. These bedforms strike approximately north-south, have an average wavelength of about 600 m, and have an average height of about 8 m and a maximum height about 15 m (Fig. 24). Both symmetrical and asymmetrical waves have been observed. The

bedforms are not only expressed on the surface, but also are remarkably well defined in the subsurface. The stratigraphic unit containing the sediment waves developed over a flat-lying reflector and attains a maximum thickness of about 120 m in the sediment wave field. In a few places the bedforms are covered by a thin layer of apparently younger sediment. One such locality occurs at the head of Pervenets Canyon, where the buried sediment waves are part of an intricate stratigraphic complex lying below a unit of parallel bedded reflectors (Fig. 25). The parallel bedded unit is generally about 20 m thick, but ranges in thickness from less than 5 m to about 110 m.

We do not know if these bedforms are relict or if some of the bedforms are presently active, nor are we certain if they indicate continuous sedimentation or discrete episodes of activity and non-activity. If these features are active, they, as well as the processes responsible for them, could represent sea-floor hazards.

Surface Waves

Currents generated by surface waves probably are a more significant factor in the transport of silt and larger-size particles on the open slope and shelf of Navarin Basin than, for example, tidal currents or the mean circulation. Bottom currents have not been measured in the lease sale area, nor are there good observations of surface waves. However, some surface wave data has been compiled in areas adjacent to and including a portion of the eastern boundary of the lease sale area (Brower and others, 1977).

Storms, and consequently storm-generated waves, are strongest and most frequent during the fall and winter (Lisitsyn, 1966; Brower and others, 1977). Waves as high as 15 m with possible periods of 9-11 seconds have been observed just to the east of the lease area (Browers and others, 1977). Waves with these heights and periods do not generate currents of sufficient strength near the bottom to erode sediments over a large portion of the shelf. Assuming a threshold value of 10 cm/sec for fine sand (Komar and others, 1972), an 11 sec, 15-m high wave generates currents strong enough to erode only fine sand and smaller grains in water shallower than 125 m. A wave 10-m high with a 15 second period, however, produces near-bottom currents greater than 10 cm/sec in water as deep as 200 m. Extreme waves, empirically estimated to be as large as 42.5 m high, can occur statistically on the average once every 100 years in the Navarin area (Brower and others, 1977). These data indicate that storm waves are a potential hazard in the Navarin Basin area.

Gas-charged sediment

Gas-charged sediment has reduced strength and bearing capacity compared to the strength of gas-free sediment (Nelson and others, 1978; Whelan and others, 1976). An increase in the concentration of gas results in an increase of excess pore pressure and a decrease in sediment stability until failure occurs. Failure of the sediment poses a potential hazard to seafloor exploitation because drilling into gas-charged sediment, disruption of the sediment by cyclic loading, or spontaneous over-pressurization may cause a sudden release of gas leading to failure of pipelines or platforms (U.S. Geological Survey, 1977).

The numerous areas of gas-charged sediment mapped in Navarin Basin (Fig. 26) are identified on the high-resolution seismic reflection profiles by acoustic anomalies such as displaced reflectors, and "wipe out" zones (Fig. 27). These anomalies are prevalent in the upper 50 to 100 m of sediment. Often these shallow anomalies coincide closely with well-developed "bright spots" that show up deeper in the section on multi-channel or medium-resolution single-channel profiles.

Gravity cores collected throughout the basin province were analyzed for hydrocarbons (methane through butanes) (Vogel and Kvenvolden, this report). All of the cores sampled contained hydrocarbon gases, but none showed significant amounts of thermogenic hydrocarbons. Three cores, two from the shelf and one from the slope, contained concentrations of methane and ethane 5 to and 10 to 20 times higher, respectively, than background values (Vogel and others, 1981). These cores also contained ratios of ethane to ethene and methane to ethane and propane that marginally suggest the presence of some thermogenic hydrocarbons. A possible explanation for the low concentrations of hydrocarbons is the short length of the cores (<6m; most of the cores collected on the shelf were <2 m long).

VOLCANIC ACTIVITY

Although no evidence of active volcanism exists in the Navarin Basin province, the volcanically active Alaska Peninsula and Aleutian Islands mark the southern border of the Bering Sea (Fig. 28). Coats (1950) lists 25 active volcanoes in the Aleutian Islands and 11 on the Alaska Peninsula. Quaternary volcanism on the Pribiloff Islands, is located less than 500 km southeast of Navarin Basin. Volcanic hazards are associated with eruption of lava and ash and the accompanying earthquakes, and the possible generation of large seismic sea waves.

Eruptions from large andesitic cones like those found on the Aleutians and the Alaska Peninsula are explosive and can spread pyroclastic material over large areas. Eruptions from basaltic volcanoes like those on the Pribilof Islands are less explosive and would have local effects.

About 21 km of ash, was erupted in Alaska in 1912 by Katmai volcano when ash was carried over distances of 2000 km or more. Ash was deposited 180 km from the volcano with a density of about 45 g/cm (Lisitsyn, 1966). According to historical data, individual ash deposits in the Bering Sea region extend 200 to 2000 km from the source. We have found minor amounts of volcanic glass in Navarin cores (see Karl and others, this report).

ICE

We have estimated ice conditions in Navarin Basin province by synthesizing data reported in Lisitsyn (1966), McRoy and Goering (1974), and Brower et al. (1977). The proposed lease area is ice-free from June through October. Migratory pack ice begins to encroach upon the northern part of the lease area in November. The pack ice is fully developed by March or April at which time the extreme southern limit of the ice edge extends over most of the lease area (Fig. 28). Ice concentrations begin to decrease in April and the ice edge continues to retreat northward through May. First year ice in the southern portion of the Bering Sea ranges in thickness from 30-71 cm, whereas ice further north can attain a thickness of 1-2 m in unstressed floes (Lisitsyn, 1966). The southern limit and concentration of the pack ice varies from year to year depending upon weather conditions--some years migratory pack ice may not affect the lease area, but in other years concentrations of ice may completely cover it.

REFERENCES CITED

Askren, D. R., 1972, Holocene stratigraphic framework southern Bering Sea continental shelf: MS Thesis, Univ. of Washington, 104 p.

Brower, W. A., Jr., Searby, H. W., Wise, J. L., Diaz, H. F., and Prechtel, A. S., 1977, Climatic atlas of the outer continental shelf waters and coastal regions of Alaska, vol. II, Bering Sea, NOAA OCSEAP Final Report-RU 347, 443 pp.

Coats, R. R., 1950, Volcanic activity in the Aleutian arc: U.S. Geol. Survey Bull. 974-B, p. 35-47.

Cooper, A. K., Scholl, D. W., and Marlow, M. S., 1976, Plate tectonic model for the evolution of the Bering Sea basin: Geol. Soc. Amer. Bull., v. 87, p. 1119-1126.

Komar, P. A., Neudeck, R. H., and Kulm, L. D., 1972, Observation and significance of deep-water oscillatory ripple marks on the Oregon continental shelf: in D. J. P. Swift, D. B., Duane, and O. H. Pilkey, eds., Shelf sediment transport: process and pattern, Dowden, Hutchinson and Ross, Inc., Stroudsbourg, Pa., P. 601-619.

Lisitsyn, A. P., 1966, Recent sedimentation in the Bering Sea (in Russian): Inst. Okeanol. Ahoc. Nauk USSR, (translated by Israel Program for Scientific Translation, available from U. S. Dept. Commerce, Clearinghouse for Fed. Sci. and Tech. Info. 1969, 614 pp.).

Marlow, M. S., Scholl, D. W., Cooper, A. K., and Buffington, E. C., 1976, Structure and evolution of Bering Sea shelf south of St. Lawrence Island: American Association of Petroleum Geologists Bulletin, v. 60, p. 161-183.

McRoy, C. P. and Goering J. J., 1974, The influence of ice on the primary productivity of the Bering Sea: in D. W. Hood and E. J. Kelley, eds., Oceanography of the Bering Sea with emphasis on renewable resources, Univ. of Alaska, Fairbanks, Alaska, p. 403-419.

Meyers, H., 1979, A historical summary of earthquake epicenters in and near Alaska: N.O.A.A. Tech. Memorandum EDS NGSDC-1, 80 p.

Nelson, Hans, Kvenvolden, K. A., and Clukey, E. C., 1978, Thermogenic gases in near-surface sediments of Norton Sound, Alaska: In, Proceedings of the 1978 Offshore Technology Society, p. 2623-2633.

Scholl, D. W., Buffington, E. C., and Marlow, M. S., 1975, Plate tectonics and the structural evolution of the Aleutian-Bering Sea region: in R. B. Forbes, ed., Contributions to the geology of the Bering Sea basin and adjacent regions: Geological Society of America Special Paper 151, p. 1-32.

U. S. Geological Survey, 1977, An investigation of Pennzoil's blow-out and loss of platform: U. S. Geological Survey unpublished administrative report, 22 p.

Varnes, D. J., 1978, Slope movement types and processes in: R. L. Schuster and R. J. Krizek, eds., Landslides, analysis and control, Natl. Acad. of Sciences, Wash. D. C., p. 11-33.

Vogel, T. M., Kvenvolden, K. A., Carlson, P. R., and Karl, H. A., 1981, Geochemical prospecting for hydrocarbons in the Navarin Basin province: American Association of Petroleum Geologists Bulletin, v. 64, no. 4.

Webster, B. D., 1979, Ice edge probabilities for the eastern Bering Sea: N.O.A.A. Technical Memorandum NWS AR-26, 20 p.

Whelan, T., Coleman, J. M., Roberts, H. H., and Suhayda, J. N., 1976, The occurrence of methane in recent deltaic sediments and its effect on soil stability: Bull. of the International Association of Engineering Geology, No. 14, p. 55-64.

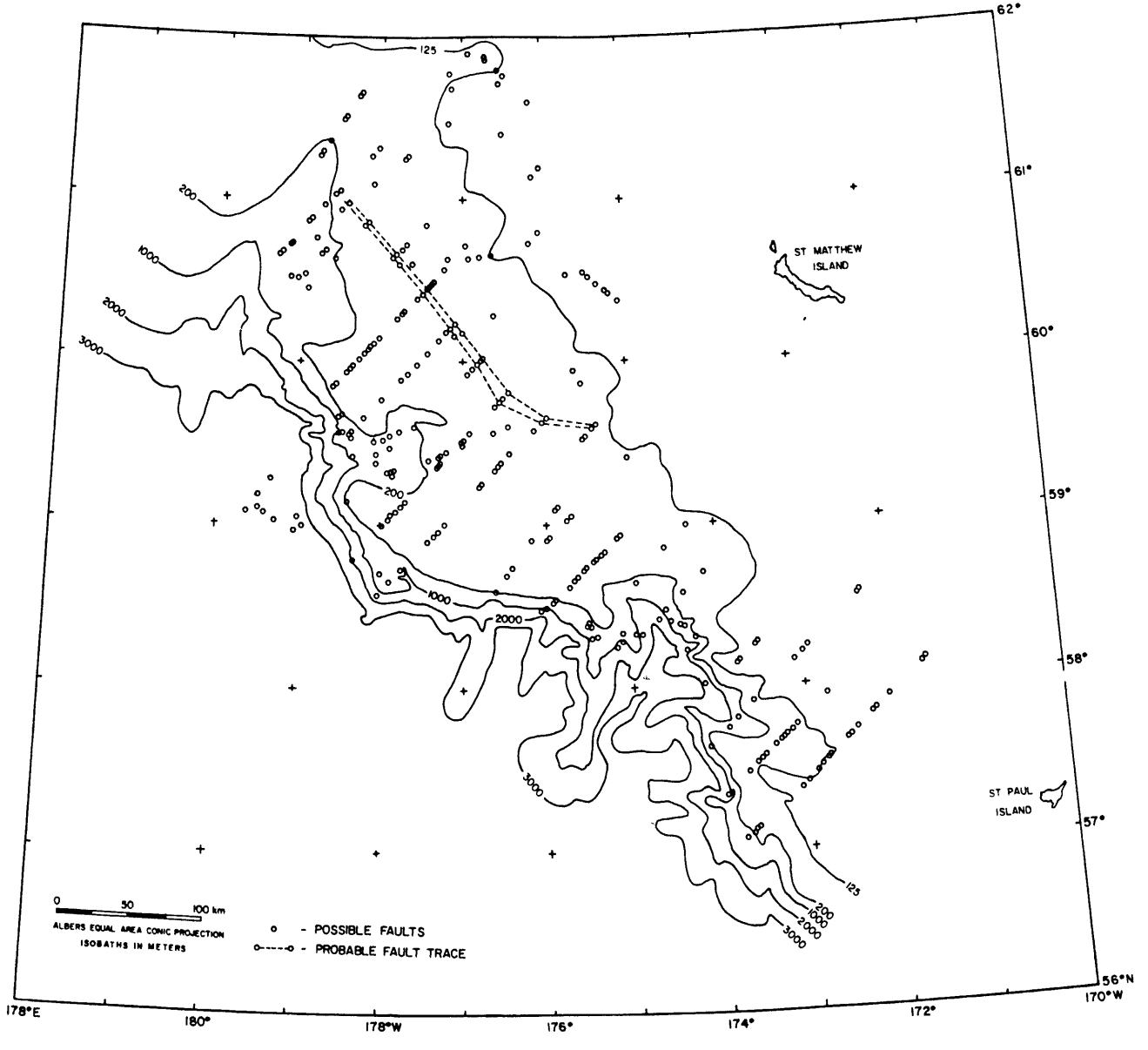

Figure 19. Preliminary map of faults in Navarin Basin province.

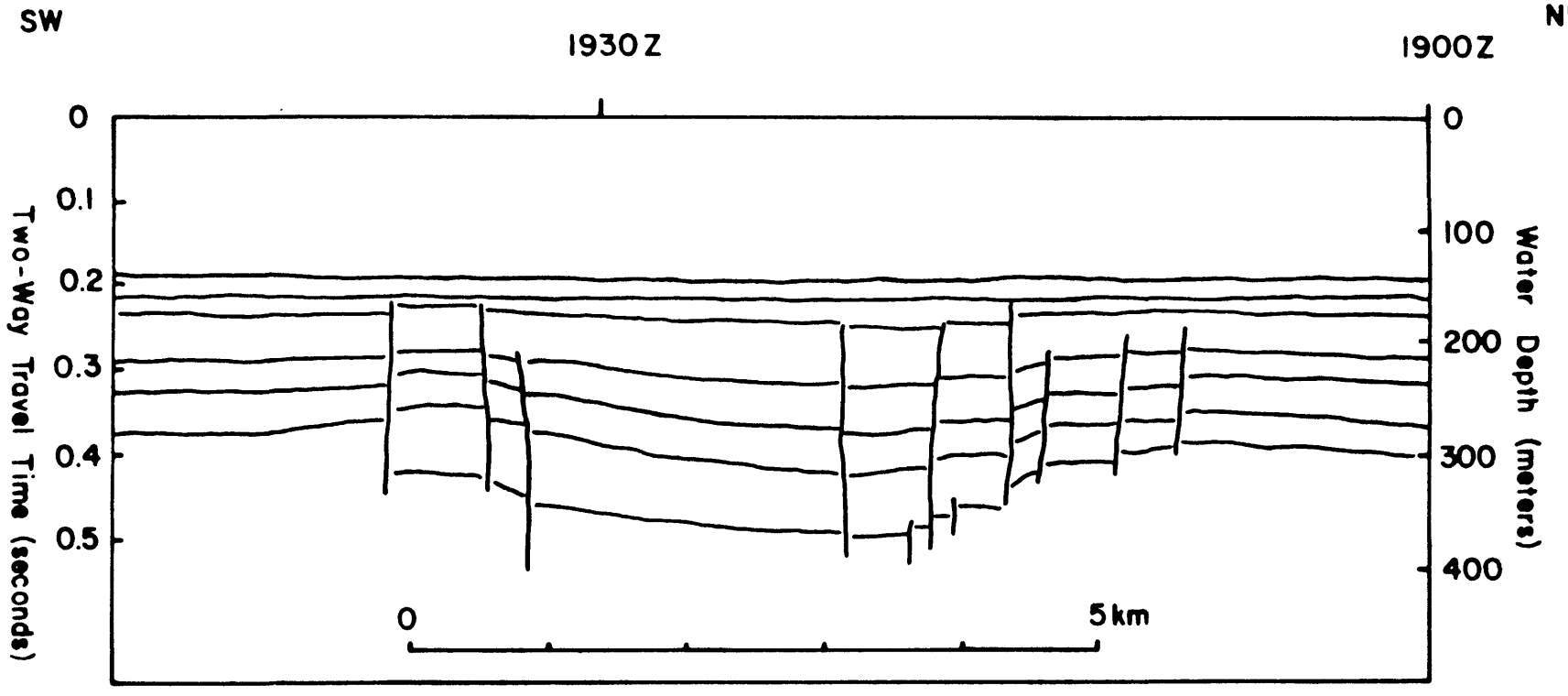

Figure 20. Interpretive line drawing of seismic-reflection profile (2-40 in^3 air guns) across graben in Navarin Basin province (see Fig. 21). Line 42, cruise DC5-80-BS/NB. Vertical exaggeration ~ 8.5 x.

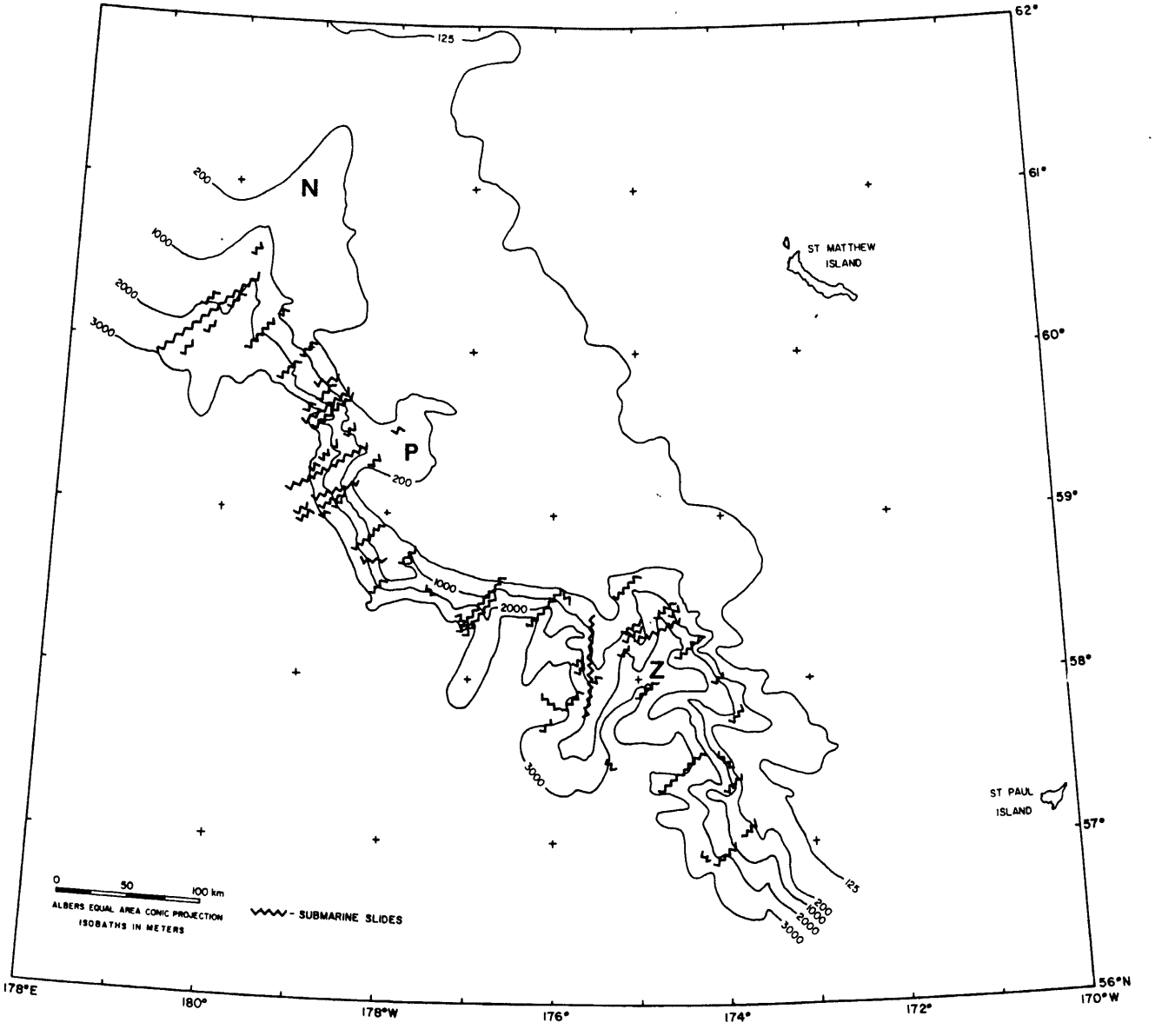

Figure 21. Preliminary map of areas of submarine landslides in Navarin Basin province. Letters N, P, Z locate Navarinsky, Pervenets, and Zhemchug Canyons.

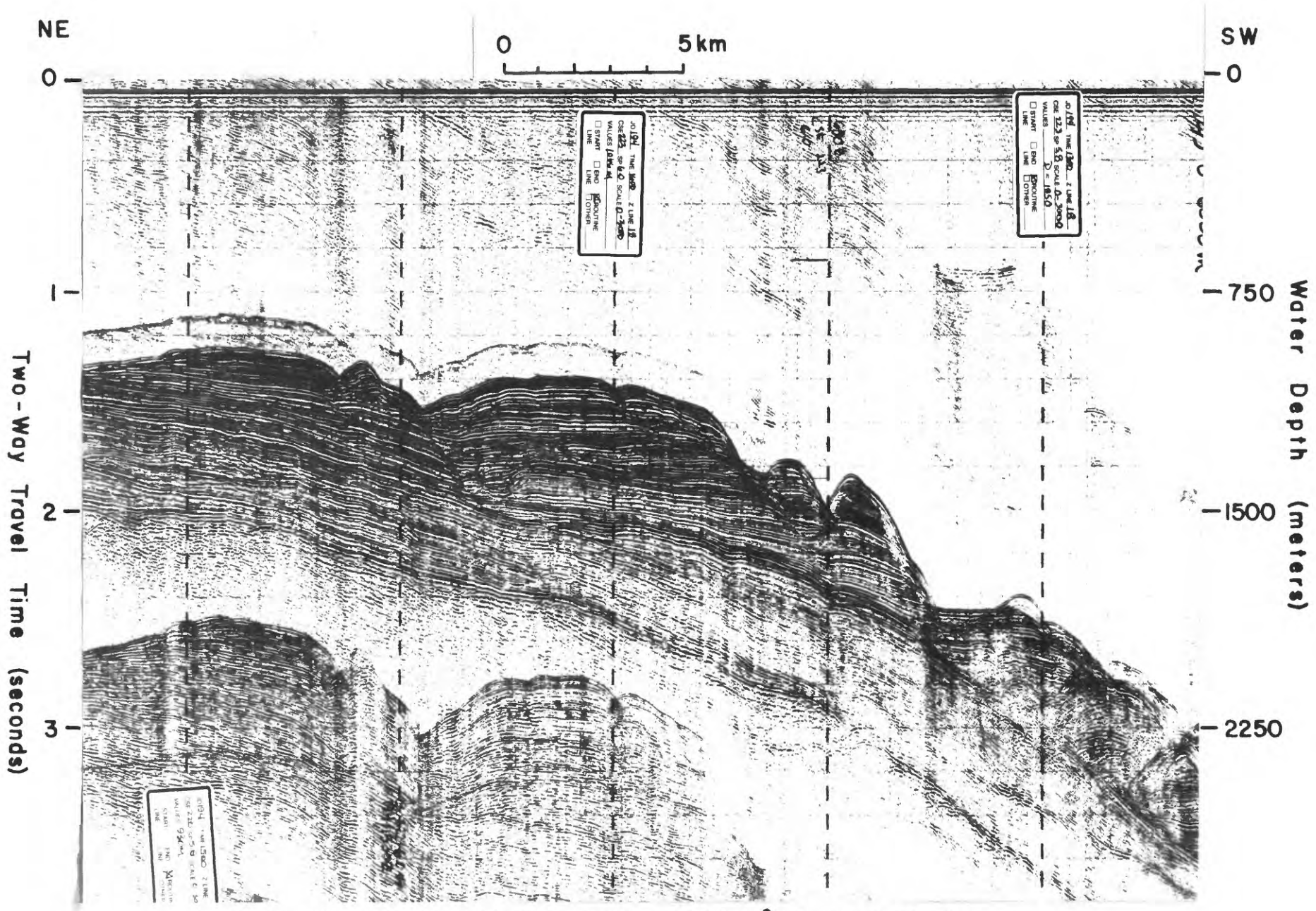

Figure 22. Seismic-reflection profile (2-40 in^3 air guns) showing slumping in Navarinsky Canyon. Note the slumps, the buried channel (∿ 1545 Z), and the associated cut and fill structures. Line 18, cruise DC4-80-BS/NB. Vertical exaggeration ∿ 10 x.

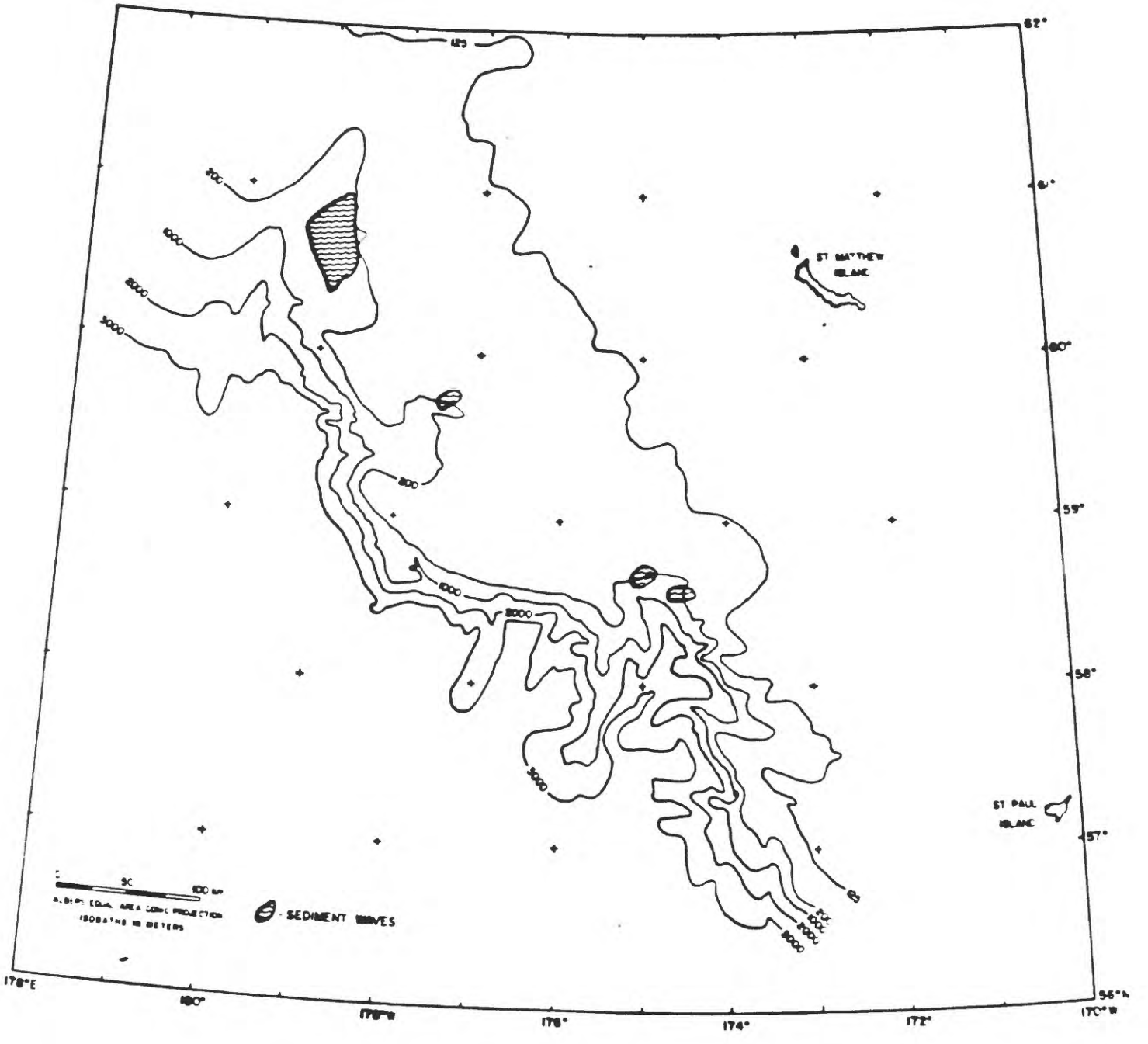

Figure 23. Preliminary map of areas of sediment waves in Navarin Basin province. Letters N, P, Z locate Navarinsky, Pervenets, and Zhemchug Canyons.

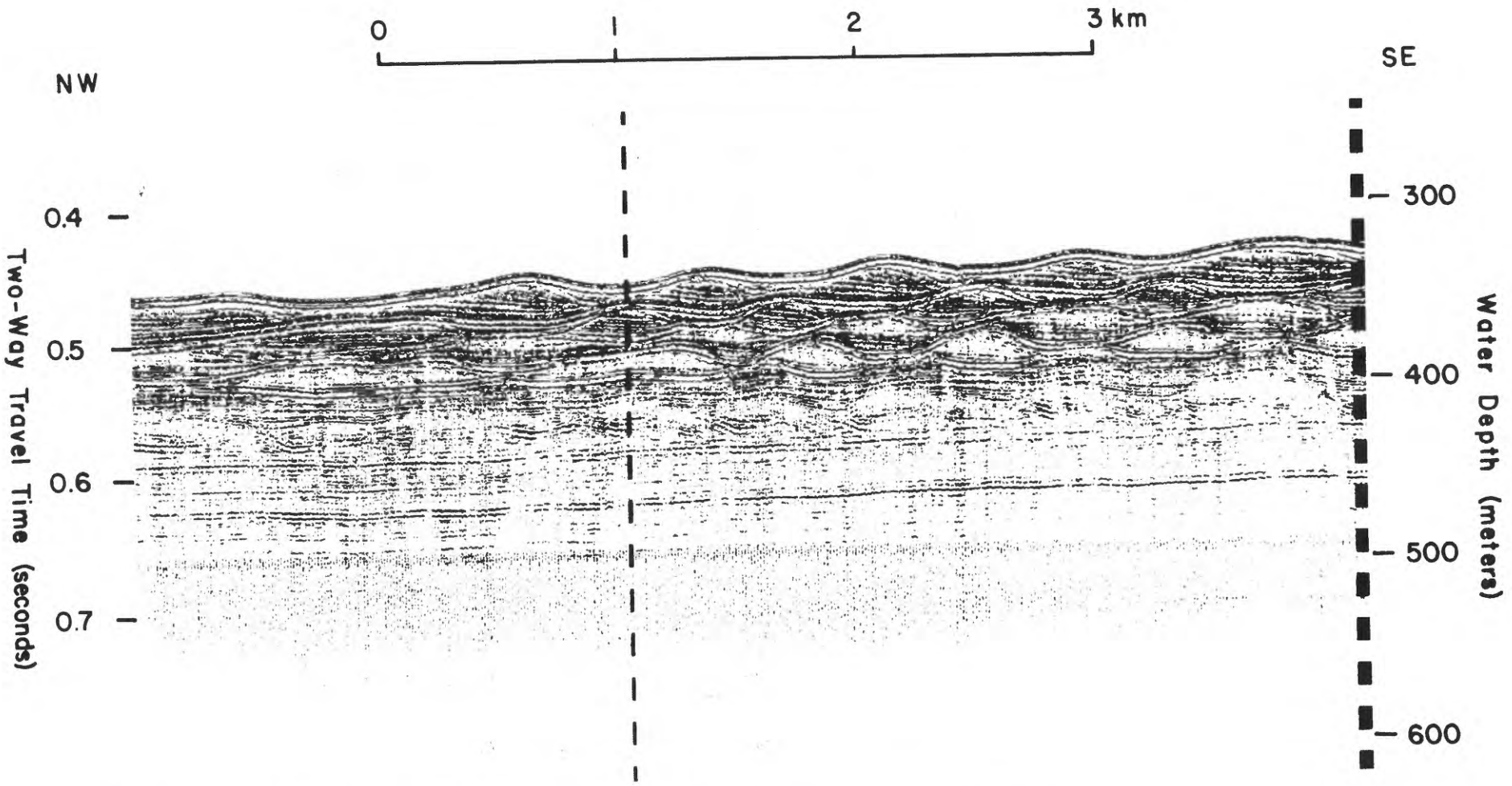

Figure 24. Seismic-reflection profile (1000J minisparker) showing sediment waves at head of Navarinsky Canyon. Line 12, DC4-80-BS/NB. Vertical exaggeration $\sim$ 7.5 x.

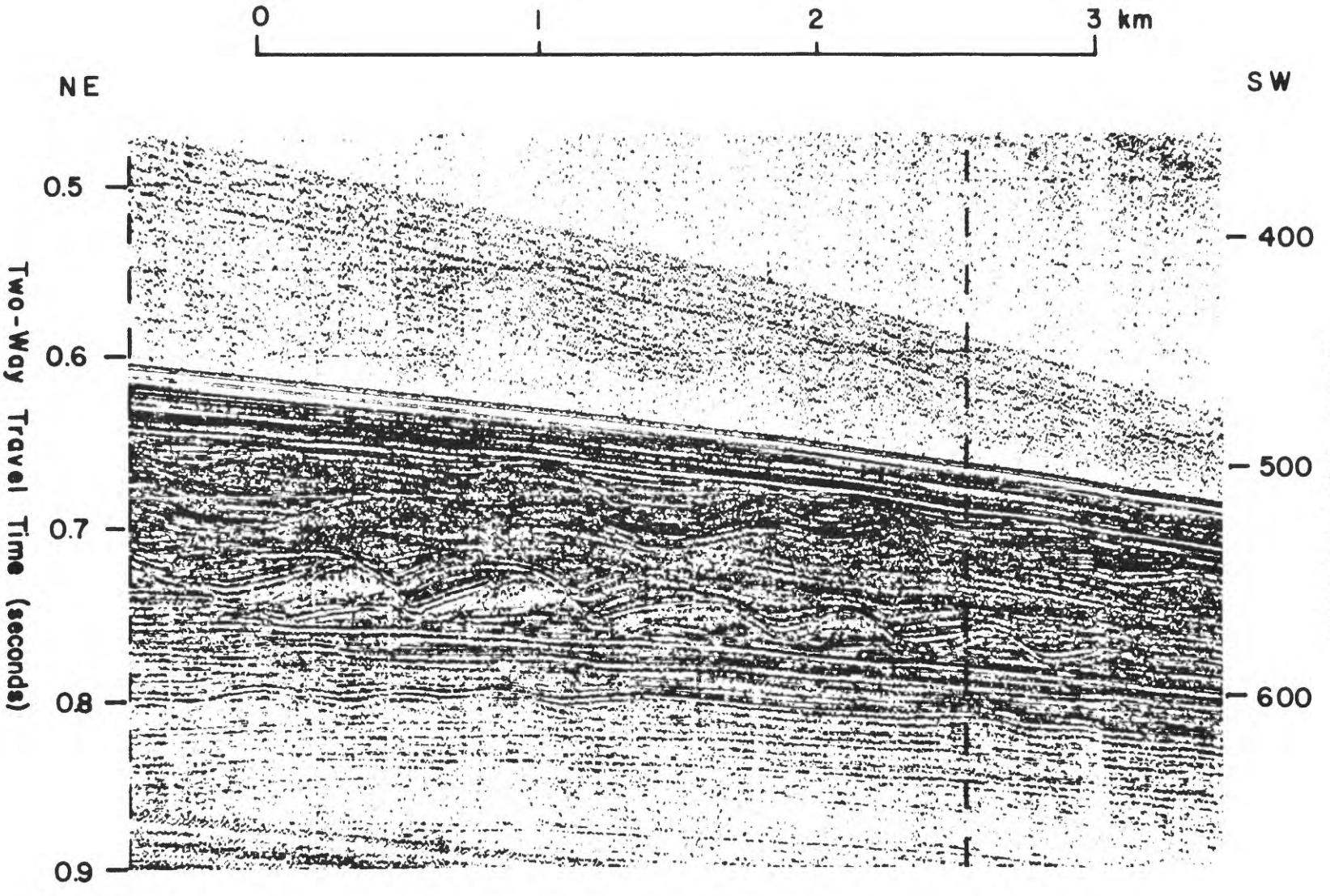

Figure 25. Seismic-reflection profile (1000J minisparker) showing sediment waves covered by about 20 m of parallel-bedded sediment at head of Pervenets Canyon. Line 43, DC5-80-BS/NB. Vertical exaggeration $\sim$ 8.5 x.

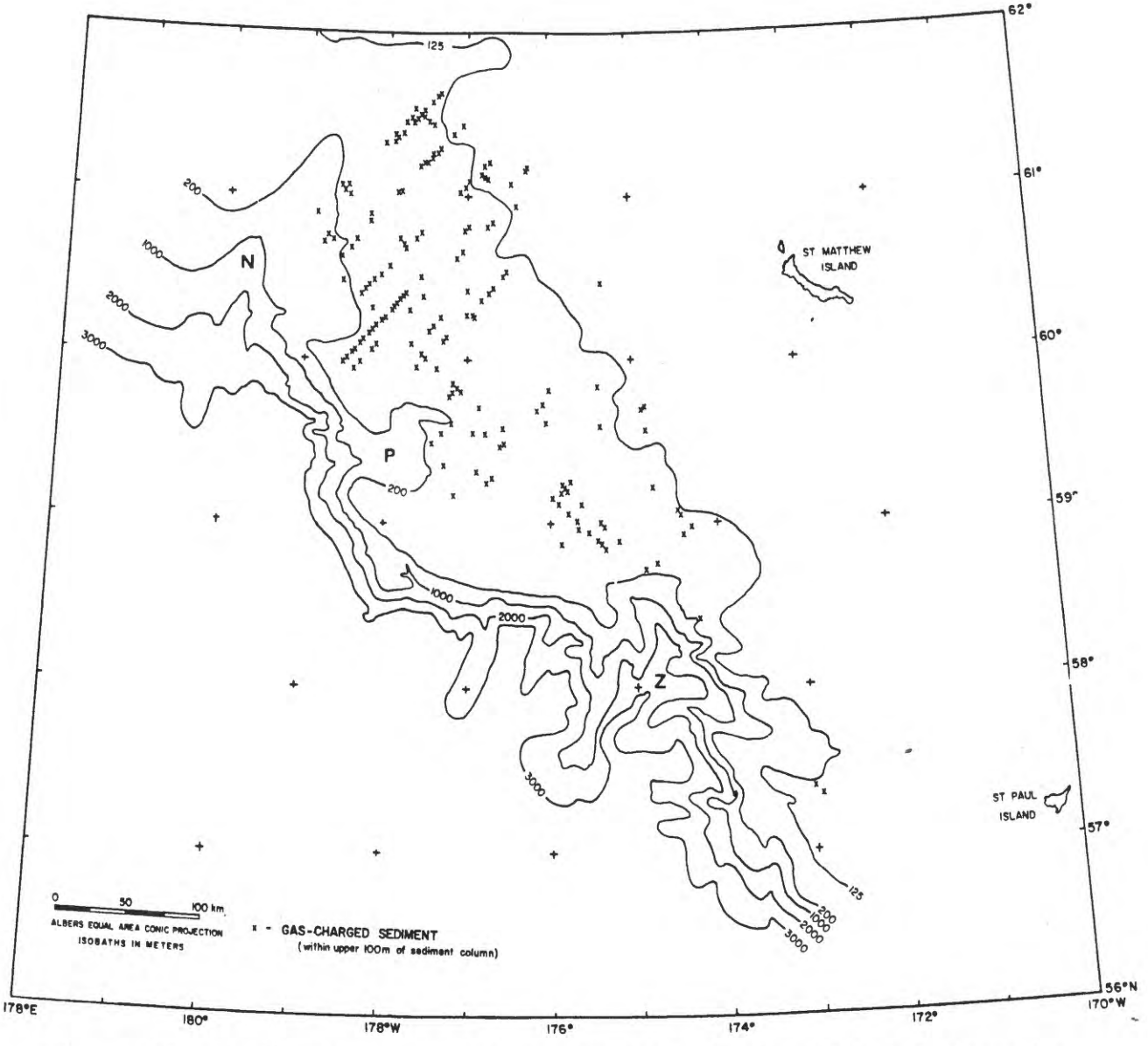

Figure 26. Preliminary map of areas of gas-charged sediment in Navarin Basin province.

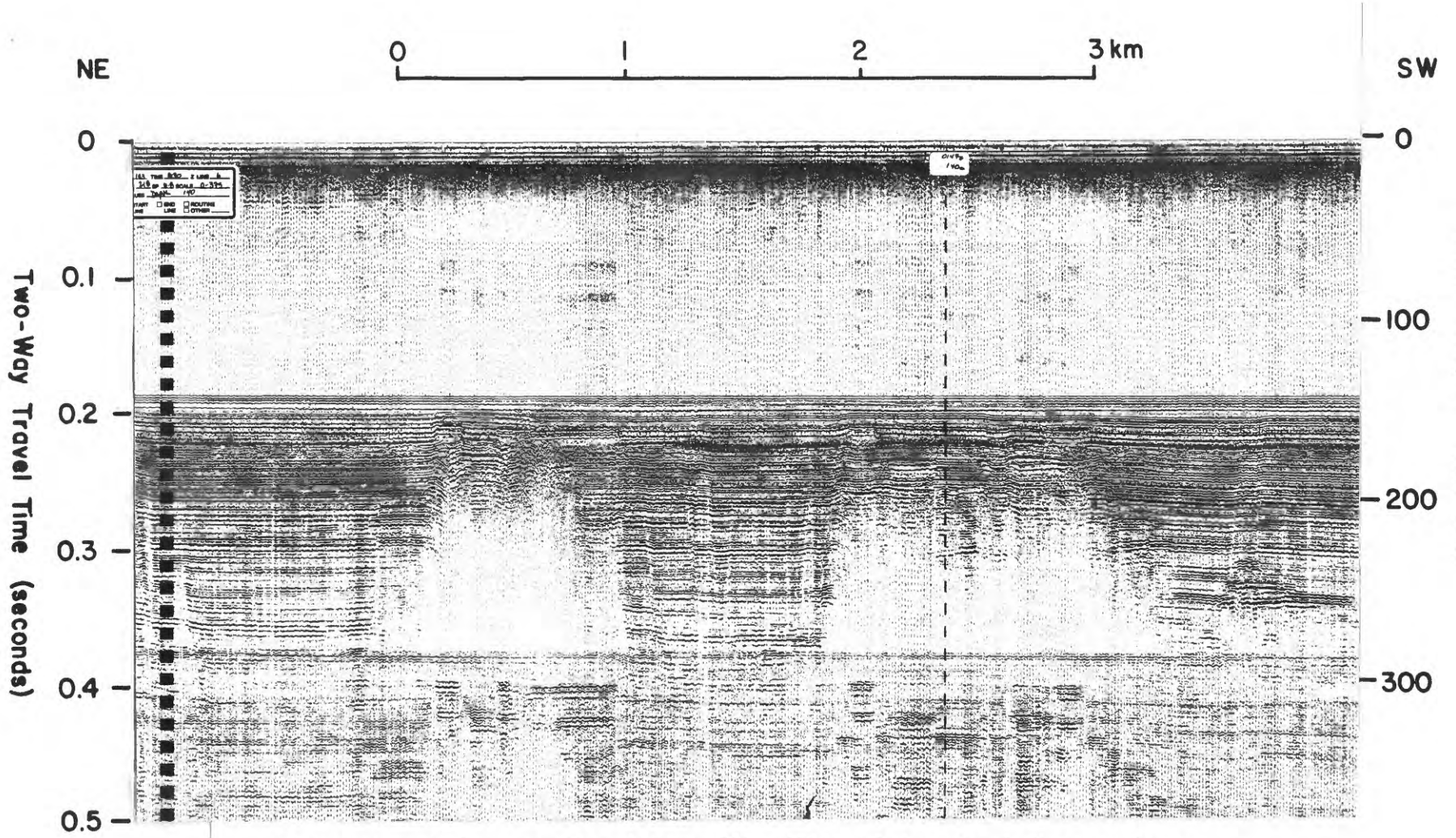

Figure 27. Seismic-reflection profile (500J minisparker) from northern part of Navarin Basin province showing acoustic anomalies interpreted to be caused by gas-charged sediment. Line 6, DC4-80-BS/NB. Vertical exaggeration $\sim$ 7.5 x.

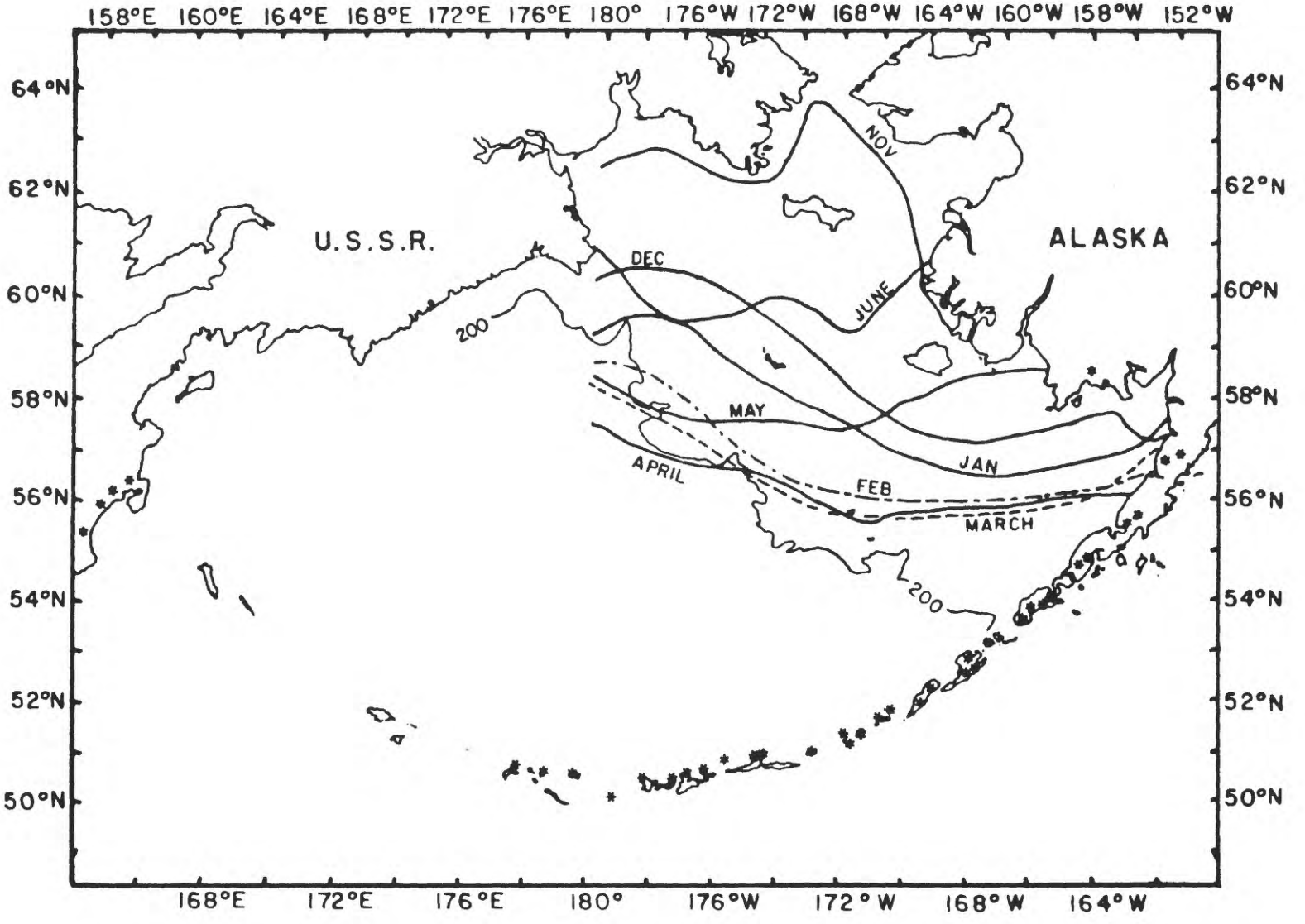

Figure 28. Location map of active volcanoes (*) (after Coates, 1950) and lines of average monthly ice-front positions (after Webster, 1979). The ice positions are for the 15th of each month and are estimated to have a 50% probability.

GEOTECHNICAL PROPERTIES OF NAVARIN BASIN SEDIMENT

Brian D. Edwards

INTRODUCTION

Cores from 68 stations have been tested to define geotechnical variables useful in describing regional changes in Navarin Basin sediment properties. The term geotechnical is applied in this study to quantitative physical characteristics of the sediment that are useful in assesssing sedimentary processes of engineering importance. Basic properties of geotechnical importance include strength and compressibility characteristics. Additional "index" variables that are known to correlate with or affect these more fundamental properties include water content, grain density, Atterberg limits (i.e. plastic and liquid limits), grain size distribution and composition of sediment.

Shipboard Techniques

A suite of 68 gravity cores was collected for stratigraphic and sedimentologic analysis. At 7 stations, replicate cores were collected and preserved in refrigeration for subsequent triaxial and consolidation testing. Shipboard testing was limited to strength measurements and subsampling for water content.

Cores were cut into multiple sections by use of a rotary knife blade cutter. Core sections designated for stratigraphic and sedimentologic analyses were then split longitudinally using a specially designed cutting system and a wire saw. Although sample disturbance is aggrevated by such longitudinal splitting, this procedure allows more frequent downcore testing while maintaining sample integrity for other analyses (e.g., X-ray radiography, photography, and textural analysis).

Strength measurements were made using a motorized Wykeham-Farrance miniature vane shear device. Tests were made at 20 cm intervals on the stratigraphic cores using a four-bladed 1/2 inch vane which was inserted into the cores so the top of the vane was buried by an amount equivalent to blade height. Torque was applied to the vane by either a torque cell that rotates the vane directly, or by a connected spring. Rotation rate of the torque cell and the top of the calibrated spring was a constant 90° per minute. When the spring system was used, torsion was measured and correlated directly with torque applied at the vane. Because of the spring's flexibility, rotation rate at the vane changed throughout the test. The method of torque measurement (spring vs torque cell) and the core state (split vs unsplit) appeared to have little impact on the general trend of the shear strength versus depth variation (Fig. 29). Vane shearing strength (S_v), is calculated from peak torque by assuming that the sediment builds a peak shearing resistance everywhere along a right-circular cylinder inscribed around the vane. This term (S_v) is commonly equated with the undrained shear strength of the sediment (S_u).

Water content and bulk density subsamples were obtained from the location of the vane test immediately following strength testing. These samples were taken with a small tube sampler and stored in sealed sample bottles for subsequent weighing and drying at the shorebased laboratory.

Replicate cores collected for more sophisticated geotechnical testing laboratory were sectioned as described above, but were not split longitudinally. Vane shear tests were conducted at the top of each unsplit core section and water content subsamples were taken at those sites. End caps were sealed on both ends of each core section. Cores were then wrapped in cheesecloth, sealed with a non-shrinking, microcrystalline wax, labelled, and stored vertically in refrigeration. The replicate cores were shipped by refrigerated air transport from Kodiak, Alaska, to storage facilities at the U.S. Geological Survey laboratory in Palo Alto, California. These cores were subsequently shipped to the commercial testing laboratory. At all times, the cores were kept in refrigeration and handled vertically.

RESULTS

Distribution of Peak Shear Strength

The areal distribution of peak undrained shear strength (S_v) at a subbottom depth of one m is shown in Figure 30. The study area can be divided physiographically into three zones: (1) shelf, (2) shelf break and uppermost slope, and (3) slope. Shelf sediment (< 200 m) typically has a peak vane shear strength (S_v) that ranges between 10 and 15 kPa (1 psi=6.9 kPa). An elongate zone of weaker sediment (<10 kPa) extends onto the central shelf from the north and reflects the presence of a tongue of fine-grained, higher water content sediment (see Karl and others, this report; Fig. 11). A zone of stronger sediment (>15 kPa) exists to the southeast although station control is too sparse to allow definition. Shear strengths in the region of the shelf break (lined area) are not shown because high sand content allows pore-water drainage during testing which compromises measured S_v values, and/or insufficient sample was recovered to warrant testing. Peak shear strength typically decreases downslope, ranging from 11 kPa near the shelf break to 3 kPa, on the abyssal floor. However, anomalously strong sediment was encountered at two stations in 3000 m of water at about 58°30'N, 178°30'W (Cores G22 and G73). Here, shear strengths are between 19 and 39 kPa.

Water Content Distribution

Sediment at a 1 m subbottom depth on the shelf has a water content that ranges between 40 and 110% by dry weight (Fig. 31). An elongate zone of water contents greater than 100% is seen in the north-central part of the shelf. This zone is coincident with the area of anomalously low peak undrained shear strength. Water content of shelf sediment gradually decreases to the southeast, with the exception of two stations that have water contents greater than 50%.

Sediment from the shelf edge and uppermost slope typically has a low water content (<50%) which correlates with increased sand percentages. Water content increases down slope and reaches a maximum (>300%; Core G 13) to the southeast in the vicinity of Zhemchug Canyon.

Consolidation State

Near-surface sediment from Navarin Basin is lightly to moderately overconsolidated (OCR: 3-4) except on the shelf where overconsolidation ratios as high as 22 are observed (Table 7). The cause of the observed overconsolidation is uncertain. Sediment on the shelf is subjected to a number of loads capable of inducing this overconsolidation state (e.g., creep, erosion of overlying material, cyclic loading, cementation, ice loading, and subaerial exposure at low sea level stands). At present, we have insufficient data to evaluate these mechanisms.

SUMMARY OF FINDINGS

An inverse correlation exists between peak undrained shear strength (S_v) and water content of Navarin Basin sediment. At a 1 m subbottom depth, a tongue of relatively weak (< 10 kPa), high water content (> 100%), fine-grained sediment extends onto the central shelf from the north. To the southeast, near the head of Zhemchug Canyon, shear strengths are anomalously high (> 15 kPa). Vane shear strengths at the shelf edge are of low reliability because of the coarse-grained texture and are not reported. Strength of the fine-grained, high water content sediment on the slope typically decreases with water depth from a high of 11 kPa near the shelf break to a low of 3 kPa at the base of the slope. Two stations of very high shear strength (19 and 39 kPa) were found at the base of the slope between Zhemchug and Pervenets Canyons.

Preliminary consolidation data indicates that the shelf sediment is lightly to heavily overconsolidated (OCR's ranging from 3 to 22 at a subbottom depth of 1 m). At present, we have insufficient data to interpret the cause of overconsolidation. It is apparent that the central shelf is more heavily overconsolidated than adjacent areas.

TABLE 7. Overconsolidation Ratios (OCR's) of near-surface sediment

Core	σ'_{vm} (kPa)	σ'_{v} (kPa)	OCR	Physiographic Province
G31	20	6.8	3	Shelf
G34	28	7.0	4	Canyon
G61	27	4.5	6	Shelf
G74	25	9.2	3	Slope
G78*	95	4.3	22	Shelf
G97	30	5.0	6	Canyon
G111	60	6.5	9	Shelf

*values 1 m subbottom depth except G78 which was determined at 58 cm.

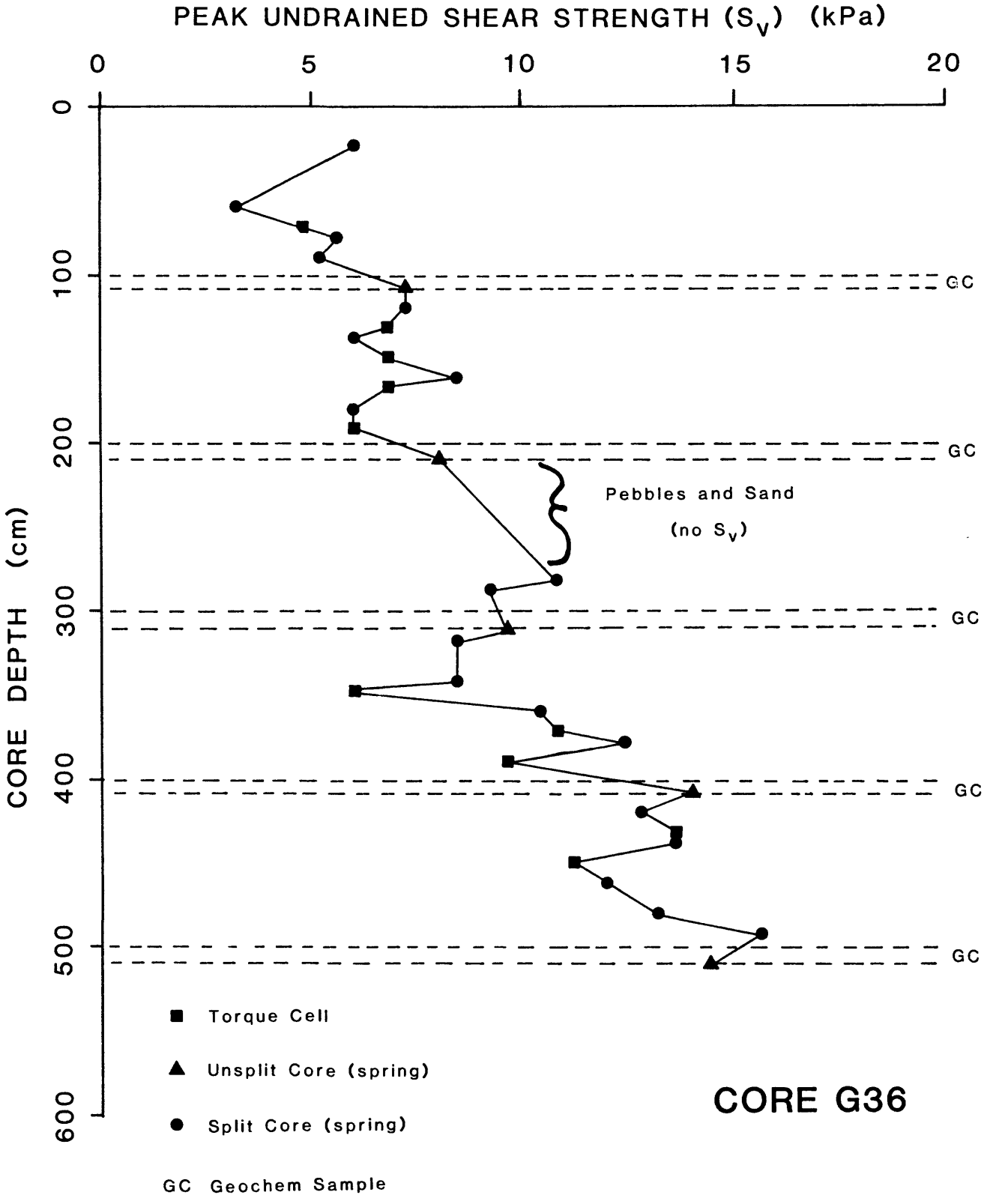

Figure 29. Peak undrained shear strength (S_v) versus core depth for core G36. Note the general increase in S_v with subbottom depth and the good correlation between strength determinations by the various methods used.

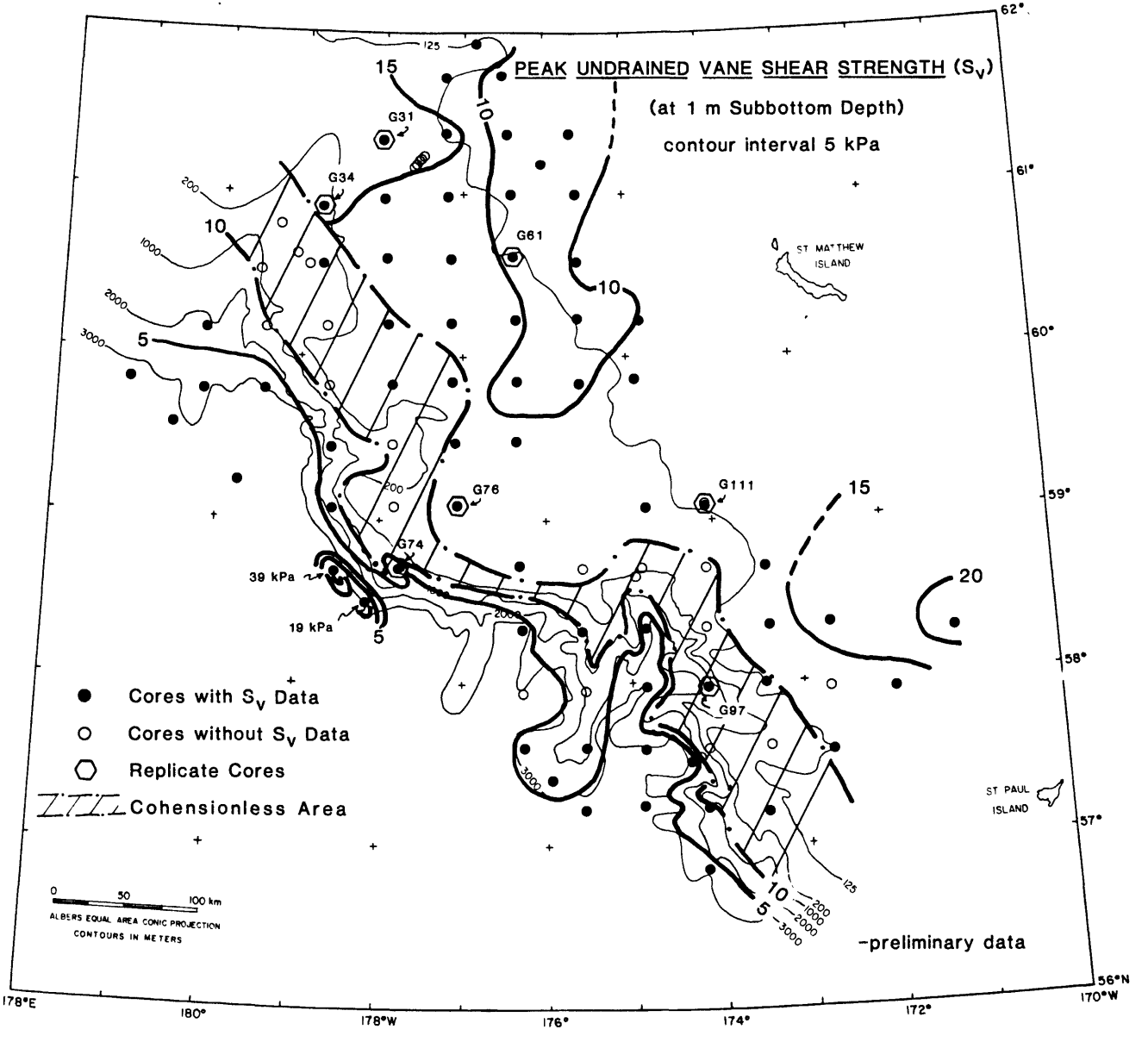

Figure 30. Areal distribution of peak undrained vane shear strength (S_v) at 1 m subbottom depth.

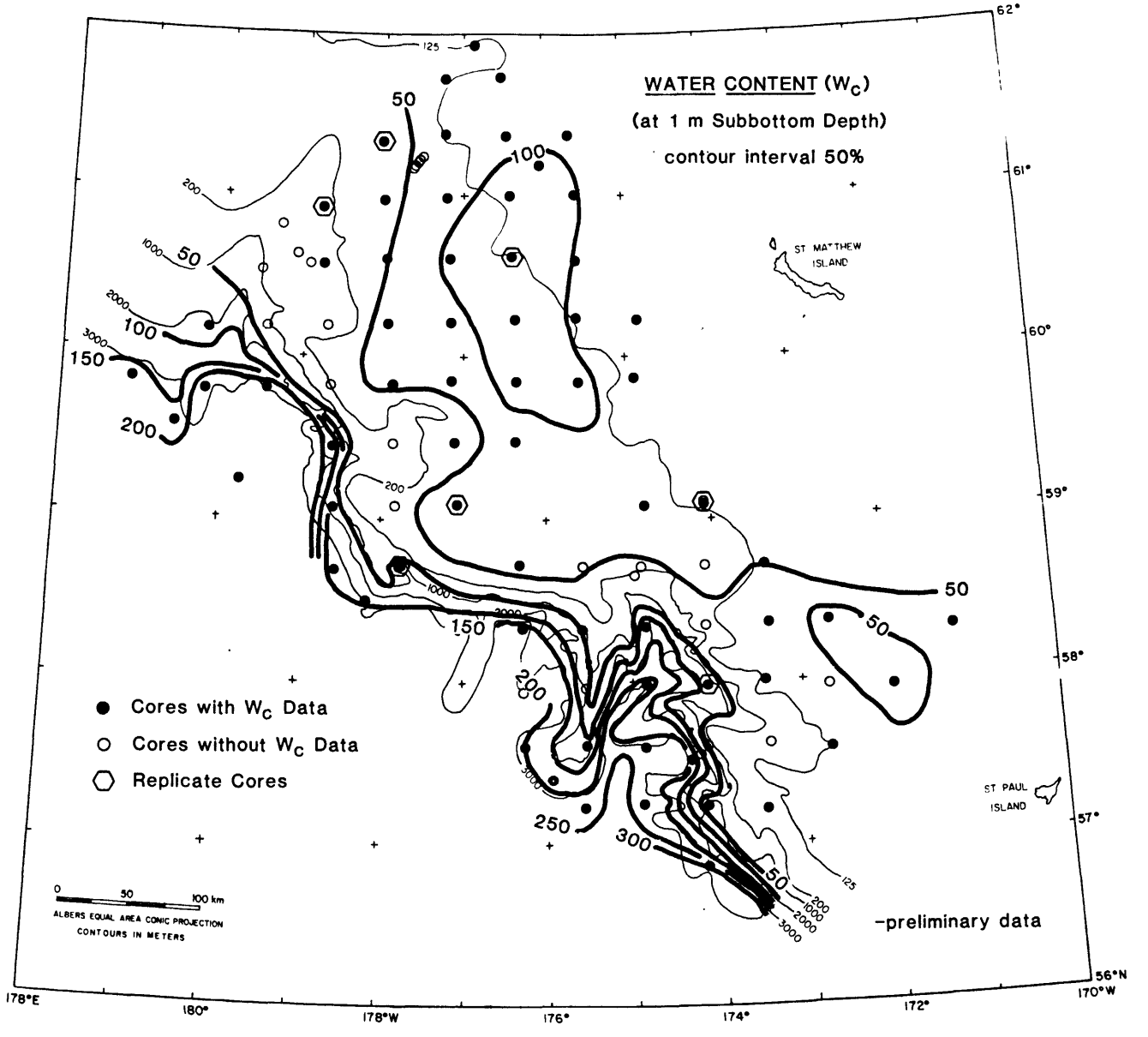

Figure 31. Areal distribution of salt-corrected water content at a 1 m subbottom depth.

HYDROCARBON GASES IN NAVARIN BASIN PROVINCE SEDIMENTS

Timothy M. Vogel and Keith A. Kvenvolden

INTRODUCTION

The first occurrence of hydrocarbon gases in marine sediments was described by Emery and Hoggan (1958) who noted these gases in the surface sediments of the Santa Barbara Basin offshore southern California. They reported concentrations of methane (C_1), ethane (C_2), propane (C_3), butanes (C_4), pentanes (C_5), and hexanes (C_6). However, since 1958 the majority of the geochemical studies devoted to gases in marine sediments have centered on the distribution and origin of methane, which is usually several orders of magnitude greater in concentration than the C_2-C_4 hydrocarbons (Reeburgh, 1969; Whelan, 1974; Martens and Berner, 1974; Claypool and Kaplan, 1974; Oremland, 1975; and Kosiur and Warford, 1979). In recent years, methods have been developed that measure the hydrocarbons C_2-C_4 at the 1 ppb level. For example, Bernard and others (1978) reported the concentrations of C_1-C_3 in sediment from the slope and shelf of the Gulf of Mexico. Whelan (1979) observed C_1-C_7 hydrocarbon gases in Deep Sea Drilling Project cores over 1000 m in length, and Whelan and others (1980) reported the occurrence of C_1-C_7 hydrocarbons in surface sediment of Walvis Bay, offshore South Africa. Kvenvolden and others (1979) reported the occurrence of C_1-C_4 hydrocarbons in sediment from Norton Sound, Alaska, and Kvenvolden and Redden (1980) observed C_1-C_4 hydrocarbon gases in sediment from the shelf, slope, and basin of the Bering Sea. Recently, models have been developed that characterize the hydrocarbon gases found in seeps in the marine environment, Bernard and others (1977) suggested the use of the ratio C_1/C_2+C_3 to help characterize the source of the hydrocarbon gases in submarine seeps. A C_1/C_2+C_3 ratio greater than 1000 is indicative of biogenic gas and a ratio less than 50 is suggestive of thermogenic gas. Cline and Holmes (1977) discussed the usefulness of the ratio $C_2/C_{2=}$. If the ratio is significantly greater than one, the hydrocarbon gas is possibly thermogenic, and if the ratio is less than one the gas is possibly biogenic. Kvenvolden and Redden (1980) cautioned that in areas where gas concentrations are low (non-seep areas), interpretation of sources of gases based on the ratio C_1/C_2+C_3 can be equivocal. The same can be said when the ratio $C_2/C_{2=}$ is used to interpret sources of gases.

This study considers the hydrocarbon gases C_1, C_2, C_3, ethene ($C_{2=}$), propene ($C_{3=}$), isobutane (i-C_4) and normal butane (n-C_4), detected by semi-quantitative analysis of sediment recovered from the Navarin Basin province in the Bering Sea. Interpretation based upon existing models and statistical evaluation of the data are presented to provide a general view of the region.

METHODS AND MATERIALS

Analytical procedures used in this work have been previously described (Kvenvolden and Redden, 1980). Cores were cut into 10-cm lengths at various intervals (usually 100-110, 200-210 cm, etc. sediment depths). Sediment from each of these 10-cm sections was placed in an unlined can (0.95 liters) that had two septa-covered holes on the side near the top. Each can was filled with distilled and degassed water. The can was sealed with a lid after a

headspace was established by removing 100 ml of water. The headspace was purged with helium through the septa. The cans were then shaken for 10 minutes to equilibrate the hydrocarbon gases in the sediment with the helium headspace. A sample of the headspace of about one-half the cans was withdrawn through a septa by a gas-tight syringe. This syringe was sealed by a valve in the syringe and stored for shore-based studies. The cans of sediment were inverted, frozen, and shipped back to the shore-based laboratory where gases in both syringes and the cans were analyzed by gas chromatography using flame ionization and thermal conductivity detectors. The cans of sediment were brought to room temperature and shaken for five minutes before portions of their headspaces were analyzed. Calculations of the gas concentrations were determined by computer comparison of the integrated area of each hydrocarbon with the integrated area of a hydrocarbon standard. Partition coefficients were calculated by repeatedly purging the headspace of some of the cans, re-equilibrating the gases by shaking the cans again, and analyzing a portion of the resulting headspace gas mixture. The partition coefficient (P.C.) is derived from the following equations:

$$P.C. = \frac{\text{amount in gas phase } (G_1)}{\text{total amount in can } (T_1)} = \frac{\text{new amount in gas phase after purge } (G_2)}{\text{new total in can after purge } (T_2)}$$

$T_2 = T_1 - G_2$, so $P.C. = 1 - \frac{G_2}{G_1}$, or generally $P.C. = 1 - \sqrt[n]{\frac{G_n}{G_1}}$ where n = # of times

For a discussion of the theory see Drozd and Novak (1979). Concentrations of the hydrocarbons are reported in nl of gas/liter of wet sediment (nl/l), except for methane, which is reported in ul of methane/liter of wet sediment (ul/l). The analytical detection limit is 1 nl of gas/liter of wet sediment. Partition coefficients used are 0.7 for C_1, and 0.5 for C_2-C_4. The partition coefficients were rounded to the nearest 0.1. Error determined from repeat analysis, duplicate cores at the same station and analytical variation is <20%.

RESULTS

Hydrocarbon gases (C_1-C_4) were observed to a subbottom depth of 520 cm in the sediments of the Navarin Basin province (Table 8). The locations of the coring sites are shown in Figure 32. Methane (C_1), was the most abundant gas, often present in concentrations several orders of magnitude larger than the other hydrocarbon gases. C_1 ranged from 2 to over 850 ul/1. The geographic distribution of C_1 at the 100-110 cm and the 200-210 cm sediment depths are shown in Figures 33 and 34, respectively. In six cores (22, 36, 37, 70, 74 and 97), anomalously high C_1 concentrations were observed. These concentrations are outside the 85% confidence interval, which is based upon the concentrations of all the samples, assuming a lognormal distribution.

Ethane (C_2) is the second most abundant hydrocarbon gas measured in the Navarin Basin province sediment. The distribution of propane (C_3) generally follows the same trend as ethane (C_2), but is less abundant. C_2 ranged from trace amounts to approximately 1500 nl/l, whereas C_3 ranged from trace amounts to about 200 nl/l. Geographic distribution of these gases at the sediment depths of 100-110 cm and 200-210 cm are shown in Figures 35-38.

The alkenes, ethene ($C_{2=}$) and propene ($C_{3=}$), are generally lower in concentration than C_2 and C_3, respectively, and the alkenes usually decrease with depth. The gas-tight syringes used for sampling contained significant amounts of $C_{3=}$, resulting from outgassing of C_3 = from the teflon plunger. No other hydrocarbon gases were outgassed in significant amounts.

Concentrations of isobutane (i-C_4) and normal butane (n-C_4) are lower than the concentrations of the lighter hydrocarbons C_1-C_3. The concentrations of i-C_4 and n-C_4 are often below the detection limit of 1 nl/l, and range to a maximum concentration of 272 and 36 nl/l, respectively. The C_5-C_7 hydrocarbons are measured as a single back-flush peak on the gas chromatogram. These hydrocarbons were seldom detected and are generally low in concentration (less than 100 nl/l). Occasionally, the C_5-C_7 concentration reached 400 nl/l. Carbon dioxide was qualitatively estimated and its concentration varied little from a mean of 2 ml/l of wet sediment. For all the samples analyzed, the C_1/C_2+C_3 ratio ranged from less than 10 to over 2000, averaging 248. The $C_2/C_{2=}$ ratio ranged from 0.2 to 198, averaging 12.

Six cores (22, 36, 37, 70, 74, and 97) have anomalous C_1 concentrations; four of these (22, 36, 37 and 74) have anomalous ethane concentrations. Three of these four cores (22, 36, and 37) have anomalous propane concentrations. The C_1/C_2+C_3 ratio in core 37 is 721, whereas the ratio in cores 22 and 36 are 70 and 60, respectively. A profile of the distribution of hydrocarbons C_1-C_3, C_1/C_2+C_3 and $C_2/C_{2=}$ ratios with depth in core 36 are shown in Figure 39. For comparison, a profile of gas concentrations with depth in core 100, in which all the gas concentrations are within the 85% confidence interval based upon a lognormal distribution, is shown in Figure 40.

DISCUSSION

Sediment in Navarin Basin province contains mixtures of gases that can be classified into four types based on the relative abundances of the hydrocarbon gases present. These four types are defined in Table 9. The first and most abundant type (Type I) has low concentrations of all the hydrocarbon gases. The typical distribution with depth of Type I gas mixture is shown on Figure 40. Type I is defined as the environmental baseline for Navarin Basin province sediment. Twenty-nine stations have Type I gas at some depth in the sediment (see Table 8).

The second type of gas (Type II) has anomalously high concentrations of C_1 and just baseline concentrations of the other hydrocarbon gases. Five cores (49, 63, 68, 102, and 105) have Type II gas. The Type II gas mixture is characterized by high C_1/C_2+C_3 ratio (greater than 450) and a low $C_2/C_{2=}$ ratio (less than two).

The third type of gas (Type III) has above-baseline concentrations of C_1 and always has anomalously high concentrations of C_2 and C_3. Eight cores (22, 25, 36, 37, 70, 71, 74, and 97) have Type III gas. The $C_1/C_2+ C_3$ ratio ranges from 56 in core 36 to 721 in core 37. The $C_2/C_{2=}$ ratio ranges from 6 in core 71 to 198 in core 22.

The fourth type of gas (Type IV) has high concentrations of at least one of the alkanes C_2-C_4. In the Navarin Basin sediments, Type IV gas is characterized by the presence of measureable quantities of i-C_4 and n-C_4. Two major groups exist within Type IV; the first group, (cores 26, 31, 41, 42, 43, 45, 50, 59, and 105) only has anomalous concentrations of C_3; the second, group, (cores 52, 54, 63, 66, 68, 73, 97, 101, and 107) has various anomalies in the C_1-C_3 hydrocarbon range. The C_1/ C_2+C_3 ratio ranges from as low as 16 to over 800 and the $C_2/C_{2=}$ ratio ranges from less than one to over 24.

In Type I gas, interpretations based on the $C_1/C_2+ C_3$ and $C_2/C_{2=}$ ratios are inconclusive because the concentrations of the hydrocarbon gases are too low for these ratios to indicate whether the gases are derived from a biogenic or thermogenic source (Kvenvolden and Redden, 1980). Although C_1 alone is often considered to be a biogenic gas, the alkanes C_2 and C_3 are often considered to be thermogenic gases. However, in open-ocean sediment isolated from any apparent thermogenic source, traces of C_2 and C_3 are found, and evidence exists that suggests that these traces can be produced by biological processes (Davis and Squires, 1954; Kvenvolden and Redden, 1980; Whelan and others, 1980; Vogel and others, 1980; Oremland and others, 1980).

Type II gas has anomalous C_1 concentrations, probably derived from microbiological activity in the surface sediment. The high concentration of C_1 in anoxic sediments resulting from microbial activity is well documented (Barnes and Goldberg, 1976; Kosiur and Warford, 1979; and Martens and Berner, 1974). The less reducing sediment of the open marine environment has biogenic C_1 present in lesser amounts (Bernard and others, 1978; Kvenvolden and Redden, 1980; Kvenvolden and others, 1981). The microbial processes that produce C_1 in both types of sediment are probably similar.

Type III gas has the molecular distribution of hydrocarbons most similar to the distribution that would suggest a thermogenic source. However, i-C_4 and n-C_4 are generally not present in anomalous concentrations in Type III. Some cores (22, 25, 36, and 74) have C_1/C_2+C_3 ratios less than 80 and $C_2/C_{2=}$ ratios greater than one. However, only cores 22 and 36 have extremely high concentrations of all three alkanes C_1-C_3. Core 36 also has detectable i-C_4 and n-C_4 at depth in the sediment. If the observed gas was from a thermogenic source at depth in the sediment, the hydrocarbon gases should increase with depth similar to core 36 (Fig. 39).

Type IV gas has a large variability in the concentrations of the hydrocarbon gases, causing conclusions to be equivocal. Type IV may be interpreted to be a mixture of thermogenic and biogenic gases. The high methane concentration could possibly be caused by the mixing of large amounts of biogenic C_1 in the surface sediments with the C_1 diffusing up from a thermogenic source. The large amounts of C_2 and C_3 seem to possibly require a thermogenic source for production. For example, if a natural gas deposit existed at depth, C_1-C_3 hydrocarbon gases would possibly diffuse upward into the surface sediment, mixing with the biogenic gas produced by microbes at the surface.

A gas mixture that has only high C_3 could be caused either by error in determining the propane concentration or by a physical or chemical process (like diffusion) reducing the concentration of the other gases.

The alkenes $C_{2=}$ and $C_{3=}$ are present in all the gas types in some quantity. These alkenes have been produced in the laboratory (Davies and Squires, 1954); $C_{2=}$ is produced in soils by bacteria (Primrose and Dilworth, 1976) and $C_{2=}$ and $C_{3=}$ have been observed in non-thermogenic gases in the southern Bering Sea (Kvenvolden and Redden, 1980) and in San Francisco Bay (Vogel and others, 1980). The processes that produce the alkanes probably differ from the biological processes that produce the alkenes. All cores (31, 54, 59, 63, 66, and 107) that have anomalous $C_{2=}$ and $C_{3=}$ concentrations, have Type IV gas. This further confuses any interpretation of the source for Type IV gas. Obviously, the high alkene concentrations imply a significant biological input to the gas detected in the surface sediments.

Cores 42-45 were taken above an acoustic anomaly that ranges to within 25 meters of the sediment surface (see Fig. 27, Carlson and Karl, this report). The gas concentrations did not show a correlation with the acoustic anomaly, possibly because either the anomaly is not due to gas-charged sediment or the gas is stopped from reaching the surface by some impenetrable sediment layer.

CONCLUSIONS

Our results show that hydrocarbon gases are common in near-surface sediment of the Navarin Basin province. Generally, the concentrations of gases are low relative to earlier observations made on sediment from Norton Sound (Kvenvolden and others, 1981). The concentrations of methane in Norton Sound, were high enough to affect the stability of the sediment and thus pose a possible geologic hazard. Measured concentrations of gases in sediment from the Navarin Basin province are much smaller; thus, we are less certain of the degree of hazard. The composition of hydrocarbon gases is variable over the province. Most of the observed gas mixtures can be attributed to microbiological activity. No significant anomalies were observed, although the gas from sediment samples from core 36 suggest that some thermogenic gas may be present. No correlation was observed between gas concentrations measured in the surficial sediment and the occurrence of an acoustic anomaly that is attributed by Carlson and Karl (this report) to possible high gas concentrations at depths of about 25 meters.

REFERENCES CITED

Barnes, R. O. and Goldberg, E. D., 1976, Methane production and consumption in anoxic marine sediments: Geology, v. 4, p. 297-300.

Bernard, B. B., Brooks, J. M., and Sackett, W. M., 1977, A geochemical model for characterization of hydrocarbon gas sources in marine sediments: Proc. 9th Offshore Tech. Conf., 1, p. 435-438.

Bernard, B. B., Brooks, J. M., and Sackett, W. M., 1978, Light hydrocarbons in recent Texas continental shelf and slope sediments: Jour. Geophys. Res., 83, p. 4053-4061.

Claypool, G. E. and Kaplan, I. R., 1974, The origin and distribution of methane in marine sediments: In Natural Gases in Marine Sediments, Kaplan, I. R., ed., Plenum, New York, p. 99-139.

Cline, J. D., and Holmes, M. L., 1977, Submarine seepage of natural gas in Norton Sound, Alaska: Science, no. 198, p. 1149-1153.

Davis, J. B. and Squires, R. M., 1954, Detection of microbially produced gaseous hydrocarbons other than methane: Science, no. 119, p. 381-382.

Drozd, J. and Novak, J., 1979, Headspace gas analysis by gas chromatography: Jour. Chromatogr., vol. 165, p. 141-165.

Emery, K. O. and Hoggan, D., 1958, Gases in marine sediments: Am. Assoc. Petrol. Geol. Bull., no. 42, p. 2174-2188.

Kosiur, D. R., and Warford, A. L., 1979, Methane production and oxidation in Santa Barbara Basin sediments: Estuarine and Coastal Marine Science, v. 8, p. 379-385.

Kvenvolden, K. A., Nelson, C. H., Thor, D. R., Larsen, M. C., Redden, G. D., Rapp, J. B., and DesMarais, D. J., 1979a, Biogenic and thermogenic gas in gas-charged sediment of Norton Sound, Alaska: Proc. 11th Offshore Tech. Conf. 1, p. 479-486.

Kvenvolden, K. A. and Redden, G. D., 1980, Hydrocarbon gas in sediment from the shelf, slope, and basin of the Bering Sea: Geochim. Cosmochim. Acta, vol. 44, p. 1145-1150.

Kvenvolden, K. A., Redden, G. D., Thor, D. R., Nelson, C. H., 1981, Hydrocarbon gases in near-surface sediment of the Northern Bering Sea. In: The Eastern Bering Sea Shelf: Oceanography and Resources, vol. 1, Ed. Hood D. W. and Calder, J. A., Gov't Print. Off.

Martens, C. S., and Berner, R. A., 1974, Methane production in the interstitial waters of sulfate-depleted marine sediments: Science, 185, p. 1167-1169.

Oremland, R. S., 1975, Methane production in shallow-water, tropical marine sediments: Appl. Microbiol., no. 30, p. 602-608.

Oremland, R. S., Culbertson, C. and Kvenvolden, K. A., 1980, Microbial formation of ethylene and ethane in anoxic estuarine sediments: Abs. Ann. Meeting Amer. Soc. Microbiol., no. 118, p. 104.

Primrose, S. B. and Dilworth, M. J., 1976, Ethylene production by bacteria: Jour. General Microbiology, no. 93, p. 177-181.

Reeburgh, W. S., 1969, Observations of gases in Chesapeake Bay sediments: Limnol. Oceanog., no. 14, p. 368-375.

Vogel, T. M., Kvenvolden, K. A., and Oremland, R. S., 1980, Hydrocarbon gases in surface sediments of San Francisco Bay, California: Abs. Ann. Meet. Pac. Div. Amer. Assoc. Advancement Sci., p. 33.

Whelan, T., 1974, Methane, carbon dioxide and dissolved sulfide from interstitial water of coastal marsh sediments: Estuarine and Coastal Marine Science, no. 2, p. 407-415.

Whelan, J. K., 1979, C_1 to C_7 hydrocarbons from IPOD holes 397 and 397A: Initial Reports Deep Sea Drilling Project, 47, part 1, p. 531-539.

Whelan, J. K., Hunt, J. M., and Berman, J., 1980, Volatile C_1-C_7 organic compounds in surface sediments from Walvis Bay: Geochim. Cosmochim. Acta, no. 44, p. 1767-1785.

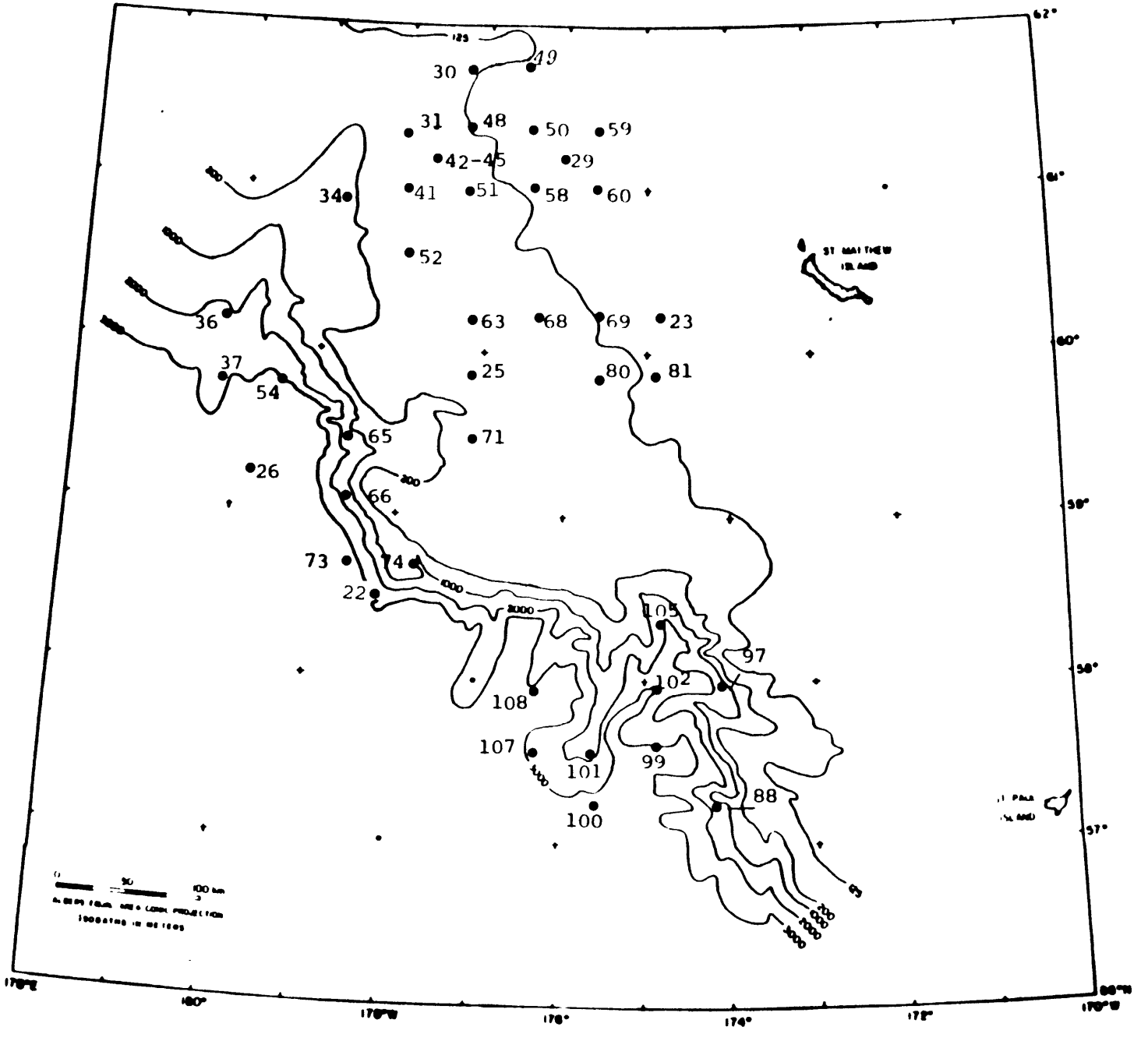

Figure 32. Map of core locations in the Navarin Basin province.

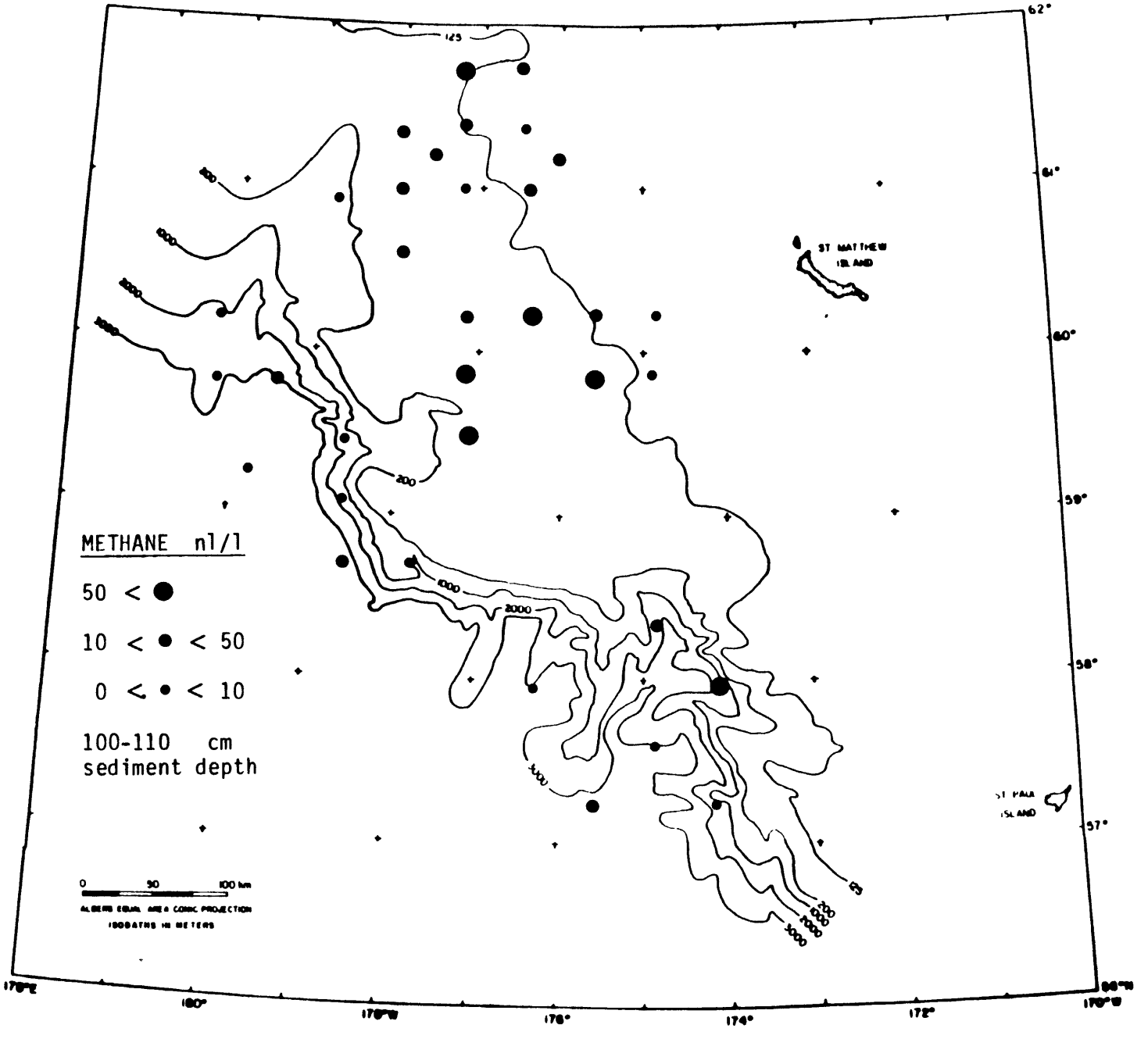

Figure 33. Distribution of methane at 100-110 cm sediment depth; reported in µl/liter of wet sediment.

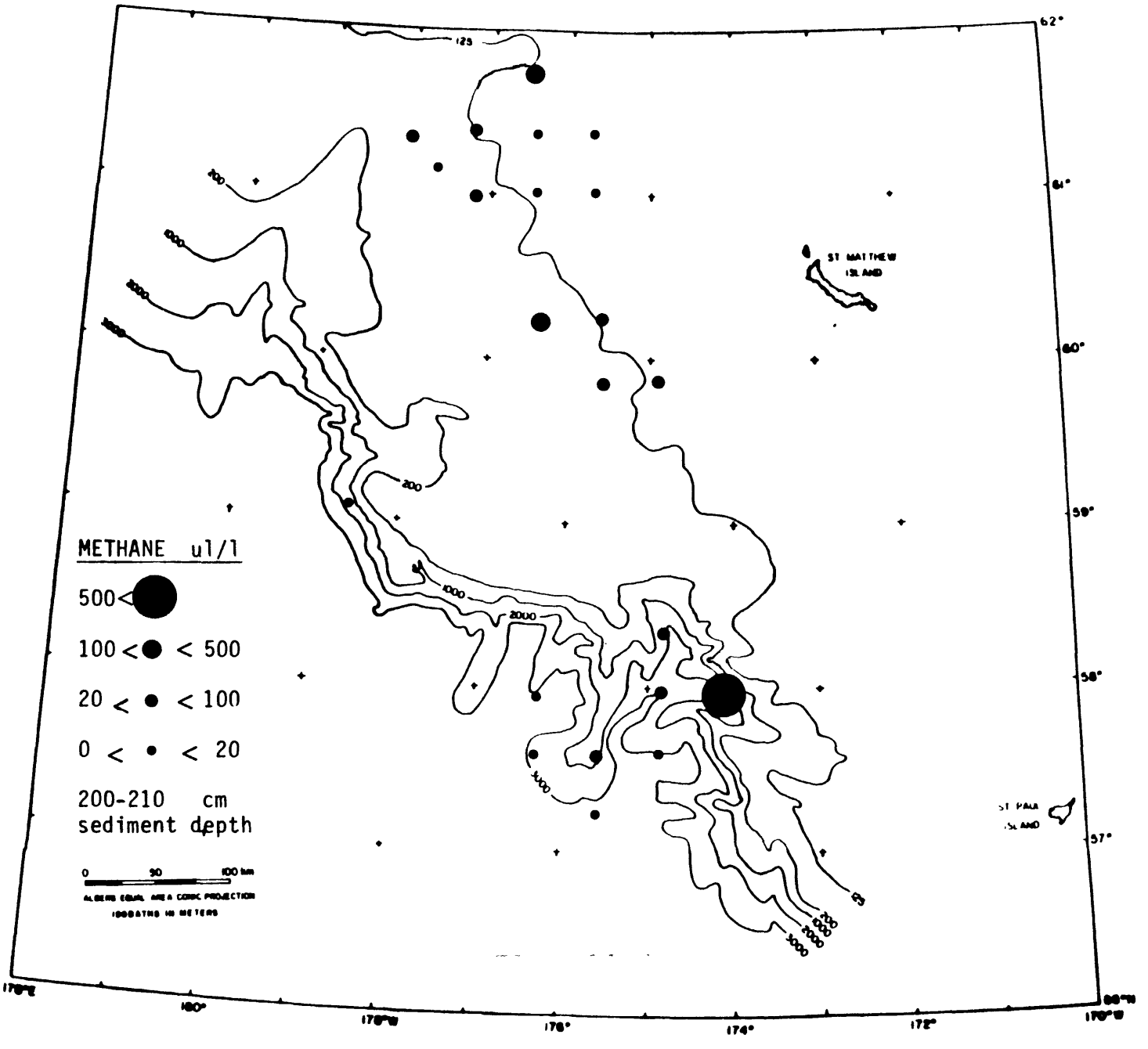

Figure 34. Distribution of methane at 200-210 cm sediment depth; reported in µl/liter of wet sediment.

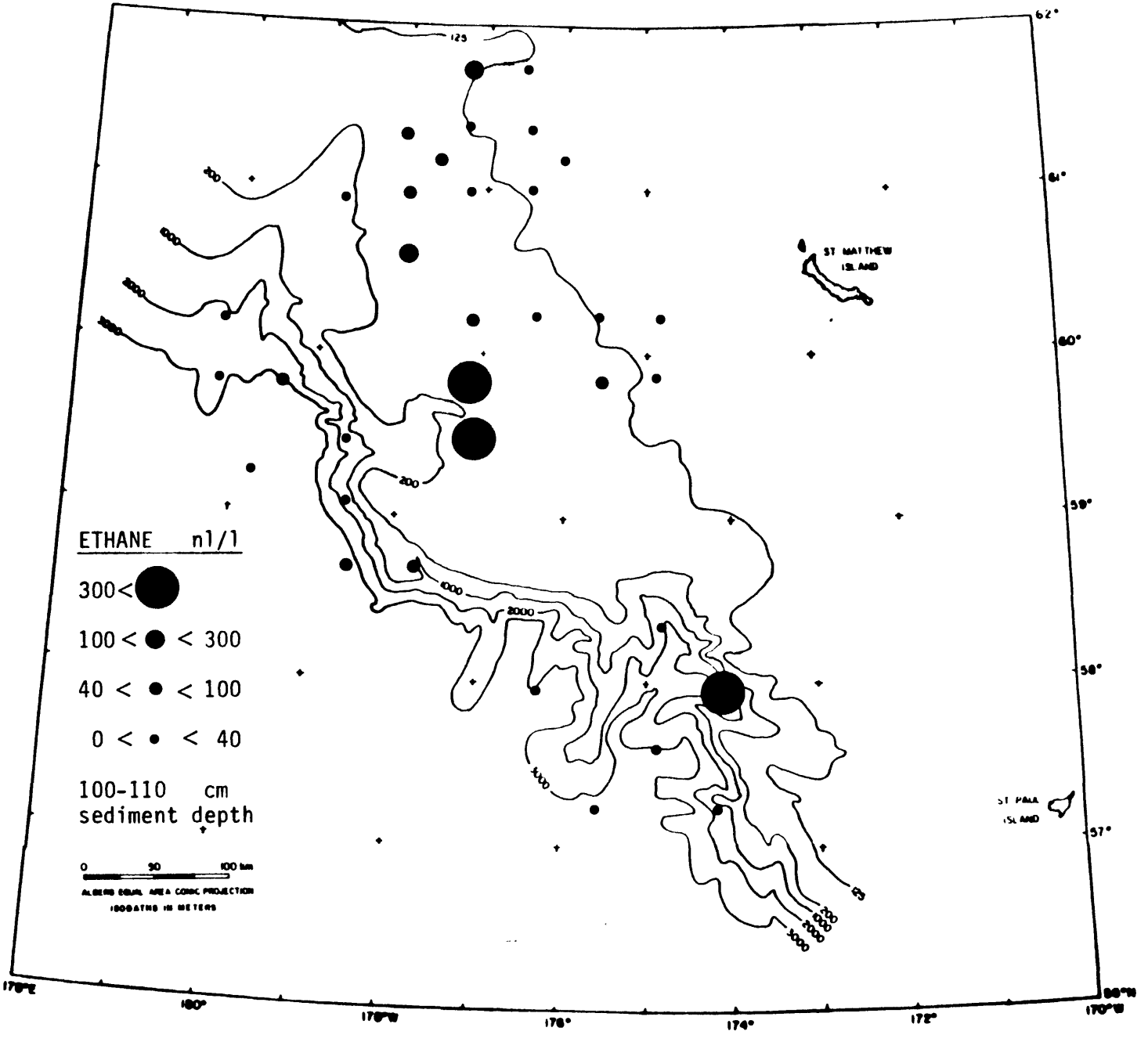

Figure 35. Distribution of ethane at 100-110 cm sediment depth; reported in nl/liter of wet sediment.

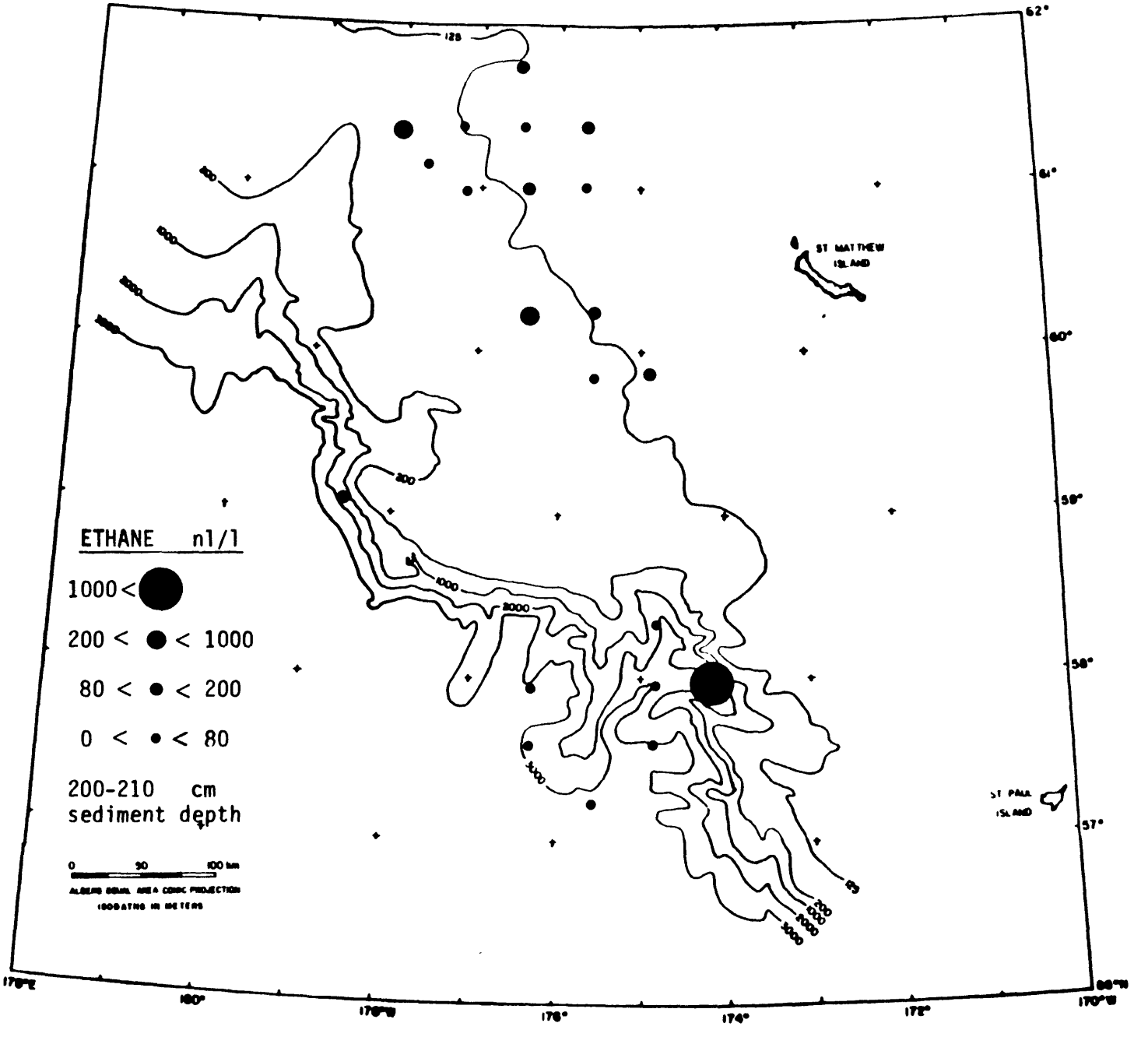

Figure 36. Distribution of ethane at 200-210 cm sediment depth; reported in nl/liter of wet sediment.

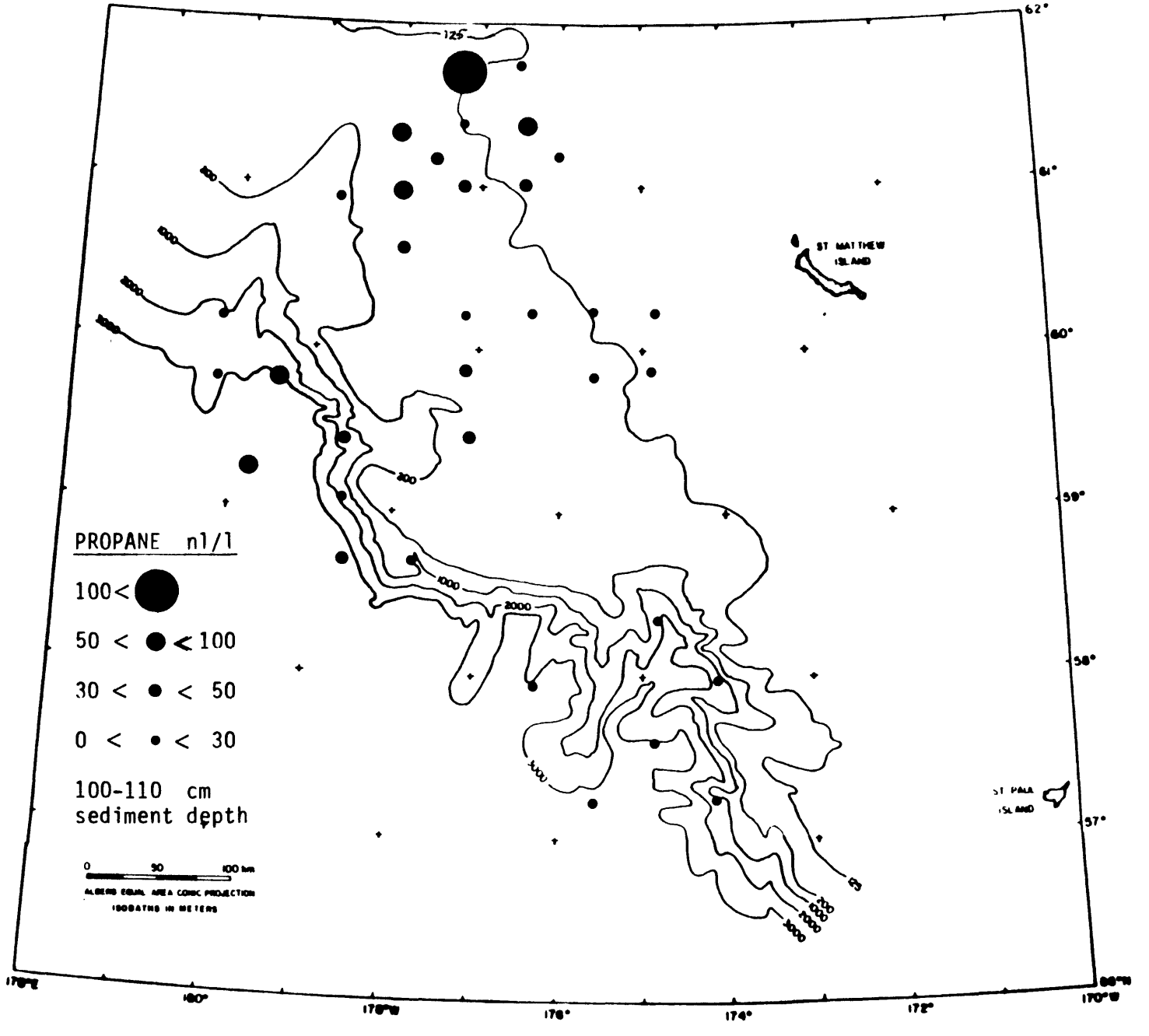

Figure 37. Distribution of propane at 100-110 cm sediment depth; reported in nl/liter of wet sediment.

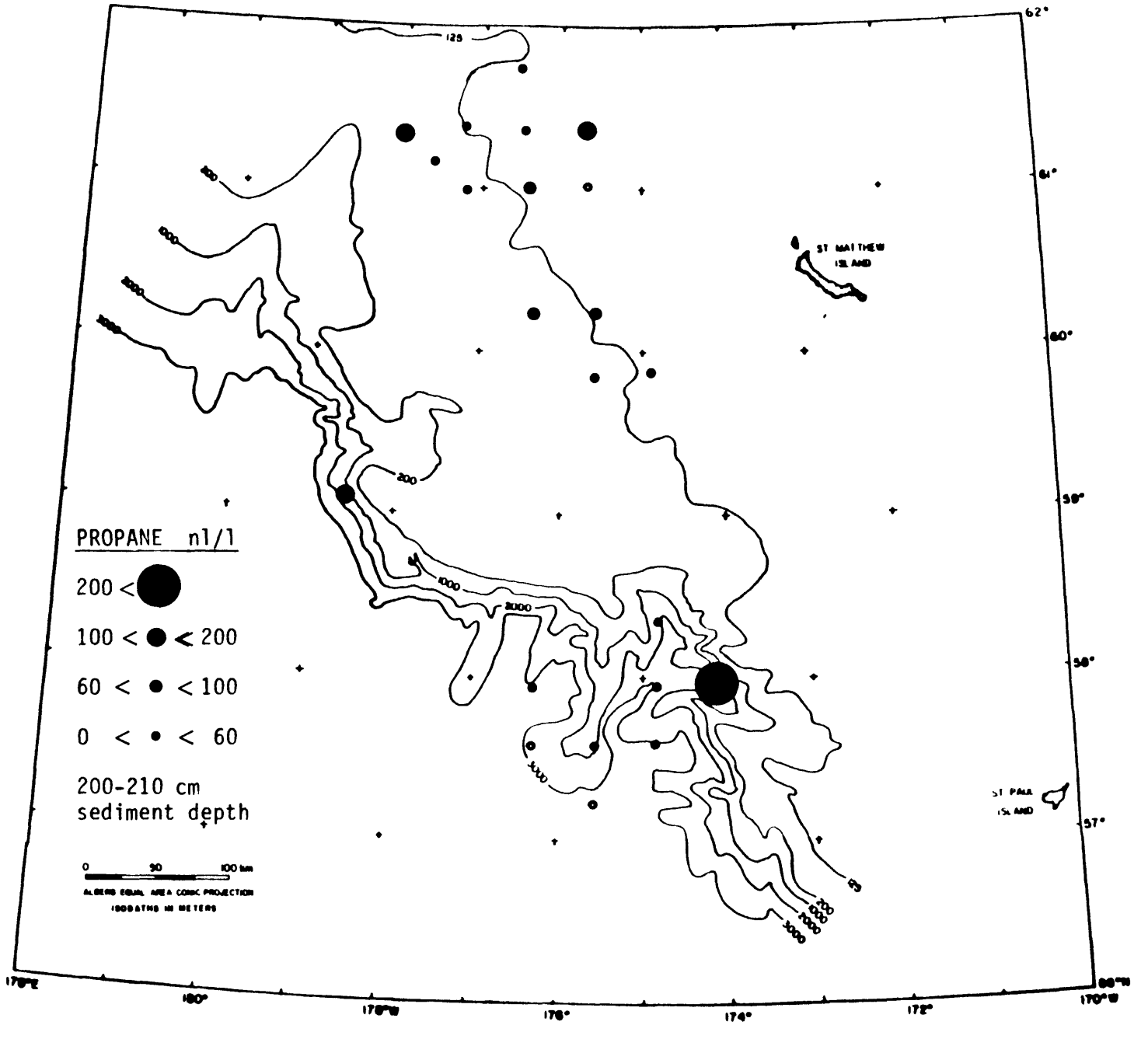

Figure 38. Distribution of propane at 200-210 cm sediment depth; reported in nl/liter of wet sediment.

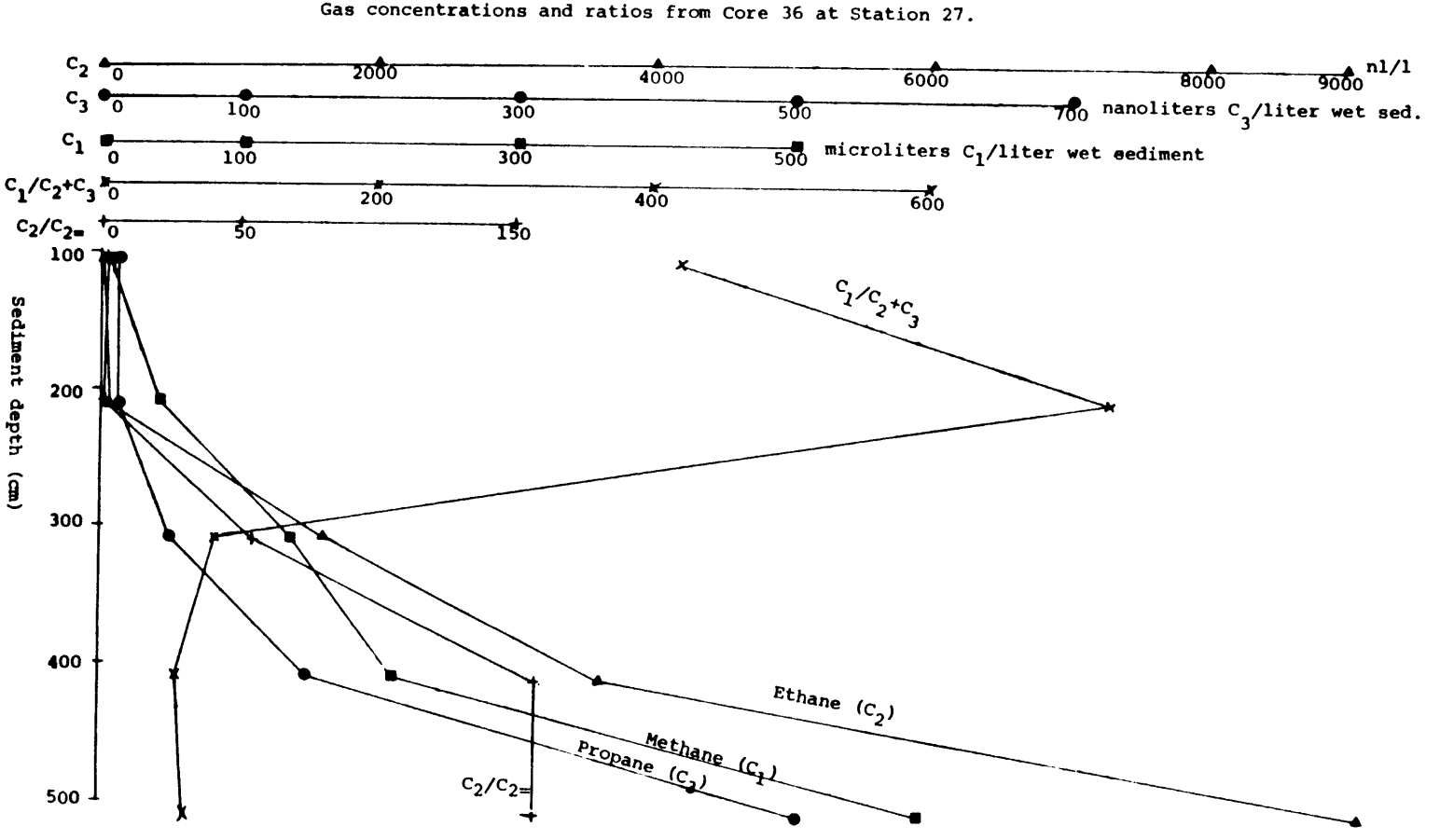

Figure 39. Graph of C_1-C_3 concentrations and C_1/C_2+C_3 and $C_2/C_{2=}$ ratios with depth in core 36.

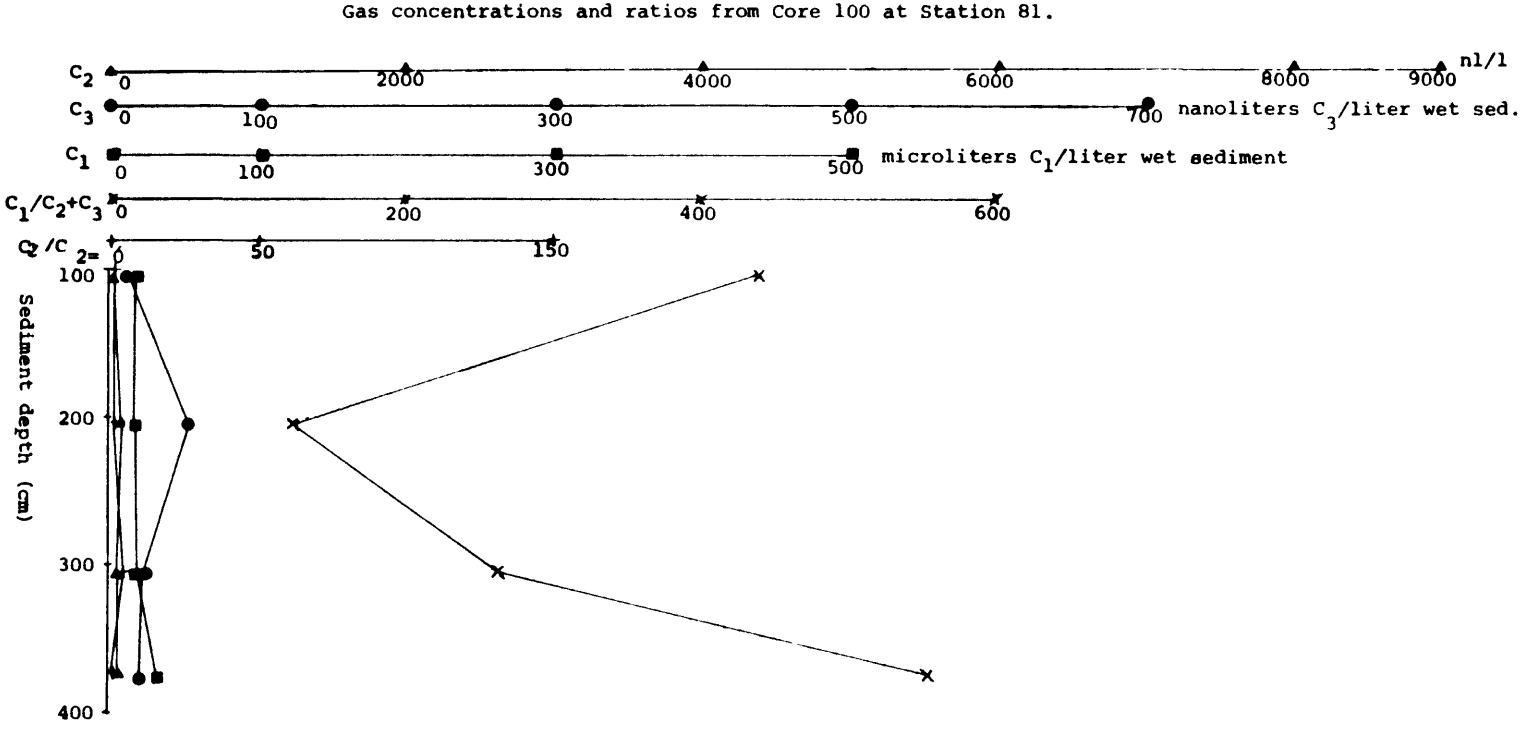

Figure 40. Graph of C_1-C_3 concentrations and C_1/C_2+C_3 and $C_2/C_{2=}$ ratios with depth in core 100. A typical type I hydrocarbon distribution.

Table 8. Hydrocarbon Gas (C_1-C_{5+}) Concentrations and Ratios from Sediment Samples from the Navarin Basin Province

Sample No. and Interval in cm	Water Depth (m)	Sta. No.	C_1 ul/l wet sed.	C_2 nl/l sed.	$C_{2:1}$	C_3	$C_{3:1}$	i-C_4	n-C_4	C_{5+}	$\frac{C_1}{C_2+C_3}$	$\frac{C_2}{C_{2:1}}$	$\frac{C_3}{C_{3:1}}$	$\frac{C_2}{C_3}$	Location Latitude	Location Longitude	Gas Type
G22 493-503	2842	16	620	8500	40	200	n.d.	10	0	0	70	200	-	40	58°29.8'	178°09.6'	III
G23 100-110	110	17	7	20	20	10	n.d.	0	0	0	190	1.2	-	2	60°14.5'	174°48.7'	I
G25 100-110	140	19	90	840	30	50	n.d.	0	6	70	100	30	-	20	59°50.8'	177°06.8'	III
G25 191-201	140	19	0	20	0	60	n.d.	0	0	20	10	-	-	0.3	59°50.8'	177°06.8'	I
G26 100-110	3373	20	7	30	20	50	n.d.	0	8	40	90	1.4	-	0.6	59°13.8'	179°43.9'	IV
G29 100-110	109	22	10	30	20	10	n.d.	0	0	0	270	1.2	-	3	61°11.4'	176°01.2'	I
G30 87-97	120	23	80	160	60	100	n.d.	6	20	20	290	3	-	2	61°43.8'	177°14.0'	III
G31 100-110	150	24	20	40	40	60	n.d.	6	8	310	170	1.0	-	0.7	61°19.9'	178°01.0'	IV
G31 200-210	150	24	30	330	160	150	120	10	8	0	70	2.0	1.3	2	61°19.9'	178°01.0'	IV
G34 100-110	210	25	7	30	30	20	n.d.	0	0	110	150	1.0	-	1.1	60°55.3'	178°46.9'	I
G34 270-280	210	25	10	60	50	20	114	0	0	0	160	1.1	0.2	3	60°55.3'	178°46.9'	I
G36 100-110	1924	27	7	6	8	10	n.d.	0	0	80	420	0.7	-	0.5	60°09.0'	179°49.0'	I
G36 200-210	1924	27	40	50	20	10	n.d.	0	0	50	730	2.0	-	5	60°09.0'	179°49.0'	I
G36 300-310	1924	27	140	1600	30	50	n.d.	0	0	30	80	50	-	32	60°09.0'	179°49.0'	III
G36 400-410	1924	27	210	3600	20	150	n.d.	0	10	30	60	160	-	24	60°09.0'	179°49.0'	III
G36 500-510	1924	27	600	9100	60	500	n.d.	8	10	440	60	160	-	18	60°09.0'	179°49.0'	III
G37 100-110	2856	28	2	0	0	0	n.d.	0	0	60	-	-	-	-	59°26.3'	179°48.3'	I
G37 431-441	2856	28	1900	1700	90	1000	0	270	20	60	700	20		2	59°26.3'	179°48.3'	III
G41 71-81	148	31	20	60	70	50	n.d.	10	10	210	130	0.9	-	1.2	60°58.3'	177°59.3'	IV
G42 100-110	141	32	20	40	40	50	n.d.	6	0	160	180	1.1	-	0.9	61°09.8'	177°37.9'	IV
G42 194-204	141	32	20	50	30	30	130	0	0	0	200	1.4	0.3	1.4	61°09.8'	177°37.9'	I
G43 100-110	148	33	10	20	30	50	n.d.	0	0	150	871	0.6	-	0.3	61°10.9'	177°36.1'	IV
G43 236-246	148	33	20	40	10	50	80	0	0	0	220	4	0.6	0.9	61°10.9'	177°36.1'	I
G44 100-110	138	34	7	20	20	0	n.d.	0	0	210	370	1.1	-		60°11.9'	177°34.2'	I
G44 190-200	138	34	10	50	60	50	120	0	0	0	100	0.8	0.5	0.9	60°11.9'	177°34.2'	I
G45 96-106	137	35	2	10	20	130	n.d.	0	0	160	20	0.7	-	0.1	61°13.1'	177°32.3'	IV
G47 74-84	134	36	1	30	0	0	n.d.	0	0	120	40		-		61°14.4'	177°30.5'	I
G48 100-110	124	37	10	30	30	20	n.d.	0	0	60	290	1.1	-	2	61°22.3'	177°13.9'	I
G48 182-192	124	37	20	50	30	30	70	0	0	0	280	1.4	0.4	2	61°22.3'	177°13.9'	I
G49 100-110		38	30	30	10	20	n.d.	0	0	50	550	2	-	2			
G49 222-232		38	100	150	30	40	80	0	0	0	530	5	0.5	4			II
G50 101-111	110	39	6	20	6	50	n.d.	0	0	120	80	3	-	0.3	61°22.3'	176°25.2'	IV
G50 208-218	110	39	10	50	20	30	50	0	0	0	150	2	0.6	2	61°22.3'	176°25.2'	I

Table 8. (Continued)

Sample No. and Interval in cm.	Water Depth (m)	Sta. No.	C_1 ul/l wet. sed.	C_2 nl/l sed.	$C_{2:1}$	C_3	$C_{3:1}$	i-C_4	n-C_4	C_{5+}	$\frac{C_1}{C_2 + C_3}$	$\frac{C_2}{C_{2:1}}$	$\frac{C_3}{C_{3:1}}$	$\frac{C_2}{C_3}$	Location Latitude	Location Longitude	Gas Type
G51 100-110	123	40	9	10	10	40	n.d.	0	0	20	160	1.1	-	0.2	60°59.2'	177°12.2'	IV
G51 207-217	123	40	30	60	30	30	80	0	0	0	300	2	0.4	2	60°59.2'	177°12.2'	I
G52 100-110	159	41	20	160	20	30	n.d.	4	0	20	100	10	-	5	60°35.6'	177°57.4'	IV
G52 167-177	159	41	80	1200	20	20	50	0	0	0	60	67	0.5	50	60°35.6'	177°57.4'	IV
G54 100-110	2929	43	20	50	50	60	n.d.	10	10	150	230	0.9	-	0.8	59°47.2'	179°25.2'	IV
G54 283-293	2929	43	60	970	130	140	40	8	10	0	60	7	4	7	59°47.2'	179°25.2'	IV
G58 100-110	118	46	10	10	20	40	n.d.	0	0	0	200	0.6	-	0.3	60°59.9'	176°24.4'	I
G58 221-231	118	46	20	80	60	60	70	0	0	0	140	1.4	0.8	1.4	60°59.9'	176°24.4'	I
G59 210-220	99	47	6	120	260	160	80	10	30	0	20	0.5	2	0.8	61°22.4'	175°39.3'	IV
G60 100-110	106	48	3	10	10	10	n.d.	0	0	0	150	1.0	-	1.0	61°00.1'	175°35.7'	I
G60 195-205	106	48	10	60	70	30	90	0	0	0	130	0.8	0.4	2	61°00.1'	175°35.7'	I
G61 100-110	125	49	1	0	0	0	n.d.	0	0	0	-	-	-	-	60°36.8'	176°23.4'	I
G61 230-240	125	49	40	90	80	60	90	0	6	0	290	1.1	0.7	2	60°36.8'	176°23.4'	I
G63 100-110	150	50	40	50	30	30	n.d.	6	6	0	470	2	-	2	60°12.7'	177°08.8'	II
G63 174-184	150	50	60	220	300	100	130	0	0	0	190	0.7	0.8	2	60°12.7'	177°08.8'	IV
G65 100-110	1609	52	3	30	40	40	n.d.	0	0	0	40	0.8	-	0.9	59°26.4'	178°35.9'	IV
G65 171-181	1609	52	40	90	60	30	130	0	0	0	350	2	0.2	4	59°26.4'	178°35.9'	I
G66 100-110	1336	53	3	20	20	20	n.d.	0	0	0	70	1.3	-	1.2	58°3.9'	178°34.7'	I
G66 200-210			4	140	170	110	120	10	0	0	20	0.9	0.9	1.4			IV
G66 300-310			4	130	130	90	90	0	10	0	20	1.0	1.0	1.4			IV
G66 400-410			8	140	30	40	70	0	0	0	40	6	0.7	3			IV
G66 520-530	1336	53	8	190	20	170	90	8	0	0	20	12	2.0	1.1	58°3.9'	178°34.7'	IV
G68 100-110	132	56	90	30	30	10	n.d.	0	0	0	2000	1.0	-	3	60°13.8'	176°20.9'	II
G68 149-159	132	56	90	110	50	40	100	0	0	0	590	2.0	0.5	2	60°13.8'	176°20.9'	IV
G69 100-110	117	58	10	10	10	20	n.d.	0	0	0	330	0.8	-	0.5	60°14.2'	175°35.5'	I
G69 193-203	117	58	40	110	60	70	130	0	0	0	230	1.7	0.6	2	60°14.2'	175°35.5'	IV
G70 198-208	142	59	160	380	30	70	150	10	0	0	360	13	0.5	6	59°51.3'	176°20.5'	III
G71 95-105	151	60	50	330	50	40	n.d.	4	8	0	140	6	-	9	59°28.0'	177°05.6'	III
G73 100-110	3170	62	20	90	50	40	n.d.	6	8	170	140	2.0	-	3	58°40.9'	178°32.2'	IV
G74 100-110	950	63	5	50	40	30	n.d.	8	8	0	60	1.3	-	2	58°42.3'	177°47.2'	I
G74 168-178	950	63	260	3000	30	60	240	0	0	0	80	110	0.3	50	58°42.3'	177°47.2'	III
G80 110-120	128	66	50	70	20	30	90	0	0	0	440	3	0.3	3	59°51.2'	175°34.3'	I
G81 100-110	117	67	5	10	0	10	n.d.	0	0	0	280	-	-	1.0	59°52.4'	174°52.8'	I
G81 199-209	117	67	30	100	30	50	140	0	0	0	180	3	0.4	2	59°52.4'	174°52.8'	I
G83 225-235	105	68	7	40	50	40	120	8	0	0	90	0.9	0.4	1.1	57°56.1'	171°56.7'	I

Table 8. (Continued)

Sample No. and Interval in cm.	Water Depth (m)	Sta. No.	C_1 ul/l wet sed.	C_2 nl/l sed.	$C_{2:1}$	C_3	$C_{3:1}$	i-C_4	n-C_4	C_{5+}	$\frac{C_1}{C_2 + C_3}$	$\frac{C_2}{C_{2:1}}$	$\frac{C_3}{C_{3:1}}$	$\frac{C_2}{C_3}$	Location Latitude	Location Longitude	Gas Type
G88 100-110	1252	72	2	10	30	10	n.d.	0	0	40	90	0.4	-	1.0	57°13.7'	174°09.8'	I
G97 100-110	1570	79	70	380	20	30	n.d.	0	0	180	180	25	-	15	57°58.6'	174°07.1'	IV
G97 192-202	1570	79	860	1360	40	220	110	30	10	0	550	35	2	6	57°58.6'	174°07.1'	III
G99 100-110	3075	80	8	20	30	10	n.d.	0	0	10	270	0.7	-	1.3	57°35.7'	174°52.5'	I
G99 200-210	3075	80	10	20	10	20	20	0	0	0	270	2	0.8	1.4	57°35.7'	174°52.5'	I
G99 300-310	3075	80	10	30	20	20	40	0	0	0	250	1.3	0.4	1.5	57°35.7'	174°52.5'	I
G99 398-408	3075	80	9	40	30	30	90	0	0	0	140	1.4	0.3	1.5	57°35.7'	174°52.5'	I
G100 100-110	3232	81	20	20	30	10	n.d.	0	0	120	440	0.7	-	1.4	57°13.5'	175°34.0'	I
G100 200-210	3232	81	20	80	40	50	70	6	10	0	120	2	0.8	1.4	57°13.5'	175°34.0'	I
G100 300-310	3232	81	20	50	10	20	30	0	0	0	260	4	0.7	2	57°13.5'	175°34.0'	I
G100 372-382	3232	81	30	40	30	20	90	0	0	0	550	1.3	0.2	2	57°13.5'	175°34.0'	I
G101 207-217	2155	82	20	90	20	30	60	0	0	0	170	4	0.4	3	57°36.5'	175°34.2'	I
G101 309-319	2155	82	50	230	30	40	100	0	0	0	180	9	0.4	6	57°36.5'	175°34.2'	IV
G102 211-221	2960	83	70	60	30	30	60	0	0	0	860	2	0.5	2	57°58.5'	174°51.4'	II
G105 100-110	2050	86	30	40	40	20	n.d.	0	10	90	540	0.9	-	2	58°20.9'	174°50.3'	II
G105 200-210	2050	86	40	70	40	30	90	0	0	0	410	2	0.3	3	58°20.9'	174°50.3'	I
G105 300-310	2050	86	50	160	130	120	140	0	20	8	170	1.2	0.8	1.4	58°20.9'	174°50.3'	IV
G107 100-110	2750	88	10	230	490	190	230	30	30	20	20	0.5	0.8	1.2	57°36.3'	176°16.5'	IV
G107 200-210	2750	88	20	200	660	200	230	20	40	30	20	0.3	0.9	1.0	57°36.3'	176°16.5'	IV
G108 100-110	3253	89	4	20	90	10	n.d.	0	0	120	120	0.2	-	2	57°57.1'	176°17.7'	I
G108 200-210	3253	89	10	30	40	40	90	0	0	0	190	0.9	0.5	0.8	57°57.1'	176°17.7'	I
G108 300-310	3253	89	20	90	70	70	90	0	0	0	100	1.3	0.8	1.3	57°57.1'	176°17.7'	I
G109 100-110	610	90	6	70	40	60	90	0	0	0	50	2	0.6	1.3	58°20.9'	175°33.8'	I

n.d.= not determined

Table 9. CLASSIFICATION OF SEDIMENT GAS TYPES

	TYPE I	TYPE II	TYPE III	TYPE IV
METHANE	LOW	HIGH	HIGH	VARIABLE
ETHANE	LOW	LOW	HIGH	VARIABLE
PROPANE	LOW	LOW	HIGH	VARIABLE
ETHENE	LOW	VARIABLE	LOW	LOW
PROPENE	LOW	VARIABLE	LOW	LOW
ISOBUTANE	LOW	LOW	LOW	LOW
N-BUTANE	LOW	LOW	LOW	LOW
C_1/C_2+C_3	VARIABLE	HIGH	LOW	VARIABLE
$C_2/C_{2=}$	LOW	LOW	HIGH	VARIABLE

DIATOMS FROM LATE QUATERNARY SEDIMENTS FROM THE NAVARIN BASIN PROVINCE

Jack G. Baldauf

INTRODUCTION

Diatoms are difficult to use as biostratigraphic indicators because no extinctions or first occurrences exist younger than 0.26 m.y., therefore, it is necessary to use fluctuations in abundance of commonly occurring species, such as Denticulopsis seminae and Nitzschia oceanica, to identify the glacial and interglacial stages of the late Quaternary and the probable Holocene/Pleistocene boundary.

METHODS AND PROCEDURE

Strewn slides of unproccesed sediment were prepared for each sample. Near top and bottom samples of each core were scanned at 500 x for age-related species. Samples from 30 core tops were used to establish the modern ecological distribution and samples taken at 15 cm intervals down two cores were used for down-core studies (Fig. 41). Strewn slides were examined in detail at 1,250 x, and the first 300 specimens encountered were tabulated to determine the abundance of individual species within each sample.

The quality of preservation for each sample was based on the absence and presence of selected diatoms. Fine, delicate species such as Thalassiosira hyalina, Thalassiothrix longessima, and Pseudopodosira elegans, were used to determine well preserved samples, whereas the presence of only heavily-silicified forms such as Coscinodiscus marginatus, C. radiatus and Rhizosolenia hebatata forma. hebatata, suggest poor preservation.

RESULTS

Cores recovered from this region were examined and all except Core 106 contain late Quaternary diatoms. Core 106 is assigned to the Denticulopsis seminae var. fossilis - D. kamtschatica Zone of Barron (1980) and is equivalent in age to the early late Pliocene. Occurrence of Pliocene sediments within this core is not surprising, because the core is located on the continental slope where down-slope transport may be a common phenomenon.

Table 10 shows the occurrences of species encountered during the examination of the surface samples. The assemblages composed of planktic and tychopelagic species (See Plate 1), represent the Arctoboreal and North Boreal diatom complexes of Jouse (1971). The abundance of individual taxa remains fairly constant throughout the study area, with the exception of Denticulopsis seminae and Nitzschia oceanica. These two species alternate in their dominance of the two identified assemblages. D. seminae comprises 22 to 40 percent of the assemblage in areas where water depths are greater than 2800 m (Fig. 42). This abundance rapidly decreases to 10 to 20 percent near the shelf break at approximately 200 m water depth, and only to 1 to 10 percent in sediment from water depths less than 200 m. This distribution pattern agrees

well with the pattern described by Sancetta (in press) for the entire Bering Sea. Nitzschia oceanica is the other common diatom species within the Navarin Basin surface sediment. This species is abundant in sediment from the shallow shelf in the northwestern portion of the study area where it composes approximately 25 percent of the assemblage (Fig. 43). The abundance of N. oceanica gradually decreases southward, across the continental slope to the deeper regions where it comprises 7-15 percent of the assemblage. This pattern of abundance is consistent with previous studies by Jouse (1962, 1967), Hasle (1965), and Kozlova and Mukhina (1967) and Sancetta (in press) who all found N. oceanica to be common in the Arctic coastal waters as well as in coastal regions of the Bering Sea. In addition, Gran (1904), Homer and Alexander (1972), and Sancetta (in press) concluded that N. oceanica is associated with ice-covered areas where ice exists for a period of at least six months.

The boundary between dominance of the floras by N. oceanica and D. seminae in surface samples closely coincides with the shelf break (Fig. 44). The southern zone, dominated by D. seminae, is confined to the Aleutian basin region, whereas the shelf zone is dominated by N. oceanica, and corresponds to the extent of ice distribution in the Bering Sea (Park and others, 1974).

The present day distribution of diatoms within surface sediments of Navarin Basin provides a foundation for ecological interpretations of diatom assemblages from stratigraphic samples. All intervals examined from Cores 13 and 26 contain diatoms of the late Quaternary Denticulopsis seminae Zone of Barron (1980). The stratigraphic assemblages are similar to those of surface samples and are dominated by D. seminae or N. oceanica with an occasionally common occurrence of Thalassiosira gravida (Fig. 45). However, in Core 26, at the intervals 231 cm and 300 cm, rare specimens of Rhizosolenia curvirostris and Thalassiosira nidulus occur, that suggest the sediment is slightly older. Well-preserved diatoms of the D. Seminae Zone exist below these two intervals, which suggests that specimens within the intervals of 231 cm and 300 cm are reworked.

Sediments in the upper 232 cm of Core 13 located in 2962 m of water are dominated by D. seminae. Denticulopsis seminae composes approximately 25 percent of the assemblage in this interval and is similar to the abundance within the surface samples. The abundance of D. seminae sharply decreases at 232 cm as the abundances of N. oceanica and T. gravida increase. This dominance of N. oceanica and T. gravida continues to the base of the core at 290 cm.

A similar pattern exists in the top 230 cm of core 26 taken in 3377 m of water. The remaining samples in core 26 show a brief increase, at 250 cm in the number of D. seminae and a decrease in the abundance of N. oceanica and T. gravida prior to the overall domination of N. oceanica and T. gravida. Minor fluctuations in the three taxa exist within the upper 227 cm but may in part result from downslope transport from Navarinsky and Pervenets Canyons, which have submarine fans that intersect near the location of core 26.

The distribution of N. oceanica in surface samples suggest this species represents a cold-water form associated with ice, whereas the distribution of

D. seminae suggests it represents a true oceanic form associated with cool waters. It is therefore possible to use this pattern to interpret the stratigraphic occurrences of dominant N. oceanica over D. seminae in cores 13 and 26 as a record of the last glacial event in the Bering Sea. Consequently, the Holocene/Pleistocene boundary may be placed immediately above the interval.

The abundance of Thalassiosira gravida, which mimics the abundance of N. oceanica throughout the core, supports this conclusion. T. gravida is a coarse, well-silicified species associated with conditions on the shelf and upper slope. Lowered sea level during a glacial stage exposes broad areas of the continental shelf to erosion and results in increased downslope transport of sediments. Concentrations of frustules of T. gravida occur at 231 cm in core 13, and 227 cm in core 26 and can be interpreted to correlate with a marine regression. The lithology of the cores lends further support to the interpreted glacial/interglacial transition. Both cores are predominately mud; however, in core 13, from 227 to 237 cm, and in core 26, from 223 to 230 cm, an interval of pebbles, gravels and shell fragments occurs. These coarse grain layers probably represent lag deposits. The top of these intervals occur exactly where the reversal of the diatom species takes place.

If the change-over in dominance of D. seminae and N. oceanica is assumed to represent the end of the last glacial event at about 11,000 years ago, then an average sedimentation rate of 22 cm/10^3 years is found in cores 13 and 26. This average sedimentation rate agrees with those calculated by Knebel and others (1974), who reported an approximate accumulation rate of 34 cm/10^3 years based on radio-carbon data.

To determine whether the D. seminae-N. oceanica reversal is a local event restricted to the immediate area, or if it can be reproduced in other areas of the Bering Sea, samples at 10 cm intervals were taken from a gravity core S3-77 6G1) recovered from the Aleutian Basin (Gardner, et al., in press). Diatom abundance data from these samples are also shown in Figure 45. The results from core 6G1 are similar to those obtained from cores 13 and 26 but suggest a lower sedimentation rate. The abundance of D. seminae in the upper 25 cm of 6G1 is 25 to 30 percent, followed down-core by a dominance of N. oceanica. A brief increase at approximately 60 cm occurs in D. seminae, a feature that also occurs in core 26. If the Holocene/ Pleistocene boundary is placed at 25 cm, this gives an average sedimentation rate of 2.25 cm/1000 years. The brief increase of D. seminae at 60 cm would reflect a warming trend that occurred about 25,000 y BP preceded by glacial conditions at about 29,000 y.BP.

CONCLUSION

Diatoms can be used to recognize glacial and interglacial events in late Quaternary sediments and allow recognition of the Holocene/Pleistocene boundary.

Cores within the study area are characterized by an assemblage dominated by D. seminae and relatively minor numbers of N. oceanica and T. gravida in the upper section of the cores. This is followed down core by an interval

where D. seminae abruptly decreases in abundance and is replaced by N. oceanica and T. gravida. This reversal is interpreted to define the Holocene/Pleistocene boundary at 11,000 y BP.

ACKNOWLEDGEMENTS

Paul Carlson and Herman Karl directed the surface and subsurface sampling within the Navarin Basin. Special thanks are given to John Barron for providing valuable assistance throughout the study, and to Kristin McDougall, John Barron and Jim Gardner for reviewing the manuscript.

REFERENCES CITED

Barron, J. A. 1980, Lower Miocene to Quaternary diatom fiostratigraphy of Leg 57, off northeastern Japan, Deep Sea Drilling Project; in Honza, E. and others, Initial Reports of the Deep Sea Drilling Project Volume LVI, LVII, Washington (U.S. Goverrment Printing Office). pp. 641-685.

Gardner, J. V., Dean, W. E., Klise, D. L., and Baldauf, J. G., in press, A climate-related oxidizing event in deep-sea sediment from the Bering Sea: Quaternary Research.

Gran, H. H., 1904, Diatomaceae from the ice-floes and plankton of the Arctic Ocean. In: F. Hansen (Editor), The Norwegian North Polar Expedition 1893-1896, IV: 1-74.

Hasle, G. R., 1965, Nitzchia and Fragilariopsis species studies in the light and electron microscopes. III The genus Fragilariopsis. Skrift. Norske videns.-Atkad. Oslo., Math.-Natur. Kl. 21 (n.s.): 1-47.

Horner, R. A. and Alexander, V., 1972, Algal populations in Arctic sea-ice: An investigatir of heterotrophy. Limnology and Oceanography 17:454-458.

Jouse, A. P., 1962. (Stratigraphic and Paleogeographic Investigations in the North-west Part of the Pacific Ocean). In Russian. Oceanol. Inst., Akad. Nauk, SSR, Moscow. 258 pp.

Jouse, A. P.,1967, Diatom floras and the history of Okhotsk and Bering Seas. In: D. Hopkins (Editor), The Bering Land Bridge. Standford University Press, Standford, California. pp. 369-372.

Jouse, A. P.,1971, Diatoms in Pleistocene sediments from the northern Pacific Ocean. In: Riedel, W. R. and Funnell B. M. (Eds.) The Micropaleontology of Oceans, Cambridge Univ. Press, Oxford. 407-421.

Knebel, H., Creager, J., and Echols, R., 1974, Holocene sedimentary framework, east-central Bering Sea continental shelf., in Herman, E. (ed.) Marine geology and oceanography of the Arctic Seas, Springer-Verlas, New York 1974, pp. 157-172.

Kozlova, O. G. and Mukhina, V. V., 1967, Diatoms and silicoflagellates in suspension and floor sediments of the Pacific Ocean: Internat. Geol. Rev. 9:1322-1342.

Lisitsyn, A. P., 1966, Recent sedimentation in the Bering Sea: Israel Program Sci. Transl., Jerusalem. Washington, D. C.: U.S. Department of Commerce, National Science Foundation, 614 pp.

Park, P. K., Gordon, L. I., and S. Alvarez-Borrego, 1974, Carbon dioxide systems of the Bering Sea In: D. W. Hood and E. J. Kelley (Editors) Oceanography of the Bering Sea, Institute of Marine Sciences, University of Alaska, Fairbanks, pp. 107-148.

Sancetta, C. (In press), Taxonomy and distribution of diatom in surface sediments of the Bering and Okhotsk Seas.

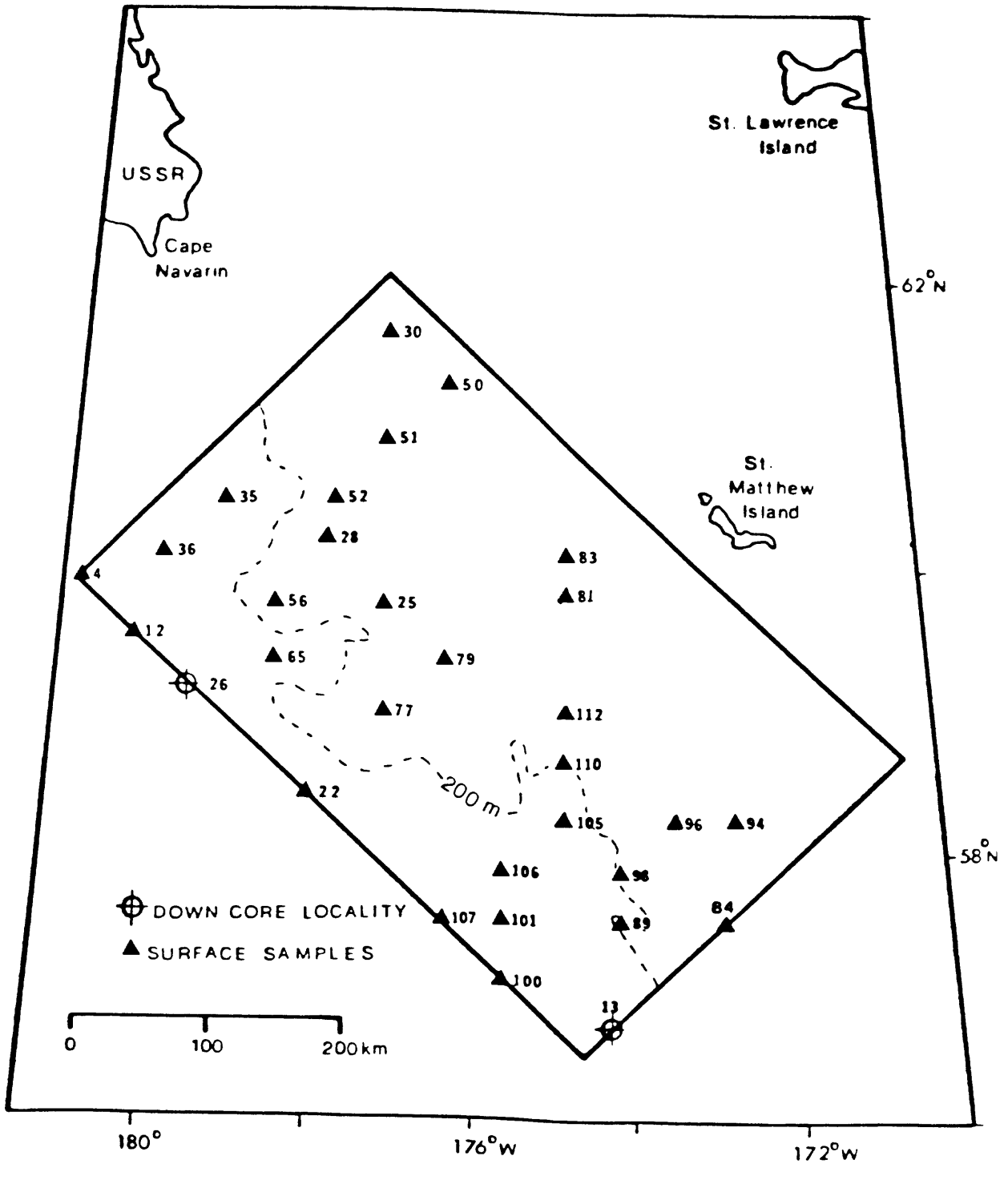

Figure 41. Location of surface samples and cores used for studies.

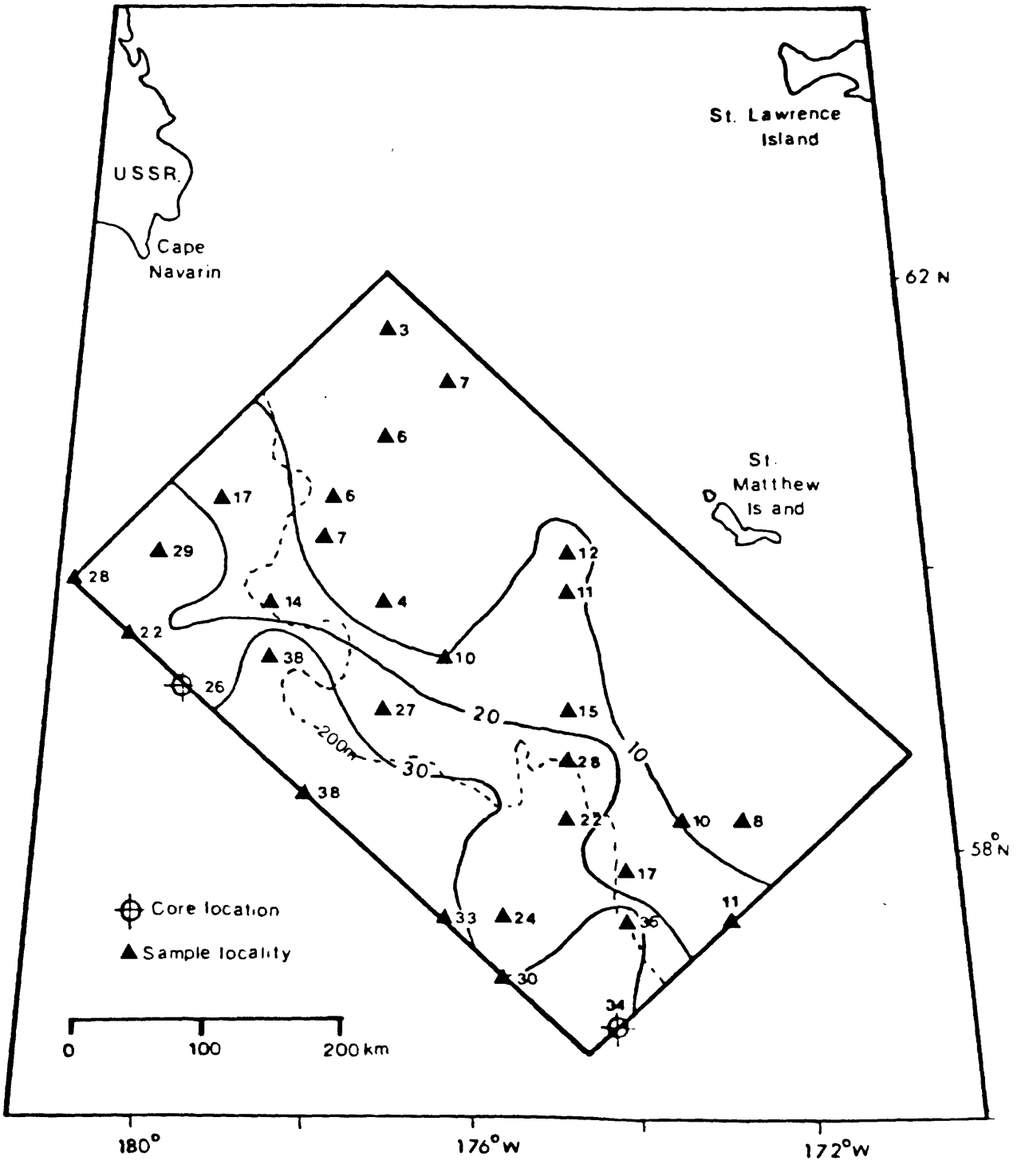

Figure 42. Distribution of Denticulopsis seminae in the surface sediments. Contours represent values of 10, 20 and 30 percent.

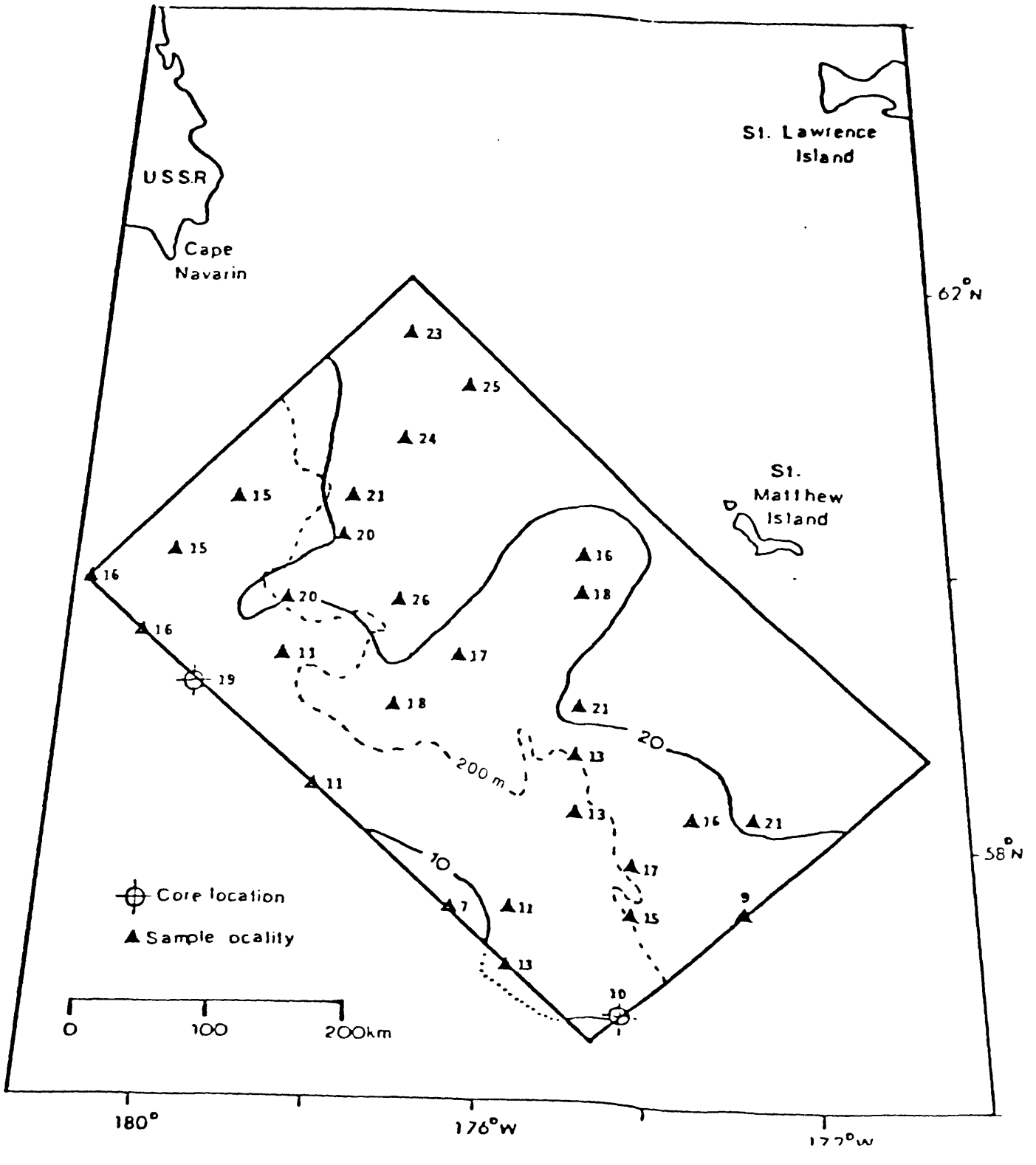

Figure 43. Distribution of Nitzschia oceanica in the surface sediments. Contours represent values of 10, 20, and 30 percent.

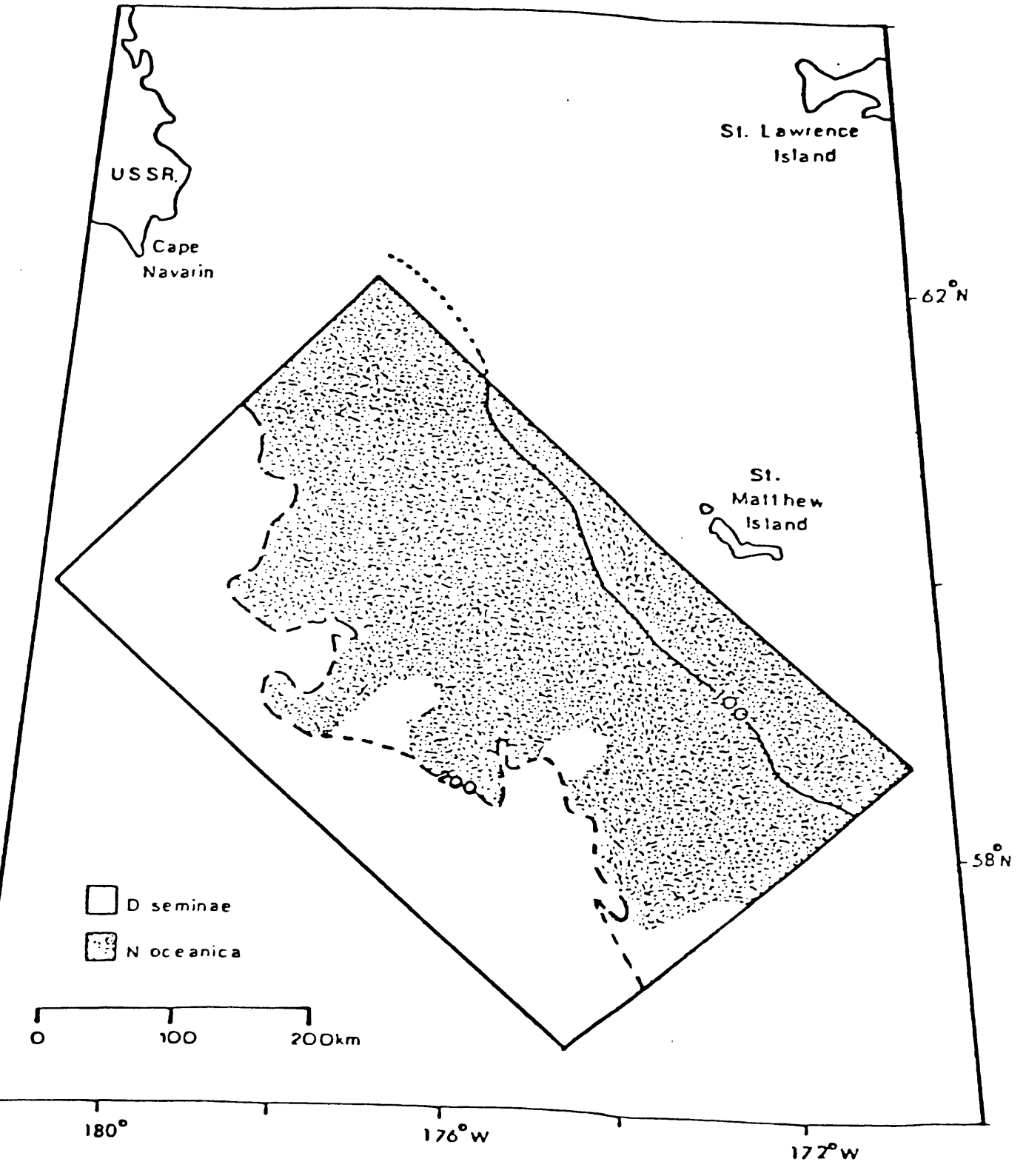

Figure 44. Area within the Navarin Basin, that is dominated by D. seminae or N. oceanica in the sediments. Contours represent depths of 100 and 200 meters. The 200 meters contour is the shelf-slope boundary.

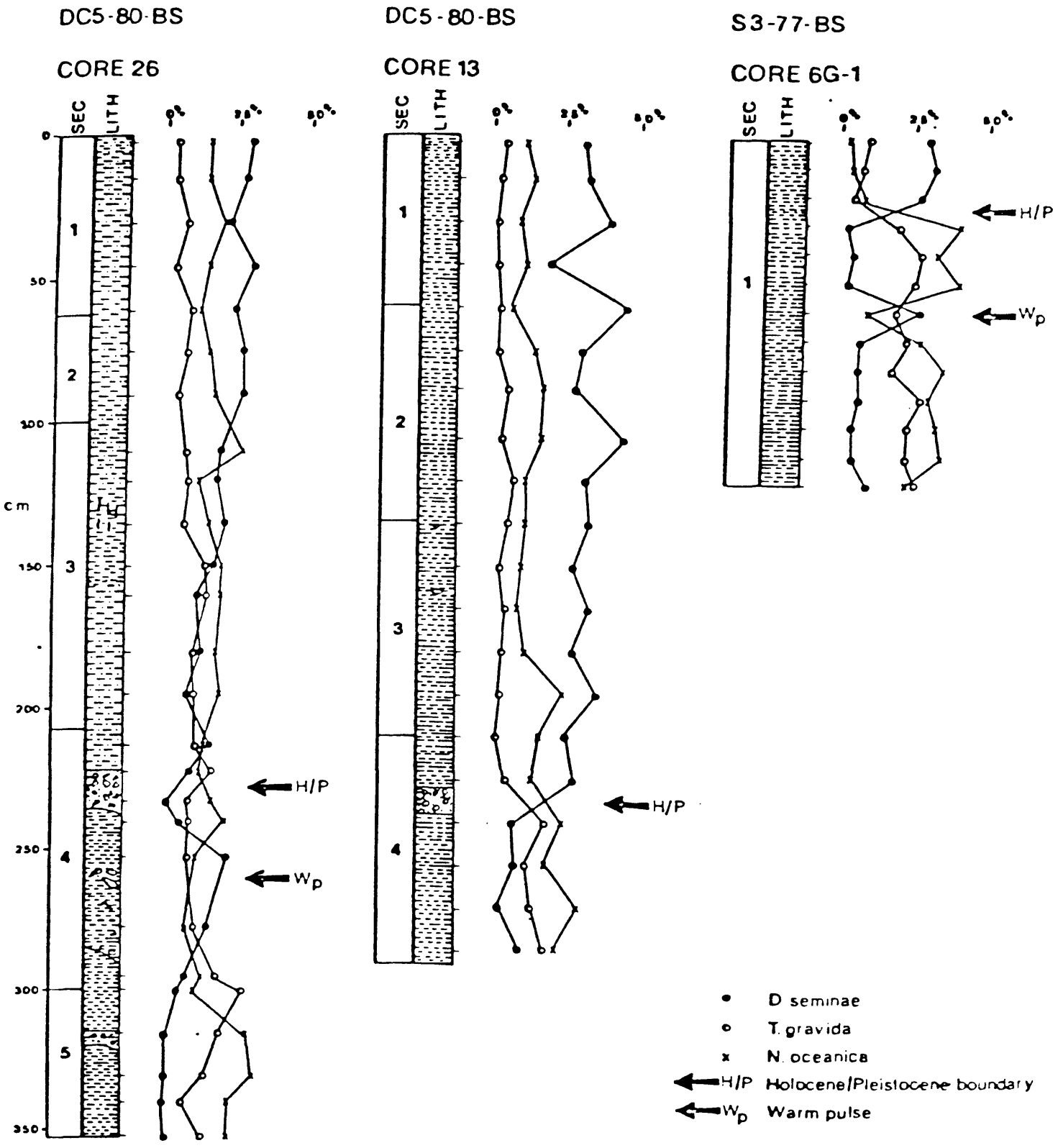

Figure 45. Down core abundance of Denticulopsis seminae, Nitzschia oceanica, and Thalassiosira gravida.

PLATE 1

Figures 1. Thalassiosira trifulata Fryxell
Sample 26-1, 75 cm; 28 μ m in diameter

2. Thalassiosira gravida Cleve
Sample 13-2, 135 cm; 25 μ m in diameter

3. Asteromphalus robustus Castracane
Sample 22-1, 2-3 cm; 56 μ m in diameter

4. Thalassiosira nordenskioldii Cleve
Sample 26-1, 75 cm; 22 μ m in diameter

5. Bacteria fragilis Gran
Sample 83-1, 0-2 cm; 20 m in diameter

6. Coscinodiscus lacustris Grunow
Sample 13-4, 79 μ m in diameter

7. Pseudopodosira elegans Sheshukova-Poretskaya
Sample 26-1, 75 cm; 17 μ m in diameter

8. Thalassiosira oestrupii
Sample 26-1, 75 cm; 8 μ m in diameter

9. Porosira glacialis (Grunow) Jørgensen
Sample 28-1, 0-2 cm4 48 μ m in diameter

10. Navicula sp. 2.
Sample 28-1, 0-2 cm; 48 μ m in length

11. Rhizosolenia hebatata f. hiemalis (Bailey) Gran
Sample 13-3, 165 cm; 84 μ m in length

12. Nitzchia oceanica (Cleve) Hasle
Sample 22-1, 2-3 cm; 28 μ m in length

13. Denticulopsis seminae (Semina) Simonsen
Sample 22-1, 2-3 cm; 34 μ m in length

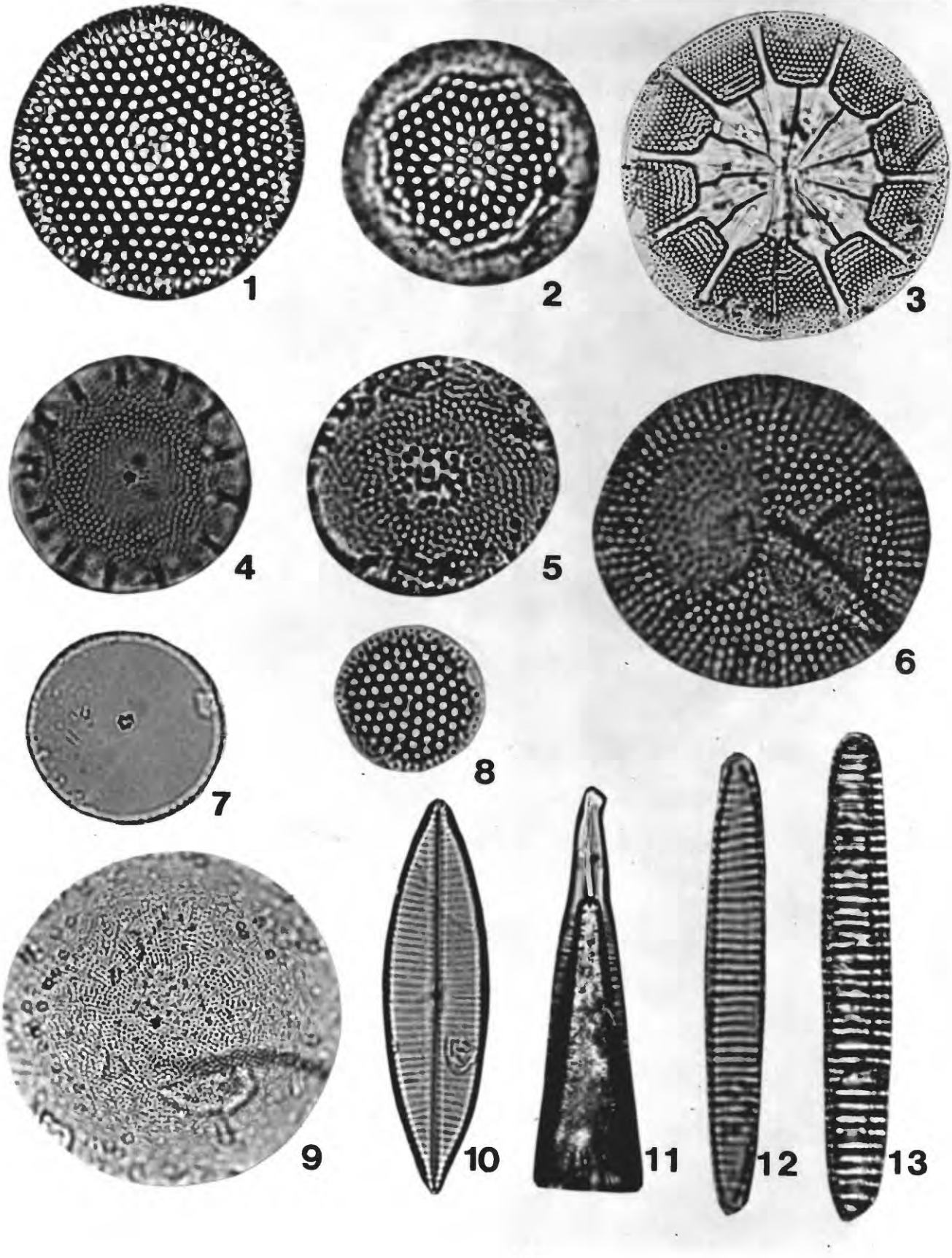
1
2
3
4
5
6
7
8
9
10
11
12
13

SPECIES \ SAMPLE	4	12	13	22	25	26	28	30	35	36	50	51	52	56	65
Actinocyclus curvatulus	-	-	0.3	-	0.6	-	-	-	-	-	-	-	0.6	1.0	-
A. divisus	0.6	0.6	0.3	0.3	1.6	0.3	2.6	0.3	1.0	0.6	1.0	1.0	0.3	1.6	-
A. ochotensis	-	-	-	1.0	-	-	-	0.6	0.6	-	-	-	1.0	1.6	-
Actinoptychus undulatus	-	-	-	-	0.6	-	0.3	-	-	-	0.6	-	-	-	0.3
A. vulgaris	-	0.3	-	0.3	-	-	-	-	-	0.3	-	-	-	-	-
Asteromphalus robustus	-	0.6	-	-	-	-	-	-	0.6	-	-	-	-	-	-
Bacteriosira fragilis	6.0	6.6	2.6	3.0	4.3	4.3	7.3	7.3	3.3	6.0	9.3	9.0	10.6	7.0	3.0
Biddulphia aurita	3.0	1.6	2.6	1.0	1.0	2.0	1.0	1.6	2.3	1.3	2.0	1.3	1.6	1.3	0.3
Coscinodiscus lacustris	-	-	-	0.3	-	-	-	0.3	-	-	0.6	-	-	-	-
C. marginatus	0.6	2.0	0.3	0.6	-	1.6	1.0	0.3	1.3	0.3	-	0.3	1.6	1.3	2.3
C. oculus-iridis	1.0	1.3	1.3	0.3	-	1.3	0.6	0.3	1.3	1.3	0.6	1.6	0.6	0.3	2.6
C. stellaris	-	-	-	-	-	-	-	-	-	-	-	-	-	-	-
C. tabularis	0.3	0.3	-	-	-	0.6	-	-	0.3	-	0.3	0.6	0.3	-	-
Denticulopsis seminae	28.0	27.0	31.3	38.3	4.0	26.0	7.3	3.0	17.0	29.0	7.0	6.3	6.0	14.3	33.0
Melosira clavigera	-	-	-	-	1.6	-	-	-	0.6	-	-	-	0.6	0.3	-
M. sulcata	1.0	1.0	0.6	2.0	7.6	1.0	2.6	5.3	3.3	2.6	3.6	5.3	3.6	4.3	1.6
Navicula sp. 1.	0.3	0.3	-	0.3	2.0	0.6	5.0	4.3	1.6	0.6	3.3	2.6	2.3	0.3	1.0
Navicula sp. 2.	-	0.3	0.3	0.3	1.0	-	0.6	-	1.3	1.6	0.6	1.3	0.6	0.6	0.6
Navicula sp. 3.	0.3	0.3	-	-	-	-	-	-	0.6	0.3	0.3	0.3	1.0	0.3	-
Nitzschia cylindrus	4.0	3.0	3.6	3.1	9.0	5.6	10.6	13.6	10.0	7.0	9.0	10.3	10.6	8.3	7.3
N. oceanica	16.3	10.6	9.6	11.0	26.3	19.0	19.3	36.0	18.6	15.0	25.6	24.3	20.6	20.3	11.3
Pleurosigma sp.	-	-	-	0.3	-	-	0.6	-	-	0.3	-	0.3	-	-	-
Porosira glacialis	1.0	2.0	1.3	1.6	2.3	3.0	4.6	2.6	3.6	3.6	2.1	1.3	6.0	3.3	4.0
Pseudopodosira elegans	1.3	3.0	-	1.3	1.3	0.6	0.6	-	0.6	-	-	1.0	-	2.6	-
Rhaphoneis sachalinensis	-	-	-	0.3	0.6	-	-	-	1.0	0.3	-	0.3	-	-	0.3
R. surirella	-	0.3	-	-	1.3	-	-	1.3	2.3	-	0.6	-	0.3	-	0.3
Rhizosolenia hebatata	2.6	3.0	4.6	3.0	1.6	3.3	1.6	0.3	2.0	1.6	0.3	1.6	2.6	2.3	2.3
R. styliformis	1.3	2.3	-	1.0	0.3	-	-	0.6	0.3	0.3	0.3	1.3	1.6	0.6	2.6
Stephanopyxis turris	-	-	-	-	-	0.6	-	-	0.3	-	-	-	-	-	0.3
Thalassionema nitzschioides	-	-	1.6	1.0	3.6	0.3	2.0	2.6	2.6	1.0	1.3	0.6	3.0	2.6	2.0
Thalassiosira decipiens	2.3	3.3	2.0	2.1	1.3	2.6	2.6	1.6	2.6	1.0	3.3	2.3	2.6	3.3	2.0
T. gravida	7.3	6.6	2.3	3.0	3.6	2.3	4.6	8.6	1.6	4.3	10.0	12.3	3.0	2.6	2.6
T. hyalina	10.0	8.0	11.0	5.6	5.6	7.6	8.6	0.6	6.6	5.0	7.0	5.0	5.0	6.0	5.3
T. leptopus	1.0	-	0.3	-	0.6	-	0.3	0.3	0.3	-	0.3	1.0	0.6	0.3	-
T. nordenskioldii	3.0	-	6.0	5.6	3.6	4.6	8.0	4.6	1.6	6.3	4.1	3.6	5.3	4.3	4.0
T. oestrupii	-	1.3	2.0	2.0	-	1.3	2.0	-	2.6	2.6	-	1.0	-	2.6	0.3
T. trifulta	6.6	8.3	10.0	7.3	4.6	10.3	3.3	2.1	5.3	6.0	3.3	2.3	3.0	3.3	5.3
T. undulosa	-	1.6	1.0	1.6	0.6	1.6	-	-	0.6	1.3	0.6	0.6	1.0	1.6	1.3
Thalassiothrix longissima	1.0	0.6	3.0	1.6	1.0	1.6	1.0	0.6	1.6	0.3	0.3	-	0.6	1.0	0.3

Table 10. Abundance (in percent) of species encountered during the examination of the surface sediments.

SPECIES \ SAMPLE	77	79	81	83	84	89	94	96	98	100	101	105	107	110	112
Actinocyclus curvatulus	-	-	-	-	0.6	0.3	-	1.0	0.3	-	0.6	0.6	-	-	-
A. divisus	0.6	0.6	2.0	2.3	2.3	1.0	0.6	0.6	-	1.0	1.0	1.0	3.0	2.0	2.3
A. ochotensis	-	-	-	-	1.0	1.0	0.6	2.0	0.3	-	1.0	1.0	-	0.6	0.6
Actinoptychus undulatus	-	0.3	0.3	0.6	-	-	0.6	1.0	-	-	-	0.3	-	-	-
A. vulgaris	-	-	-	-	-	-	-	-	-	-	-	-	-	-	-
Asteromphalus robustus	-	-	-	-	-	-	-	-	-	0.6	-	-	-	-	-
Bacteriosira fragilis	7.6	7.0	7.3	6.0	5.3	3.0	7.0	6.0	4.3	4.3	3.6	4.6	4.3	6.6	5.6
Biddulphia aurita	1.3	0.6	1.0	1.6	2.3	2.3	1.3	1.3	1.0	0.3	2.3	2.0	1.6	3.3	0.6
Coscinodiscus lacustris	-	0.3	0.3	-	-	-	-	-	-	-	-	0.3	-	-	0.3
C. marginatus	0.3	2.0	1.0	1.3	1.3	1.6	0.3	0.6	1.3	1.6	0.6	0.6	1.6	-	1.0
C. oculus-iridis	-	0.6	0.6	0.3	1.6	2.0	1.0	1.0	1.0	0.6	1.3	1.3	1.3	0.6	0.6
C. stellaris	-	-	-	-	0.3	0.3	-	-	-	-	-	-	-	-	-
C. tabularis	-	-	-	-	-	0.6	-	-	0.3	1.3	-	1.0	-	-	0.3
Denticulopsis seminae	27.6	10.0	10.6	13.0	11.3	37.0	9.6	10.3	17.6	28.0	24.0	22.3	33.3	15.0	14.6
Melosira clavigera	-	0.3	-	3.0	1.6	-	2.6	0.6	0.6	-	-	1.0	-	0.1	0.3
M. sulcata	2.3	5.0	11.6	14.0	7.6	2.3	9.3	5.3	4.0	2.0	2.6	6.0	1.0	3.6	10.0
Navicula sp. 1.	0.3	1.6	2.3	0.3	1.3	0.3	1.0	3.0	1.6	1.0	0.3	2.0	-	-	-
Navicula sp. 2.	-	0.6	-	0.3	1.0	0.6	0.3	-	1.3	-	-	-	-	-	-
Navicula sp. 3.	-	0.3	1.0	1.0	-	0.3	-	0.3	0.3	-	-	0.3	-	-	-
Nitzschia cylindrus	6.6	9.3	6.0	6.6	7.6	1.0	8.0	9.6	9.3	3.0	3.0	6.6	4.6	5.6	4.3
N. oceanica	16.6	16.6	17.6	15.3	9.0	5.6	21.0	15.6	17.6	13.0	11.0	13.0	7.0	21.0	21.6
Pleurosigma sp.	-	0.6	-	0.3	-	-	-	-	-	0.3	-	-	-	-	-
Porosira glacialis	1.3	3.3	1.3	3.3	4.0	2.6	4.0	3.3	3.6	2.0	2.6	1.6	4.0	1.6	2.0
Pseudopodosira elegans	2.0	1.0	0.6	0.3	1.0	-	2.6	-	-	1.0	1.6	0.6	0.6	1.0	0.6
Rhaphoneis sachalinensis	0.3	1.3	0.3	0.6	-	-	0.3	0.3	-	-	-	-	-	-	-
R. surirella	-	-	-	-	2.0	-	2.0	1.3	2.0	-	0.3	0.6	-	-	1.6
Rhizosolenia hebatata	2.3	3.0	2.0	0.3	1.3	2.3	2.3	0.6	2.3	2.6	5.3	1.3	3.0	1.3	2.3
R. styliformis	1.6	1.3	0.3	1.3	2.3	2.0	1.6	0.6	2.0	3.3	1.6	2.0	0.6	0.6	0.3
Stephanopyxis turris	-	-	-	-	-	-	-	-	-	-	0.3	-	-	-	-
Thalassionema nitzschioides	0.6	1.6	-	2.6	4.6	4.0	2.3	4.0	3.0	0.6	3.0	3.3	1.6	0.6	4.0
Thalassiosira decipiens	3.3	4.3	2.3	3.3	3.6	1.6	1.3	2.6	3.0	3.0	1.0	2.0	2.3	1.2	2.3
T. gravida	5.6	6.3	10.0	7.0	1.0	2.3	3.6	4.3	1.3	2.6	4.0	3.3	4.3	5.3	3.0
T. hyalina	3.0	5.3	5.0	3.6	4.0	6.3	2.6	4.0	7.6	7.6	5.3	7.0	7.3	4.6	6.0
T. leptopus	-	-	0.3	-	0.3	-	0.3	-	0.3	0.3	-	0.6	0.6	-	-
T. nordenskioldii	6.0	4.6	4.6	1.6	5.3	4.0	3.0	5.6	1.6	6.6	6.0	4.3	3.6	3.3	5.6
T. oestrupii	2.0	2.0	1.3	2.3	2.6	1.0	1.0	1.6	0.6	1.0	0.3	1.3	2.6	0.6	0.6
T. trifulta	7.3	6.6	5.6	6.0	8.3	10.3	5.0	6.0	6.0	7.3	17.0	6.3	8.3	2.6	4.3
T. undulosa	0.6	1.3	0.3	-	0.6	0.3	0.6	1.3	0.6	0.6	0.3	1.6	1.6	0.6	1.3
Thalassiothrix longissima	-	-	-	1.0	0.6	1.3	1.0	1.0	0.6	1.6	0.6	1.3	1.0	0.3	0.6

Table 10| %Abundance (in percent) of species encountered during the examination of the surface sediments. (cont'd)

PRELIMINARY REPORT ON BENTHIC FORAMINIFERS FROM NAVARIN BASIN PROVINCE, BERING SEA, ALASKA

Paula J. Quinterno

INTRODUCTION

Previous studies of benthic foraminifers in the Bering Sea are mostly confined to areas to the north and west (Saidova, 1967; Lisitsyn, 1966) and to shallow-water areas to the east and northeast of the study area. (Anderson, 1963; Knebel and others, 1974) of the study area. The distribution of benthic foraminifers in the present study area was determined in 49 subsamples from water depths of 91m to 3420 m. Fourteen of these subsamples are from core tops or grab samples (Fig. 46), and 33 are from various depths within the cores. The goals of this study are to determine the distribution of benthic foraminifers in surface sediment and to record stratigraphic changes of the fauna with depth.

METHODS

Five of the 14 surface samples were preserved in 70% ethyl alcohol and stained with Rose Bengal shortly after they were collected. Rose Bengal stains protoplasm a deep pink, thereby distinguishing living foraminifers from dead specimens. This method is not without error; for example, foreign organic material such as bacteria or worms on or within the tests, may take the stain and be mistaken for foraminiferal protoplasm. Also, if the tests are thick or amber-colored, the stain is difficult to see.

The sampling techniques used to collect the cores in this study disturbed the upper few centimeters of sediment. Just before the sampler hits bottom, it creates a shock wave that scatters some of the surface sediment. All gravity cores collected on this cruise were turned horizontally to remove the liner in order to facilitate handling on deck. If the upper section of a core consisted of water-saturated sediment, some of the slurry was lost and some probably mixed with sediment deeper in the core. Because foraminifers live in the upper few centimeters of sediment, it is not likely that a representative sample of the living population was obtained. Therefore, results of live studies are approximations.

Samples (both preserved and unpreserved) were processed by washing over a 62 μm mesh sieve to remove silt and clay. Preserved samples were air dried to prevent protoplasm from shrinking; unpreserved samples were dried in an oven. In samples with abundant terrigenous material, foraminifers were concentrated by floating in carbon tetrachloride. A microsplitter was used to obtain a representative split of approximately 300 benthic foraminifers, but the actual number of benthic foraminifers in the splits ranged from 3 to 2860. Foraminifers were mounted on cardboard slides, identified, and the percentage of each species in the assemblage was calculated (Table 11).

DISTRIBUTION OF FORAMINIFERS

Forty-five calcareous and 20 agglutinated benthic species have been identified in the samples examined (Table 11).

Calcareous Species

The maximum water depth at which calcareous benthic foraminifers have been found in the Bering Sea is 3500 m; agglutinated species occur from shallow depths to depths greater than 3500 (Saidova, 1967).

Calcareous benthic foraminifers are present in all but 4 of the samples (Table 11). The exceptions are a G-14 (2-3 cm) from 91 m water depth, which contains all agglutinated specimens; G-6 (19-20 cm and 80-81 cm) from a water depth of 113 m -- both intervals are barren of calcareous and agglutinated specimens; and G-106 (55-58 cm) from 1785-m water depth which contains several fragments of poorly-preserved large, agglutinated forms tentatively identified as Hyperammina and Rhabdammina.

Calcareous benthic foraminifers in the samples studied are well- to poorly-preserved (Plates 2A and 2B). Both abrasion during transport and dissolution seem to affect preservation. Although Elphidium tests look robust, broken specimens are common. Dissolution also affects this genus; in some surface samples the entire calcareous test has been dissolved, leaving only the amber-colored organic inner lining (Plate 2B). Calcareous specimens in G-13 (240 cm) and G-12 (582-584 cm) show definite signs of dissolution. Tests are dull and grainy and features are obscure. These samples are from water depths of 2962 and 3164 m, respectively.

Agglutinated Species

Previous studies in the Bering Sea have reported the highest percentages of agglutinated foraminifers at water depths of less than 200 meters and also at depths greater than 2500 m (Anderson, 1963 and Saidova, 1967). This trend was not observed in the present study. Percentages varied from high to low at all water depths. There is, however, a definite decrease in the percentage of agglutinated foraminifers with depth in the cores (Figs. 47, 48, and 49; Table 11). This decrease could be attributed to poor preservability; the organic cement binding the grains together may be destroyed after the tests are buried, or to present conditions which provide a more-favorable habitat for agglutinated forms and less favorable for calcareous forms than did past conditions.

The large, agglutinated foraminifers, Hyperammina and Rhabdammina, in core G-106 (55-58 cm) differ from the agglutinated specimens near the top of this core (5-8 cm) and from those of all other samples analyzed (Table 11). The fauna at 55-58 cm resembles the faunas found in Bering Sea dredge samples which were dated as possibly early Tertiary (Robert Arnal, personal communication). Although age-diagnostic foraminifers are absent from G-106 (55-58 cm), the general character of the fauna and the lithology (well-consolidated mud with shale fragments) suggests a pre-Quaternary age.

Down-core Studies

All the benthic foraminifer species found in these cores have representatives that are still living today, so evolutionary extinctions cannot be used here for stratigraphic interpretation. Fluctuating abundances of certain species, however, may be useful for deciphering Quaternary history.

Elphidium is generally considered to be restricted to the shelf, yet high percentages of this genus occur in 3 cores from water depths greater than 1900 m (Figs. 47, 48, 49). These occurences may indicate a change in environmental conditions at the time of deposition. Percentages of Elphidium in G-13 increase from less than 5% in the intervals examined above 227 cm to 35% and 22% at 230-231 cm and 235-236 cm, respectively. A decrease to 8% or less occurs below 240 cm (Fig. 47). Elphidium reaches a maximum of 74% at 330 cm in G-26 and a maximum of 20% at 325 cm in G-36 (Figs. 48 and 49). These maxima are associated with sediment consisting of sands and gravelly sands. This coarse sediment is overlain by diatom ooze in G-13 and G-26 which extends from the core top down to 220 cm. Diatom ooze is the dominant sediment type in surface samples from the continental slope of the Navarin Basin province (Karl and others, this report). Coarse sediment on the slope may have been displaced from shelf depths. Lowering of sea level during Pleistocene glaciation caused much of the flat shelf to be exposed. Shallow-water faunas could have been easily transported downslope or ice rafted into the deep-water environment. Furthermore, cores 36, 26, and 13 are located near the mouths of Navarinsky, Pervenets, and Zhemchug Canyons, respectively (Fig. 46); where downslope sediment transport would have been facilitated.

Baldauf (this report) concludes that fluctuating abundances of the diatoms D. seminae, N. oceanica, and T. gravida can be used to identify the Holocene/Pleistocene boundary in cores G-13 and G-26 (Figs. 50 and 51). He states that N. oceanica is a cold-water species associated with ice, whereas D. seminae is a true oceanic species associated with cool waters. The change in dominance from D. seminae to N. oceanica marks the transition from glacial to interglacial conditions that occurred about 11,000 years ago. The maximum abundance of Elphidium in G-13 occurs at Baldauf's proposed Holocene/Pleistocene boundary (Fig. 50). Although Elphidium does not show a peak at 220 cm in G-26 (the proposed Holocene/Pleistocene boundary), the peak at 330 cm correlates with another decrease of D. seminae (Fig. 51).

Faunas from Low-Oxygen Environments

Low diversity, high abundance benthic foraminiferal assemblages are typical in sediments where the dissolved oxygen content of the overlying water is less than 1 ml/l. A few species of the genera Bolivina, Buliminella, Fursenkoina, and Globobulimina often dominate the fauna.

Benthic foraminiferal faunas at 2 depth intervals in G-66 are similar to the low-oxygen faunas described by Douglas and Heitman (1979) from the southern California borderland and by Ingle and Keller (1980) from the eastern Pacific margin. Frequency percentages of the most abundant species from 2 depth intervals in G-66 are presented in Table 12.

Table 12. Percentages of benthic foraminifers from 2 intervals in G-66

Core 66 (1336 m deep)	380-382 cm	385-387 cm
Buliminella tenuata	45%	52%
Bolivina pacifica	25	25
Fursenkoina spp.	23	6
Globobulimina auriculata	4	4

The 380-382-cm interval of G-66 is a dark greenish gray and olive gray laminated mud. The sand-size fraction is approximately 90% foraminifers, dominated by the few species shown in Table 12. Previous studies have shown that laminated sediments are common where dissolved oxygen content of the overlying water is less than 1ml/l; these conditions are unfavorable for most scavenging macro-invertebrates, so there are few organisms to disturb the sediment. Although the fauna at 385-387 cm in G-66 is similar to the fauna at 380-382 cm (Table 12), the sediment is very different. The lower interval (385-387 cm) is coarse material made up largely of volcanic ash. The sediment below 390 cm changes abruptly to mud (similar to sediment at 380-382 cm), but the fauna does not change significantly. The coarse layer is probably an air-borne volcanic ash deposit, and if found in other cores in the Navarin Basin province, could be a useful stratigraphic marker.

Live Species

Rose Bengal stain was used to recognize live foraminifers in 5 surface samples, and the percentage of each species in the live fauna was calculated. The composition of the live and dead species in surface samples G-59, G-32, S-110, and G-40 are similar for each station. This is not the case at G-26 (Tables 11 and 13). Eighteen species were present in G-26, but only 6 of these species (33%) were represented by both live and dead specimens. Elphidium, a genus usually restricted to shelf depths, made up 8% of the total fauna (Table 11) in G-26 (3373 m. water depth). All specimens of Elphidium were dead and poorly preserved. Displacement, possibly by downslope transport in Pervenets Canyon, could account for the discrepancy between living and dead species in core G-26.

Table 13. Similarity of live and dead species

Sample no.	Total no. of species	No. of species represented by both live and dead	% of species in common
G-59	18	14	78
G-32	26	23	88
S-110	32	24	75
G-40	27	20	74
G-26	18	6	33

ACKNOWLEDGMENTS

I wish to thank Carol Hirozawa, Michael Mullen, and Susan Vath for their help in preparing the samples for this study and Robert Arnal, Joyce Blueford, Paul Carlson, and Herman Karl for critically reviewing an earlier version of the manuscript.

REFERENCES

Anderson, G. J., 1963, Distribution patterns of Recent foraminifera of the Bering Sea: Micropaleontology, v. 9, no. 3, p. 305-317.

Douglas, R. G. and Heitman, H. L., 1979, Slope and basin benthic foraminifera of the California borderland: SEPM Special Publ. no. 27, p. 231-246.

Ingle, J. C. and Keller, G., 1980, Benthic foraminiferal bio-facies of the eastern Pacific margin between 40° S and 32° N, in Field, M. E., and others (eds.), Quaternary Depositional Environments of the Pacific Coast: Pacific Coast Paleogeography Symposium 4, Los Angeles, Soc. Econ. Paleo. and Mineralogists, p. 341-355.

Knebel, H. J., Creager, J. S., and Echols, R. J., 1974, Holocene sedimentary framework, east-central Bering Sea continental shelf, in Herman, Y. (ed.), Marine Geology and Oceanography of the Arctic Seas: New York, Springer-Verlag, p. 157-172.

Lisitsyn, A. P., 1966, Recent sedimentation in the Bering Sea in Russian): Inst. Okeanol. Akad. Nauk. USSR, (translated by Israel Program Sci. Transl., Jerusalem, Washington, D.C., U.S. Dept. Commerce, National Sci. Foundation, 614 p.

Saidova, Kh. M., 1967, Depth changes in Bering Sea during the Upper Quaternary, as indicated by benthonic foraminifera, in Hopkins, D. (ed.), The Bering Land Bridge: Stanford Univ. Press, p. 364-368.

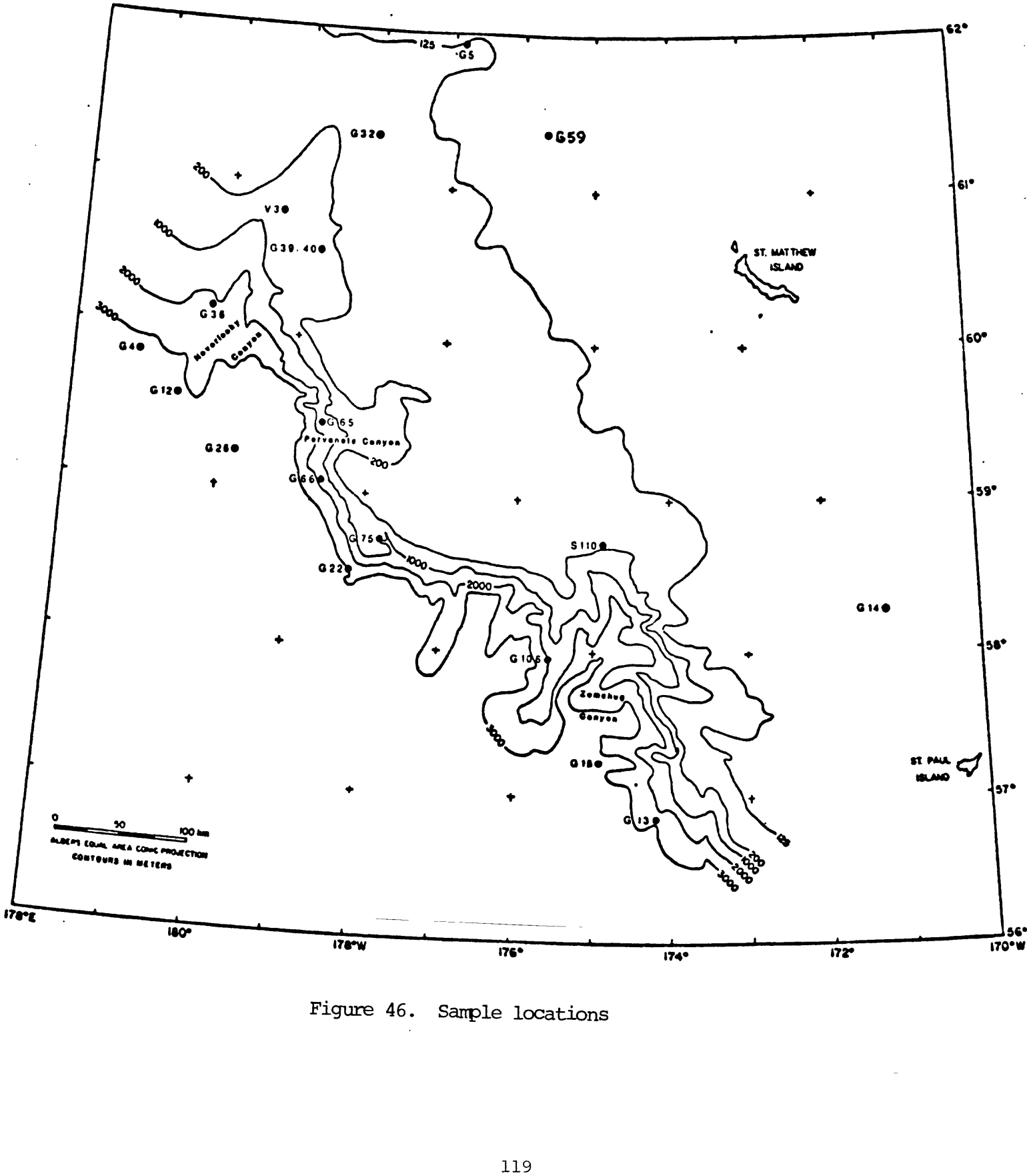

Figure 46. Sample locations

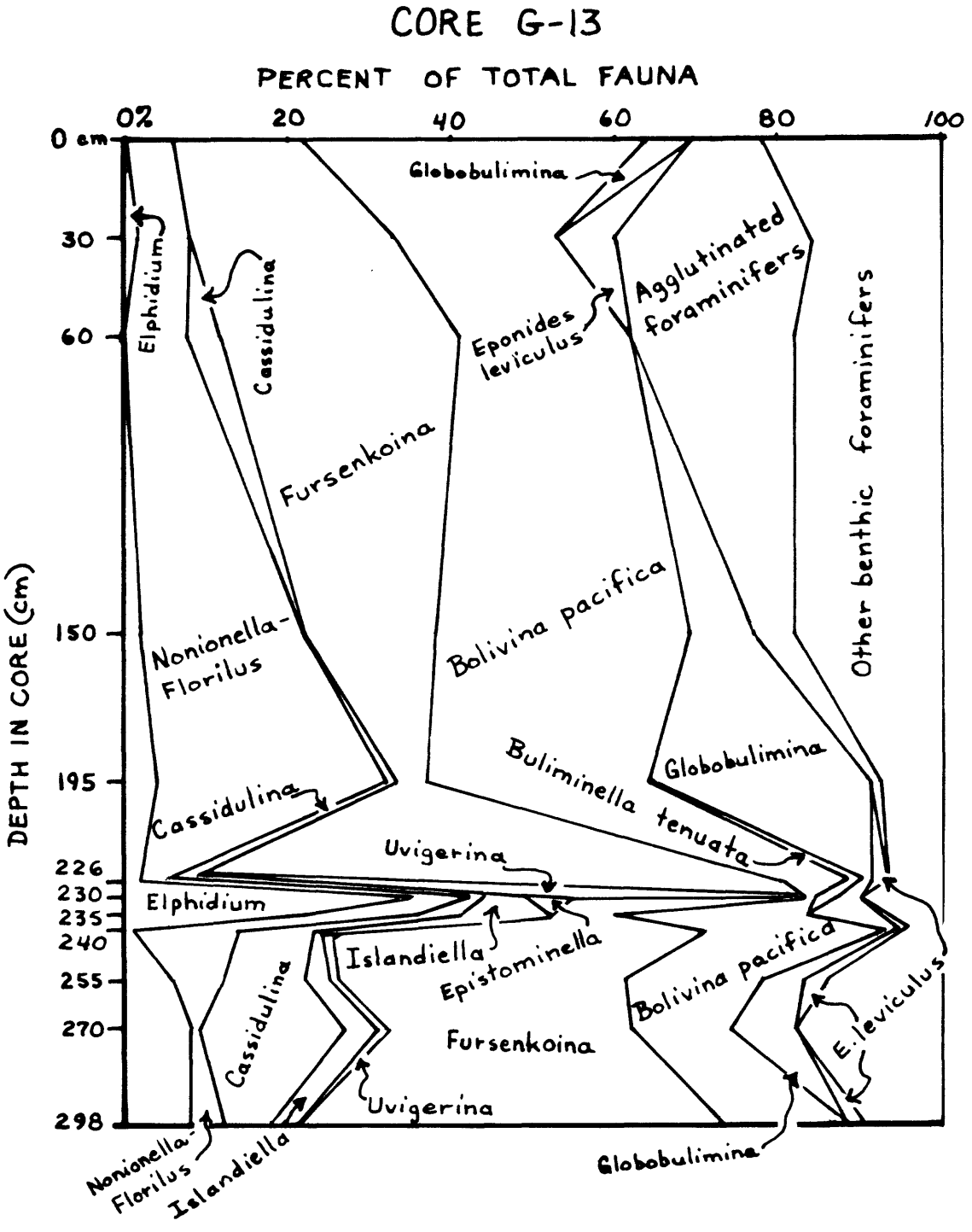

Figure 47 Distribution of benthic foraminifers with depth in Core G-13.

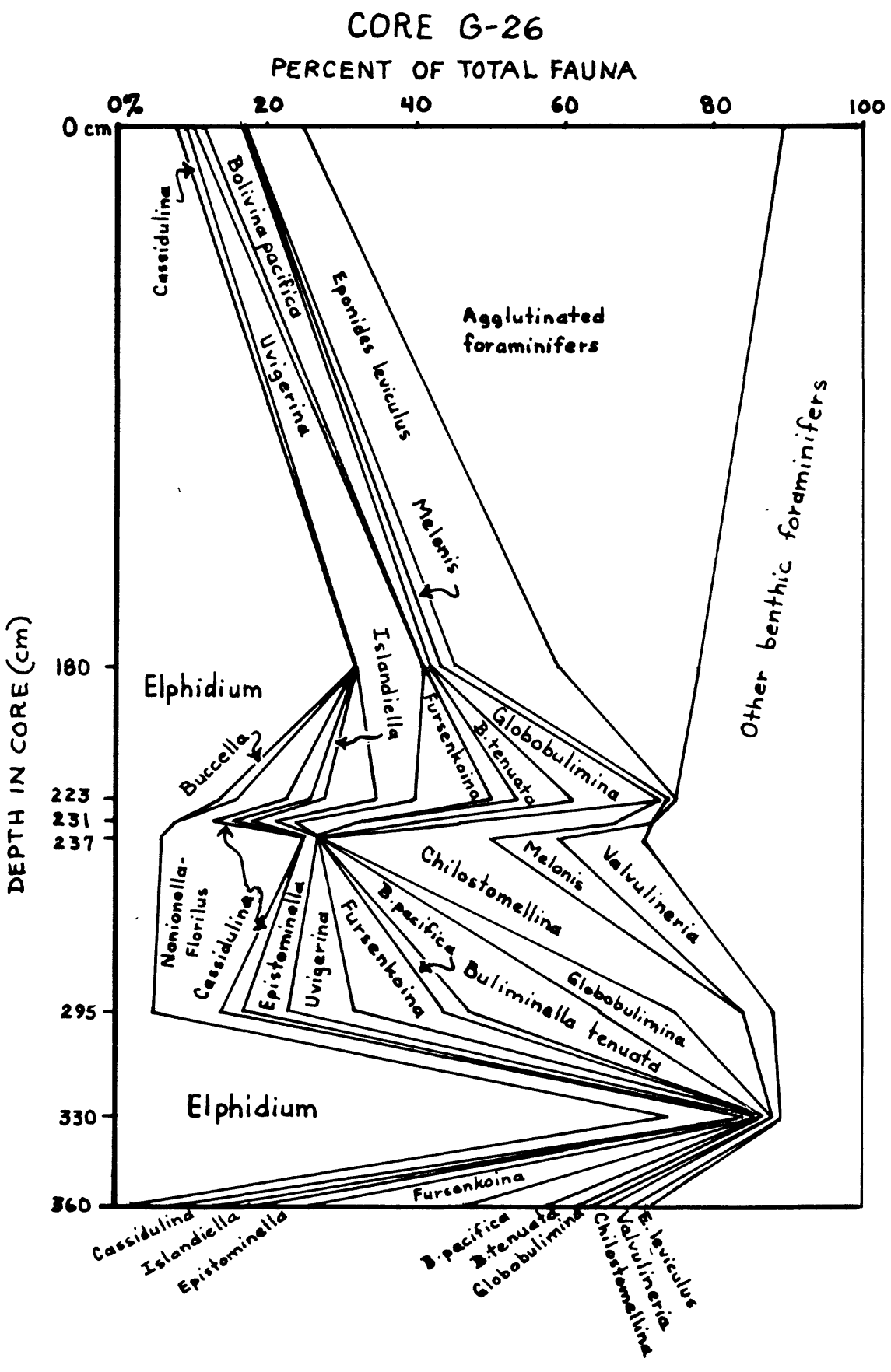

Figure 48. Distribution of benthic foraminifers with depths in Core G-26.

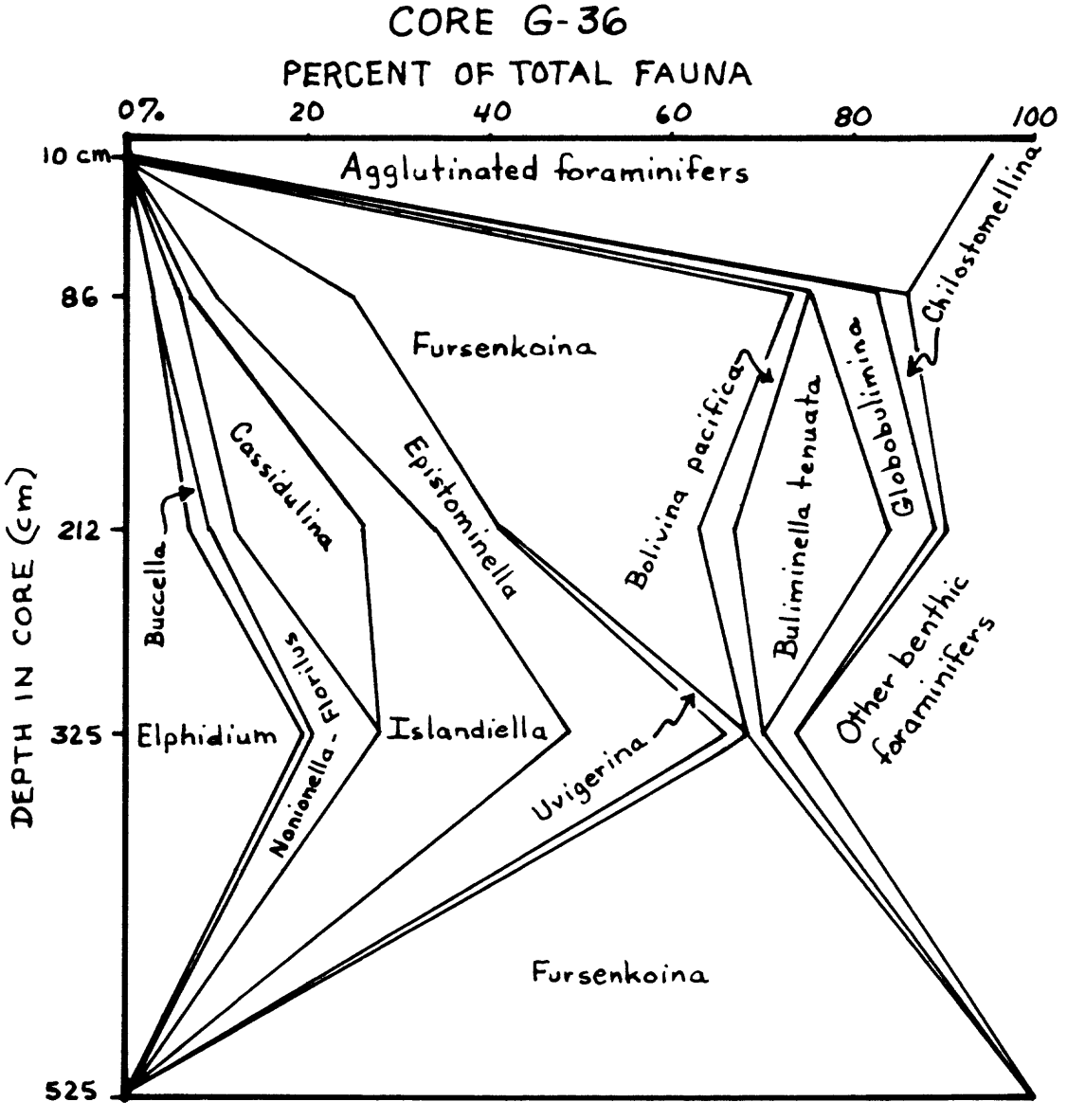

Figure 49. Distribution of benthic foraminifers with depth in Core G-36.

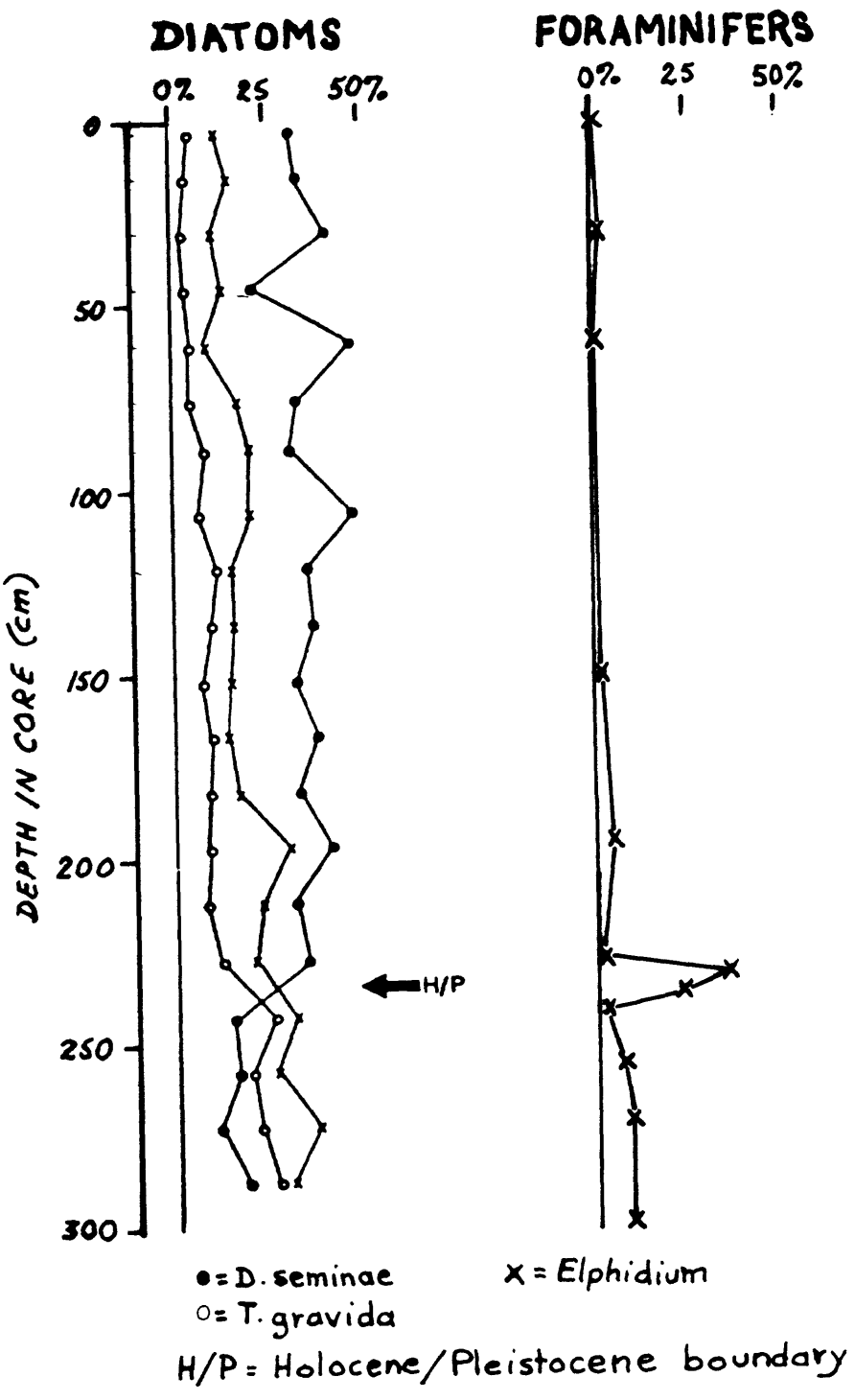

Figure 50. Downcore distributions of diatoms and foraminifers in Core G-13.

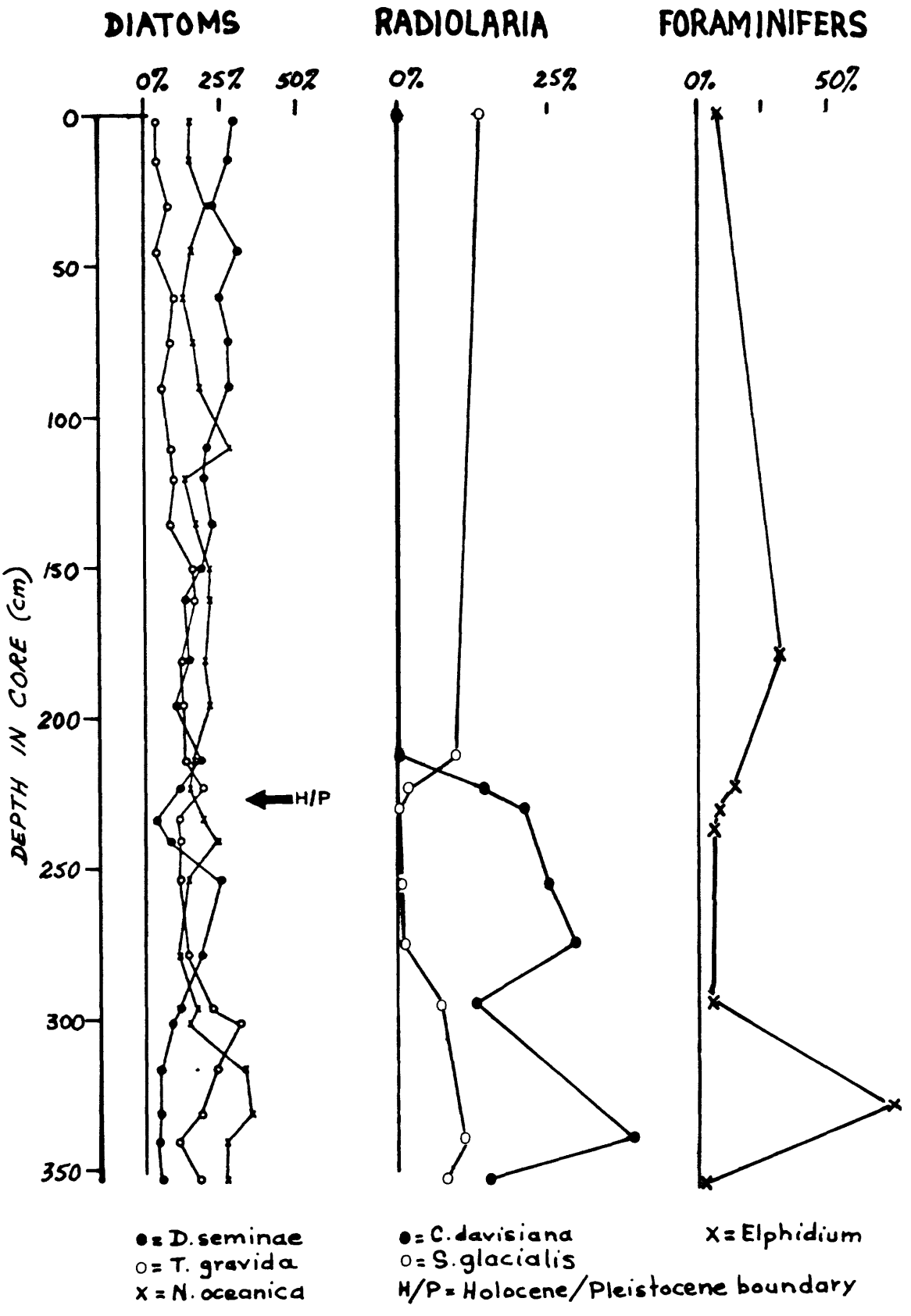

Figure 51. Downcore distributions of diatoms, radiolarians, and foraminifers in Core G-26.

PLATE 2

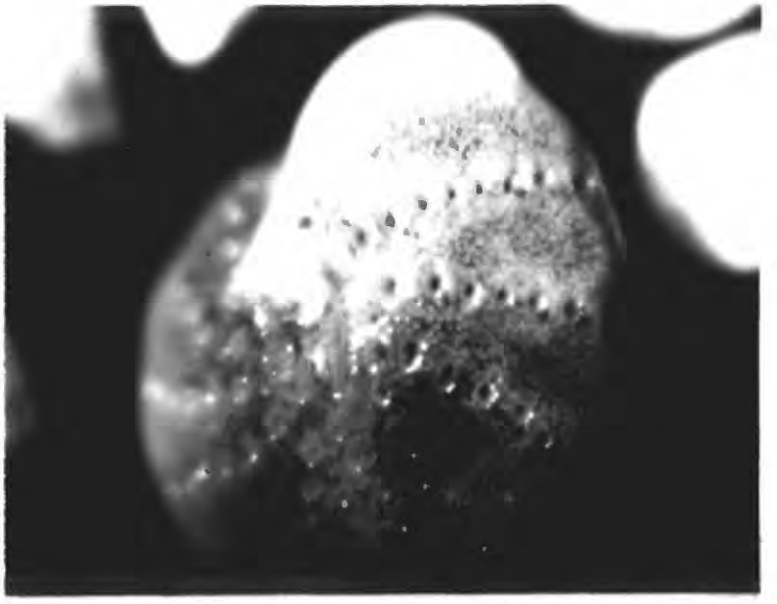

A. Well-preserved *Elphidium* sp. from S-110 (x60)

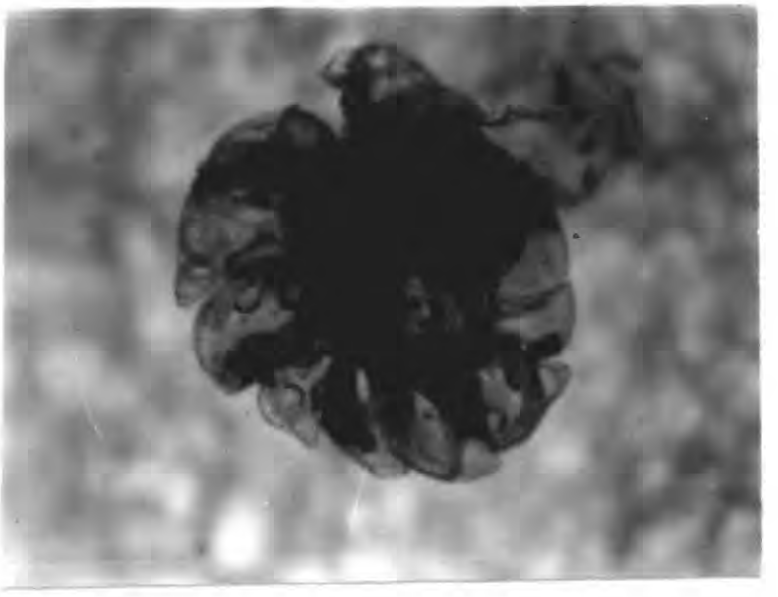

B. Organic inner lining of *Elphidium* sp. from G-54, 0-2cm (x100)

CORE NUMBER AND DEPTH IN CORE / SPECIES	G-14 2-3cm	G-59 0-2cm	G-6 19-20cm	80-81cm	G-32 0-2cm	S-110	G-39	G-40 0-2cm	V-3	G-75 10-12cm	G-66 380cm	385cm	G-65 181cm	G-106 5-8cm	55-58cm	G-36 10-12cm	86-88cm	212-214cm	325-327cm	525-527cm	G-22 2-3cm
WATER DEPTH(m)	91	99	113		150	164	220	220	524	951	1336		1609	1785		1924					2842
Adercotryma glomeratum*	x	x(2)			9(14)	11(15)	3	12(15)	4							2					
Alveolophragmium crassimargo*					2(2)	1(3)		6(13)													
Ammoscalaria tennuimargo*																86					
Ammotium cassis*	x	x(5)			x																
Bathysiphon sp *	35	37(18)			2(3)	1(1)		x(2)	x												
Bigenerina sp *																					
Bolivina decussata					x(1)		1		7								1	x	1		
Bolivina pacifica		x			2(4)			2(5)	x	1	25	25	8				2	4	2		42
Bolivina seminuda										6											
Bolivina striatula																					
Bolivina spp						(x)															
Buccella spp		1(1)			4(6)	3(1)	3	x(1)	1				x				x	2	1		
Bulimina spp			N	N																	
Buliminella elegantissima									X												
Buliminella tenuata			E	E							45	52						17			
Cassidulina californica						1(1)	x									2					
Cassidulina limbata			R	R															x		
Cassidulina sp		4(8)			4(6)	4(5)	4	1(3)	1	2		1	10				1	14			
Cassidulinoides sp			R	R								x	x					x			
Chilostomella sp																1					
Chilostomellina fimbriata			A	A							1		6				4	1			4
Cibicides sp						(x)			1								x	x			
Cribrostomoides scitulus*	4		B	B																	
Cyclammina cancellata*																4					
Dentalina sp							x														
Eggerella advena*	35	2(2)			17(12)	7(3)	15	20(10)	13												
Elphidium clavatum var.		15(8)			7(6)	1	x		1	6	x		26				3	7	20		1
Elphidium frigidum						1(1)															
Epistominella pacifica									21	2	x	3					12	x	18		
Epistominella vitrea					10(9)	16(24)	17	7(6)	24		x		1				3	7			
Eponides leviculus						2(3)	1	1	1			1	x					x			
Eponides spp																					19
Fissurina spp		x(x)				x(x)			x									x	x		2
Florilus labradoricus		x(1)			2(2)	2		(2)	4	7	x	2	19				3	3	7		
Fursenkoina spp		22(43)			3(2)		x	5(8)	1		23	6	16				48	22		100	11
Globobulimina auriculata					1(2)				x	3	4	4	2	14			8	5	4		
Gyroidina spp																					
Haplophragmoides bradyi*					x	1(1)		1(1)	x							5					

Table 11 Relative frequency percentages of benthic foraminifers from the Navarin Basin province
X = less than 1%. * = agglutinated species
Data for 'live' species is shown in parentheses

CORE NUMBER AND DEPTH IN CORE / SPECIES	G-14 2-3cm	G-59 0-2cm	G-6 19-20cm	80-81cm	G-32 0-2cm	S-110	G-39	G-40 0-2cm	V-3	G-75 10-12cm	G-66 380cm	385 cm	G-65 181 cm	G-106 5-8cm	55-58 cm	G-36 10-12cm	86-88 cm	212-214cm	325-327cm	526-527cm	G-22 2-3cm
WATER DEPTH(m)	91	99	113		150	164	220	220	524	951	1386		1609	1785		1924					2842
Haplophragmoides columbiense *		S				x (x)			x												
Hyperammina sp (fragments=F)*															F						
Islandiella spp					2 (1)	x (x)	2	1 (x)									3	8	21		
Karreriella sp.*																					
Lagena spp					x (x)	x	x	x	x	x		x	1				x	x	x		
Melonis pompilioides																					
Nonionella pulchella									7			1									
Nonionella turgida digitata							x	2(5)					3				x	x			5
Nonionella spp			N	N														x			
Pelosina variabilis*																1					
Protelphidium orbiculare			E	E				x										x			
Pseudononion auricula						1(2)	2	2(4)	x				3				5	2	x		
Pullenia salisburyi			R	R		x(x)		x(x)													
Pyrgo spp																					
Quinqueloculina spp			R	R					x												
Recurvoides spp*		3(4)			2(3)	1(2)	1	x(1)	x												
Reophax spp *	x	1(3)	A	A	5(8)	3(3)	1	(1)	x	x						55					5
Rhabdammina sp (fragments=F)*															F						
Spiroplectammina biformis*	16	7(2)	B	B	13(7)	5(1)	3	13(4)	5					28				x			
Textularia sp *	2	5(6)			6(6)	8(3)	2	8(3)						28							5
Trifarina angulosa					3(3)	20(17)	32	(8)	2	1			x								
Triloculina trihedra																	x	x	x		
Trochammina spp.*	6				x(x)	2(3)			1					14		2					2
Uvigerina (costate)					1(x)	5(4)	9	1(2)	1	69		4	2					x	2		
Uvigerina (smooth)																		x	x		1
Uvigerina (hispid)																					
Valvulineria sp										2		1							x		
other calcareous species						x							1				4	3	3		1
other agglutinated species		(3)			x (1)	1 (2)		x (1)	1					14							
Percentagglutinated	88	55	0	0	56	41	25	60	24	0	0	0	0	84	94		0	0	0	0	11
NUMBER OF BENTHIC SPECIMENS COUNTED TOTAL	628	1747	0	0	681	1441	309	591	2860	211	679	325	370	7	fragments	89	568	666	360	3	74
(LIVE)		(727)			(292)	(557)		(238)													

Table 11 (continued)

SPECIES \ CORE NUMBER AND DEPTH IN CORE	G-13 0-2cm	30 cm	60 cm	150 cm	195 cm	226-227cm	230-231cm	235-236cm	240 cm	255cm	270 cm	298-299cm	G-12 582-584cm	G-4 0-2cm	8-9 cm	296 cm	G-26 0-2cm	180cm	223-226cm	231-232 cm	237cm	295-300cm	330cm	360cm	G-15 50-100cm	195-196 cm
WATER DEPTH(m)	2962												3164	3222			3373								3420	
Adercotryma glomeratum*		2															16(10)									
Alveolophragmium crassimargo*																	1(3)									
Ammoscalaria tennuimargo*																		1								
Ammotium cassis*																										
Bathysiphon sp*									x																	
Bigenerina sp*																	1									
Bolivina decussata						x					x	x														x
Bolivina pacifica	42	20	21	31	27	8	1	23	22	17	12	15	6	42			5	1	4			3		11		1
Bolivina seminuda	3			5	7														1	1						1
Bolivina striatula																										4
Bolivina spp							3		1	1			29						1					2		
Buccella spp						x			x	x	x	x							2			x	1			1
Bulimina spp																			x							x
Buliminella elegantissima								2		1									x			x		1		
Buliminella tenuata						2	3	x					13						7	7		18		4		8
Cassidulina californica																			3	1						x
Cassidulina limbata																			x	1						
Cassidulina sp			4	x	1	5	2	5	9	10	18	6	x				1(3)		3	1		3		3	9	4
Cassidulinoides sp							3						x			3			1	2		x	1	2		1
Chilostomella sp				1															3			1				x
Chilostomellina fimbriata					1				x			x	17							21	21	9		2		1
Cibicides sp								x				x	x				1	7	x	9	6		7	1		1
Cribrostomoides scitulus*																										
Cyclammina cancellata*																										
Dentalina sp												x							x							x
Eggerella advena*		9	12	2	1									2				1								
Elphidium clavatum var		2		2	4	1	35	22	1	6	8	8	8	15	50	x	8	32	14	8	6	5	74	2	64	16
Elphidium frigidum																										
Epistominella pacifica						1	6	x											5	3		5		2		10
Epistominella vitrea						1			1	1		x	1						2		2	1	1	4		4
Eponides leviculus		7				2			1	3		2				26	8(3)	14	1					2		x
Eponides spp				x				2		3	7		3	2	17	1		2	1		9		1			
Fissurina spp											x	1						3	x				3	2		
Florilus labradoricus	3	2		9	20	x	7	4			1	1	4	5					7	5	11	8	10	2	27	8
Fursenkoina spp	16	25	29	16	4	68	1	8	45	34	30	52	8	2			1		10	9		12		21		3
Globobulimina auriculata	5			8	27	1	3	8	1	5	8		1	5	17	11		1	12	6		10	1	2		9
Gyroidina spp																		1	x			1		x		x
Haplophragmoides bradyi*																										

Table 11 (continued)

CORE NUMBER AND DEPTH IN CORE / SPECIES	G-13 0-2cm	30 cm	60 cm	150 cm	195 cm	226-227cm	230-231cm	235-236cm	240 cm	255 cm	270 cm	298-299cm	G-12 302-304 cm	G-4 0-2 cm	8-9 cm	296 cm	G-26 0-2 cm	190 cm	228-225 cm	231-232 cm	237 cm	295-300 cm	330 cm	360 cm	G-15 50-100 cm	195-196 cm
WATER DEPTH (m)	2962												3164	3232			3373								3420	
Haplophragmoides columbiense*				1																						
Hyperammina sp.*																										
Islandiella spp.							5	11	1	3	4	3							2	1		1		2		3
Karreriella sp.*																		1								X
Lagena spp.						X	X	X	X		X	X	X						X	1	2	X		X		X
Melonis pompilioides											X							2	1	5	9	X				X
Nonionella pulchella																										
Nonionella turgida digitata	3		8	11	8	1		10	13	6		3									8	1		1		X
Nonionella spp.	4					2													X					2		
Pelosina variabilis*																										
Protelphidium orbiculare																			X							
Pseudononion auricula	3								X	1		2					1					X				
Pullenia salisburyi																			X							
Pyrgo spp.																	1			2						
Quinqueloculina spp.									X								1			3		X		1		
Recurvoides spp.*																										
Reophax spp.*	3	4		1										8			34(7)	10								
Rhabdammina sp.*																										
Spiroplectammina biformis*	6	4															2									
Textularia sp.*				X										8				6								
Triforina angulosa																			X	1		X				X
Triloculina trihedra	3			1							X	X						1	X		2			2		
Trochammina spp.*		2	8	1										2			11(7)									
Uvigerina (costate)						1	87												5	2		8				14
Uvigerina (smooth)									1	1	1	X	3	5	17	45	1	9	1			1	1	X		2
Uvigerina (hispid)											X									1						
Valvulineria sp.							1						2			13			X		11	4	1	3		1
other calcareous species	15	13	17	9		5		X	2	7	4	1	1	2			4	5	2	11	12	4		27		
other agglutinated species		2																								
Percent agglutinated	9	24	20	5	1	0	0	0	X	0	0	0	0	20	0	0	65	19	0	0	0	0	0	0	0	0
NUMBER OF BENTHIC SPECIMENS COUNTED (TOTAL)	38	44	24	225	90	402	662	183	396	321	177	368	489	40	6	233	153	87	493	102	53	567	120	298	11	868
(LIVE)																	(29)									

Table 11 (continued).

RADIOLARIA FROM THE NAVARIN BASIN PROVINCE, BERING SEA

Joyce R. Blueford

INTRODUCTION

Although several biostratigraphic studies describe radiolarian faunas in the North Pacific (Hays, 1970; Nigrini, 1970; Sachs, 1973; Kling, 1971 and 1973; Ling, 1970; Robertson, 1975; and Kruglikova, 1976 and 1977), The only comprehensive study of the radiolarian fauna from surface sediments from the Bering Sea is by Ling and others (1970). Many north Pacific species are not found in the Bering Sea. Radiolarians from the surface layer in the Sea of Okhotsk (Kruglikova, 1975) are similar to those analyzed for this report.

The purpose of this preliminary survey of radiolaria is threefold. First, it establishes what species are present in the upper 600 cm of the sediment; secondly, it suggests useful species for stratigraphy; and thirdly, it suggests areas of further studies that may yield useful stratigraphic and environmental information.

METHODS

It was concluded after a preliminary scan of prepared foraminiferal samples that samples from cores collected in water depths deeper than 200 m contained the most abundant and diverse radiolaria fauna. Therefore, a concentrated effort was made on deep water cores as shown in Figure 52. Samples were taken from the top and bottom of most of the cores. Some cores, such as 12, 26, 109, and 115, were sampled at intermediate levels as well.

Samples were washed through a 52 mm mesh sieve. Because carbonate and organic contents were low, the usual method of adding HCl and hydrogen peroxide was not used. Radiolaria from samples that contain a high percentage of diatoms were concentrated by first drying the sample, then putting half of the sample on a watch glass, then pouring it into another watchglass. The first watchglass is wiped clean and the process is repeated about 4 or 5 times. Diatoms tend to adhere to the watchglass that does not have the bulk of the sample because of static electricity. Radiolaria are concentrated in the sample and strewn slides are then made. The entire slide was scanned in an effort to look at the total assemblage.

RESULTS

The radiolarian fauna of the Bering Sea is different from that of the North Pacific in being more diverse with endemic arctoboreal and cosmopolitan species (Kruglikova, 1977). The Navarin Basin province assemblage is similar to the assemblage in surface sediment throughout the Bering Sea (Ling and others, 1970) and the Sea of Okhotsk (Kruglikova, 1975). This may be due in part to oceanographic current and water mass patterns.

Seventy different species were identified from Navarin Basin province cores (Table 14). Their abundance as a group in samples collected from the slope and rise is second only to diatoms. The following species are found to be most abundant in this area (in decreasing order): Stylochlamidium venustum

(Bailey), Spongotrochus glacialis Popofsky group, Cycladophora (?) cornuta (Bailey), Cycladophora davisiana Ehrenberg, Stylodictya aculeata Jorgensen, Acanthodesmiidae gen. et. sp. indet. A, Lithelius sp., Stylatractus pyriformis (Bailey)? emend Kruglikova, Dictyophimus gracilipes Bailey, Prunopyle antarctica Dreyer, Acanthodesmia micropora (Popofsky), Arachnocorys (?) dubius Dogiel and Stylodictya validispina Jorgensen. Table 15 shows the abundance of all species counted in this study.

The occurrence of Lychnocanoma grande in some samples (Table 15) is noteworthy in that this species has been shown in studies of Pacific Ocean cores to be stratigraphically significant (see e.g., Robertsen, 1975; Kruglikova, 1976). Not enough samples have been examined, however, to determine the significance of L. grande in the Navarin cores.

REFERENCES CITED

Casey, R. Price, A. and Swift, C., 1972, Radiolarian definition and paleoecology of the late Miocene to E. Pliocene in S. California: in Proceedings of the Pacific Coast Miocene Biostratigraphic Symposium S.E.P.M., p. 226-238.

Cleve, P. T., 1899, Plankton collected by the Swedish Expedition to Spitzbergen in 1898: Swedish Acad. Sci., Bandel 32, No. 3.

Dogiel, V. A. and V. V. Reshnetnyak, 1952, Material on radiolarians of the northwestern part of the Pacific Ocean: Invest. Far East Seas USSR, publication III.

Hays, J. D., 1970, Stratigraphy and evolutionary trends of radiolaria in north Pacific deep sea sediments: GSA Memoir 126, p. 185-218.

Hays, J. D., 1971, Faunal extinctions and reversals of the earth's magnetic field: GSA v. 82, p. 2433-2447.

Hulsemann, Kunigunde, 1963, Radiolarions in plankton from the Arctic drifting station T-3: Arctic Ins. of N.A. Tech. Paper No. 13, p. 5-43.

Jorgensen, E., 1905, The protist plankton and the diatoms in bottom samples: Bergens Mus. Skrifter, no. 7, p. 49-151, pls. 6-18.

Kling, S., 1971, Radiolaria: Leg 6 DSDP; in Fisher, A. G., Heezen, B. C., and others, Initial Reports Deep Sea Drilling Project, v. 6, Washington, D.C., p. 1069-1096.

Kling, S., 1973, Radiolaria from east north Pacific, DSDP Leg 18: in Kulm, L. D., von Huene, R., and others, 1973, Initial Reports Deep Sea Drilling Project, v. 18, Washington D.C., p. 617-641.

Kruglikova, S. B., 1975, Radiolarians in the surface layer of the sediments of the Okhotsk Sea. Oceanology, v. XV, Acad. of Sciences USSR.

Kruglikova, S. B., 1976, Radiolarians in the upper Pleistocene sediments of the boreal and northern subtropical zones of the Pacific Ocean: Oceanology, v. XVI, Acad. of Sci. USSR.

Kruglikova, S. B., 1977, Peculiarities of the distribution of radiolarians in the sediments of the boreal and subtropical zones of the Pacific Ocean in the Pleistocene: Oceanology, v. XVII, Acad. of Sci. USSR.

Ling, H. Y., 1973, Radiolaria: Leg 19, Deep Sea Drilling Project: in Creager, J. S., Scholl, D. W., and others, Initial Reports Deep Sea Drilling Project, v. 19, Washington, D.C., p. 777-797.

Ling, H. Y., and others, 1970, Polysystine radiolaria from Bering Sea surface sediments: in Proceedings of II Plankt. Conference, Rome, p. 705-729.

Nigrini, C., 1970, Radiolarian assemblages in the north Pacific and their application to a study of Quaternary sediments in core V20-130: GSA Memoir, 126, p. 139-183.

Nigrini, C. and Moore, T., 1979, A guide to modern radiolaria, Cushman Foundation Sp. Publ. No. 16, p. 212.

Petrushevskaya, M. G., 1967, Antarctic spumelline and nasselline radiolarians: Issled. Fauny Morei 4 (12) Rez. biol. Issled., Sov. Antarkt. Eksped. 1955-1958, 3, p. 5-186.

Reshetnyak, V. V., 1966, Deep Water Phaeodaria Radiolaria of the northwest Pacific Ocean, Akad. of Sci. USSR, Ins. of Zoology, no. 94.

Riedel, W. R., 1958, Radiolaria in Antarctic sediments, Rept. BANZ Antarctic Research Exped., ser. B, v. 6, pt. 10, p. 217-255.

Robertson, J., 1975, Glacial to interglacial oceanographic changes in the northwest PAcific, including a continuous record of the last 400,000 yrs., Ph.D. dissertation, Columbia University, New York, p. 326.

Sachs, H. M., 1973, Late Pleistocene history of the north Pacific: evidence from a quantitative study of radiolaria in core V21-173: Quaternary Research 3, p. 89-98.

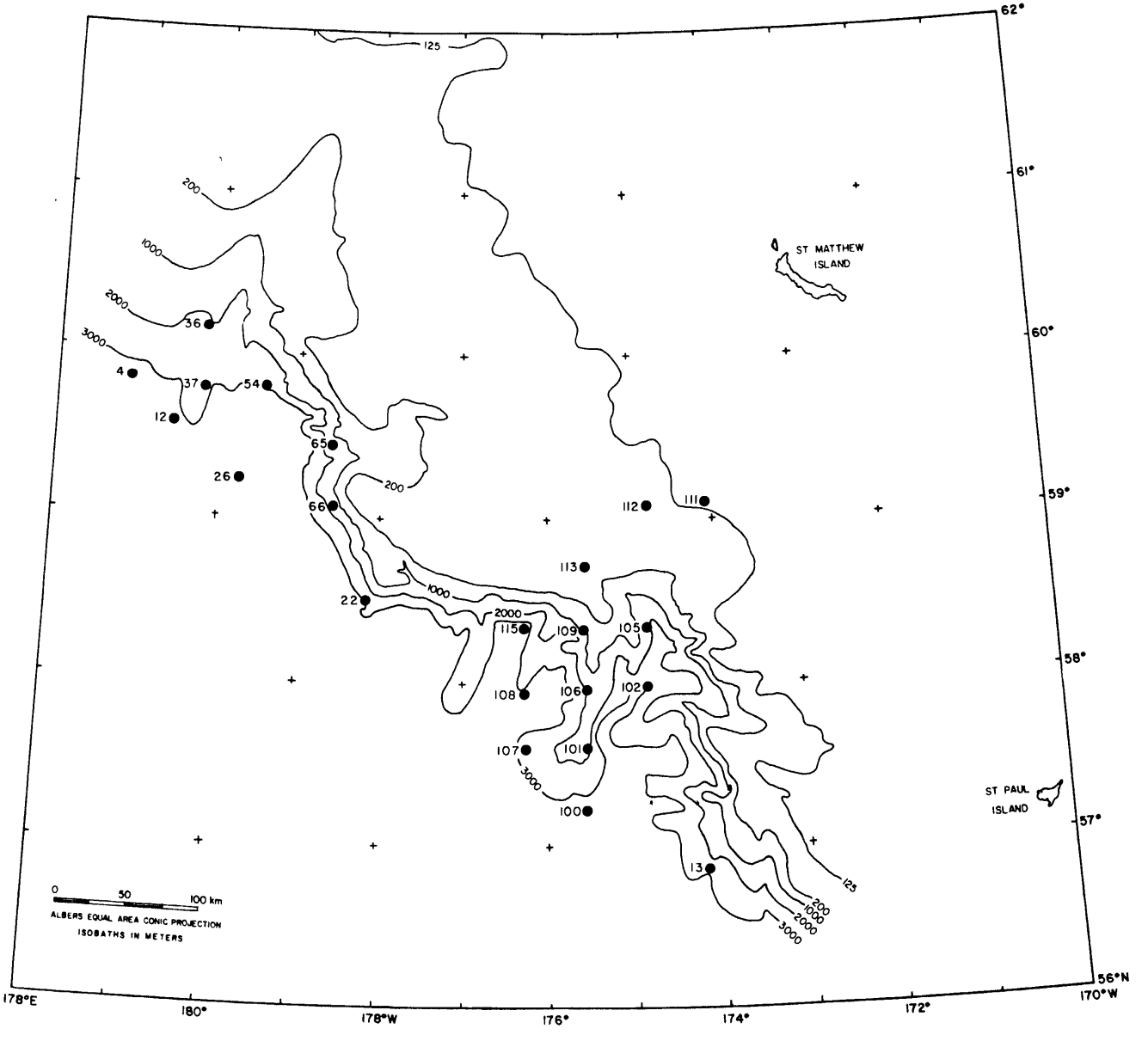

Figure 52. Location map of cores analysed for radiolarians.

Table 14. LIST OF RADIOLARIAN SPECIES FOUND IN NAVARIN BASIN

Species Name	Taxonomic Reference	Percentage of samples in which species occur (62 total samples)
*1,2Acanthodesmia micropora (Popofsky)	Kruglikova, 1975	63
*1,Acanthodesmiidae gen. et.sp. indet A	Kling, 1973	81
Acanthodesmiidae gen. et.sp. indet B		44
Acanthosphaera sp. indet.		2
*1,2,Arachnocorys dubius Dogiel	Dogiel, 1952	58
Artostrobiidae sp. indet.		3
Artostrobus annulatus (Bailey)	Ling et al., 1970	8
Botryocampe inflata (Bailey)	Kruglikova, 1974	32
Botryostrobus auritus (Ehrenberg)	Nigrini and Moore, 1978	40
Carposphaera sp. indet. A		55
Carposphaera sp. indet. B		27
Carposphaera sp. indet. C		37
Carposphaera sp. indet. D		16
Cenosphaera cristata Haeckel	Riedel, 1958	35
Cenosphaera sp. indet. A		23
Cenosphaera sp. indet. B		6
Cornutella profunda Ehrenberg	Casey, 1972	32
Cromyechinus borealis (Cleve)	Hulseman, 1963	2
*2,Crytopera laguncula Haeckel	Haeckel, 1887	42
*1,2,Cycladophora ? cornuta (Bailey)	Kruglikova, 1974	82
*1,2,Cycladophora davisiana Ehrenberg	Ling et al., 1970	76
Dictyocephalus papillosus (Ehrenberg)	Riedel, 1958	37
*1,Dictyophimus gracilipes Bailey	Petrushevskaya, 1967	74
*2,Dictyophimus hirundo (Haeckel group)	Nigrini and Moore, 1978	45
Dictyophimus sp. indet.		13
Diploplegma banzare Riedel	Riedel, 1958	29
Echinomma delicatulum (Dogiel)	Kruglikova, 1975	42
Echinomma sp. indet.		5
Eucecryphalus histricosus Hulseman	Hulseman, 1963	15
Eucyrtidium hexagonatum Haeckel	Nigrini and Moore, 1978	11
Euphysetta elegans Bogert	Reshetnyak, 1966	5
Helisoma sp. indet.		47
Lipmanella dictyoceras (Haeckel)	Kling, 1973	2
Lirella mela (Cleve)		2
*1,Lithelius? sp.	Petrushevskaya, 1967	32
*2,Lithomitra arachnea (Ehrenberg)	Ling, 1970	29
*2,Lychnocanoma grande Campbell	Casey, 1972	35
Peridium minutum Cleve	Cleve, 1899	11
Peridium sp. indet.		11
Peripyramis circumtexta Haeckel	CAsey, 1972	55
Phaeodaria gen. et. sp. indet. A		2
Phaeodaria gen. et. sp. indet. B		11
Plagoniidae gen. et. sp. indet.		15

Plectacantha oikiskos Jorgensen	Jorgensen, 1905	13
Polysolenia arktios Nigrini	Nigrini, 1970	18
Polysolenia sp. indet.		8
*1,2,Prunopyle antarctica Dreyer	Riedel, 1958	68
Pterocanium korotnevi (Dogiel)	Nigrini and Moore, 1978	58
Pterocanium sp. indet.		2
*2,Pterocorys hirundo Haeckel	Kruglikova, 1974	56
Rhizoplegma boreale (Cleve)	Ling et al., 1970	47
Saccospyris robustus Kruglikova	Kruglikova, 1974	2
Sethoconus ? tabulatus (Ehrenberg)	Petrushevskaya, 1967	2
*2,Siphocame aquilonaris (Bailey)	Ling et al., 1970	37
*1,Spongotrochus glacialis Popofsky	Nigrini and Moore, 1978	74
Spongurus pylomaticus Riedel	Kruglikova, 1974	44
Spongurus sp.	Ling et al., 1970	31
*2,Stylacontarium acquilonium (Hays)	Hays, 1971	55
*1,Stylatractus pyriformis (Bailey)	Kruglikova, 1974	61
Stylatractus univerus	Hays, 1971	6
*1,2,Stylochlamidium venustum (Bailey)	Kruglikova, 1974	90
*1,2,Stylodictya aculeata Jorgensen	Nigrini and Moore, 1978	76
*1,Stylodictya validispina Jorgensen	Kruglikova, 1974	58
Tetraphormis enneastrum (Haeckel)	Hulseman, 1963	3
Theoperidae gen. et. sp. indet. A		6
Theoperidae gen. et. sp. indet. B		29
Theoperidae gen. et. sp. indet. C		5
Tholospyris borealis (Bailey)	Kruglikova, 1974	34
*2,Tholospyris spinosus Kruglikova	Kruglikova, 1974	56
Triceraspyris antarctica (Haecker)	Casey, 1972	6

* Detailed information given in Table 15a and 15b.
1. Species that are abundant.
2. Possible stratigraphic or environmental indicators.

species \ depth in core-cm	4 - 0	4 - 295	12 - 0	12 - 68	12 - 140	12 - 210	12 - 310	12 - 400	12 - 490	12 - 567	13 - 0	13 - 285	22 - 30	22 - 136	22 - 148	26 - 0	26 - 212	26 - 223	26 - 231	26 - 255	26 - 275	26 - 295	26 - 340	26 - CC	36 - 80	36 - 630	36 - CC	37 - 30	37 - CC	54 - 98	54 - CC	65 - 0
Acanthodesma micropora	x	2	1	1	3	3	0	2	4	4	2	3	2	x	1	2	x	2	0	8	2	3	2	2	0	0	1	0	2	1	2	0
Acanthodesmidae sp. indet. A	5	4	5	4	6	x	2	2	2	4	x	4	x	2	1	3	4	5	3	8	2	x	0	5	0	9	1	0	0	2	2	0
Arachnocorys dubius	2	x	0	x	x	x	x	x	0	0	1	0	3	x	0	2	4	0	3	0	1	1	x	0	0	0	0	2	2	3	1	0
Crytopera laguncula	x	0	0	0	1	2	2	1	x	x	0	x	1	0	0	x	2	0	0	8	x	x	2	x	0	0	1	0	0	0	0	0
Cycladophora ? cornuta	4	5	5	4	11	11	27	29	55	27	5	20	3	2	17	5	9	12	18	17	14	18	11	8	0	23	23	6	26	6	34	3
Cycladophora davisiana	x	26	2	x	1	26	22	21	12	19	x	5	x	x	36	0	x	14	21	25	28	13	39	15	7	14	25	2	22	0	24	0
Dictyophimus gracilipes	2	2	5	2	5	2	2	2	x	1	10	7	4	2	x	6	7	2	6	0	3	2	2	x	4	0	1	6	6	15	6	2
Dictyophimus hirundo	1	0	0	1	2	x	x	1	x	x	2	2	1	0	0	0	0	2	0	0	1	0	0	0	0	0	0	0	0	0	x	3
Lithelius ? sp.	3	4	2	2	3	x	3	1	x	3	6	12	x	0	3	2	7	5	12	17	7	9	6	2	4	14	3	5	3	5	2	3
Lithomitra arachnea	2	0	x	1	x	0	0	2	2	1	1	0	x	0	7	x	0	2	6	0	1	1	2	x	0	5	0	0	0	0	x	0
Lychnocanoma grande	0	0	x	0	x	0	x	x	0	0	0	7	x	0	0	x	0	18	3	0	5	8	2	9	32	5	8	0	0	0	x	0
Prunopyle antarctica	5	5	5	4	1	4	3	10	5	8	x	3	3	12	5	4	4	3	3	0	x	7	6	9	0	0	4	6	3	3	5	0
Pterocorys hirundo	x	0	x	0	1	0	2	1	3	2	0	2	1	0	x	0	2	2	3	0	x	x	0	5	7	0	0	2	5	1	x	0
Siphocampe aquilonaris	3	8	2	3	x	0	0	0	0	0	x	0	7	2	4	2	3	0	0	0	3	3	0	x	0	0	0	0	0	1	0	0
Spongotrochus glacialis	10	9	13	10	10	6	5	6	5	7	13	6	13	11	9	14	8	2	0	0	1	7	6	4	4	0	4	13	2	11	4	44
Stylacontarium acquilonium	0	x	3	2	x	0	2	x	x	1	2	0	2	5	0	0	x	2	0	0	x	x	0	2	0	0	4	6	0	0	0	0
Stylatractus pyriformis	2	4	4	3	11	4	4	2	0	4	8	5	3	3	0	8	8	0	0	8	3	1	0	1	0	0	4	8	0	8	0	0
Stylochlamidium venustum	21	11	33	35	14	9	11	2	2	4	12	4	18	35	1	26	21	2	0	0	1	4	2	4	14	0	5	22	8	20	6	32
Stylodictya aculeata	5	4	2	3	2	18	2	9	6	10	2	7	3	0	2	x	4	0	0	0	3	7	7	6	4	9	8	2	2	1	5	2
Stylodictya validispina	2	x	x	x	0	x	x	2	x	1	1	2	x	0	0	3	2	0	0	0	x	x	x	x	0	0	0	3	2	1	x	0
Tholospyris spinosus	2	1	1	3	x	x	x	0	0	0	x	x	9	3	3	7	x	2	5	0	x	1	0	x	4	5	3	2	2	2	0	3
other species	31	15	22	22	29	15	13	4	8	4	21	11	22	28	9	17	15	31	19	9	25	18	11	28	20	16	4	15	15	19	14	8
total species counted	385	310	103	306	303	117	194	204	628	228	212	218	174	167	152	224	197	49	33	12	285	149	122	625	28	22	77	64	123	147	234	59

Table 15a. Abundance, shown in % of total assemblage of cores 4 to 65. Species used are those identified in table 1 as either abundant or potientially stratigraphically significant. (x = less than 1%)

species \ depth in cm	64-19	64-cc	100-21	100-cc	101-1	101-cc	102-30	102-cc	105-0	105-cc	106-15	106-28	106-43	107-30	107-cc	108-59	108-113	108-cc	109-5	109-226	109-232	109-cc	111-cc	112-0	112-cc	113	115-6	115-224	115-244	115-cc
Acanthodesma micropora	0	6	0	4	0	2	0	3	0	0	2	2	0	3	5	0	0	3	0	0	0	0	0	0	0	0	1	2	1	2
Acanthodesmidae sp. indet. A	0	4	5	5	8	5	4	1	6	5	4	5	0	2	2	3	5	3	6	0	0	0	0	0	0	0	2	5	2	3
Arachnocorys dubius	0	0	10	x	2	1	14	30	6	10	2	5	0	x	0	0	x	x	0	0	0	0	0	0	0	0	4	x	1	x
Crytopera laguncula	0	1	0	x	0	x	0	0	0	0	0	0	0	0	2	0	x	2	0	0	0	0	0	0	0	0	x	0	2	2
Cycladophora? cornuta	6	21	7	25	2	32	4	4	0	0	2	2	0	2	34	0	x	24	0	14	0	0	0	0	0	0	8	9	39	35
Cycladophora davisiana	17	3	5	7	x	16	0	1	12	5	0	17	6	x	11	2	0	14	0	29	0	0	0	0	0	0	0	3	13	14
Dictyophimus gracilipes	2	11	12	3	3	x	0	3	0	0	4	12	0	5	5	0	x	x	0	0	0	0	0	0	0	0	4	2	2	2
Dictyophimus hirundo	x	1	2	x	1	0	0	x	0	0	0	0	0	x	2	x	x	1	0	0	0	0	0	0	0	0	x	1	2	2
Lithelius ? sp.	x	10	2	5	1	3	0	2	0	14	6	5	6	3	3	3	4	1	0	0	26	0	0	0	0	0	4	7	1	2
Lithomitra arachnea	0	0	0	2	0	0	0	1	0	0	0	5	13	0	1	0	x	x	0	0	0	0	0	0	0	0	0	0	2	x
Lychnocanoma grande	0	8	0	x	x	0	4	0	0	0	0	2	0	0	0	0	0	0	0	9	0	0	0	0	0	0	0	0	x	x
Prunopyle antarctica	6	0	2	4	3	10	4	x	0	0	0	0	0	3	3	2	2	14	0	0	0	0	0	0	0	0	4	3	8	8
Pterocorys hirundo	0	3	0	2	2	1	0	0	0	0	4	0	0	x	2	x	x	3	0	0	0	0	0	0	0	0	0	x	x	x
Siphocampe aquilonaris	x	0	0	0	0	0	4	2	0	0	0	0	0	2	0	2	5	0	2	0	0	0	0	0	0	0	x	1	0	0
Spongotrochus glacialis	17	1	10	7	22	5	7	9	24	14	17	14	6	16	1	18	13	7	29	14	25	0	75	85	52	45	11	15	6	3
Stylacontarium acquilonium	2	0	0	x	x	0	11	x	6	0	4	0	0	2	1	5	6	1	0	0	0	0	0	0	0	0	x	3	x	x
Stylatractus pyriformis	0	0	0	3	3	x	7	3	0	0	2	0	0	2	3	x	1	x	0	0	0	0	0	0	0	0	6	8	3	4
Stylochlamidium venustum	28	10	25	8	31	7	26	15	35	28	24	0	0	40	3	49	47	8	55	14	0	0	17	10	39	27	35	28	3	6
Stylodictya aculeata	4	4	0	4	4	3	0	3	0	5	4	0	6	x	5	2	x	13	0	9	0	0	8	0	0	0	x	2	8	9
Stylodictya validispina	0	0	0	x	1	2	0	1	0	0	2	0	0	x	4	2	2	4	0	0	0	0	0	0	0	0	4	4	1	3
Tholospyris spinosus	x	1	0	x	4	x	0	0	0	5	0	0	6	2	0	x	2	0	0	0	0	0	0	0	0	0	5	2	2	0
other species	9	16	20	21	15	13	46	20	11	10	19	23	57	18	13	12	13	7	8	11	50	0	0	5	9	10	12	7	8	7
total species counted	108	72	98	105	104	256	81	270	17	21	54	42	16	205	188	131	329	237	49	21	4	0	12	20	23	11	166	337	380	389

Table 15b. Abundance, shown in % of total assemblage of cores 4 to 65. Species used are those identified in table 1 as either abundant or potientially stratigraphically significant. (x = less than 1%)

A PRELIMINARY REPORT ON AMINO ACID DIAGENESIS IN FOSSIL MOLLUSKS RECOVERED FROM THE NAVARIN BASIN PROVINCE, BERING SEA

David J. Blunt and Keith A. Kvenvolden

INTRODUCTION

Fossil mollusks were recovered in marine sediments from the Navarin Basin province, Bering Sea. The relative age of the fossil mollusks can be calculated from the amount of amino acid diagenesis that has occurred within the fossil shell since the organism's death. Correlation and geochronology of marine sedimentary deposits can be accomplished using the diagenesis of amino acids in mollusk shells. Reviews and recent advances using this method can be found in Hare and others (1980).

Theory

Individual amino acids that are no longer being biologically reproduced in the protein of the shell matrix undergo a stereochemical change from the L-enantiomer (living optical configuration having a mirror image) to the D-enantiomeric configuration during hydrolysis. The process of interconversion is called racemization. Over time, a mixture of L- and D-amino acids results. The kinetics of racemization can be expressed as a reversible first-order reaction:

$$\text{L - amino acid} \underset{k_D}{\overset{k_L}{\rightleftharpoons}} \text{D - amino acid}$$

where k_L and k_D are the respective reaction rate constants for the L- and D-amino acid enantiomers. The integrated rate expression for the racemization reaction as derived by Bada and Schroeder (1972) is:

$$\ln\left(\frac{1 + D/L}{1 - D/L}\right) - \ln\left(\frac{1 + D/L}{1 - D/L}\right)_{t=o} = 2kt \qquad (1)$$

where k is the racemization rate constant, D/L is the ratio of D- and L- amino acid enantiomers, and t is time. The logarithmic term at t=o is evaluated by measuring the D/L ratios in modern specimens.

MATERIALS AND METHODS

Samples

Gravity cores selected for this study were recovered in the northern Navarin Basin province (Fig. 52). Bottom water temperatures in the region are about 2° C, but they are related to the hydrographic regime in some complex fashion (Herman Karl, personal communication).

Fossil mollusks selected for amino acid analysis are reported in Table 16 together with gravity core numbers and subbottom depths. Of the ten gravity cores selected for this study, only in cores 42 and 44 were samples recovered from more than one depth interval. Seven articulated samples were recovered.

Methodology

The procedures used to extract and quantitate amino acid residues in the total amino acid fraction (both free and bound) in mollusk shell are fully described in Kvenvolden and others (1981). Briefly, about 0.2 g of shell material is hydrolyzed in 6 N HCL for 20 hours at 110° C. The hydrolysate is then dried and redissolved in a pH 1 norleucine standard. The mixture is applied to DOWEX 50 W x 8 (H^+) cation exchange resin. Amino acids are eluted with 2N NH_4OH. The eluate is subsequently split; half is quantitated by automatic ion-exchange chromatography and half is derivatized as a penta-fluoropropionyl-amino acid-(+)-2 butyl ester and analyzed for amino acid D/L ratios by gas chromatography.

RESULTS

Amino acid compositions in twelve mollusks recovered in sediments from the Navarin Basin province are reported in residues per 10^3 (Table 17). Relative differences in amino acid composition between each species can be detected by this method of presentation. For example, the specimens of Nuculana have relative concentrations of about 200 for aspartic acid, proline and glycine, whereas the specimens of Macoma have relative concentrations that are about 25-50% lower for the same three amino acids. Mya truncata, Yoldia myalis, Clinocardium nuttallii and Cyclocardia crebricostata also show relative differences in their amino acid compositions. Total amino acid concentrations are quite variable and range from 22.7 micro-moles per gram of shell (um/g) in Cyclocardia crebricostata to 6.12 um/g in Mya truncata.

Amino acid D/L ratios for aspartic acid, alanine, glutamic acid, phenylalanine, proline, leucine, and valine are reported for each specimen (Table 18). The highest D/L ratio was consistently measured in aspartic acid and the lowest D/L ratio was consistently measured in valine. The highest aspartic acid D/L ratio was measured to be 0.379 in Nuculana radiata (core no. 26, 227 cm), and the lowest was measured to be 0.071 in Macoma sp. (core no. 6, 10 cm). The highest valine D/L ratio was measured to be 0.056 in Yoldia myalis (core no. 42, 60 cm), and the lowest valine D/L ratio was measured to be 0.027 in Macoma sp. (core no. 6, 10 cm). The D/L ratios of alanine, glutamic acid, phenylalanine, proline, and leucine in all samples were measured to be between the limits of aspartic acid and valine (0.379-0.027).

DISCUSSION

Correlation and Geochronology

Relative correlation and geochronology of sediments from Navarin Basin province using amino acid diagenesis in fossil mollusks is possible, providing the shells have not been reworked. Shells that were living in situ probably have not been disarticulated, and seven articulated samples were recovered at

five different stations (see Table 16). All of the specimens of Nuculana are articulated. These samples provide a means of relative geochronology and correlation. Clearly from Table 18 the amino acid D/L ratios in N. radiata from core no. 26 are higher than the amino acid D/L ratios in N. radiata from core no. 50. Both of these samples were recovered from about the same subbottom depth interval which indicates that different sedimentation rates, erosion and/or non-deposition has occurred in these cores. Samples of Macoma are more likely to have been reworked as is suggested by their disarticulated state (with the exception of core no. 44). However, the D/L ratios of Macoma obliqua and Macoma brota recovered from subbottom depths of 200 cm in core 44 and 217 cm in core 62 respectively are distinctly greater than the D/L ratios in the two Macoma sp. samples recovered from subbottom depths of only 10 cm in core 6 and 13 cm in core 59. This is an expected result for samples recovered in situ.

Isoleucine and leucine are two amino acids that are commonly used for correlation and geochronology in fossil mollusk shells (for example, see Mitterer, 1974; Wehmiller and others, 1977; Kvenvolden and others, 1979; and Miller and others, 1979). Aspartic acid and glutamic acid have also been used in correlation and geochronology of fossil estuarine deposits (Kvenvolden and others, 1979). Only leucine will be applied in this preliminary report.

Application of amino acid geochronology is possible providing the factors that affect leucine racemization in each sample have been properly assessed. Leucine geochronology should include three major factors: 1) applicability of linear racemization kinetics; 2) assessment of in situ temperature history and 3) species effects on racemization kinetics. Linear racemization kinetics using equation 1 can be applied in this study because the highest leucine D/L ratio measured is only 0.116 and it has been reported that non-linear kinetics occur in mollusks at leucine D/L ratios greater than ~ 0.3 (Wehmiller and Belknap, 1978). The in situ temperature history is perhaps the most difficult factor to assess, and the present bottom water temperature of ~ 2° C will be tentatively used for calculations. Species effects on leucine racemization kinetics are apparent when samples having the same time and temperature history are compared. Species effects between Nuculana, Macoma, and Clinocardium will be discussed in the following section.

Leucine Calibration

Specimens of Nuculana, Macoma, Clinocardium and Mya all of which have been measured for leucine D/L ratios and have been recovered from radiocarbon dated localities, are reported on Table 19. Temperature histories are based on long-term climatological records for the region. Temperature histories of ~ 10° C have been estimated for samples from the Puget Lowland (see Miller and Hare, 1980; Kvenvolden and others, 1981). The Mya truncata from Anchorage is estimated to have a temperature history of ~ 2° C (Miller and Hare, 1980). Differences in leucine D/L ratios between Nuculana, Macoma and Clinocardium are small and the leucine D/L ratios are probably too low to distinguish species characteristics for these samples with this limited comparison. These samples have the same magnitude of D/L ratio as the Navarin Basin province samples.

However, the leucine D/L ratio for Mya truncata is about 50% lower than others of about the same age. This difference is a result of its lower (~ 2° C) temperature history. This illustrates a necessity for proper assessment of temperature history.

The leucine racemization rate constant used in equation 1 must reflect the diagenetic temperature history that the sample has experienced. The variables of time and temperature recorded in Navarin Basin province sediment need further study. A preliminary estimate of a leucine rate constant usable in the Navarin Basin province can be calculated from the Washington and Alaskan localities that have been radiocarbon-dated and have temperature histories that can be calculated. Leucine racemization rate constants can be calculated using the Arrhenius relationship:

$$\ln\left(\frac{k_2}{k_1}\right) = \frac{Ea\ (T_2 - T_1)}{R\ (T_2\ T_1)} \qquad (2)$$

where k_2 and k_1 are the leucine racemization rate constants; the leucine racemization activation energy (Ea) is assumed to be 29.4 kcal/mole for all samples; the gas constant R is 1.987; and T_2 and T_1 are the respective estimated temperature histories in degrees Kelvin for each sample.

Leucine rate constants from Table 19 can be calibrated by the method of Bada and Protsch (1973) using equation 1. These calibrated rate constants and calculated temperatures can be applied to equation 2 and a leucine rate constant at 2° C can be calculated for Nuculana, Macoma, and Clinocardium. The leucine racemization rate constant calculated at 2° C for each species is: Nuculana, $(1.73 \pm 0.23) \times 10^{-6}$; Macoma, $(1.78 \pm 0.09) \times 10^{-6}$; and Clinocardium, 1.45×10^{-6}. Leucine rate constant determined for Macoma and Clinocardium are tentatively applied to Yoldia and Cyclocardia. Since the calibrated Mya truncata already has a temperature history of 2° C, the calibrated rate constant of 2.31×10^{-6} will be used in calculations.

Age and Accumulation Rates

The calibrated leucine rate constants at 2° C and the measured leucine D/L ratios from fossil mollusks in the Navarin Basin province results in ages from equation 1 that range from 5,600 years in core 59 to 53,000 years in core 26 (Table 20). It must be restated that the present lack of a local in situ temperature calibration site within the Navarin Basin province prohibits these ages as being considered "absolute". For example, an average temperature history of about 6° C for bottom water temperatures will reduce the calculated ages by as much as 50 percent. It is encouraging to note that the ages determined from two depth intervals in cores 42 and 44 are in the correct geochronological order. The oldest age of 53,000 years is calculated from an articulated Nuculana from core 26. The radiolarian Lychnocanum grande which may have become extinct about 35,000 to 40,000 years ago (Joyce Blueford, personal communication) occurs with the Nuculana in core 26. However, diatom assemblages of this antiquity are not present in core 26 (Jack Baldauf,

personal communication). The articulated Nuculana in core 26 may have been reworked perhaps from submarine slumping.

The preliminary age calculations can be used to evaluate minimum accumulation rates in cores collected on the shelf, slope, and basin in the Navarin Basin province. Sample reworking, erosion and/or non-deposition of sediment will result in minimum accumulation rates being calculated. Minimum average accumulation rates range from 0.6 to 16 cm/10^3 years (Table 20). Aveerage accumulation rates along the shelf are quite variable and range from 0.6 cm/10^3 years in core 28 to as high as 16 cm/10^3 years in core 50. The paucity of microfauna in core 28 may be attributed to dilution of microfauna by rapid accumulationn (Paula Quinterno, personal communication). The contrasting slower accumulation rate using amino acid geochronology in core 28 suggests that the top of the core has undergone erosion or that the non-articulated Cyclocardia has been reworked and redeposited during conditions of rapid accumulation. The average minimum accumulation rate above the 200 m contour in the northern Navarin Basin province is about 7 cm/10^3 years, using amino acid geochronology.

Core 66, collected in 1336 m of water, has a minimum average sedimentation rate of 1.4 cm/10^3 years. This apparent accumulation rate is low, perhaps from erosion and/or non-deposition above the articulated Yoldia myalis located at a subbottom depth of 60 cm. Core 26, collected in 3337 m of water, is calculated to have a minimum average accumulation rate of 4.3 cm/10^3 years.

SUMMARY

Fossil mollusks recovered from sediments in Navarin Basin province were analyzed for amino acid content and stereochemistry. Concentrations of individual amino acids reported in residues per 10^3 characterize species of Nuculana, Macoma, Clinocardium, Yoldia, Cyclocardia and Mya. Amino acid D/L ratios show variable extents of racemization between the limits of valine and aspartic acid. Geochronology using leucine racemization is limited, mainly due to the lack of in situ temperature history and local calibration samples. Tentative amino acid geochronology based on an average temperature history of 2° C results in age estimations which range from 5,600 years to 53,000 years. Minimum average accumulation rates on the shelf range from 0.6 to 16 cm/10^3 years and average about 7 cm/10^3 years. The interpretation of accumulation rates using fossil mollusks must take into account sample reworking and sediment erosion and/or non-deposition.

REFERENCES CITED

Bada, J. L. and Schroeder, R. A., 1972, Racemization of isoleucine in calcareous marine sediments: kinetics and mechanism: Earth and Planet. Sci. Lett., v. 15, p. 223-231.

Bada, J. L. and Protsch, R., 1973, Racemization reaction of aspartic acid and its use in dating fossil bones: Proc. Nat. Acad. Sci., v. 70, p. 1331-1334.

Hare, P. E., Hoering, T. C., and K. King, Jr., 1980, Biogeochemistry of Amino Acids: New York, Wiley, 558 p.

Kvenvolden, K. A., Blunt, D. J., and H. E. Clifton, 1979, Amino acid racemization in Quaternary shell deposits at Willapa Bay, Washington: Geochim. Cosmochim. Acta, v. 43, p. 1505-1520.

Kvenvolden, K. A., Blunt, D. J., McMenamin, M. A., and S. E. Strahan, 1981, Geochemistry of amino acids in shells of the bivalve mollusk Saxidomus: In Proc. of the Ninth Internatl. Meeting on Organic Geochem., in press.

Miller, G. H., Hollin, J. T., and J. T. Andrews, 1979, Aminostratigraphy of U.K. Pleistocene deposits: Nature, v. 281, p. 539-543.

Miller, G. H. and P. E. Hare, 1980, Amino acid geochronology: Integrity of the carbonate matrix and potential of molluscan fossils: In Hare, P. E., Hoering, T. C., and K. King, Jr., eds., Biogeochemistry of Amino Acids: New York, Wiley, 558 p.

Mitterer, R. M., 1974, Pleistocene stratigraphy in southern Florida based on amino acid diagenesis in fossil Mercenaria: Geology, v. 2, p. 425-428.

Wehmiller, J. F. and D. F. Belknap, 1978, Alternative kinetic models for the interpretation of amino acid enantiomeric ratios in Pleistocene mollusks: examples from California, Washington and Florida: Quat. Res., v. 9, p. 330-348.

Wehmiller, J. F., Lajoie, K. R., Kvenvolden, K. A., Peterson, E., Belknap, D. F., Kennedy, G. L., Addicott, W. O., Vedder, J. G., and R. W. Wright, 1977, Correlation and chronology of Pacific coast marine terrace deposits of continental United States by fossil amino acid stereochemistry - technique evaluation, relative ages, kinetic model ages and geologic implications: U.S. Geol. Surv. Open-file Report 77-680, 197 p.

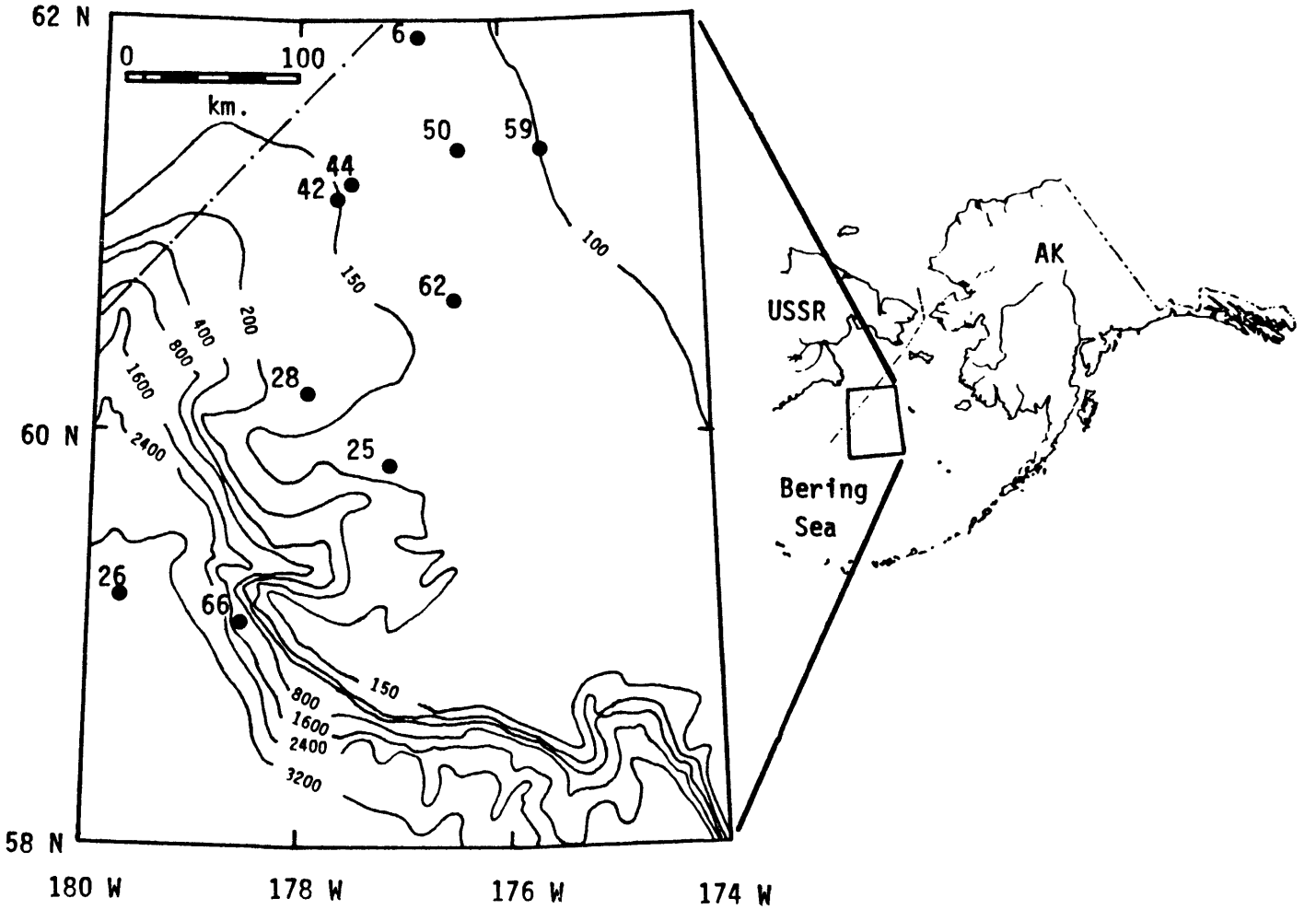

Figure 53. Location of gravity cores in the northern Navarin Basin province where fossil mollusks were studied. Bathymetry is in meters.

Table 16. Sample Identification and Subbottom Depths in Gravity Cores Recovered in the Navarin Basin Province, Bering Sea

Station No.	Gravity Core No.	Subbottom Depth cm	Sample
3	6	10	Macoma sp. (not art.)
19	25	173	Mya truncata (not art.)
20	26	223-230	Nuculana radiata (art.)
21	28	8	Cyclocardia crebricostata (not art.)
32	42	97	Clinocardium nuttallii (art.)
32	42	170	Nuculana fossa (art.)
34	44	125	Nuculana fossa (art.
34	44	200-206	Macoma cf. M. obliqua (art.)
39	50	219-230	Nuculana radiata (art.)
47	59	13-14	Macoma sp. (not art.)
49	62	214-220	Macoma brota (not art.)
53	66	60	Yoldia myalis (art.)

1. Specimens identified by L. Marincovich, USGS, Menlo Park

2. (not art.)= sample not articulated; (art.)= sample articulated

Table 17. Amino Acid Residues/10^3 in Molluscan Fauna Recovered in the Navarin Basin Province

Sample	Nuculana	Nuculana	Nuculana	Nuculana	Macoma	Macoma	Macoma	Macoma	Mya	Yoldia	Clinocardium	Cyclocardia
Core No.	26	50	42	44	44	62	6	59	25	66	42	28
Subbottom Depth cm.	∿ 227	∿ 225	170	125	∿ 203	∿ 217	10	∿ 14	173	60	97	8
Aspartic acid	198	197	207	220	145	147	109	114	289	226	241	96
Threonine	46	46	48	45	58	54	52	60	50	40	46	33
Serine	46	56	54	48	68	77	66	81	53	58	53	50
Glutamic acid	63	65	65	67	109	113	78	84	70	103	67	46
Proline	205	199	217	215	141	117	150	143	100	114	125	56
Glycine	186	196	183	162	166	156	226	188	175	194	205	414
Alanine	58	60	67	58	97	93	87	105	83	86	48	56
Valine	63	56	58	56	49	53	48	46	45	64	58	30
Methionine	12	14	7	7	15	16	28	34	8	12	23	7
Isoleucine	17	13	14	14	20	28	26	21	19	24	26	18
Leucine	24	21	22	25	45	48	39	46	27	33	30	29
Tyrosine	22	24	21	29	25	24	26	19	17	26	27	61
Phenylalanine	7	5	6	6	21	23	18	16	7	9	10	32
Histidine	13	10	4	3	10	14	15	10	6	NR	NR	17
Lysine	35	31	28	30	27	31	29	27	47	NR	41	47
Arginine	7	8	7	14	3	5	3	4	6	11	< 1	7
Total Concentration (um/g)	8.54	13.7	14.8	18.6	8.06	9.41	16.7	8.72	6.12	12.2	11.8	22.7

Table 18. Amino Acid D/L Ratios in Molluscan Fauna Recovered in the Navarin Basin Province

Sample	Nuculana	Nuculana	Nuculana	Nuculana	Macoma	Macoma	Macoma	Macoma	Mya	Yoldia	Clinocardium	Cyclocardia
Core No.	26	50	42	44	44	62	6	59	25	66	42	28
Subbottom Depth cm.	∿ 227	∿ 225	170	125	∿ 203	∿ 217	10	∿ 14	173	60	97	8
Aspartic acid	0.379	0.233	0.300	0.241	0.227	0.206	0.071	0.075	0.213	0.299	0.206	0.099
Alanine	.164	.084	.115	.091	.093	.078	.035	.038	.096	.127	.074	.048
Glutamic acid	.136	.080	.097	.076	.090	.073	.042	.047	.080	.089	.073	.060
Phenylalanine	.160	.102	.124	.106	.106	.086	.038	.058	NR	.103	.093	.050
Proline	.122	.058	.074	.063	.104	.081	.034	.034	.109	.158	.067	.045
Leucine	.116	.049	.073	.053	.074	.058	.036	.035	.061	.102	.060	.046
Valine	.040	.030	.037	.031	.046	.037	.027	.022	.04	.056	.043	.041

Table 19. Calibration Localities Used for Age Calculation by Leucine Racemization

Sample	Sample/ Locality No[1]	Leucine D/L	^{14}C Age	k_{leu}^{2} ($\times 10^{-6}$)	T[3]	Location[4]
Nuculana fossa	80-37	0.105	11,640±275 (W-940)	6.89	∿ 10	Cedarville, WA
Nuculana fossa	80-24	.142	13,010±170 (UW-32)	9.07	∿ 10	Penn Cove, WA
Macoma calcarea	80-37	.125	11,640±275 (W-940)	8.63	∿ 10	Cedarville, WA
Macoma sp.	80-24	.126	13,010±170 (UW-32)	7.82	∿ 10	Penn Cove, WA
Clinocardium nuttallii	79-3	.112	13,010±170 (UW-32)	6.72	∿ 10	Penn Cove, WA
Mya truncata	77-MTA-1 (ml552)	.055	13,000±	2.31	∿ 2	Bootlegger Cove, Anchorage, AK

[1] Samples from the Puget Lowland, Washington, collected with D. Easterbrook, Western Washington University. Alaskan Mya received as an interlaboratory calibration sample, 1977, with G. Miller, INSTAAR, University of Colorado

[2] For all calculations a leucine $D/L_{t=o}$ of 0.025 was used

[3] Average diagenetic temperature estimated from long-term temperature records

[4] Washington radiocarbon dated localities can be found in Easterbrook, 1969. Alaskan locality reported in Miller and Hopkins, 1980

Table 20. Leucine Racemization Age and Sedimentation Rate in Cores from the Navarin Basin Province, Bering Sea

Gravity Core No.	Subbottom Depth cm.	Estimated Sample[1] Age 2C	Minimum[2] Sedimentation Rate (cm x10^{-3}yr)	Reworked[3] Sample
6	10	6,200±300	1.6	(?)
25	173	16,000	10	(?)
26	223-230	53,000±6,000	4.3	(?)
28	8	14,000±	0.6	(?)
42	97	24,000	4	-
42	170	28,000±3,000	6.1	-
44	125	16,000±2,000	7.8	-
44	200-206	28,000±2,000	7.3	-
50	219-230	14,000±2,000	16	-
59	13-14	5,600±300	2.4	(?)
62	214-220	19,000±1,000	11	(?)
66	60	43,000±2,000	1.4	-

[1]Error reported is from the calibrated rate constant. An increase of 4C in average temperature history will decrease the calculated age by as much as 50%

[2]Assuming constant sedimentation and sediment surface is at time zero

[3]Disarticulated samples possibly reworked